INVESTIGATION OF NORMAL VISION AND NEURO-OPHTHALMIC DISORDERS USING NONLINEAR SYSTEMS IDENTIFICATION METHODS

BY

RASA RUSECKAITE

A THESIS SUBMITTED FOR
THE DEGREE OF DOCTOR OF PHILOSOPHY OF
THE AUSTRALIAN NATIONAL UNIVERSITY

FEBRUARY 2004

VISUAL SCIENCES GROUP
RESEARCH SCHOOL OF BIOLOGICAL SCIENCES
THE AUSTRALIAN NATIONAL UNIVERSITY

STATEMENT

I declare that the results presented in this thesis are my own original work and were obtained under the supervision of dr. T. Maddess and dr. AC. James. None of the material has been presented for the award of any other degree or diploma in any other university or institute of higher education.

Some of the work described in this thesis is being prepared for publication:

James AC., Ruseckaite R., Maddess T., Effect of sparseness and dichoptic presentation upon multifocal visual evoked potentials (Visual Neurosci, submitted, 2004)

Maddess T., James AC., Ruseckaite R., Bowman EA.., Hierarchical decomposition of dichoptic multifocal visual evoked potentials (Visual Neurosci, submitted, 2004)

Ruseckaite R., Maddess T., James AC., Sparse multifocal stimuli for detection of multiple sclerosis (Visual Neurosci, prepared for submission, 2004)

Ruseckaite R., Maddess T., James AC., Comparing multifocal frequency doubling illusion visual evoked potentials and automated perimetry for normal and multiple sclerosis patients (Invest Ophthalmol Vis Sci, prepared for submission, 2004)

Rasa Ruseckaite

February 2004

ACKNOWLEDGEMENTS

I would like to thank my supervisor dr. T. MADDESS and my advisor dr. AC. JAMES whose broad knowledge of scientific issues and support have been of great value to me and essential for the completion of this work.

I also give my thanks to dr. G. DANTA who allowed me to experiments on patients suffering from multiple sclerosis. I would like to thank to my colleagues and the staff in the Research School of Biological Sciences for helping me with my experiments and volunteering to be my experimental subjects.

In addition I would like to thank all my friends (Mappoulo, Veronica, Noi, Ana, Reza…) outside the laboratory for giving me their time and support, and many unforgettable moments.

Above all, I wish to thank to my dear Mother, ANTANINA RUSECKIENE for her constant support and loving care she have given me during all these years.

My PhD study has been supported by an Australian National University Scholarship.

Rasa Ruseckaite

February 2004

ABSTRACT

This thesis principally describes multifocal visual evoked potentials (mfVEPs) recorded to different levels of temporal sparseness. mfVEPs were recorded and compared in Normal and Multiple Sclerosis (MS) subjects. According to the new MS diagnostic criteria of McDonald et al. (2001), MS patients tend to have abnormal looking waveforms. Their responses are also delayed and smaller than those obtained from Normal subjects. In many previous studies (Halliday *et al.*, 1972; Frederiksen *et al.*, 1991; Tan & Leong, 1992; Andersson & Siden, 1995), conventional VEPs were employed for the detection of the above mentioned features, appearing in MS evoked potentials. Later Fortune et al. (2002; 2003) showed that conventional VEPs were not equivalent to multifocal VEPs, which can be a useful tool in detecting the multiple damaged location of the visual field. My thesis describes the usefulness and diagnostic value of mfVEPs in MS. The thesis consists of four chapters.

The first chapter describes different temporal levels (sparseness) of multifocal visual stimuli. Here I discuss monocularly and dichoptically presented multifocal visual stimuli and the responses recorded from 13 Normal subjects. Dichoptically tested mfVEPs to sparser stimuli are larger and more consistent across the regions. The signal to noise ratios shows that the recording time could be reduced at about 3 times to achieve a good response quality to sparser stimuli. This result is very important in recording mfVEPs from MS patients.

The second chapter discusses multifocal responses obtained from Normal and MS subjects. It describes a number of diagnostic parameters and different discriminant models. Those parameters are extracted from the responses recorded to all four temporal visual stimuli, but the most sensible model, able to diagnose 98% of MS patients correctly contains three parameters, describing signal size, latency and shape, extracted from the Pattern Pulse stimulus only.

Chapter III describes mfVEPs also recorded to the frequency doubling (FD) illusion stimuli. Visual field perimetry tests, based on FD technology (FDT) were also applied. The analysis of FD effect in Normal and MS subjects is described in the third chapter. The main result in this chapter is that the Pattern Pulse parameters combined with FD mfVEPs measures (eg. amplitudes and FDT thresholds) also provide high diagnostic sensitivities.

In the last chapter I examine the binocular responses obtained to Pattern Pulse stimulus in Normal and MS subjects. They are larger than compared to monocular responses recorded from any single eye, but binocular responses do not have any significant differences in their latencies.

My thesis illustrates the high diagnostic value of multifocally recorded visual evoked responses and clearly show the high sensitivities of 98% in MS patients, compared to sensitivities obtained by means of traditional MS diagnostic techniques (i.e. conventional VEP stimulus and MRI) (Martinelli *et al.*, 1987; Frederiksen *et al.*, 1991).

Bibliography

ANDERSSON, T. & SIDEN, A. (1995). An analysis of VEP components in optic neuritis. *Electromyogr Clin Neurophysiol* **35,** 77-85.

FORTUNE, B. & HOOD, D. (2003). Conventional pattern-reversal VEPs are not equivalent to summed multifocal VEPs. *Invest Ophthalmol Vis Sci* **44,** 1364-1375.

FORTUNE, B., HOOD, D. & JOHNSON, C. (2002). Comparison of conventional and multifocal VEPs. In *ARVO*, pp. 2126, Ft. Lauderdale.

FREDERIKSEN, J., LARSSON, H., OLESEN, J. & STIGSBY, B. (1991). MRI, VEP, SEP and biothesiometry suggest monosymptomatic acute optic neuritis to be a first manifestation of multiple sclerosis. *Acta Neurol Scand* **83,** 343-350.

HALLIDAY, A., MCDONALD, W. & MUSHIN, J. (1972). Delayed visual evoked response in optical neuritis. *Lancet* **1,** 982-985.

MARTINELLI, V., COMI, G., LOCATELLI, T., DELLA SALA, S. & SOMAZZI, L. (1987). Assessment of visual function in MS patients: comparative study of some diagnostic tests. *Ital J Neurol Sci* **Suppl,** 121-124.

MCDONALD, W., COMPSTON, A., EDAN, G., GOODKIN, D., HARTUNG, H., LUBLIN, F., MAFARLAMD, H., PARTY, D., POLMAN, C., REINGOLD, S., SANDBERG-WOLLHEIM, M., SIBLEY, W., THOMPSON, A., VAN DEN NOORT, S., WEINSHENKER, B. & WOLINKSY, J. (2001). Recommended diagnostic criteria for multiple sclerosis: guidelines from the international panel on the diagnosis of multiple sclerosis. *Ann Neurol* **50,** 121-127.

TAN, C. & LEONG, S. (1992). Evoked response study among Malaysian multiple sclerosis patients. *Singapore Med J* **33,** 575-580.

ABBREVIATIONS

BIN	binocular
BOS	bipolar occipital straddle
CI	confidence interval
CL	confidence limit
Com	communalities
CNS	central nervous system
CSD	current source density
CSF	cerebrospinal fluid
cVEP	conventional visual evoked potential
DR	diabetic retinopathy
EEG	electroencephalogram
ERG	electroretinogram
FD	frequency doubling
FD mfVEP	frequency doubling multifocal visual evoked potential
FDT	frequency doubling technology
FFT	fast Fourier transformation
HLA	human leukocyte antigen
IMP	improvement
IOP	intraocular pressure
IPL	inner plexiform layer
ISCEV	international society for clinical electrophysiology of vision
LDA	linear discriminant analysis
LE	left eye
LGN	lateral geniculate nucleus

LQ	liquid crystal
mfERG	multifocal electroretinogram
mfVEP	multifocal visual evoked potential
MRI	magnetic resonance imaging
MS	multiple sclerosis
NT	implicit time of the first negativity
NT_F	the longest fitted delay of the first negativity
N1	the first negativity
OD	right eye
ON	optic neuritis
OS	left eye
OPL	outer plexiform layer
PC	principal component
PCA	principal component analysis
PERG	pattern electroretinogram
POAG	primary open angle glaucoma
PT	the implicit time of the first positivity
P1	the first positivity
RE	right eye
RMS	root mean square
ROC	receiver operator curve
RP	retinitis pigmentosa
RR	relapsing remitting
RRMS	relapsing remitting multiple sclerosis
QDA	quadratic discriminant analysis
SC	superior colliculus

SE	standard error
SITA	Swedish interactive threshold algorithm
SNR	signal to noise ratio
STD	standard deviation
TON	traumatic optic neuropathy
URV	ultraviolet radiation
VEP	visual evoked potential
V1	striate visual cortex

LIST OF TABLES

LIST OF FIGURES

CONTENTS

Introduction

The Visual System

The Eye

The human visual system consists of the eye, optic nerve, and the brain which processes image information (Henry & Vidyasagar, 1977; Wandell, 1995b). Figure I.1 shows the basic structure of the human eye: the pupil, the iris, the sclera, and the cornea. The pupil is the aperture of the eye, through which light enters and then goes on to be projected onto the surface of the retina. The iris is a ring of muscular tissue, constricting and relaxing in order to narrow or widen the opening of the pupil. The sclera is the "white" of the eye, which functions as the main supportive wall of the eyeball. The cornea is a transparent layer of tissue that covers the pupil and the iris.

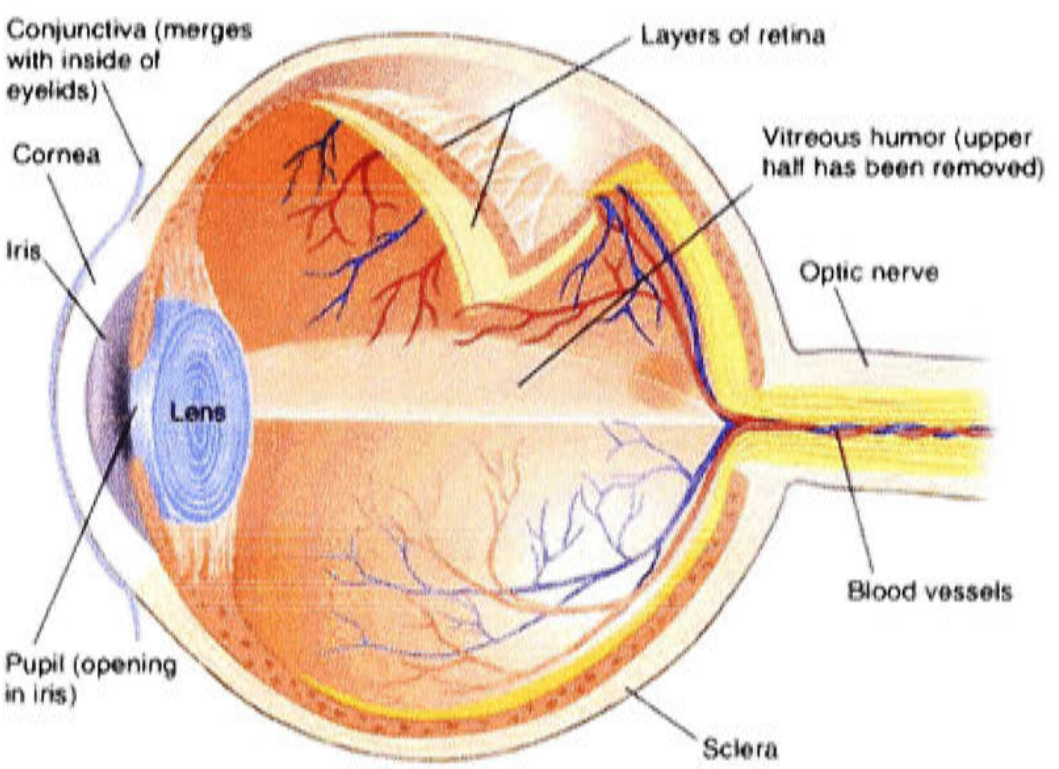

Figure I.1 Sagittal section of the adult human eye. When light arrives at the eye, it enters through the pupil, bordered by the iris. Light is brought into focus on the retina by the cornea and lens. Before that it must pass through the transparent vitreous and several retinal layers (reproduced from http://psych.athabascau.ca/html/Psych402/Biotutorials/).

The Retina

The retina is a neural tissue that includes the photoreceptive cells located on the inner surface of the eye. The primate retina is approximately 0.5 mm thick and consists of three layers of cell bodies and two layers, containing the synaptic interconnections between the neurons (Curcio & Allen, 1990; Wassle *et al.*, 1990; Wassle & Boycott, 1991; Dacey, 1993; Dacey & Lee, 1994).

In the centre of the retina is the optic nerve, a circular to oval white area measuring about 2 x 1.5 mm across. The major blood vessels of the retina radiate from the centre of the optic nerve. A blood vessel-free reddish spot, the fovea which is 4.5-5 mm or two and half disc diameters, can be seen to the temporal side of the disc. The fovea is situated at the centre of the area known as the macula (Henry & Vidyasagar, 1977).

The optic nerve contains the ganglion cell axons running to the brain and incoming and outgoing blood vessels opening into the retina to vascularize the retinal layers and neurons (Hartline, 1940; Henry & Vidyasagar, 1977; Wassle *et al.*, 1990; Dacey, 1993). The ganglion cells, which are the output neurons of the retina, lie innermost in the retina closest to the lens and front of the eye. The photoreceptors (i.e. the rods and cones) lie outermost in the retina against the pigment epithelium and choroid (Henry & Vidyasagar, 1977; Wassle *et al.*, 1990; Dacey, 1993).

The outer nuclear layer of the retina contains cell bodies of the rods and cones. The inner nuclear layer contains cell bodies of the bipolar, horizontal and amacrine cells and the ganglion cell layer contains cell bodies of ganglion cells and displaced amacrine cells (Wassle *et al.*, 1989). The first area of neuropil is the outer plexiform layer (OPL)

where connections between rod and cones, and vertically running bipolar cells and laterally oriented horizontal cells occur. The second neuropil of the retina is the inner plexiform layer (IPL). It functions as a relay station for the afferent-information-carrying nerve cells, the bipolar cells, to connect them to ganglion cells (Fig. I.2). Varieties of laterally - and afferently - directed amacrine cells interact in further networks to influence the ganglion cell signals. At the end of these processes message concerning the visual image is transmitted to the brain along the optic nerve (Henry & Vidyasagar, 1977; Wassle *et al.*, 1990; Dacey, 1993).

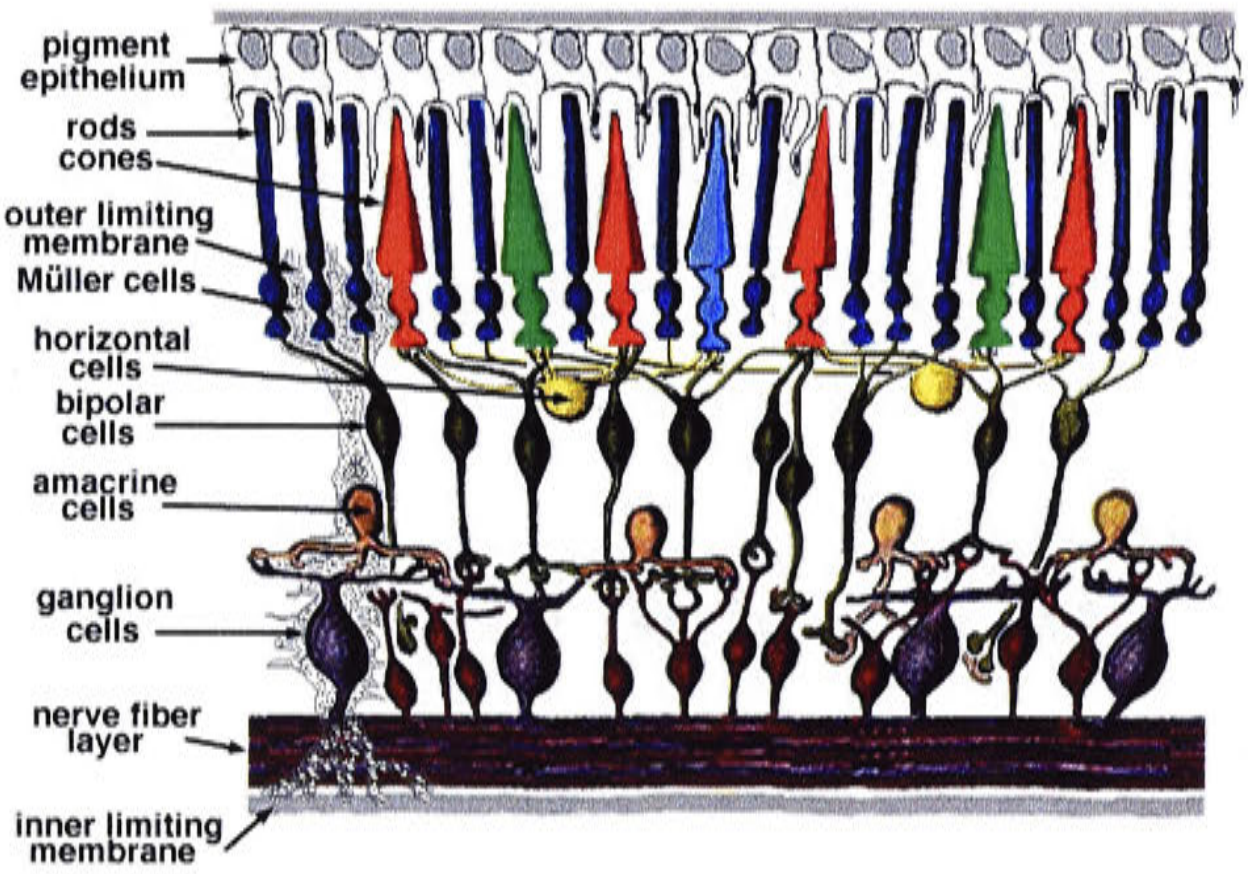

Figure I.2 Retina layers. A simplistic wiring diagram of the retina emphasizes only the sensory photoreceptors and the ganglion cells with a few interneurons connecting the two cell types (reproduced from http://webvision.med.utah.edu/sretina.html#overview)

The Visual Pathway

Human eyes are placed in the head so that they lie on each side of the midline of the face. This position has significant implications for the *visual field*. When humans look in any particular direction, they see a measurable amount of visual "space". This space is called the visual field. The extent of the visual field can be mapped by simply moving an object around in front of the forward fixated eyes until it disappears from view.

The eyes gather visual information from the environment. The retinal information exits the eye via the optic nerve (i.e. the nerve containing the axons of retinal ganglion cells and extending from the eye to the optic chiasm). Then the information branches to the lateral geniculate nucleus (LGN) of the thalamus, the pretectum and the superior colliculus (SC) (Henry & Vidyasagar, 1977; Bullier, 2001). The LGN receives the information from the two half-retinae projecting to the contralateral hemifield (eg. R LGN from R temporal and L nasal retinae) (Henry & Vidyasagar, 1977). The LGN of primates typically consists of six layers. The four superficial layers containing neurons with small cell bodies are called parvocellular layers. The two deeper layers contain neurons with large cell bodies and are called magnocellular. There are also cell bodies between these two layers in regions, called the intercalated zones (Henry & Vidyasagar, 1977; Shapley & Perry, 1986).

A large number of scientific studies have been done on the retinal ganglion cells and their properties in cats (Enroth-Cugell & Robson, 1966; Cleland & Levick, 1974; Wassle *et al.*, 1975; Victor & Shapley, 1979a; Victor, 1988) and monkeys (Gouras, 1968; De Monasterio & Gouras, 1975; Schiller & Malpeli, 1977; Kaplan & Shapley, 1982; Derrington & Lennie, 1984; Perry & Cowey, 1985; Blakemore & Vital-Durand, 1986; Silveira *et al.*, 1989; Wassle *et al.*, 1989). The retinal ganglion cells were

classified on the basis of their neural responses, and their distribution was compared in regards of their axon terminals in the LGN. In cats, cells, known as X cells, are driven by linear receptive field centre and surround mechanisms, whilst the Y cells also receive signals from an array of non-linear sub-units. The responses of both cell types are also very sensitive to contrast changes (Enroth-Cugell & Robson, 1966; Hochstein & Shapley, 1976; Victor *et al.*, 1977; Shapley & Victor, 1978; Victor & Knight, 1979; Victor & Shapley, 1979a; Shapley & Victor, 1980).

The remaining cells in the ganglion cell population are sometimes known as W. Those W cells, including the Y ones often project to the SC, whereas the X cells project straight to the LGN (Rodieck & Brening, 1983; Shapley & Perry, 1986; Dacey *et al.*, 2003).

In monkeys the major retinal ganglion cell types are sometimes classified as P and M cells. This classification is based according to their destination in the LGN. The P cells project to the parvocellular layers of the LGN. They also have small receptive fields and are poorly sensitive to luminance contrast (Gouras, 1968; De Monasterio, 1978; Shapley & Perry, 1986; Dacey *et al.*, 2003). The M cells project to the magnocellular layers and they are sensitive to luminance contrast. There are two groups of M cells: M_X and M_Y. In M_X cells the response is linear, when in M_Y cells it is not (Kaplan & Shapley, 1982; Marrocco *et al.*, 1982 ; Blakemore & Vital-Durand, 1986; Shapley & Perry, 1986; Benardete *et al.*, 1992; Benardete & Kaplan, 1999).

There are P_X and P_Y cells known in monkeys, but only few P_Y cells have been reported (Benardete *et al.*, 1992). The K cells which project to the koniocellular group in the LGN have been compared to those W cells in cats (Irvin *et al.*, 1986; Casagrande, 1994).

As described above, the responses of both X and Y cell types, and their primate equivalents, are sensitive to luminance contrast changes. This can be explained in part by the retinal gain control effect, reviewed in the paper of Maddess et al. (1998) and described by Shapley and Victor (1978). The gain control operates such that at moderate to high temporal frequencies the response is relatively amplified for higher contrast stimuli. In the cat the retinal gain control is strongest in the Y cells (Shapley & Victor, 1978; Victor & Shapley, 1979a, b). In the monkeys the contrast gain control is strongest in the M_Y cells (Kaplan & Shapley, 1982; Marrocco *et al.*, 1982). Retinal gain control has been confirmed in primate M-cells and it does not exist in P-cells (Derrington & Lennie, 1984; Benardete *et al.*, 1992).

Figure I.3 represents the visual pathway (Walsh, 1990c), viewed from above. The top rectangle divided into quarters symbolizes the field of vision; the dot in the centre is a fixation spot. The left half of the visual field projects onto the right half of each retina. From the retina axons pass through corresponding portions of the optic nerves to the chiasm, where fibers from the nasal half of the retina cross to the opposite side. The temporal half fibers from the right retina remain uncrossed (Henry & Vidyasagar, 1977; Hubel, 1988).

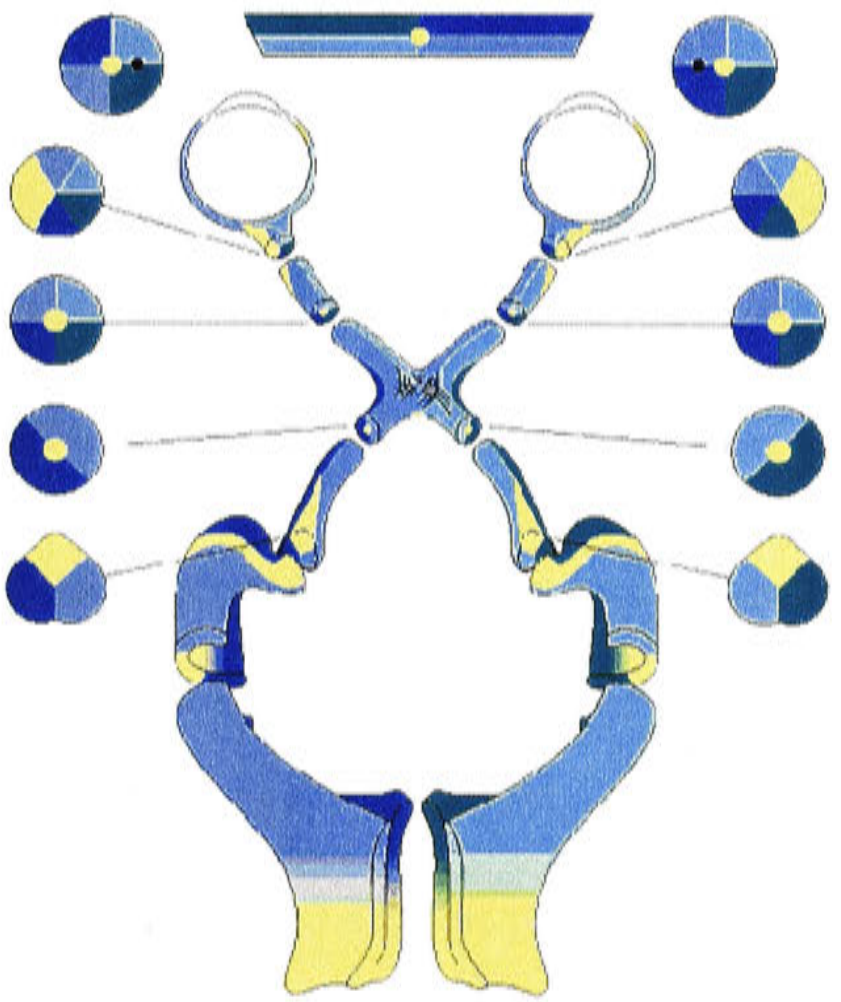

Figure I.3 Central optic pathways. The left side of the visual field is mapped to the visual cortex of the right hemisphere of the brain, and the right side to the left hemisphere (reproduced from Walsh TJ, *Visual fields. Examination and interpretation,* 1990, American Academy of Ophthalmology)

From the LGN, visual information goes to the primary visual cortex, which processes visual input and then sends it off to other areas of the brain for higher order processing and perception (see reviews by Bullier (2001), Henry & Vidyasagar (1977) or Hubel, 1982)).

The Visual Cortex

The human cerebral cortex is a 2 mm thick sheet of neurons with a surface area of about 1400 cm^2. The visual cortex is the part of the cerebral cortex that is responsible for processing visual stimuli. It is located at the anterior of the brain in the occipital lobe. A ridge or convolution of the cerebral cortex is called a gyrus, while each shallow surface is called a sulcus (Horton & Hoyt, 1991) (also see review by Dougherty *et al.* (2003)). The most visible sulci are used as markers to partition the human brain into four lobes: frontal, temporal, parietal and occipital.

The greatest part of the visual signal from the retina and the LGN arrives at a single area within the occipital lobe of the cortex called the primary visual cortex (V1) (Henry & Vidyasagar, 1977; Hubel, 1988; Horton & Hoyt, 1991; Dougherty *et al.*, 2003). The extrastriate visual cortex (Fig.I.4) is the place where the highest level of image processing is done.

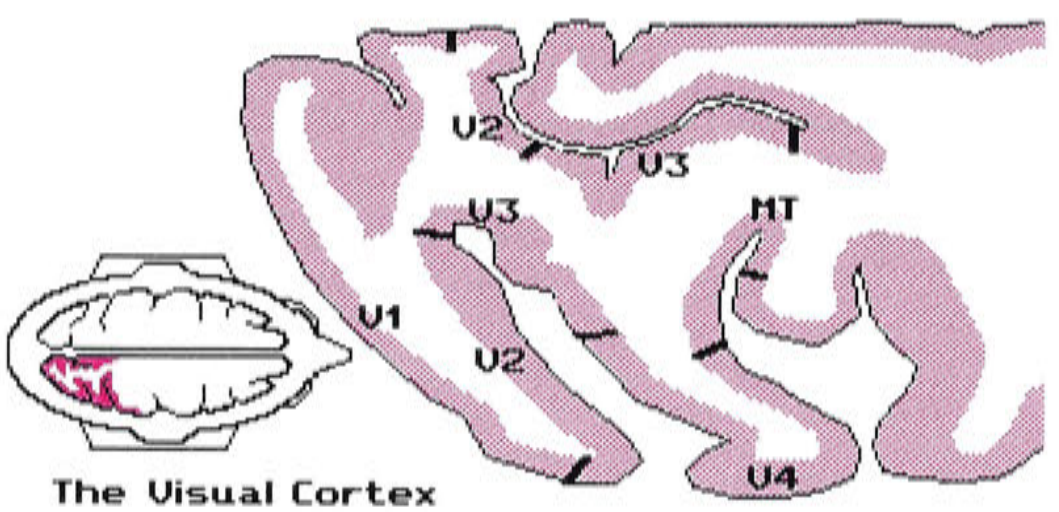

Figure I.4 The V1. Nearly all-visual information reaches the cortex via V1, the largest and most important visual cortical area. This area is also known as striate cortex. Other areas of visual cortex are known as extra striate visual cortex; the more important areas are V2, V3, V4 and MT, also known as V5 (reproduced from http://www.biols.susx.ac.uk/home/George_Mather/Linked%20Pages/Physiol/Cortex.html).

The occipital visual cortex is divided into 5 separate areas, V1 to V5 (Hubel, 1982, 1988; Wandell, 1995a). In humans the structure of V1 is complicated by the presence of a horizontal folding of the cortex called the calcarine sulcus, and the longitudinal division of the brain into left and right hemispheres. V1 contains 6 major layers of cells, and several sublaminae in certain layers. Cells in V1 seem to be arranged into functional groups, each of which is responsible for processing input of certain information. This region, which has a white band of myelinated fibres, represents about 15% of the whole neocortical surface in the macaque monkey, though it is probably only about 5% of the neocortex in man (see review by Dougherty *et al.* (2003)). It is the most complex region of the cortex with at least 6 identifiable layers (layer 1 is close to the cortical surface, layer 6 adjoins the white matter below) even though it is only about 0.5mm thick in the monkey (Hubel & Wiesel, 1968).

Layer 1 is nearly aneuronal, composed predominantly of dendritic and axonal connections. Approximately 20% of the neurons in layers 2-6 are inhibitory interneurons (GABAergic) that make major contributions to the function of V1 circuits but do not project axons outside this area (Fitzpatrick *et al.*, 1987; Hubel, 1988). Layers 2 and 3 (the "supergranular" layers) contain many excitatory projection neurons that send axons to extrastriate cortical regions. Layer 4 (the "granular" layer) is divided into 4 horizontal sublayers: 4A, 4B, 4Ca, and 4Cb. Layers 4Ca and 4Cb are the major recipients of afferent innervation from the LGN. The LGN magnocellular (M) and parvocellular (P) layers project to 4Ca and the 4Cb, respectively. Thus, the M and P streams remain segregated at this stage (but see qualification below) (Schein & De Monasterio, 1987). Layers 5 and 6 (the "infragranular" layers) contain many afferent excitatory projection neurons that project back to the LGN to provide feedback to this relay area (Lund *et al.*, 1975; Rockland & Pandyab, 1979), for more details also see the

review by Felleman *et al.* (1991). Following processing in this region, the visual neuronal impulses are directed to the secondary visual cortex or V2. V2 then projects to V3, V4, and V5. Each of these areas is also subdivided and sends information to any other areas of the brain that process visual information. This general arrangement is subdivided into three parallel pathways (Hubel, 1988; Felleman & Van Essen, 1991; Wandell, 1995a; Dougherty *et al.*, 2003).

The visual field position of retinal ganglion cells is roughly preserved by the spatial organization within the LGN layers (Curcio & Allen, 1990; Erwin *et al.*, 1999). Both the LGN and the striate cortex thus exhibit a precise point-to-point, but slightly distorted map of the visual field (Conoly & Van Essen, 1984). This map reflects the precise and orderly arrangement of connections along the retinogeniculate striate pathway. This arrangement is referred to as retinotopic organization. There are two retinotopic maps in the striate cortex, one for each eye, and they are in register with one another. Each half of the visual field is mapped to the contralateral hemisphere and the upper and lower fields are mapped in reverse. The primary visual cortex is organized with respect to three principles: retinotopic representation, stimulus orientation (eg. orientation columns) and ocular dominance (eg. ocular dominance columns) (Fig.I.5). In any one column of cells, the information processed relates to a single locus in visual space, an angle of orientation, an input from one or both eyes (Lund *et al.*, 1975; Horton & Hoyt, 1991).

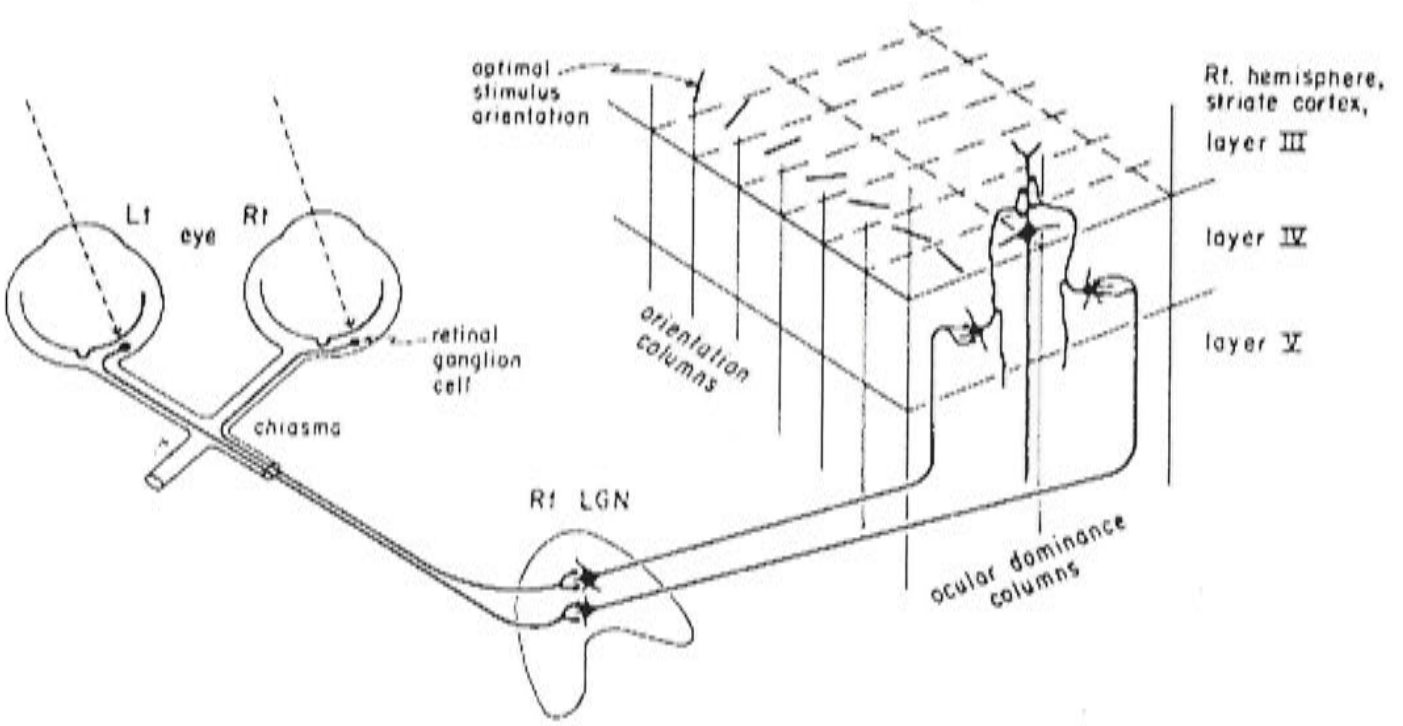

Figure I.5 The striate cortex is organized into intersecting sheets of cells, where each of them is representing progressively changing optimum stimulus orientation, and the other an alternation of dominance of input of left and right eyes. The right half of the retinae of both eyes projects to the right hemisphere, and inputs from corresponding points of the two retinae converge on single cells within striate cortex (reproduced from Wiesel, TN and Hubel, DH, *Laminar and columnar distribution of geniculo-cortical fibers in the macaque monkey,* J Comp Neurol, 146:421-450,1972)

The signals in area V1 are also retinotopically organized. From electrophysiological studies on monkeys, the location of receptive fields can be measured with an electrode that penetrates tangentially through layer 4C, traversing through the ocular dominance columns (Hubel & Wiesel, 1972; Hubel *et al.*, 1978; Hubel, 1982; Horton & Hoyt, 1991). Neurons with receptive fields in the central visual field are located in the posterior calcarine sulcus (Fig.I.6), while the neurons with the peripheral receptive fields are located in the anterior portions of the sulcus (Horton & Hoyt, 1991).

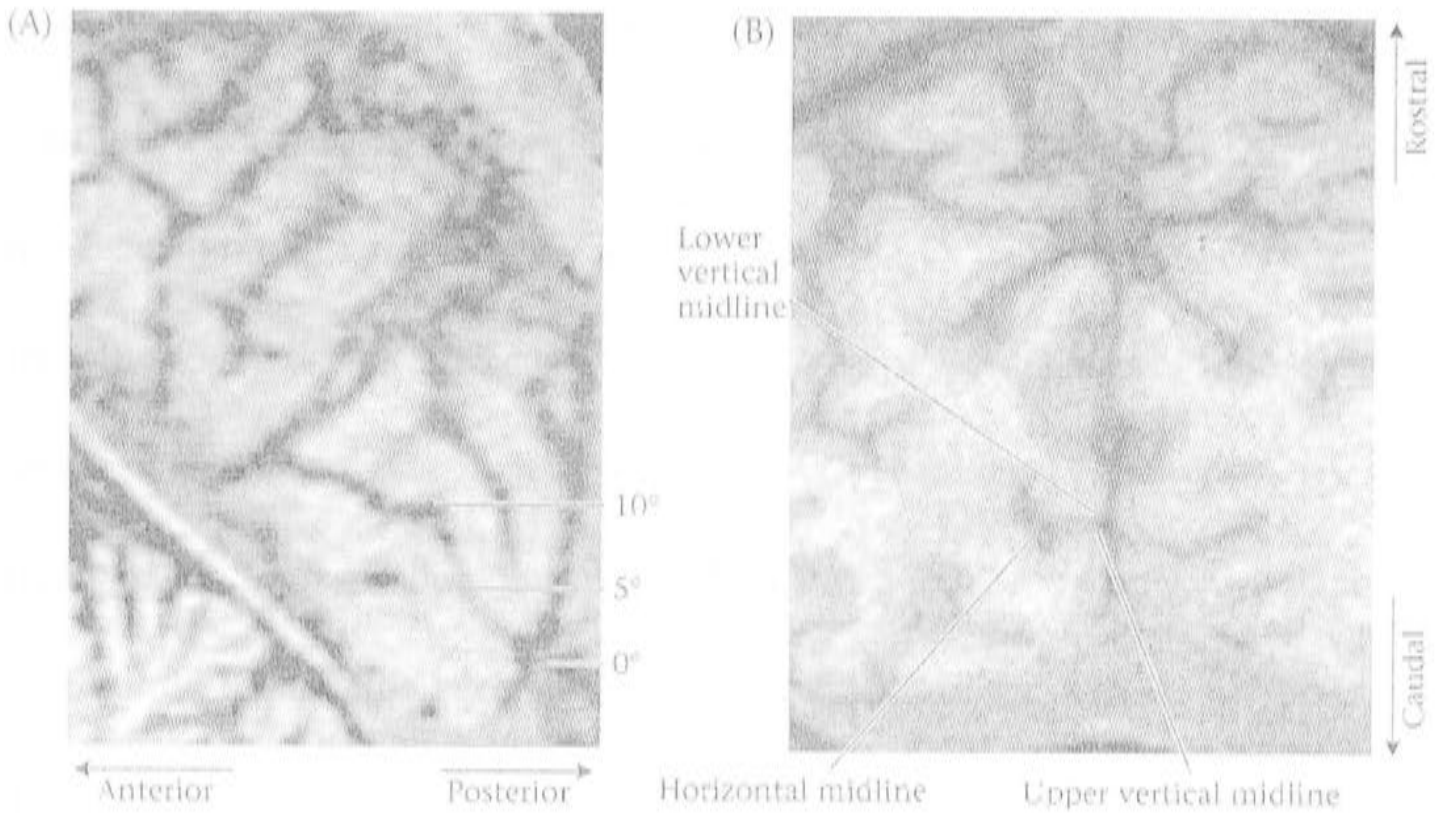

Figure I.6 A) is a sagittal view; the calcarine is a long sulcus that extends in about 4 cm. The visual eccentricities of the receptive fields of neurons at different locations are shown. B) is the coronal view of the calcarine sulcus, the receptive fields of neurons fall along a semicircle within the visual field. Neurons with receptive fields on the upper, middle and lower sections of semicircle of constant eccentricity are found on the lower, middle and upper parts of the calcarine sulcus respectively (reproduced from Wandell, BA, *Foundations of vision*, 1995).

Perimetry and Frequency Doubling Technology

Perimetry

Perimetry and visual field testing are very important for detecting ocular disorders that differentially degrade peripheral vision and central vision, such as in glaucoma and other retinal diseases or neurological disorders (Johnson *et al.*, 1999). Techniques for performing visual field testing have existed for 200 years (Duke-Elder & Jay, 1969).

The simplest form of visual field testing is the confrontation field. During the test examiner faces a patient and brings them to close one eye and fixate examiner's nose with the other eye. The examiner tests the extent of patient's visual field by moving a finger or a pen; or tests each of the visual field quadrants by asking the patient to count fingers or to compare the colour of objects presented simultaneously to the vertical or horizontal hemifields (Welsh, 1961; Frisen, 1973).

Kinetic perimetry is performed by means of a tangent screen or more commonly a hemispherical bowl device such as the Haag-Streit (Goldmann) perimeter. The patient looks at a small fixation point while small white targets are moved from the periphery towards the fixation point along a number of different meridians (Johnson & Keltner, 1987; Stewart *et al.*, 1988).

Static perimetry is a technique where the patient also looks into a white hemispherical bowl at a small fixation point in the centre. At fixed, stationary locations in the visual field, stimuli are briefly presented and the patient presses a response button when stimulus is seen. The size of stimulus remains constant and the luminance varies according to a staircase procedure (Walsh, 1990c; Johnson *et al.*, 1999).

The Humphrey Visual Field Analyser is a computerized static perimeter that tests a patient's ability to see lighted dots across their entire field of vision (Walsh, 1990c). The machine sequentially displays these dots in varying degrees of size and

brightness across a patient's central and peripheral vision to determine their threshold at each location. Threshold testing of visual fields identifies the limit of the sensitivity of the eye at programmed locations in the visual field. Based on patient's responses to the dots, the computer prepares a map of the patient's visual field. This test usually takes from 5 to 20 minutes. The Humphrey Visual Field Analyser has become an industry standard machine for the diagnosis and monitoring glaucoma and other ocular and neurological diseases (Walsh, 1990c; Blumenthal *et al.*, 2000; Burnstein *et al.*, 2000; Maddess *et al.*, 2000a; Sekhar *et al.*, 2000; Wong & Sharpe, 2000; Budenz *et al.*, 2002; Schimiti *et al.*, 2002; Wall *et al.*, 2002; Gillespie *et al.*, 2003; Vesti *et al.*, 2003).

The most common Humphrey test is the 24-2, which examines the central 24° (radius) of vision. The Humphrey 10-2 test permits monitoring of patients with very restricted fields (central 10°) (Caprioli & Zulauf, 1991) and the 30-2 tests more peripheral points (Heijl, 1985; Wong & Sharpe, 2000). The following strategies are available for the 24-2, 10-2 and 30-2 tests:

- **Full Threshold** - makes the least assumptions about the patient's vision. The brightness of the stimulus is varied at each location in order to find the threshold value (Heijl, 1985).
- **SITA Standard** (Swedish Interactive Threshold Algorithm). With the benefit of research into visual fields, the SITA test is able to make predictions of threshold values by analysing the patient's previous responses. The results are calculated using all of the data collected, so errors may be identified and corrected automatically (Sekhar *et al.*, 2000; Budenz *et al.*, 2002; Schimiti *et al.*, 2002)}.
- **SITA Fast** is the fastest threshold test, best used with reliable subjects (Schimiti *et al.*, 2002).

- **Stimulus Size** is full threshold test, which may be performed using different stimulus sizes. These equate to the stimulus sizes used by the Goldman Perimeter (Wilensky *et al.*, 1986; Caprioli & Zulauf, 1991).
- **Stimulus Colour.** The Humphrey test is normally carried out using a white stimulus against a white background. The stimulus colour may be changed when monitoring colour dependent changes. Colour perimetry can be a powerful tool to detect early glaucomatous damage (Sample & Weinreb, 1990; Snepvangers & Van den Berg, 1990).

The Octopus 201, 2000 and 500 perimeters (i.e. simplified versions of the standard perimetry) are similar to the Humphrey ones, except they produce an audible sound before the stimulus presentation, whereas the Humphrey instruments are quiet. This click before may keep the patient alert and prevent from blinking during the test (Caprioli & Zulauf, 1991).

Frequency Doubling Technology

Frequency Doubling Technology (FDT) is a new technique that has been designed for a rapid and effective detection of visual field loss due to glaucoma and other ocular diseases (Maddess, 1989; Maddess *et al.*, 1997; Johnson *et al.*, 1999; Maddess *et al.*, 1999). Over a range of high temporal and low spatial frequencies, counterphase flickering gratings produce the spatial frequency doubling (FD) illusion (Fig.I.7), in which the apparent brightness of the grating varies at twice its real spatial frequency (Kelly, 1966, 1981).

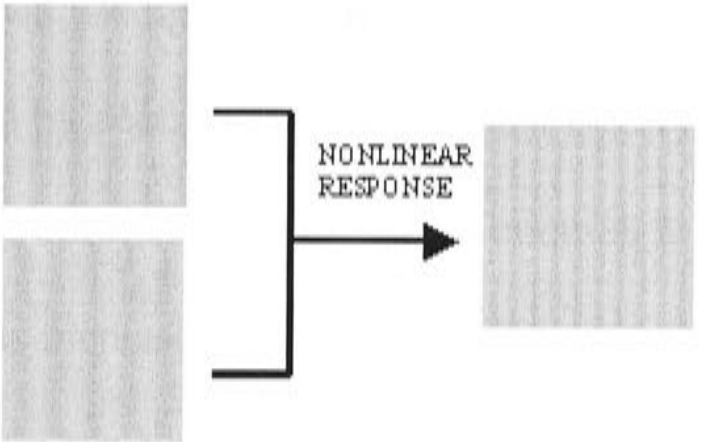

Figure I.7 Illustration of the stimuli, based on frequency doubling techniques. While presenting the stimulus on the display, temporal frequencies overlap with counter phase flicker, providing the nonlinear response, which is interpreted as frequency doubling stimulus (reproduced from Johnson, CA et al. *A primer for frequency doubling technology,* 1998 *Humphrey* Systems)

The FDT method is based on the assumption that the low spatial frequencies in combination with high temporal frequencies primarily stimulate cells of the magnocellular layers of the LGN (Maddess & James, 1998; Johnson *et al.*, 1999). FDT perimetry was developed for detection of localised flaws of abnormalities of perception in the visual field. The original form of perimeter (Fig.I.8), patented at ANU by Maddess et al. (1989, 1991) is manufactured by Welch Allyn (Skaneateless NY, USA). It uses 17 stimulus locations for the C-20 stimulus presentation pattern, the stimulus consisting of four targets per quadrant and a central stimulus (Fig.I.9). A newer version of the device, the Matrix, can use up to 52 stimuli in a test grid like the HFA 24-2 test. The FD tests are performed by determining the contrast threshold for each of the target locations in the display. If a stimulus is detected, its contrast is decreased for the next presentation, and if not, it is increased.

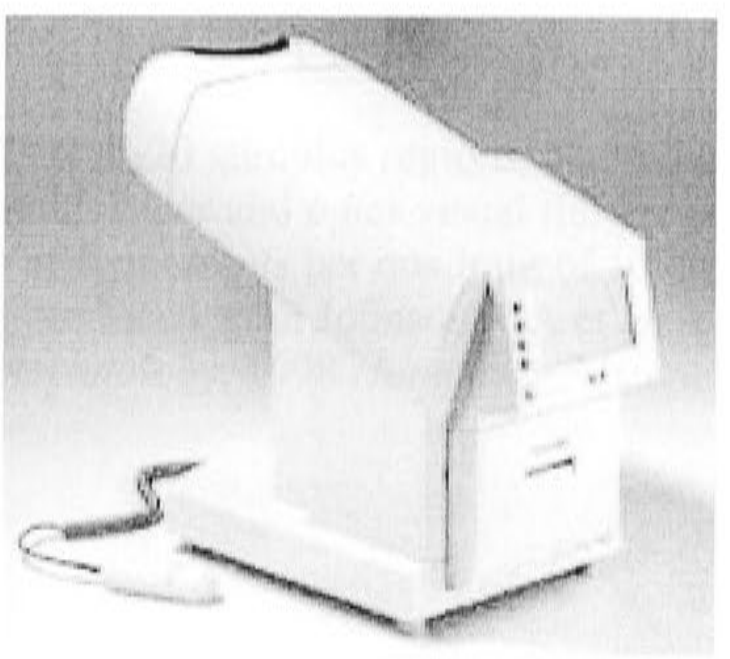

Figure I.8 FDT perimeter (reproduced from Johnson, CA et al. *A primer for frequency doubling technology,* 1998 Humphrey Systems)

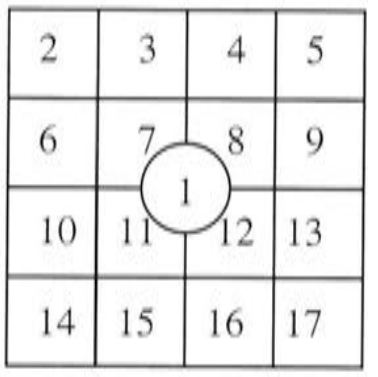

Figure I.9 Illustration of the FDT C-20 stimulus regions. The visual field is divided into quadrants where each contains inner and outer visual field regions. The stimulus presentation pattern consists of four targets per quadrant of 10 deg. in diameter, and a central 5 deg. radius target (reproduced from Johnson, CA et al. *A primer for frequency doubling technology*, 1998 *Humphrey* Systems)

Electroretinograms

The electroretinogram (ERG) is the summed electrical response of the retina, produced by a visual stimulus (Granit, 1933; Gouras, 1970). The physiological ability of the retina to respond to differing standards of illumination results in a duplicity of responses from rods and cones, i.e., a photopic and scotopic response, depending whether the retina is light adapted or dark adapted (Thomas & Lamb, 1999). The ERG measures the electrical activity of the cells within the retina in response to light stimulation. The ERG is considered the primary diagnostic test for retinal dystrophies and degenerations (including retinitis pigmentosa (Berson & Howard, 1971)), as well as inflammatory (Dodt, 1987), vascular and toxic disorders (Asi & Perlman, 1992).

The ERG has 2 major components: the negative-going a-wave, followed by the positive-going b-wave (Granit, 1933; Hood & Birch, 1982). The leading edge of the a-wave provides a direct measure of photoreceptor activity, and the b-wave reflects (Fig.I.10) the action of glial and other cells (Perlman, 1983; Heynen & Van Norren, 1985a; Asi & Perlman, 1992).

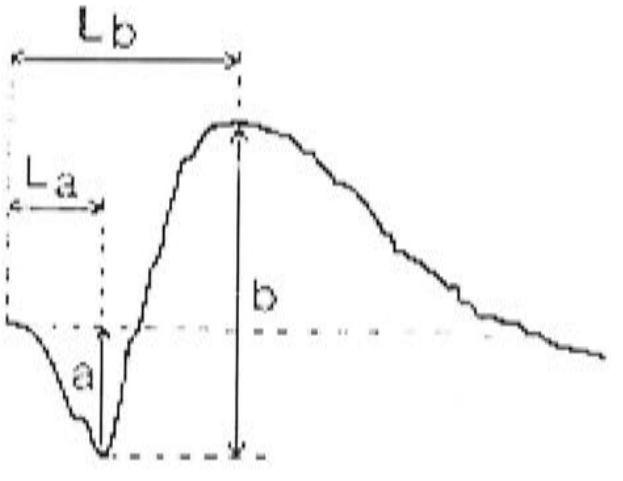

Figure I.10 The ERG response from a human contains the a-wave and the b-wave. La and Lb are the time-to-peaks for both waves (reproduced from http://webvision.med.utah.edu/ERG.html).

The a-wave is derived from the retinal photoreceptors, the rods and cones (Granit, 1933; Perlman, 1983; Heynen & Van Norren, 1985a; Thomas & Lamb, 1999; Paupoo *et al.*, 2000). Applying current source density analysis (which will be discussed in a subsequent section) to electrophysiological recordings of the intra-retinal ERG responses at different retinal depths further reveals the location of the b-wave (P-II) generators (Newman, 1980; Heynen & Van Norren, 1985b).

The only retinal elements that have a spatial distribution similar to the b-wave sources and sinks are the Müller glial cells (Miller & Dowling, 1970; Miller, 1973; Nicholson & Freeman, 1975; Newman, 1980). Intracellular recording from Müller cells in the Necturus retina supported Faber's ideas (Miller & Dowling, 1970) that the slow depolarising response of Müller cells to a light stimulus followed a temporal pattern similar to that of the ERG b-wave recorded from the same retina.

Furthermore, the amplitude-stimulus intensity relationship was similar for the Müller cell photo responses and the ERG b-wave. Based on these observations, Miller and Dowling (1970) suggested that depolarisation of the Müller cell membrane in the distal retina resulted in extracellular currents that were expressed as the b-wave. A change in the extracellular concentration of ions that permeate through the Müller cells' membrane would cause a change in membrane potential. The most effective are potassium ions (Miller, 1973).

Flash ERG and PERG

The flash ERG is a recording of the eye's electrical response to a ganzfield (wide field) flash of light accomplished by placing an electrode on the surface of the eye, typically

on the cornea. The flash ERG is produced by the action of the photoreceptors and by in the proximal retina such as bipolar and Müller cells (Miller & Dowling, 1970).

While the flash ERG tests the photoreceptors and associated glial cells (Hood & Birch, 1990), the pattern evoked ERG (PERG) has been proposed to reflect the activity of ganglion cells or structures closely dependent upon ganglion cell integrity. The PERG measures the eye's electrical response to an alternating (eg. flashing or reversing) patterned checkerboard stimuli (Korth, 1983; Azzopardi *et al.*, 1998; Marmor & Zrenner, 1999), also see the reviews by Zrenner (1990) and Bach *et al.* (2000). Compared to the flash ERG, The PERG is a very small signal, typically of 0.5 – 10 μV per region, depending on stimulus characteristics (Marmor & Zrenner, 1999; Bach *et al.*, 2000).

To answer the question whether the PERG and ERG were generated by different retinal cell populations, Maffei and Fiorentini (1982) devised a very interesting experiment: they recorded the ERG in response to homogenous light flashes as well as to pattern reversal stimuli before and after transsection of the optic nerve in cat retina. They found that the PERG progressively reduced while the ERG elicited in response to temporally modulated flashes appeared unaffected by nerve sectioning and remained after the PERG was extinguished (Fig. I.11). Afterwards it was suggested that the PERG source supposed to be located in the inner retina which is different from the ERG b – wave location.

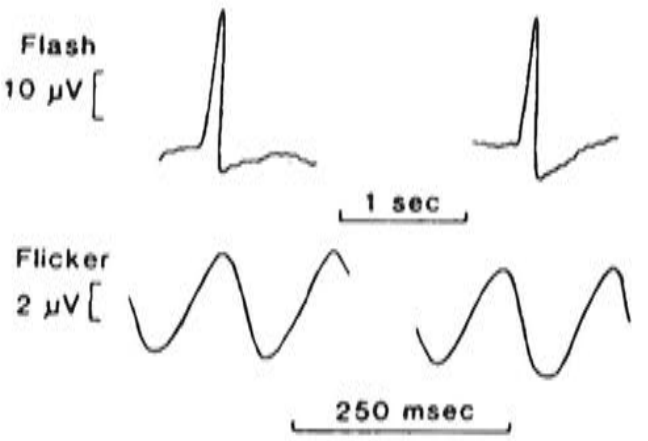

Figure I.11 The ERG response to 50 msec light flashes and to light flickering at 8 Hz recorded from two eyes 4 months after transection of the right optic nerve (reproduced from Zrenner E, *The physiological basis of the pattern electroretinogram*, 1990, Pergamon Press)

Earlier studies by Groneberg (as reviewed by Zrenner (1990)) showed that the PERG gradually disappeared in patients with a transsected optic nerve in one eye due to head injury. In the meantime, the ERG to the flash did not change. Later clinical studies observed the similar abnormalities (Dawson *et al.*, 1982; Azzopardi *et al.*, 1998; Shorstein *et al.*, 1999; Viswanathan *et al.*, 2000). Subsequent experiments in monkeys (Maffei *et al.*, 1985) also showed the validity of these observations in the primate visual system. As a result of these observations, it can be stated, that the origin of the PERGs is connected to ganglion cell activity.

Current Source Density (CSD) Analysis

CSD analysis has helped to provide further evidence of the origins of the PERG, as reviewed by (Zrenner, 1990). It solved the question about the localization of sources and sinks in certain retinal layers, and establishes localization different from the sources of the b-wave.

The CSD was studied by Nicholson and Freeman (Nicholson & Freeman, 1975), and also by Newman (1980). The general basics to perform current CSD were described by Zrenner et al. (1986) and Baker et al. (1988). Figure I.12 illustrates the positioning of stimulating and recording electrodes for CSD. The ERG depth is recorded with a micropipette electrode, tip diameter being of 5 μm. The point where the microelectrode contacted the retina is detected from effects on the electrical recording and on the resistance readings. When the resistance increase at about 300 – 400 microns of the retina depth, it indicates that the distal end of the retina is contacted. The signals are recorded in vitreous, as shown in Figure I.12 (Nicholson & Freeman, 1975; Zrenner *et al.*, 1986; Zrenner, 1990).

According to Maffei et al. (1982; 1985), at least of half of the fundamental uniform field-evoked CSD originates in the distal 40 –50% of the retina, corresponding to the photoreceptor layer. The photoreceptor generator currents as well as receptor – bipolar synaptic currents are candidates for the generators of the uniform field response (Maffei & Fiorentini, 1982; Maffei *et al.*, 1985).

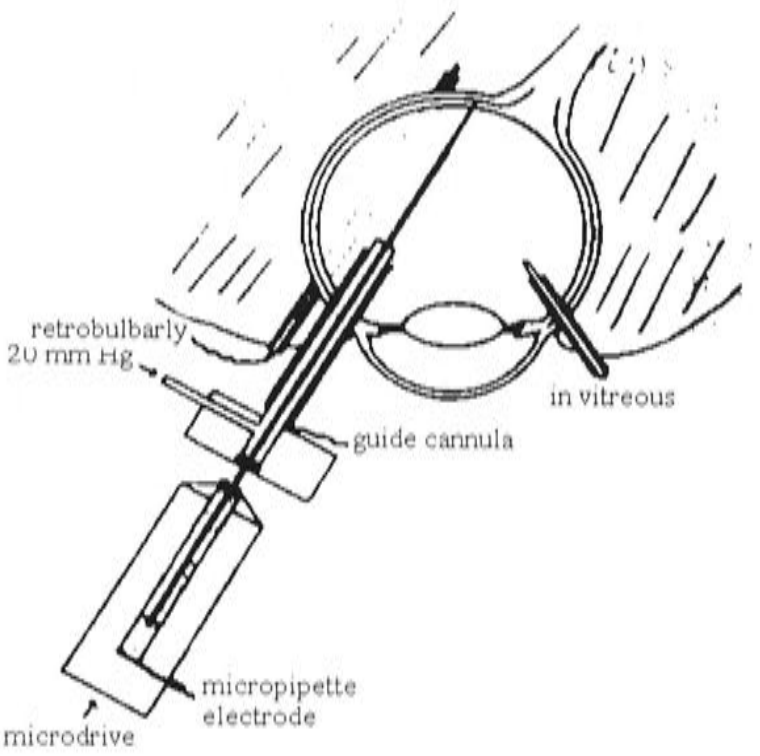

Figure I.12 The CSD analysis, positioning of stimulating and recording electrodes (reproduced from Zrenner E, *The physiological basis of the pattern electroretinogram*, 1990, Pergamon Press)

Multifocal Methods and White Noise Analysis

Chaos in Greek mythology is a great abyss out of which titans emerged (Sakai *et al.*, 1988). The concept of chaos was introduced by Wiener (1935), where he gave a mathematical foundation to the statistical mechanics of chaotic behaviour such as motion of gas molecules of turbulent flow. Gaussian white – noise is aderivation of the fundamental chaos using a Gaussian white-noise input the system input can be mathematically defined by a series of Wiener integrals (Sakai *et al.*, 1988). Wiener was the first to propose using a Gaussian white noise signal to test a system. Such a white noise has a flat spectrum, having independent values at every moment and a Gaussian or normal distribution. White – noise analysis can be extended to multi-input systems. The simplest case is the two-input experiment performed on concentric (or biphasic) receptive fields in the vertebrate retina (Marmarelis & Naka, 1973b; Mancini *et al.*, 1990). As discussed by James (1992), Victor (1992), Sutter (1992), Chichilnisky (2001) and Klein (1992), the multi – input white noise analysis is invaluable in visual neuroscience.

In the section that follows I will discuss the following aspects of the white noise theory: the orthogonalization, the calculation of the kernels from experimental data and the kernels of particular nonlinear systems (Victor, 1992).

Measurement of the Wiener Kernels of a Nonlinear System by Cross Correlation

The most important property of the linear system is superposition, defined as $S_1 + S_2 = R_1 + R_2$. It means, that if stimulus S_1 leads to a response and if the stimulus S_2 provides $S_1 + S_2$, then it leads to the response $R_1 + R_2$ (Victor, 1992). The nonlinear system is a system which does not show the superposition principle. An excellent example of a

nonlinear system is the visual system. A nonlinear system with a white Gaussian noise input is shown in the Figure I.13. Here the input *x(t)* to a system A is a white Gaussian process. The output *y(t)* of the system is represented by the orthogonal expansion (Lee & Schetzen, 1965):

$$y(t) = \sum_{n=0}^{\infty} G_n[h_n, x(t)] \qquad \text{(I.1)}$$

h_n here is the set of Wiener kernels on the nonlinear system, and G_n is a complete set of orthogonal functions. In this manner, a nonlinear system is characterized by the set of Wiener kernels h_n. The zero order kernel h_n is a constant; the first order kernel $h_1(\tau_1)$ is the linear kernel equivalent to the unit impulse response of a linear system. The second order kernel $h_2(\tau_1, \tau_2)$ is the quadratic kernel. The *n*th – order kernel is $h_n(\tau_1, ..., \tau_n)$.

The first order kernel can be estimated, as shown in the Figure I.14, by applying x(t) to A and the delay circuit B, multiplying their outputs *y(t)* and $y_1(t)$, and averaging the product for various values of the delay time σ. It can be expressed as follows:

$$h_1(\sigma) = \frac{1}{K}\overline{y(t)\,y_1(t)} \qquad \text{(I.2)}$$

Figure I.13 A nonlinear system with a white Gaussian noise input

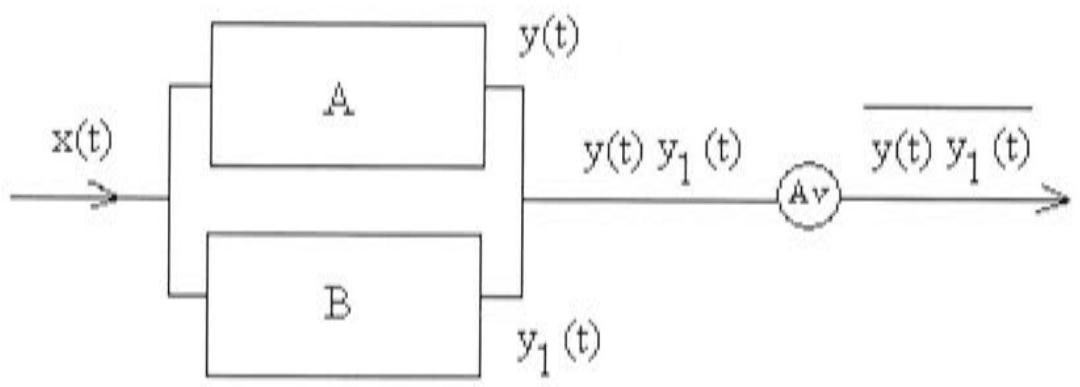

Figure I.14 Measurement of the first order kernel. A is unknown nonlinear system, B is an adjustable delay σ

The second order kernel can be estimated in similar way: we apply *x(t)* to the unknown nonlinear system and a two-dimensional delay circuit and then take the average of the product of their outputs for various value of the delay times σ_1 and σ_2. The second order kernel is expressed as follows:

$$h_2(\sigma_1,\sigma_2) = \frac{1}{2K^2}\overline{y(t)y_1(t)}, \quad for\ \sigma_1 \neq \sigma_2 \qquad (I.3)$$

The third and the *n*th order Wiener kernels are measured are estimated in the similar manner, and the Eq. I.4 expresses the measurement for the *n*th order kernel:

$$h_n(\sigma_1,.....,\sigma_n) = \frac{1}{n!K^n}\overline{\{y(t) - \sum_{m=0}^{n-1} G_m[h_m, x(t)\}y_n(t)}, \quad for\ all\ \sigma_1,.....,\sigma_n \qquad (I.4)$$

The detailed measurement of Wiener kernels by cross correlation is described by Lee & Shetzen (1965).

M-sequences

Multifocal analysis, using the m-sequence methodology, developed by Sutter et al. (1991; 1999), as implemented in the VERIS system (Electro – Diagnostic Imaging, San Mateo, CA) has been applied in many studies. The multi-input multifocal m-sequence technique has been referred to as a white noise analysis (Klein, 1992; Victor, 1992; Sutter, 2000). This technique is also a cross-correlation technique, where the binary m-sequences are used to emulate a random process. A schematic representation of a binary m-sequence is shown in the Figure I.15.

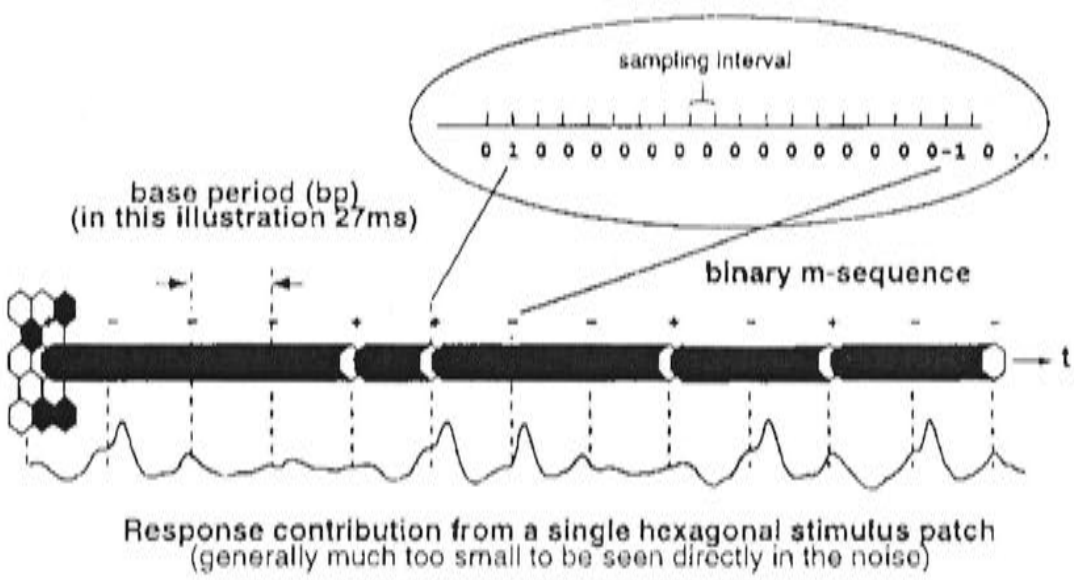

Figure I.15 A schematic representation of the flash stimuli of one of the hexagons in the VERIS stimulus array. The inset shows the sampling intervals. A bright (+1) hexagon indicates that the stimulus is flashed at the beginning of the first sampling interval, otherwise (-1). All other locations are 0s (reproduced from Sutter E, *The interpretation of multifocal binary kernels*, Doc Ophthalmol, 100:47-75, 2001).

The series I_i used for cross-correlation consist of +1 and –1. +1 if in the first sampling interval all base periods there was a stimulus, and –1 if otherwise. All other locations contained 0s (i.e. a weight of 0 and do not contribute). It was assumed that several data points were collected in each base period. The expression for cross- correlation can be rewritten as follows:

$$K_j^1 = \sqrt{\frac{1}{n}} \sum_{i=1}^{n} R_i * I_{i-j} = \sqrt{\frac{1}{n}} \sum_{i=1}^{n} R_{j+i} * I_i \qquad \text{(I.5)},$$

where for each j, the response R is added with the corresponding lag I and weight I_i. Lags could have a weight of –1 or +1. Those with 0 lags do not contribute. The cross - correlation of the response to random stimuli with auto-products of the stimulation sequence leads to a series of kernels (Lee & Schetzen, 1965; Sutter, 1991; Klein, 1992; Victor, 1992; Sutter, 2000, 2001). The cross - correlation for the derivation of the first kernel is equal to averaged separately all the response epochs following a stimulus and all those without stimulus and also subtracting the second averaging from the first.

Figure I.16 illustrates the derivation of the first order kernel and the second order kernel. The general rules for the extraction of the higher order kernels are similar: for a slice of order k, specific sequences of k consecutive base intervals are considered (Sutter, 1991, 2000, 2001).

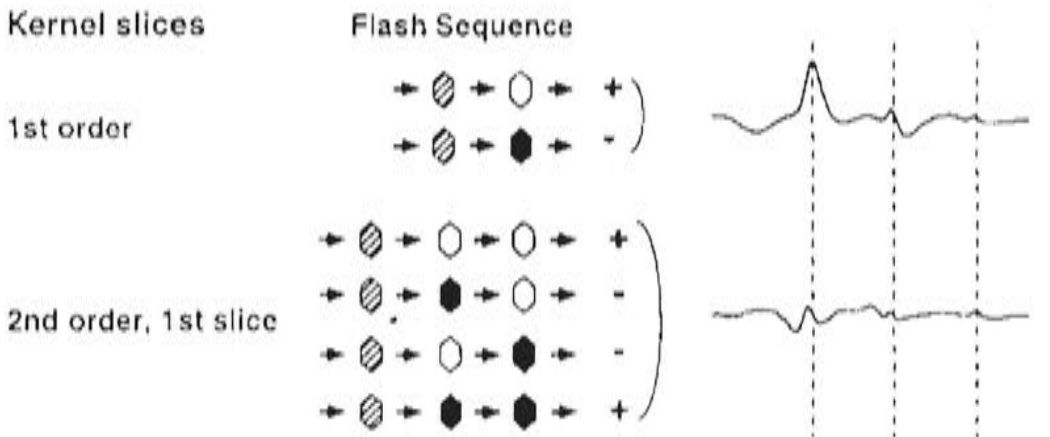

Figure I.16 The schematic illustration of the first order and the second order kernels. The white hexagon means "flash", the black hexagon symbolizes "no flash" and the dashed hexagon means "50% flash, 50% no flash" (reproduced from Sutter E, *The interpretation of multifocal binary kernels*, Doc Ophthalmol, 100:47-75, 2001).

Sutter (2001) has shown a relationship between kernels slices of different order. He described an example of the first order kernel and the first slice of the second order kernel, where, apparently the second base period of the first order kernel and the first base period of the second order slice differ only in rows where they contain no stimulus. The same rule can be applied for the higher order kernels. When the base period is smaller than the response duration, the higher order contributions are superimposed on the lower order slices with the corresponding lag. When the base period is very small, the kernels become similar to those obtained with Gaussian white noise stimulation (as reviewed by Sutter (2001)).

The Advantages of M-sequences

There are several advantages of m-sequences:

1. m-sequences uniformly test all possible stimulus sequences.
2. They have near-perfect autocorrelation functions. This property minimizes the problems of non - orthogonality, arising during estimation of kernels (Sutter, 1992, 2001) with truncated sequences.
3. It can happen that estimated kernels overlap (Sutter, 1992, 2001). In this case m-sequences can determine at which points and in which kernels those overlaps occurs.

While m-sequences are designed for nonlinear systems, they can be ideally used in processing of the visual system data, such as multifocal electroretinograms or visual evoked potentials.

Multifocal ERG and Clinical Studies

The multifocal ERG (mfERG) enables simultaneous recordings from a multitude of separate retinal regions (Sutter & Tran, 1992; Hood *et al.*, 1998; Kondo *et al.*, 1998; Hood *et al.*, 1999; Wilhelm *et al.*, 2000; Hood *et al.*, 2002a; Poloschek & Sutter, 2002). It has become a very popular tool for studying normal and abnormal retinal function. In the multifocal procedure, small retinal areas are independently stimulated. Multifocal cone ERGs have a biphasic waveform with negative and positive components and are relatively easy to record (Marmor *et al.*, 1999). Multifocal rod ERGs can also be measured from local regions of the retina (Friedburg *et al.*, 2001), but these responses are relatively small and noisy compared to those from the cones (Hood *et al.*, 1998; Hood *et al.*, 1999). A typical mfERG set up is given in the Figure I.17.

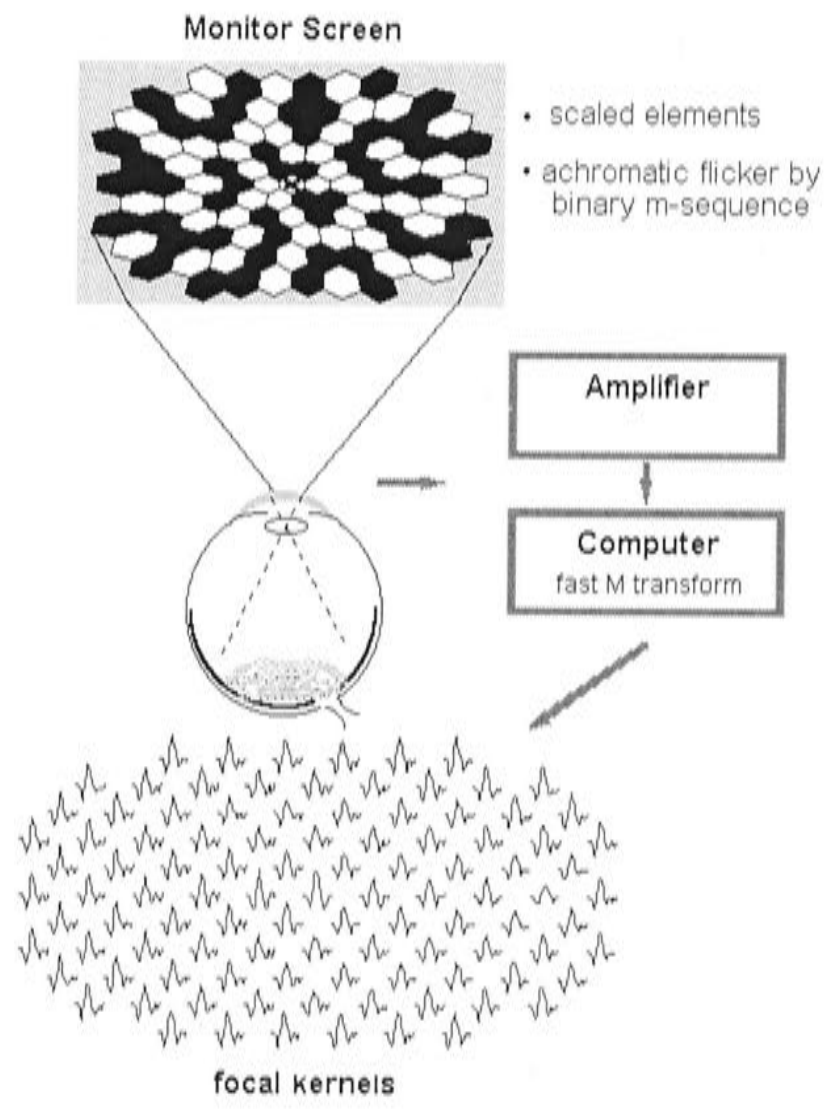

Figure I.17 A typical multifocal recording set up (reproduced from http://www.octopus.ch/products/default.htm)

Recent studies (Hood *et al.*, 1999; Hood *et al.*, 2001; Hood *et al.*, 2002a) investigated whether the mfERG was linked to ganglion cell activity or not. It was found that the monkey's mfERG contained a component that originated from the neurons in the retina producing action potentials, ganglion cells and their axons and probably amacrine cells. This component contributes to the optic nerve head component described in the human mfERG (Sutter & Bearse, 1999). Hood et al. (1999; 2001; 2002a) discussed an inner retinal component in humans as well, but he did not establish that this component was a ganglion cell component. Sano et al. (2002) showed that the ganglion cells also contributed to the 1st order kernel of the mfERG.

Previous research has shown the value mfERGs in clinical studies for the diagnosis of glaucoma (Hood & Zhang, 2000; Klistorner *et al.*, 2000; Maddess *et al.*, 2000b, a; Fortune *et al.*, 2002a) or other ocular diseases, such as diabetic retinopathy (Fortune *et al.*, 1999a), optic neuritis (Sano *et al.*, 2002), choroidal nevi and melanomas (Muscat *et al.*, 2002) or many other ophthalmic diseases.

Visual Evoked Potentials

Visual evoked potentials (VEPs) are electrical potentials recorded from the occipital cortex in response to a systematic change in some visual event such as a flashing light or contrast alternating chequered pattern (Towle *et al.*, 1991; Bodis Wollner, 1992; Nuwer, 1997; Kremlacek *et al.*, 1999; Odom *et al.*, 2003). They are sensitive to abnormalities at all stages of visual processing, including multiple sclerosis (Chiappa, 1983; Matthews & Small, 1983; Sala *et al.*, 1987; Towle *et al.*, 1991; Frederiksen & Petrera, 1999) and glaucoma (Graham *et al.*, 1999; Parisi *et al.*, 2001; Bengtsson, 2002; Thienprasiddhi *et al.*, 2003).

Types of VEPs

There are different types of specialized VEPs used in worldwide laboratories: steady state, sweep, motion, chromatic or color, dichoptic, stereo-elicited, multi-channel, hemi-field, multifocal, multi-frequency or LED Goggle VEPs. Most of these above-mentioned types of VEPs are not covered by the International Society for Clinical Electrophysiology of Vision (ISCEV) Standard (Harding *et al.*, 1995; Odom *et al.*, 2003). The three most popular VEP stimuli are pattern reversal, pattern onset/offset and flash (Odom *et al.*, 2003). Motion VEPs are recorded as well and can be compared to pattern reversal VEPs, as they have some similarities in terms contrast dependency (Bach & Ullrich, 1997; Gopfert *et al.*, 1999).

Pattern Reversal VEPs

The pattern reversal stimulus consists of black and white checks that alterate phase (eg. black to white and white to black) repeatedly at a specified number of reversals per

second. The stimulus should be defined in terms of the visual angle of each check, the reversal frequency, the number of reversals, the mean luminance, the pattern contrast and the field size (Harding *et al.*, 1995; Bach & Ullrich, 1997; Gopfert *et al.*, 1999; Shawkat & Kriss, 2000; Heinrich & Bach, 2001; Odom *et al.*, 2003l). Figure I.18 illustrates the example of the pattern reversal stimulus.

VEPs recorded in response to pattern reversal stimuli have been used to evaluate optic neuritis (Andersson & Siden, 1995), optic neuropathy (Ikejiri *et al.*, 2002) glaucoma (Parisi *et al.*, 2001), retinal disorders (Xu *et al.*, 2001) and multiple sclerosis (Sand *et al.*, 1990; Andersson *et al.*, 1991; Frederiksen *et al.*, 1991b; Roder, 1991; Towle *et al.*, 1991; Bodis Wollner, 1992).

Flash VEPs

The flash VEP should be elicited by a flash of light that subtends a visual field of at least 20 deg. (Odom *et al.*, 2003). The responses are much more variable across subjects than pattern VEPs but show little interocular asymmetry. They maybe useful when optical factors such as media capacities prevent the valid use of pattern stimuli.

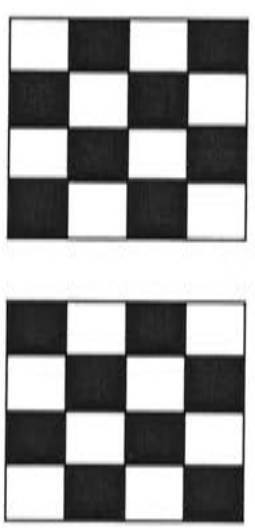

Figure I.18 An example of the pattern reversal visual stimulus wherein the appearance of a test stimulus exchanges check colouring. If the checks have contrasts -1 and 1 then the temporal alternation corresponds to multiplication with -1 at regular intervals.

Pattern Onset/Offset VEPs

For the pattern onset/offset stimulus a pattern is abruptly exchanged with a diffuse background (eg. when a contrast pattern appears from a uniform background of identical mean luminance, is present for a short time, and then disappears) (Harding *et al.*, 1995; Odom *et al.*, 2003). The ISCEV standard requires the stimulus to be defined in terms of the visual angle of each check (Harding *et al.*, 1995; Odom *et al.*, 2003). The reversing pattern is more common and useful in clinical practice, some scientific research on the pattern onset/offset VEPs was reported by Kremlacek et al. (1999; 2002), Suttle et al. (1999; 2000), Hoffman et al. (2003) and others.

Principal Component Analysis of VEPs

Principal Components Analysis (PCA) studies suggested that VEPs consisted of two basic components (C.I and C.II) (Jeffreys, 1971; Jeffreys & Axford, 1972). According to their results, C.I and C.II had spatially separate sources, and also the sources of C.I, originated in the striate cortex. Di Russo et al. (2001) also analyzed the initial VEP components and found that C.I. arose from the primary visual cortex, whereas the C.II. was coming from extrastriate cortical areas 18 – 19 (Jeffreys, 1971; Jeffreys & Axford, 1972; Bodis Wollner *et al.*, 1992; Manahilov *et al.*, 1992; Clark & Hillyard, 1996; Martinez *et al.*, 2001). Maier et al. (1987) also showed that C. I. and C.II. had their origins in two different cortical regions. Di Russo et al. (2001) summarized previous studies regarding the cortical visual areas that generate the first and the second component of pattern-onset VEP. Many researchers (Jeffreys, 1971; Jeffreys & Axford, 1972; Bodis Wollner *et al.*, 1992; Manahilov *et al.*, 1992; Clark & Hillyard, 1996;

Martinez *et al.*, 2001) showed that CI originated mostly from the Brodmann's area 17, striate cortex.

Review of the Previous VEP Studies

A number of VEP study have been performed on animals, such as mice, rats, cats and monkeys. Peachey et al. (2003) in their paper reviewed the visual electrophysiology literature, covering techniques used to record ERG and VEP from the mouse. He also reviewed how these techniques have been applied to characterize the functional implications of gene mutation or manipulation in the mouse retina. According Peachey et al. (2003), models of retinal disease in mice are very close to these pathologies in humans; therefore, in conclusion, the results described in their paper could contribute to the study of vision in other mammals.

Padnick et al. (1999) examined properties of the flash VEP recorded intracortically in cat primary visual cortex. The scientists were interested to know whether the VEP recording depth was a relevant factor to the size, shape and latency of the response. They also investigated the effect of variability in individual animals in order to establish the connection between the stimulus duration and anaesthetics used in the experiments and other factors. To discover the origin of VEP components in cats' visual cortex Padnick (1999) applied the CSD analysis and found that early potentials were generated in the layer 4 of the Area 17.

Pardue et al. (2001) studied the VEPs to infrared stimulation in normal cats and rats. This study covers the aspects of retinal degenerative diseases and possible methods of its detection, which could be potentially applied in humans.

VEPs and their components were investigated in monkeys too. Padmos et al. (1973) in his paper described flashed patterns in VEPs recorded from monkeys. The

researchers also reviewed the detection of luminance by first order summing models (Padmos *et al.*, 1973) as well as a centre – surrounding antagonistic mechanisms enhancing responses to spatial frequency selectivity and contour detection models. The main goals of this study were to detect the response differences in men and monkeys, as well as to examine the effect of electrode depth when recording intracortically. Padmos (1973) reported that contour specificity could not be observed on the scalp of monkey. He found that in monkey the enhanced response to patterned stimuli could satisfactorily be explained by assuming spatial frequency selectivity by a centre-surround antagonistic receptive field structure.

Steady state visual evoked responses in the alert primate *Macaca fasicularis* were investigated and reported by Nakayama et al. (1982). Those researchers aimed to compare the existence of narrow spatial and temporal frequency tuning (Tyler *et al.*, 1978). The second goal of the study was to verify the existence of multi-limbed linear functions when plotting VEP amplitude versus log contrast function, which has been reported before in humans by Cambell et al. (1970) and Apkarian et al. (1981). The scientists also discovered a match between the extrapolated VEP thresholds and psychophysics in monkeys and humans (Campbell & Maffei, 1970). These findings suggested that the steady state VEPs could reflect the activity of two distinct neural mechanisms responsive to pattern stimulation.

Shroeder et al. (1991) investigated the striate cortical contribution to the surface-recorded pattern reversal VEPs in the alert monkeys. As the visual capacities of these monkeys and humans are very similar and the opportunities for direct intracranial recording in humans are limited, therefore the monkeys were chosen to be the study object. These scientists examined the laminar profiles of VEPs, CSD and concomitant activity in the area 17 recorded simultaneously at incremental depths using multi contact electrodes. The results of this study suggested the possibility of differentiating

synaptic stages and cellular processes reflected in the human VEPs, based on homologies with simian VEP components.

A very important and interesting study of scalp VEPs and intra-cortical responses to chromatic and achromatic stimuli in primates was reported by Kulikowski et al. (2002). A major observation of this paper was that the VEPs of monkeys could be used to evaluate the integrity of the visual pathway and the quality of spatial and colour vision without any invasion techniques or training. In this paper researchers considered correlation between multi-unit responses and intra-cortical VEPs, correlation between scalp and intra-cortical VEPs, as well as chromatic VEPs. Kulikowski (2002) also discussed the differences between human and monkey scalp-recorded VEPs. If there was a close similarity between men and primates in chromatic VEPs, differences emerged when recording achromatic VEPs. Human achromatic VEPs consist of a prominent positive wave, which in low spatial frequencies are similar for onset, offset and reversal, consistent with their original in the responses of transient neurones. This fact was also discussed in the earlier published papers of the same author (Kulikowski, 1974, 1978). Differently from humans, in monkeys achromatic VEPs consist of more negative waves which distort onset-offset symmetry.

To assess stereopsis in rhesus monkeys Janssen et al. (1999) used VEPs as well. He found that VEPs to random dot stereograms recorded from monkeys could be reliably recorded and remarkably similar to those of human beings, using an identical stimulus paradigm.

A number of investigators studied and reported VEPs obtained to different levels of contrast. Parker et al. (1982) and Nakayama et al. (1982) in their studies described the change in gain of the VEP amplitudes at different levels of contrast. The Figure I.19 illustrates this finding and shows the relationship between the VEP amplitude and

contrast; the slope is steeper at high levels of contrast which results from foveal and parafoveal activity (Campbell & Maffei, 1970).

Kulikowski et al. (1978) in his studies on contrast also showed that activation of mechanisms responsible for movement or pattern detection supposed to depend on stimulus characteristics. They stated that at relatively low rates of stimulations (1-2Hz) so called "transient" VEPs could be obtained, meaning that pattern detection depends on standing contrast, whilst movement detection is a function of contrast change (Kulikowski, 1978).

Spekjreise et al. (1973) regarded the distinction between luminance and contrast processing. The scientists concluded that VEPs to contrast stimulation could not be derived from luminance responses, as they had a quality on their own.

A psychophysical and electrophysiological study of responses to chromatic and luminance contrast in glaucoma was reported in the paper of Porciatti et al. (1997). He showed that the visual dysfunction in glaucoma occurred mainly because of the damage of M – cells being not selective for the M-pathway. The main conclusion of this study was that the responses to equiluminant colour-contrast stimuli might be of diagnostic value.

Lopes de a Faria et al. (1998) in their research measured contrast sensitivity function using contrast sweep VEPs. Those scientists showed that contrast sensitivity function could have a diagnostic value when assessing visual functions, where standard visual acuity tests would not able to detect particular ocular diseases.

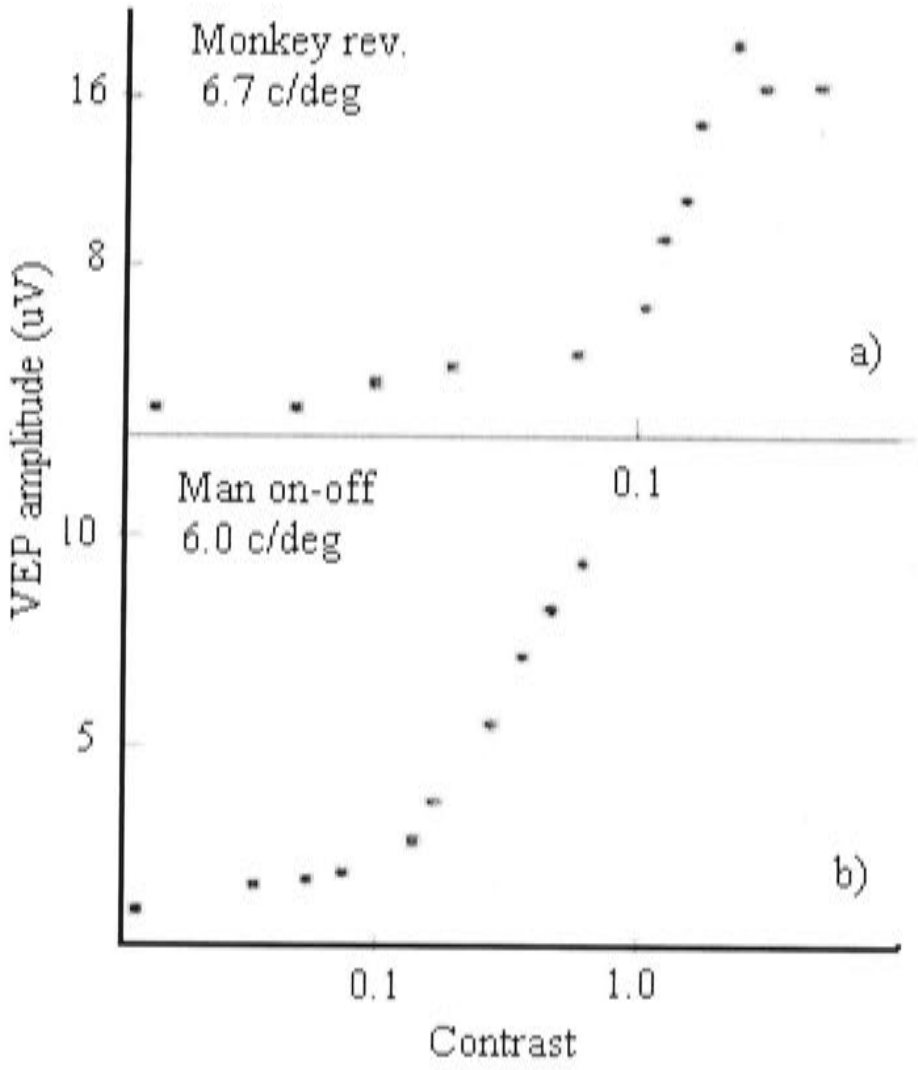

Figure I.19 a) Data replotted from Nakayama & Mackeben (1982), (b) Amplitude of N1-P1 wave of human "onset" replotted from Parker *et al.*(1982)

Bodis Wollner (1977) in his study on recovery from cerebral blindness called attention to the diagnostic value of grating pattern VEPs by describing in detail a case in which VEPs measurement established the diagnosis of an organic lesion. He showed that VEP measurements provided electrophysiological evidence of cerebral blindness and therefore could be used for the further diagnostics.

In patients with disease of the optic nerve (e.g. multiple sclerosis) the VEPs to the pattern stimuli are usually delayed (Halliday *et al.*, 1972; Asselman *et al.*, 1975; Kjaer, 1980). They could be delayed due to the other diseases as well. As described in the study of Ashworth et al. (1978), VEPs showed increased latency of the response due to astrocytoma of the corpus callosum (tumour). After recording VEPs from the patient, the scientists found no demyelination evidence, but they suggested that the tumour interfered with nerve fibre conduction, which could account for the delay in the VEPs.

Halliday et al. (1976) also studied pattern VEPs in compression of the anterior visual pathways. Pattern VEPs have been recorded in 19 patients with compression of the optic nerve, chiasm or tract, verified at operation. The study group included patients with orbital tumours, intracranial meningiomas, craniopharyngiomas and pituitary tumours. The scientist found abnormal VEPs, however, the incidence of delayed response was much lower, instead, and some absent responses were reported. Asymmetric VEPs in this study were associated with visual field defects. The similar study of Blumhardt (1977) reported on the P100, positive component of pattern VEPs and findings were similar to the ones as described above.

Oka et al. (2001) reviewed VEP studies on visual processing of figural geometry. He showed that a specific trend in VEP peak latencies could be revealed to relate figure perception with figural symmetries. Very similar work on figure salience was done by Romani et al. (1999).

Multifocal Visual Evoked Potentials (mfVEPs)

The traditional VEP has limitations when applied to visual field testing (Hood *et al.*, 2000b). With traditional VEPs responses are obtained at only few locations within a single testing sessions and those responses are mixed from unaffected and affected brain and optic nerve regions (Hood *et al.*, 2000a; Hood & Zhang, 2000; Hood *et al.*, 2000b). By using the multiple-input method or mfVEPs, it is possible to obtain local field defects in patients with ganglion cell or optic nerve damage. mfEVPs analysis refers to the simultaneous characterization of response properties for multiple visual field locations (Baseler *et al.*, 1994; Baseler & Sutter, 1995; James, 2003).

As mentioned in a review by Baseler et al. (1994), the use of large – area stimulation can result in a substantial loss of information. The precise localization of cortical sources contributing to scalp potentials requires stimuli to be small enough in order to avoid signal cancellation. Baseler et al. (1994) demonstrated that significant responses could be collected concurrently from very small stimuli at a multitude of visual field locations within recording time being reasonably short. To achieve as short as possible recording duration associated with multiple stimulus locations, the multifocal responses were obtained by means of the binary m - sequence method, described above in this thesis.

The mfVEP technique is a promising new method to identify functional deficits (Yu & Brown, 1996; Slotnick *et al.*, 1999; Hood *et al.*, 2000a; Hood & Zhang, 2000; Betsuin *et al.*, 2001; Hasegawa & Abe, 2001), but it could be limited by the large intersubject variability of the responses found in normal subjects (Klistorner *et al.*, 1998a; Graham *et al.*, 1999; Hood *et al.*, 2000b; Hood *et al.*, 2002b; Kikuchi *et al.*, 2002; Zhang *et al.*, 2002; Balachandran *et al.*, 2003; Chan *et al.*, 2003; Thienprasiddhi *et al.*, 2003). Klistorner et al. (2001) in their study reported the method of using the

underlying EEG amplitude to normalize an individual's mfVEP responses. This reduces intersubject variability by 25%. This variability is due largely to anatomical differences in the visual cortex, such as location of calcarine sulcus in relation to the placement of the external electrodes and differences in the local folding of the cortex within V1 (Baseler *et al.*, 1994; Hood & Zhang, 2000; Dougherty *et al.*, 2003; Thienprasiddhi *et al.*, 2003).

There are several ways to reduce the variability of mfVEP respones:

- Applying an interocular comparison of the monocular mfVEP responses (Graham *et al.*, 1999; Hood *et al.*, 2000b; Thienprasiddhi *et al.*, 2003), allowing the detection of early and localized damage of the ganglion cells or optic pathway.
- Choosing a stimulus check size (Balachandran *et al.*, 2003) that generates the largest amplitude and compensates for cortical scaling.
- Adding additional channels to record mfVEPs (Hood *et al.*, 2002b; James, 2003).
- Since mfVEPs can be small, distinguishing them from noise can be difficult, therefore Zhang at al. (2002) and James (2003) suggested to apply a signal -to-noise (SNR) analysis of mfVEPs, which also helps to reduce the intersubject variability by selecting responses from different electrodes.

MfVEP Stimulation

For the recording of mfVEPs, cortically scaled stimuli (Klistorner *et al.*, 1998a; Klistorner & Graham, 1999; Slotnick *et al.*, 1999; Hood *et al.*, 2000b; Klistorner & Graham, 2001; Balachandran *et al.*, 2003; James, 2003) often are used. The checkerboard can be divided into a number of stimulus regions, and each region can flash on or off, or show checks having reverse contrast. The term "cortically scaled"

(Fig. I.20) means the manner in which both checks and the regions of stimulus increase in size with increasing eccentricity (Baseler *et al.*, 1994; James, 2003) in order that each check stimulates an approximately equal area of V1. Each check stimulates an equal number of V1 areas. In the present study VEPs were recorded in response to a multifocal stimulus in which many visual stimuli were presented concurrently.

Recording and Electrode Placement

VEPs are usually recorded using gold cup electrodes providing superior conductivity, attached to the scalp with conductive paste. In some cases many electrodes are placed over the entire cranial area, but for some studies it is sufficient to use only a few electrodes and to place them on the scalp over the occipital lobe.

Several studies (Baseler *et al.*, 1994; Baseler & Sutter, 1995; Klistorner *et al.*, 1998a; Klistorner *et al.*, 1998b; Hood *et al.*, 2002b; Kikuchi *et al.*, 2002) have compared the conventional and new electrode placements. According to the international 10-20 system, the conventional monopolar electrode placement uses the Oz (active electrode) and Fz (reference electrode) positions according. This placement was recommended by the ISCEV standards (Harding *et al.*, 1995; Odom *et al.*, 2003) and it favoured responses from the lower visual field. This happens mostly due to conduction of signal and the complicated anatomy of retino-cortical projections from different parts of the visual field and extreme convolution of the cortex (Klistorner *et al.*, 1998b).

Baseler et al. (1994; 1995) showed that it was possible to improve the upper field responses by means of pseudorandom presented

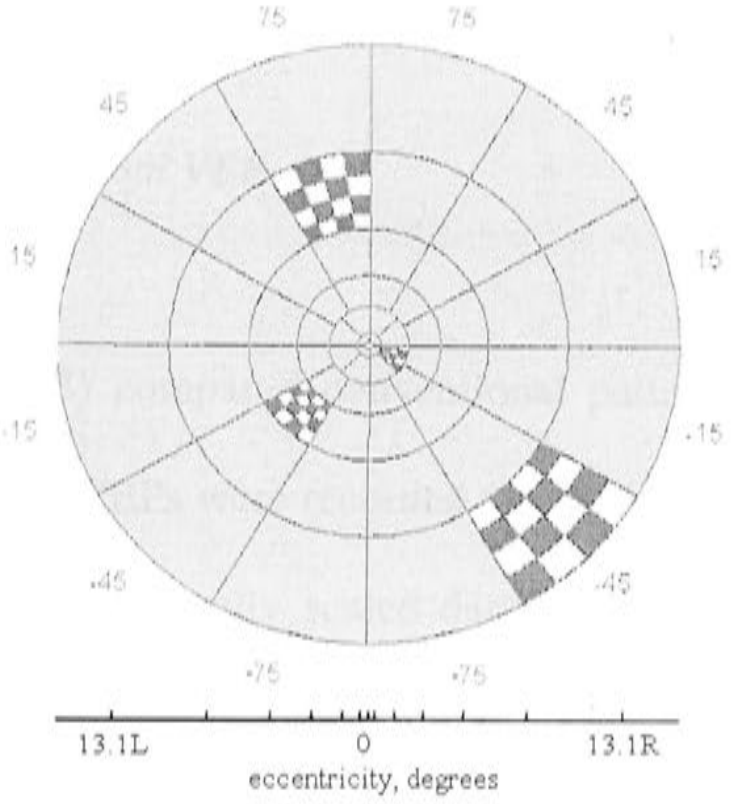

Figure I.20 A 60-region cortically scaled dartboard multimodal stimulus, with four sample regions (*checkers*), illustrating the pattern pulse stimulus (reproduced from James A, *The pattern pulse multifocal visual evoked potential*, Invest Ophthalmol Vis Sci, 44:879-890, 2003)

multifocal stimulation and cortical scaling of the size of stimulated patches up to 7 deg. eccentricity.

The study of Klistorner *et al.* (1998a; 1998b) used a bipolar occipital straddle (BOS) electrode technique with one electrode being placed above the inion, the reference electrode below it, and an earth electrode being placed on the ear or forehead. The technique (Klistorner *et al.*, 1998b) allows more equal signals to be obtained from the upper and lower visual field.

Multifocal VEPs vs. Conventional VEP

Fortune et al. (2002b; 2003) compared conventional pattern reversal VEPs (cVEPs) with mfVEPs. In this study cVEPs were recorded to a wide field chequerboard stimulus and mfVEPs to a 60 regions cortically scaled dartboard stimulus. It was shown that full-field cVEPs could not be simply related to the sum of the mfVEP responses, even when they were recorded under the similar conditions. According to Fortune et al. (2003), mfVEPs to fast m-sequence stimulation showed a strong polarity reversal between upper and lower hemifield waveforms. Other scientists have also observed this effect and assumed that it reflected the convolution of the calcarine fissure in V1, as the dipoles reverse orientation there which should result in an inverted response polarity (Slotnick *et al.*, 1999; Di Russo *et al.*, 2001; James, 2003).

The second difference was found in mfVEPs implicit times: they were faster than for cVEPs. Fortune also showed that the amplitudes of the cVEPs were much larger than for mfVEPs. According to these results it was stated that the sources of cVEPs and mfVEPs were different. Based on those results, Fortune suggested that mfVEPs were dominated by contributions from V1 whereas cVEPs were proposed to be influenced by extrastriate sources.

Diseases of Vision in Which Perimetry is Useful

Multiple Sclerosis

Overview

Multiple Sclerosis (MS) is an inflammatory disease of the Central Nervous System (CNS), affecting mainly the brain, spinal cord and optic nerve. MS is a disease of the "white matter" tissue (Waxman, 1983). The white matter consists of myelinated nerve fibres, which are responsible for transmitting communication signals both internally within the CNS and between the CNS and the sensory apparatus of the rest of the body. MS is characterized by areas of focal demyelination (plaques) disseminated throughout the neuraxis in both space and time (Chiappa, 1983; Waxman, 1983; Conlon *et al.*, 1999; Brinar, 2002).

MS has its onset in the third decade of human age, with more cases being between the age of 30 and 50 years (Waxman, 1983; Poser & Brinar, 2002a; Pugliatti *et al.*, 2002). This disease is more common in women, with a male/female ratio 1.4 and 2 (Waxman, 1983; Hawkes, 2002). According to Swank et al. (1987), before becoming disabled, MS patients are active, energetic and highly productive. They are intelligent and vital individuals, physically they are of average height and weight and usually attractive.

The MS incidence and prevalence rate increases with increasing distance from the equator (Waxman, 1983). This means that people living in higher latitudes the North or South have a greater possibility of getting MS. In Australia the highest prevalence rates are reported from originally British, Scottish and Irish communities but these do not exceed half the frequency observed in most parts of the British Isles (Pugliatti *et al.*, 2002). Van der Mei et al. (2001) examined associations of regional MS prevalence within Australia and ultraviolet radiation (UVR) levels experienced by a significant

proportion of the population in several regions. The correlation was stronger than that between URV exposure and prevalence of melanoma. A close association was found between the theoretical prevalence predicted by the UVR and the real MS prevalence by region. Van der Mei also discussed the correlation between the UVR and bright sunshine hours. According the results of this study, the light itself could be an important factor, whilst an increased amount of light would decrease melatonin production in human body and therefore decreasing of the autoimmune system would cause MS.

As reviewed by Sadovnick (2002), MS results from an interaction of genetic and environmental factors. MS also appears to be oligogenic, eg. with more than one gene involved. The human leukocyte antigen (HLA) is not "a deterministic" gene for MS (Poser & Brinar, 2002a; Sadovnick, 2002).

There are different types of MS: Relapsing/Remitting, Secondary Progressive, Progressive Relapsing, Primary Progressive (Poser & Brinar, 2002a). Other terms are often used to describe rarer forms of MS including benign MS, Malignant MS, chronic progressive MS, transitional/progressive MS, Devic's disease and Balo's concentric diseases (Swank & Dugan, 1987). The most common form is Relapsing Remitting (RRMS), which is characterised by relapses during which time new symptoms appear and/or old ones worsen. The relapses are followed by remissions, when patients fully or partially recover. Relapses can last for days or weeks, or longer with recovery very being slow but steady (Waxman, 1983; Poser, 2000; Kesselring & Klement, 2001; McDonald *et al.*, 2001; Poser & Brinar, 2002a, b).

Symptoms

Early symptoms of MS include numbness and/or paresthesia, mono- or paraparesis, double vision, optic neuritis, ataxia, and bladder control problems (Waxman, 1983; Kurtzke, 1985; Swank & Dugan, 1987; Prineas *et al.*, 1993; Hawkes, 2002). Symptoms also include upper motor neuron signs, i.e., increased spasticity, increasing para- or quardriparesis. Vertigo, incoordination and other cerebellar problems, depression, emotional lability, abnormalities in gait, dysarthria, fatigue and pain are also commonly seen in most MS patients (Waxman, 1983; Foong *et al.*, 2000; Kesselring & Klement, 2001). Some patients have facial palsy (Fukazawa *et al.*, 1997), or such unusual complaints as upside-down vision (Dogulu & Kansu, 1997).

Diagnosis

There is no single test for MS and it is not even certain that it is only one disease (Waxman, 1983; Swank & Dugan, 1987; Brinar, 2002). People who have finally been diagnosed with definite MS will have been through several diagnostic stages, often requiring months or years for a final decision (Jongen *et al.*, 1997; Leocani *et al.*, 2000; Poser, 2000; Brinar, 2002). The Schumacher criteria are a set of diagnostic criteria that were developed in 1965 and are still commonly used by neurologists to make a clinical diagnosis of multiple sclerosis. These criteria are still commonly used by neurologists to make a clinical diagnosis of MS. The Schumacher criteria were updated in 1983 by the Poser Criteria and these are:

- Clinically definite MS: 2 attacks and clinical evidence of 2 separate lesions; 2 attacks, clinical evidence of one and paraclinical evidence of another separate lesion.

- Laboratory supported Definite MS: 2 attacks, either clinical or paraclinical evidence of 1 lesion, and cerebrospinal fluid (CSF) immunologic abnormalities (eg.;1 attack, clinical evidence of 2 separate lesions & CSF abnormalities; 1 attack, clinical evidence of 1 and paraclinical evidence of another separate lesion, and CSF abnormalities (McMillan *et al.*, 2000). CSF is a fluid that circulates in the space within the spinal cord and brain. It protects the brain and spinal cord from injury by acting like a liquid cushion (Sand & Sulg, 1990; Jongen *et al.*, 1997).

- Clinically probable MS: 2 attacks and clinical evidence of 1 lesion; 1 attack and clinical evidence of 2 separate lesions; 1 attack, clinical evidence of 1 lesion, and paraclinical evidence of another separate lesion.

- Laboratory supported probable MS: 2 attacks and CSF abnormalities.

According to a more recent set of criteria (McDonald *et al.*, 2001), the focus remains on the objective demonstration of dissemination of lesions in both time and space. There are additional requirements in making the diagnosis:

  - Positive MRI scans, showing dissemination in time or space (Frederiksen *et al.*, 1991a; McDonald *et al.*, 2001; Sastre-Garriga *et al.*, 2003; Sicotte *et al.*, 2003).
  - Positive VEPs, which show the delayed but well preserved, wave forms (Matthews & Small, 1983; Frederiksen *et al.*, 1991b; Roder, 1991; Towle *et al.*, 1991; McDonald *et al.*, 2001).

Treatment of MS

While there is no curative treatment available for MS, a number of medications can be used to treat the disease symptomatically (Swank & Dugan, 1987; Poser & Brinar, 2002b). Corticosteroids are the medications of choice for treating the exacerbations of MS symptoms. Interferonß-1B (*Betaseron*) as well as Interferonß-1a (*Avonex*) are used to reduce the frequency and severity of relapses (Miller, 1997; Conlon *et al.*, 1999; Narayanan *et al.*, 2001; Sena *et al.*, 2003). Specific medications are also available to treat fatigue, pain, spasticity, bladder control problems, etc. (Poser & Brinar, 2002b). In the future, medications aimed at reducing specific autoimmune responses, and medications designed to assist in remyelination will help improve the quality of life of MS patients (Kappos, 1988; Weinshenker *et al.*, 1996).

Optic Neuritis

Optic Neuritis (ON), inflammation of the optic nerve (Kurtzke, 1985; Celesia *et al.*, 1990; Frederiksen *et al.*, 1991c), is a condition typically involving the young adult population. The initial attack is unilateral in 70% of adult patients and bilateral in 30%. The mean age of onset of ON is in the third decade of life (Frederiksen *et al.*, 1991c), but can occur from the first to the seventh decades. The annual incidence of ON ranges from 1.4 to 6.4 new cases per 100,000 populations (Frederiksen *et al.*, 1991c). It is reported that one third of ON patients will go on to have MS (Frederiksen *et al.*, 1991c).

ON typically presents with a triad of symptoms: loss of vision, dyschromatopsia and eye pain (Waxman, 1983; Wang *et al.*, 2001). The usual sign of ON is a loss of vision that usually is rapid in onset, occurring over a few hours or days (Waxman, 1983; Ebers, 1985; Kurtzke, 1985). The classic description of ON is: "the patient sees nothing and the doctor sees nothing" (Fig.I.21).

Figure I. 20 The left eye, affected by optic neuritis (reproduced from http://www.mult-sclerosis.org/opticneuritis.html).

The patient says complains of a decrease in vision, but the doctor can not find any signs on ophthalmoscopy. This happens because of the location of the ON, predicting the type of field defect that is produced (Walsh, 1990b). The defect usually shows as a central scotoma and affects the axial portion of the nerve (Fig.I.22).

The visual loss may be subtle or profound, with even a single plaque causing complete loss of vision in one eye. The vision can be 6/6 with the only symptoms being blurred vision on exertion or other isolated symptoms. Visual loss may occur over hours to days. The most popular ON detection test is the perimeter (Walsh, 1990b). It helps to define the site of pathology along the visual pathways. Sometimes patients are unaware of peripheral vision loss, especially when it occurs in one eye; therefore the perimeter is a useful instrument with which to assess the pattern of visual field loss not only in the central regions, but as well as in the periphery. mfVEPs are also employed in the detection and tracking ON (Halliday *et al.*, 1972; Frederiksen *et al.*, 1991b; Frederiksen & Petrera, 1999; Hood *et al.*, 2000a; Hood *et al.*, 2000b).

The prognosis for functional visual recovery from ON is usually good. The majority of patients recover visual acuity of 6/9 or better. Most cases will recover visual acuity in a few months, although the patients will often report some residual visual defect. Overall, in a patient with ON, the vision may improve, but the risk for development of MS is high.

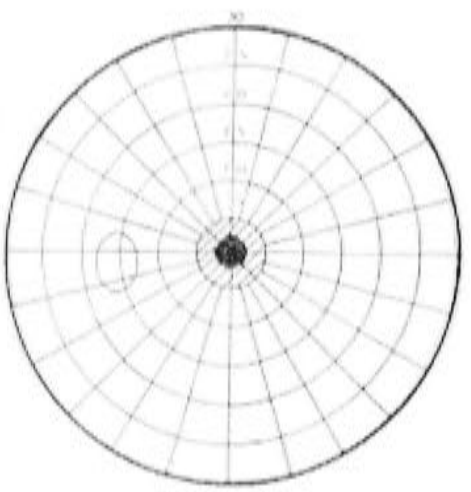

Figure I.22 A field defect with a central scotoma, but with a full peripheral field (reproduced from Walsh TJ, *Visual fields. Examination and interpretation,* 1990, American Academy of Ophthalmology)

Glaucoma

Overview

The other example of conditions that affect vision and can be detected my perimeters and mfVEPs is glaucoma. Glaucoma is a disease characterized by the death of retinal ganglion cells and intraocular pressure (IOP) that is greater than the tolerance of the affected eyeball (Duke-Elder & Jay, 1969; Leske, 1983; Crawford *et al.*, 2000). Glaucoma is the second leading cause of blindness in the developed world, and it is estimated that 6.7 million of the 66.8 million people affected globally are bilaterally blind as a result (Duke-Elder & Jay, 1969).

Glaucoma can be caused by genetic and developmental anomalies, and can take various forms: Open-angle, Acute angle-closure, chronic angle-closure, "Normal (or low) tension", Childhood and Congenital. In adults, the most common form is the primary open-angle glaucoma (POAG) (Duke-Elder & Jay, 1969). It is characterized by optic disc abnormalities and visual field defects (Atkin *et al.*, 1980; Leske, 1983; Landers *et al.*, 2002).

Symptoms

While in its early stages glaucoma is symptomless, its symptoms can differ depending on the type. As the disease progresses, however, vision begins to deteriorate. Symptoms include loss of peripheral vision, increased IOP (Fraser *et al.*, 1999; Gillies *et al.*, 2000; Landers *et al.*, 2002), difficulty focusing on close objects, seeing colored rings or halos around lights, headaches along with eye pain for acute forms of glaucoma, difficulty-adjusting eyes to the dark. In some cases blurred vision, nausea and vomiting can appear (Leske, 1983).

Diagnosis

There is no standard for diagnosis of glaucoma, but detection is usually based on three different clinical tests: tonometry, fundoscopy and perimetry (Maddess, 1989; Caprioli, 1991; Johnson *et al.*, 1999; Maddess & Severt, 1999; Goldbaum *et al.*, 2002; Gillespie *et al.*, 2003). Tonometry is used to determine the IOP, fundoscopy is a visual examination of the optic disk, and perimetry looks for localised flaws or abnormalities of perception in the visual field. Abnormalities of the visual field in glaucoma patients often occur in patterns that correspond to the anatomy of the nerve fiver layer of the retina and its projection to the optic nerve (Walsh, 1990a) (Fig.I.23). The typical nerve fiber bundle defects are the arcuate scotoma, nasal step and temporal-sector defects.

Treatment

Treatment of glaucoma is mainly based on controlling and reducing the IOP. Generally the first stage of glaucoma treatment is beta-blocker eye drops (Mietz *et al.*, 2001). Most cases of glaucoma can be controlled with a single drug or drug combinations, but some patients may require or select surgery (Oostenbrink *et al.*, 2000; Demir *et al.*, 2003).

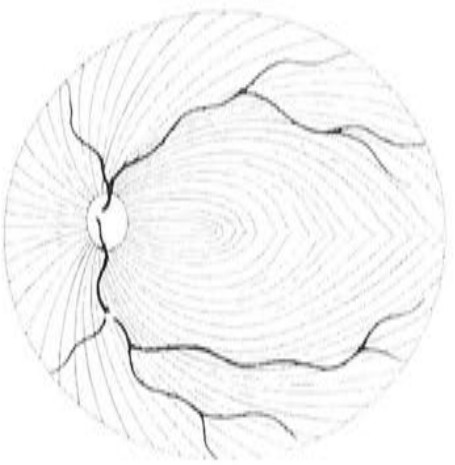

Figure I.23 Damage to discrete bundles of the nerve fibers usually happening at the superior and inferior poles of the disc, rises the visual field loss typical in glaucoma (reproduced from Walsh TJ, *Visual fields. Examination and interpretation,* 1990, American Academy of Ophthalmology)

Retinitis Pigmentosa

Overview

Retinitis Pigmentosa (RP) does not have clearly identifiable symptoms. For some people, the loss of sight is slow and there may be only a small loss (Berson & Howard, 1971). Others have periods of rapid loss, often with years in between with no apparent decline. The symptoms of disorder usually become apparent between the ages of 10 and 30 years. In the more common types of RP, a person will have a history of visual problems at dusk or in poor light, so-called night blindness, and a gradual reduction in the field of vision, loss of the outer edges, resulting in a tendency to trip over things (Hood & Birch, 1996; Robson *et al.*, 2003).

Diagnosis and Treatment

The main RP features visible on the fundus are the retinal blood vessels, which spread out from a pale, whitish disc (Robson *et al.*, 2003), the head of the optic nerve and in the centre a somewhat denser area called the macular (Hood *et al.*, 1999). Central vision could be involved and might deteriorate at a lower rate than in the periphery. Assessing central cone function might be of value in predicting retention of central loss.

The study of Iarossi *et al.* (2003) suggests the potential clinical use of the present mfERG method to characterize local cone system dysfunctions in RP. Paranhos et al. (1999) suggest using pattern reversal VEPs to evaluate visual function of the RP patients as well. Patients suffering from RP need to wear glasses.

Diabetic Retinopathy

Overview

Diabetic retinopathy (DR), is a complication of diabetes and a leading cause of blindness (Bek & Helgesen, 2001). It occurs when diabetes damages the tiny blood vessels inside the retina, the light-sensitive tissue at the back of the eye (Verma *et al.*, 2003).

Diagnosis and Treatment

DR is detected during a comprehensive eye exam including visual acuity test, dilated eye exam (eg. drops are placed in eyes to dilate the pupils) or tonometry. To identify local retinal abnormalities in diabetic patients with retinopathy Fortune et al.(1999b) employed mfERGs. The results of Fortune at al. (1999b) and Onozu et al. (2003) showed smaller mfERG amplitudes and delayed implicit times in DR patients, and also demonstrated that this sort of analysis could be a highly sensitive method of assessment of local retinal function in diabetes.

To prevent progression of diabetic retinopathy, people with diabetes should control their levels of blood sugar, blood pressure, and blood cholesterol. Sometimes DR is treated with laser surgery as well.

Summary

Vision is a very complex process, consisting of retinal, thalamic, and cortical processing stages. Pathology can occur at any of these stages, and at any time. Two common pathologies of vision are glaucoma and ON, caused by MS. Perimetry is commonly used to detect glaucoma, and it has proven to have the best sensitivity and specificity (Johnson *et al.*, 1999; Maddess *et al.*, 1999; Maddess & Severt, 1999). MfVEP is one of the possible ON and MS detection techniques, showing delayed response waveforms (Hood *et al.*, 2000b).

Multifocal VEPs and Clinical Application

The mfVEPs have become more reproducible (Graham *et al.*, 1999) and resulted as useful tool to quantify visual field defects. In the recent studies of Betsuin at al. (2001) mfVEPs were used to detect the visual field defects such as bitemporal hemianopia due to a pituitary adenoma, retrobulbar optic neuritis, homonymous hemianopia due to a subcortical haemorrhage, homonymous quadrantanopia due to multiple sclerosis and homonymous quadrantanopia due to multiple brain infarction. In all cases good correspondence was found between the perimetrically determined visual field defects and the mfVEPs, which were significantly small in the particular visual field locations.

A large number of mfVEPs studies (Graham *et al.*, 1999; Hood & Zhang, 2000; Klistorner *et al.*, 2000; Hasegawa & Abe, 2001; Parisi *et al.*, 2001; Bengtsson, 2002; Goldberg *et al.*, 2002; Chan *et al.*, 2003; Thienprasiddhi *et al.*, 2003) have been performed in research on glaucoma. According to those studies, mfVEPs appear to be a useful tool to assess visual field damages to the above-mentioned disease. Graham et al.(1999) in his study showed that mfVEP amplitudes correlated well with visual field

defects seen in glaucoma patients. Here the amplitudes were compared with the corresponding perimetric thresholds. Multifocal objective perimetry was also explored and compared to mfVEPS in Goldberg et al. (Goldberg *et al.*, 2002) study. The above-mentioned studies showed that the mfVEPs could provide a breakthrough in assessing glaucoma, but some problems, such as variability of the signal with different electrode placements, effects of visual acuity, age and other factors should be considered.

VEPs and mfVEPs can be also used to identify changes of the visual field caused by ON and MS. Multiple studies (Dawson *et al.*, 1982; Andersson *et al.*, 1991; Frederiksen *et al.*, 1991a; Frederiksen *et al.*, 1991c; Roder, 1991; Jones, 1993; Andersson & Siden, 1995; Frederiksen & Petrera, 1999; Hood *et al.*, 2000a; Hood *et al.*, 2000b; Betsuin *et al.*, 2001; Ikejiri *et al.*, 2002; Hidajat & Goode, 2003) showed that ON patients tend to have smaller signals and prolonged or strange looking waveforms. Hood et al. (2000a) in his study reported that mfVEPs would be more useful than conventional VEPs in assessing visual field defects caused by ON because of the ability to obtain recordings from multiple regions of the visual field. In study of three ON patients they found that not all regions were equally affected. These results clearly show the mfVEPs ability to spot the damaged optic nerve locations. For disorders such as MS or ON, deficits that are localized within the optic nerve may be masked by undamaged fibers when a conventional wide-field stimulus is used; therefore conventional stimulus is not able to detect those lesions along the optic nerve (Maddess & James, 1998; James, 2003).

Current MS Diagnostic Techniques

As it is not easy to detect pathology, diagnostic techniques need to be very reliable. According to the new MS diagnostic criteria (McDonald *et al.*, 2001), the disease could be detected by means of CSF, MRI or VEPs. Diagnostic sensitivity of 75% and specificity of 92% of CSF in MS was reported by (McMillan *et al.*, 2000; Sastre-Garriga *et al.*, 2003). A negative result of CSF does not rule out MS, also it has relatively poor sensitivity (Kempster *et al.*, 1987; McMillan *et al.*, 2000).

As reviewed by Dalton *et al.* (2002) the development of MS using the new MRI criteria offered a high sensitivity of 83%, specificity of 83%, positive predictive value of 75%, negative predictive value of 89% and accuracy of 83% after a year for clinically definite MS. Previous studies (Mushlin *et al.*, 1993 ; Brex *et al.*, 2001; Jin *et al.*, 2003; Rovaris *et al.*, 2003; Sastre-Garriga *et al.*, 2003; Sicotte *et al.*, 2003) reported high MRI sensitivity in diagnosing MS, and when lesions are detected on MRI, the MS is the likely diagnosis versus conversion disorder. If lesions are not detected, the diagnosis can be ruled out.

VEPs are recommended and useful to identify patients at risk for developing clinically definite MS. Previous studies (Burki, 1981; Neima & Regan, 1984; Colon, 1987; Martinelli *et al.*, 1987; Novak *et al.*, 1988; Sand *et al.*, 1990; Frederiksen *et al.*, 1991b; Scaioli *et al.*, 1991; Van Diemen *et al.*, 1992; Iriarte *et al.*, 1993; Porciatti & Sartucci, 1996; Duska & Denislic, 2000; Sartucci *et al.*, 2001) showed VEPs' abnormalities in 82% of MS patients. According to the above quoted scientific studies, the sensitivity of conventional VEPs range is between 25% and 83%, when the specificity varies between 63% and 88%.

The above mentioned MS and ON diagnostic sensitivities are not high enough and, therefore it is necessary to look for and investigate new more reliable diagnostic tools, able to detect the disease at higher sensitivities.

In this thesis I will discuss non-linear system identification methods applied to the early detection of MS and ON. The sensitivity of these methods and tools is about 98 %, which is much higher than the traditional MS and ON diagnostic tools. My research described in this thesis is based on the responses recorded from Normal, MS and ON subjects to sparse pattern reversal mfVEP, FD mfVEP and FDT stimuli.

Bibliography

ANDERSSON, T. & SIDEN, A. (1995). An analysis of VEP components in optic neuritis. *Electromyogr Clin Neurophysiol* **35,** 77-85.

ANDERSSON, T., SIDEN, A. & PERSSON, A. (1991). A comparison of clinical and evoked potential (VEP and median nerve SEP) evolution in patients with MS and potentially related conditions. *Acta Neurol Scand* **84,** 139-145.

APKARIAN, P., NAKAYAMA, K. & TYLER, C. (1981). Binocularity in the human evoked otential: facilitation, summation, and suppression. *Elektroencephalogr Clin Neurophysiol* **51,** 32-48.

ASI, H. & PERLMAN, I. (1992). Relationships between the electroretinogram a-wave, b-wave and oscillatory potentials and their application to clinical diagnosis. *Doc Ophthalmol* **79,** 125-139.

ASHWORTH, B., MALONEY, A. & TOWNSEND, H. (1978). Delayed visual evoked potentials a with bilateral disease of the posterior visual pathway. *J Neuro Neurosurg Psych* **41,** 449-451.

ASSELMAN, P., CHADWICK, D. & MARSDEN, C. (1975). Visual evoked responses in the diagnosis and management of patients suspected of multiple sclerosis. *Brain* **98,** 261-282.

ATKIN, A., WOLKSTEIN, M., BODIS WOLLNER, I., ANDERS, M., KELS, B. & PODOS, S. (1980). Interocular comparison of contrast sensitivities in glaucoma patients and suspects. *British J Ophthalmol* **64,** 858-862.

AZZOPARDI, P., KING, S. & COWEY, A. (1998). Pattern electroretinograms after cerebral hemispherectomy. *Brain* **124,** 1228-1240.

BACH, M., HAWLINA, M., HOLDER, G., MARMOR, M., MEIGEN, T., VAEGAN & MIYAKE, Y. (2000). Standard for pattern electroretinography. *Doc Ophthalmol* **101,** 11-18.

BACH, M. & ULLRICH, D. (1997). Contrast dependency of motion-onset and pattern-reversal VEPs: interaction of stimulus type, recording site and response component. *Vision Res* **37,** 1845-1849.

BAKER, C., HESS, R., OLSEN, B. & ZRENNER, E. (1988). Current source density analysis of linear and nonlinear components of the primate electroretinogram. *J Physiol* **407,** 155-176.

BALACHANDRAN, C., KLISTORNER, A. & GRAHAM, S. (2003). Effect of stimulus check size on multifocal visual evoked potentials. *Doc Ophthalmol* **106,** 183-188.

BASELER, H. & SUTTER, E. (1995). M and P components of the VEP and their visual field distribution. *Vision Res* **37,** 675-690.

BASELER, H., SUTTER, E., KLEIN, S. & CARNEY, T. (1994). The topography of visual evoked response properties across the visual field. *Electroencephalogr Clin Neurophysiol* **90,** 65-81.

BEK, T. & HELGESEN, A. (2001). The regional distribution of diabetic retinopathy lesions may reflect risk factors for progression of the disease. *Acta Ophtalmol Scand* **79,** 501-505.

BENARDETE, E. & KAPLAN, E. (1999). The dynamics of primate M retinal ganglion cells. *Visual Neurosci* **16,** 355-368.

BENARDETE, E., KAPLAN, E. & KNIGHT, B. (1992). Contrast gain control in the primate retina: P cells are not X-like, some M cells are. *Visual Neurosci* **8,** 483-486.

BENGTSSON, B. (2002). Evaluation of VEP perimetry in normal subjects and glaucoma patients. *Acta Ophthalmol Scand* **80,** 620-626.

BERSON, E. & HOWARD, J. (1971). Temporal aspects of the electroretinogram in sector retinitis pigmentosa. *Arch Ophthalmol* **86,** 653-665.

BETSUIN, Y., MASHIMA, Y., OHDE, H., INOUE, R. & OGUCHI, Y. (2001). Clinical application of the multifocal VEPs. *Cur Eye Res* **22,** 54-63.

BLAKEMORE, C. & VITAL-DURAND, F. (1986). Organization and post-natal development of the monkey's lateral geniculate nucleus. *J Physiol* **380,** 453-491.

BLUMENTHAL, E., SAMPLE, P., ZANGWILL, L., AC, L., KONO, Y. & WEINREB, R. (2000). Comparison of long-term variability for standard and short-wavelength automated perimetry in stable glaucoma patients. *Am J Ophthalmol* **129,** 309-313.

BLUMHARDT, L., BARRETT, G. & HALLIDAY, A. (1977). The asymmetrical visual evoked potential to pattern reversal in one half field and its significance for the analysis of visual defects. *Br J Ophthalmol* **61,** 454-421.

BODIS WOLLNER, I. (1977). Recovery from cerebral blindness: evoked potential and psychophysical measurements. *Electroencephalogr Clin Neurophysiol* **42,** 178-184.

BODIS WOLLNER, I. (1992). Sensory evoked potentials: PERG, VEP, and SEP. *Cur Opin Neurol Neurosurg* **5,** 716-726.

BODIS WOLLNER, I., BRANNAN, J., NICOLL, J., FRKOVIC, S. & MYLIN, L. (1992). A short latency cortical component of the foveal VEP is revealed by hemifield stimulation. *Elektroencephalogr Clin Neurophysiol* **84,** 201-208.

BREX, P., MISZKIEL, K., O'RIORDAN, J., PLANT, G., MOSELEY, I. & THOMPSON, A. (2001). Assessing the risk of early multiple sclerosis in patients with clinically isolated syndromes: the role of follow up MRI. *J Neurol Neurosurg Psychiatry* **70,** 390-393.

BRINAR, V. (2002). The differential diagnosis of multiple sclerosis. *Clin Neurol Neurosurg* **104,** 211-220.

BUDENZ, D., RHEE, P., FEUER, W., MCSOLEY, J., JOHNSON, C. & ANDERSSON, D. (2002). Sensitivity and specificity of the Swedish interactive threshold algorithm for glaucomatous visual field defects. *Ophthalmol* **109,** 1052-1058.

BULLIER, J. (2001). Review. Integrated model of visual processing. *Bain Research Reviews* **36,** 96-107.

BURKI, E. (1981). [Visual evoked potentials, contrast sensitivity and color perception in patients with optic neuritis and multiple sclerosis] (abstract). *Klin Monastbl Augenheilkd* **179,** 161-168.

BURNSTEIN, Y., ELLISH, N., MAGBALON, M. & HIGGINBOTHAM, E. (2000). Comparison of frequency doubling perimetry with Humphrey visual field analysis in a glaucoma practise. *Am J Ophthalmol* **129,** 328-333.

CAMPBELL, F. & MAFFEI, L. (1970). Electrophysiological evidence for the existence of orientation and size detectors in the human visual system. *J Physiol* **207,** 635-652.

CAPRIOLI, J. (1991). Automated perimetry in glaucoma. *Am J Ophthalmol* **111,** 235-239.

CAPRIOLI, J. & ZULAUF, M. (1991). *Automated perimetry for advanced users.* Yale Eye Center, Yale.

CASAGRANDE, V. (1994). A third parallel visual pathway to primate area V1. *Trends Neurosci* **17,** 305-310.

CELESIA, G., KAUFMAN, D., BRIGELL, M., TOLEIKIS, S., KOKINAKIS, D., LORANCE, R. & LIZANO, B. (1990). Optic neuritis: a prospective study. *Neurology* **40,** 919-923.

CHAN, H., TAM, W., CHEN, C. & NG, N. (2003). The detection of small stimulated field defects using multifocal VEPs. *Ophthalmol Physiol Opt* **23,** 205-212.

CHIAPPA, K. (1983). *Evoked potentials in clinical medicine.* Raven Press, New York.

CHICHILNISKY, E. (2001). A simple white noise analysis of neuronal light responses. *Network: Comput Neural Syst* **12,** 1-15.

CLARK, V. & HILLYARD, S. (1996). Spatial selective attention affects early extrastriate but not striate components of the visual evoked potential. *J Cogn Neurosci* **8,** 387-402.

CLELAND, B. & LEVICK, W. (1974). Brisk and sluggish concentrically organized ganglion cells in the cat's retina. *J Physiol* **240,** 421-456.

COLON, E. (1987). The contribution of evoked potentials to the diagnosis of demyelinating diseases (abstract). *Ital J Neurol Sci* **Suppl,** 97-102.

CONLON, P., OKSENBERG, J., ZHANG, J. & STEINMAN, L. (1999). The immunobiology of multiple sclerosis: an autoimmune disease of the central nervous system. *Neurobiol Disease* **6,** 149-166.

CONOLY, M. & VAN ESSEN, D. (1984). The representation of the visual fields in parvicellular and magnocellular layers of the lateral geniculate nucleus in the macaque monkey. *J Comp Neurol* **226,** 544-564.

CRAWFORD, M., HARWERTH, R., SMITH III, E., SHEN, F. & CARTER-DAWSON, L. (2000). Glaucoma in primates: cytochrome oxidase reactivity in parvo-magnocellular pathways. *Invest Ophthalmol Vis Sci* **2000,** 1791-1802.

CURCIO, C. & ALLEN, K. (1990). Topography of ganglion cells in human retina. *J Comp Neurol* **300,** 5-25.

DACEY, D. (1993). Morphology of a small-field bistratified ganglion cell type in the macaque and human retina. *Visual Neurosci* **10,** 1084-1098.

DACEY, D. & LEE, B. (1994). The "blue-on" opponent pathway in primate retina originates from a distinct bistratified ganglion cell type. *Nature* **367,** 731-735.

DACEY, D., PETERSON, B., ROBINSON, F. & GAMLIN, P. (2003). Fireworks in the primate retina: in vitro photodynamics reveals diverse LGN-projecting ganglion cell type. *Neuron* **37,** 15-27.

DALTON, C., BREX, P., MISZKIEL, K., HICKMAN, S., MACMANUS, D., PLANT, G., THOMPSON, A. & MILLER, D. (2002). Application of the new McDonald criteria to patients with clinically isolated syndromes suggestive of multiple sclerosis. *Ann Neurol* **52,** 47-53.

DAWSON, W., MAIDA, T. & RUBIN, M. (1982). Human pattern-evoked retinal responses are altered by optic atrophy. *Invest Ophthalmol Vis Sci* **22,** 796-803.

DE MONASTERIO, F. (1978). Properties of concentrically organized X and Y ganglion cells of macaque retina. *J Neurophysiol* **41,** 1394-1417.

DE MONASTERIO, F. & GOURAS, P. (1975). Functional properties of ganglion cells of the Rhesus monkey retina. *J Physiol* **251,** 167-195.

DEMIR, T., TURGUT, B., CELIKER, U., OZERCAN, I., ULAS, F. & AKYOL, N. (2003). Effects of octrotide acetate and amniotic membrane on wound healing in experimental glaucoma surgery. *Doc Ophthalmol* **107,** 87-92.

DERRINGTON, A. & LENNIE, P. (1984). Spatial and temporal contrast sensitivities of neurones in lateral geniculate nucleus of macaque. *J Physiol* **357,** 219-240.

DI RUSSO, F., MARTINEZ, A., SERENO, M., PITZALIS, S. & HILLYARD, S. (2001). Cortical sources of the early components of the visual evoked potential. *Hum Brain Mapping* **15,** 95-111.

DODT, E. (1987). The electrical response of the human eye to patterned stimuli: clinical observations. *Doc Ophthalmol* **65,** 271-286.

DOGULU, C. & KANSU, T. (1997). Upside down reversal of vision in multiple sclerosis. *J Neurol* **244,** 461-472.

DOUGHERTY, R., KOCH, V., BREWER, A., FISCHER, B., MODERSITZKI, J. & WANDELL, B. (2003). Visual field representations and locations of visual areas V1/2/3 in human visual cortex. *J Vis* **3,** 586-598.

DUKE-ELDER, S. & JAY, B. (1969). Glaucoma hypotony. In *Diseases of the lens*, pp. 379-391. Henry Kimpton, London.

DUSKA, M. & DENISLIC, M. (2000). Diagnostic sensitivity of neurophysiological tests in multiple sclerosis. In *6th Internet World Congress for Biomedical Sciences*.

EBERS, G. (1985). Optic neuritis and multiple sclerosis. *Arch Neurol* **42,** 702-704.

ENROTH-CUGELL, C. & ROBSON, J. (1966). The contrast sensitivity of retinal ganglion cell of the cat. *J Physiol* **187,** 517-552.

ERWIN, E., BAKER, F., BUSEN, W. & MALPELI, J. (1999). Relationship between laminar topology and retinotopy in the Rhesus lateral geniculate nucleus: results from a functional atlas. *J Comp Neurol* **407,** 92-102.

FELLEMAN, D. & VAN ESSEN, D. (1991). Distributed hierarchical processing in the primate cerebral cortex. *Cereb Cortex* **1,** 1-47.

FITZPATRICK, D., LUND, J., SCHMECHEL, D. & TOWLES, A. (1987). Distribution of GABAergic neurons and axon terminals in the macaque striate cortex. *J Comp Neurol* **264,** 73-91.

FOONG, J., ROZEWICZ, L., THOMPSON, A., MILLER, D. & RON, M. (2000). A comparison of neuropsychological deficits in primary and secondary progressive multiple sclerosis. *J Neurol* **247,** 97-101.

FORTUNE, B., BEARSE, M., CIOFFI, G. & JOHNSON, C. (2002a). Selective loss of an oscillatory component from temporal retinal multifocal ERG responses in glaucoma. *Invest Ophthalmol Vis Sci* **43,** 2638-2647.

FORTUNE, B. & HOOD, D. (2003). Conventional pattern-reversal VEPs are not equivalent to summed multifocal VEPs. *Invest Ophthalmol Vis Sci* **44,** 1364-1375.

FORTUNE, B., HOOD, D. & JOHNSON, C. (2002b). Comparison of conventional and multifocal VEPs. In *ARVO*, pp. 2126, Ft. Lauderdale.

FORTUNE, B., SCHNECK, M. & ADAMS, A. (1999a). Multifocal electroretinogram delays reveal local retinal dysfunction in early diabetic retinopathy. *Invest Ophthalmol Vis Sci* **40,** 2638-2651.

FRASER, S., BUNCE, C. & WORMALD, R. (1999). Risk factors for late presentation in chronic glaucoma. *Invest Ophthalmol Vis Sci* **40,** 2251-2257.

FREDERIKSEN, J., LARSSON, H., NORDENBO, A. & SEEDORFF, H. (1991a). Plaques causing hemianopsia or quadrantanopsia in multiple sclerosis identified by MRI and VEP. *Acta Ophthalmol Copenh* **69,** 169-177.

FREDERIKSEN, J., LARSSON, H., OLESEN, J. & STIGSBY, B. (1991b). MRI, VEP, SEP and biothesiometry suggest monosymptomatic acute optic neuritis to be a first manifestation of multiple sclerosis. *Acta Neurol Scand* **83,** 343-350.

FREDERIKSEN, J., LARSSON, H., OTTOVAY, E., STIGSBY, B. & OLESEN, J. (1991c). Acute optic neuritis with normal visual acuity. Comparison of symptoms and signs with psychophysiological, electrophysiological and magnetic resonance imaging data. *Acta Ophthalmol Copenh* **69,** 357-366.

FREDERIKSEN, J. & PETRERA, J. (1999). Serial visual evoked potentials in 90 untreated patients with acute optic neuritis. *Survey Ophthalmol* **44,** 54-62.

FRIEDBURG, C., THOMAS, M. & LAMB, T. (2001). Time course of the flash response of dark- and light- adapted human rod photoreceptors derived from the electroretinogram. *J Physiol* **534,** 217-242.

FRISEN, L. (1973). A versatile color confrontation test for the central visual field: a comparison with quantitative perimetry. *Arch Ophthalmol* **89,** 3-9.

FUKAZAWA, T., MORIWAKA, F., HAMADA, K., HAMADA, T. & TASHIRO, K. (1997). Facial palsy in multiple sclerosis. *J Neurol* **244,** 631-633.

GILLESPIE, B., MUSCH, D., GUIRE, K., MILLS, R., LICHTER, P., JANZ, N., WREN, P. & GROUP, C. S. (2003). The collaborative initial glaucoma treatment study: baseline visual field and test-retest variability. *Invest Ophthalmol Vis Sci* **44,** 2616-2620.

GILLIES, W., BROOKS, A. & STRANG, N. (2000). Management and prognosis of end-stage glaucoma. *Clin Exper Ophthalmol* **28,** 405-408.

GOLDBAUM, M., SAMPLE, P., CHAN, K., WILLIAMS, J., LEE, T., BLUMENTHAL, E., GIRKIN, C., ZANGWILL, L., BOWD, C., SENJOWSKI, T. & WEINREB, R. (2002). Comparing machine learning classifiers for diagnosing glaucoma from standard automated perimetry. *Invest Ophthalmol Vis Sci* **43,** 162-169.

GOLDBERG, I., GRAHAM, S. & KLISTORNER, A. (2002). Multifocal objective perimetry in the detection of glaucomatous field loss. *Am J Ophthalmol* **133,** 29-39.

GOPFERT, E., MULLER, R., BREUER, D. & GREENLEE, M. (1999). Similarities and dissimilarities between pattern VEPs and motion VEPs. *Doc Ophthalmol* **97,** 67-79.

GOURAS, P. (1968). Identification of cone mechanisms in monkey ganglion cells. *J Physiol* **199,** 533-547.

GOURAS, P. (1970). Electroretinography: some basic principles. *Invest Ophthalmol* **9,** 557-569.

GRAHAM, S., FRACS, F., KLISTORNER, A., GRIGG, J. & BILLSON, F. (1999). Objective perimetry in glaucoma: recent advances with multifocal stimuli. *Survey Ophthalmol* **43,** 199-209.

GRANIT, R. (1933). The components of the retinal action potential in mammals and their relation to the discharge in their optic nerve. *J Physiol* **77,** 207-239.

HALLIDAY, A., MCDONALD, W. & MUSHIN, J. (1972). Delayed visual evoked response in optical neuritis. *Lancet* **1,** 982-985.

HALLIDAY, A., HALLIDAY, E., KRISS, A., MCDONALD, W. & MUSHIN, J. (1976). The pattern-evoked potential in compression of the anterior visual pathways. *Brain* **99,** 357-374.

HARDING, F., ODOM, J., SPILLEERS, W. & SPEKREIJSE, H. (1995). Standard for visual evoked potentials 1995. *Vision Res* **36,** 3567-3572.

HARTLINE, H. (1940). The receptive fields of optic nerve fibers. *Am J Physiol* **130,** 690-699.

HASEGAWA, S. & ABE, H. (2001). Mapping of glaucomatous visual field defects by multifocal VEPs. *Invest Ophthalmol Vis Sci* **42,** 3341-3348.

HAWKES, C. (2002). Is multiple sclerosis a sexually transmitted infection? *J Neurol Neurosurg Psychiatry* **73,** 439-443.

HEIJL, A. (1985). The Humphrey field analyser, construction and concepts. In *Sixth International Visual Field Symposium*. ed. JUNK, W., pp. 44-84, Boston.

HEINRICH, S. & BACH, M. (2001). Adaptation dynamics in pattern-reversal visual evoked potentials. *Doc Ophthalmol* **102,** 141-156.

HENRY, G. & VIDYASAGAR, T. (1977). Evolution of mammalian visual pathways. In *Evolution of the eye and visual system*. ed. CRONLY-DILLON, J. & GREGORY, R. Macmillan Press, Scientific & Medical.

HEYNEN, H. & VAN NORREN, D. (1985a). Origin of the electroretinogram in the intact macaque eye-I. *Vision Res* **25,** 697-707.

HEYNEN, H. & VAN NORREN, D. (1985b). Origin of the electroretinogram in the intact macaque eye-II. *Vision Res* **25,** 709-715.

HIDAJAT, R. & GOODE, D. (2003). Normalisation of visual evoked potentials after optic neuritis. *Doc Ophthalmol* **106,** 305-309.

HOCHSTEIN, S. & SHAPLEY, R. (1976). Linear and nonlinear spatial subunits in Y cat retinal ganglion cells. *J Physiol* **262,** 265-284.

HOFFMAN, M., STRAUBE, S. & BACH, M. (2003). Pattern-onset stimulation boosts central multifocal VEP responses. *J Vis* **3,** 432-439.

HOOD, D., BEARSE, M., SUTTER, E., VISWANATHAN, S. & FRISHMAN, L. (2001). The optic nerve head component of the monkey's (Macaca mulatta) multifocal electroretinogram (mERG). *Vision Res* **41,** 2029-2041.

HOOD, D. & BIRCH, D. (1982). A computational model of the amplitude and implicit time of the b-wave of the human ERG. *Visual Neurosci* **8,** 107-126.

HOOD, D. & BIRCH, D. (1990). A quantitative measure of the electrical activity of human rod photoreceptors using electroretinography. *Visual Neurosci* **33,** 1605-1618.

HOOD, D. & BIRCH, D. (1996). Abnormalities of the retinal cone system in retinitis pigmentosa. *Vision Res* **36,** 1699-1709.

HOOD, D., FRISHMAN, L., SASZIK, S. & VISWANATHAN, S. (2002a). Retinal origins of the primate multifocal ERG: implications for the human response. *Invest Ophthalmol Vis Sci* **43,** 1673-1685.

HOOD, D., GREENSTEIN, V., FRISHMAN, L., HOLOPIGIAN, K., VISWANATHAN, S., SEIPLE, W., AHMED, J. & ROBSON, J. (1999). Identifying inner retinal contributions to the human multifocal ERG. *Vision Res* **39,** 2285-2291.

HOOD, D., ODEL, J. & ZHANG, X. (2000a). Tracking the recovery of local optic nerve function after optic neuritis: a multifocal VEP study. *Invest Ophthalmol Vis Sci* **41,** 4032-4038.

HOOD, D., WLADIS, E., SHADY, S., HOLOPIGIAN, K., LI, J. & SEIPLE, W. (1998). Multifocal rod electroretinograms. *Invest Ophthalmol Vis Sci* **39,** 1152-1162.

HOOD, D. & ZHANG, X. (2000). Multifocal ERG and VEP responses and visual fields: comparing disease - related changes. *Doc Ophthalmol* **100,** 115-137.

HOOD, D., ZHANG, X., GREENSTEIN, V., KANGOVI, S., ODEL, J., LIEBMANN, M. & RITCH, R. (2000b). An interocular comparison of the multifocal VEP: a possible technique for detecting local damage to the optic nerve. *Invest Ophthalmol Vis Sci* **41,** 1580-1587.

HOOD, D., ZHANG, X., HONG, J. & CHEN, C. (2002b). Quantifying the benefits of additional channels of multifocal VEP recording. *Doc Ophthalmol* **104,** 303-320.

HORTON, J. & HOYT, W. (1991). The representation of the visual field in human striate cortex. *Arch Ophthalmol* **109,** 816-824.

HUBEL, D. (1982). Exploration of the primary visual cortex, 1955-78. *Nature* **299,** 515-524.

HUBEL, D. (1988). *Eye, brain and vision*. Scientific American, New York.

HUBEL, D. & WIESEL, T. (1968). Receptive fields and functional architecture of monkey striate cortex. *J Physiol* **195,** 215-243.

HUBEL, D. & WIESEL, T. (1972). Laminar and columnar distribution of geniculo-cortical fibers in the macaque monkey. *J Comp Neurol* **146,** 421-450.

HUBEL, D., WIESEL, T. & STRYKER, M. (1978). Anatomical demonstration of orientation columns in macaque monkey. *J Comp Neurol* **177,** 361-380.

IAROSSI, G., FALSINI, B. & PICCARDI, M. (2003). Regional cone dysfunction in retinitis pigmentosa evaluated by flicker ERGs: relationship with perimetric sensitivity losses. *Invest Ophthalmol Vis Sci* **44,** 866-874.

IKEJIRI, M., ADACHI-USAMI, E., MIZOTA, A., TSUYAMA, Y., MIYAUCHI, O. & SUEHIRO, S. (2002). Pattern visual evoked potentials in traumatic optic neuropathy. *Ophthalmol* **216,** 415-419.

IRIARTE, J., DE CASTRO, P., ARTIEDA, J., ZUBIETA, J. & MARTINEZ-LAGE, J. (1993). [Paraclinical tests in multiple sclerosis. Clinical correlation and predictive value] (abtsract). *Neurologia* **8,** 53-58.

IRVIN, G., NORTON, T., SESMA, M. & CASAGRANDE, V. (1986). W-like response properties of interlaminar zone cells in the lateral geniculate nucleus of a primate (Galago crassicaudatus). *Brain Res* **363,** 254-274.

JANSSEN, P., VOGELS, R. & ORBAN, G. (1999). Assessment of stereopsis in rhesus monkeys using visual evoked potentials. *Doc Ophthalmol* **95,** 247-255.

JAMES, A. (1992). Nonlinear operator network models of visual processing. In *Nonlinear vision: determination of neural receptive fields, function, and networks*. ed. PINTER, R. & NABET, B., pp. 31-74. CRC Press, Ann Arbor.

JAMES, A. (2003). The pattern pulse multifocal visual evoked potential. *Invest Opthalmol Vis Sci* **44,** 879-890.

JEFFREYS, D. (1971). Cortical source locations of pattern-related visual evoked potentials recorded from the human scalp. *Nature* **229,** 502-504.

JEFFREYS, D. & AXFORD, J. (1972). Source locations of pattern-specific components of human visual evoked potentials. I. Component of striate cortical origin. *Exp Brain Res* **16,** 1-21.

JIN, Y., DE PEDRO-CUESTA, J., HUANG, Y. & SODERSTROM, M. (2003). Predicting multiple sclerosis at optic neuritis onset (abstract). *Mult Scler* **9,** 135-141.

JOHNSON, C. & KELTNER, J. (1987). Optimal rates of movement for kinetic perimetry. *Arch Ophthalmol* **105,** 73-75.

JOHNSON, C., WALL, M., FINGERET, M. & LALLE, P. (1999). *A primer for frequency doubling technology*. Welch Allyn, Inc., Dublin, CA.

JONES, S. (1993). Visual evoked potentials after optic neuritis. Effect of time interval, age and disease dissemination. *J Neurol* **240,** 489-494.

JONGEN, P., LAMERS, K., COESBURG, W., LEMMENS, W. & HOMMES, O. (1997). Cerebrospinal fluid analysis differentiates between relapsing-remitting and secondary progressive multiple sclerosis. *J Neurol Neurosurg Psychiatry* **63,** 446-451.

KAPLAN, E. & SHAPLEY, R. (1982). X and Y cells in the lateral geniculate nucleus of macaque monkeys. *J Physiol* **330,** 125-123.

KAPPOS, L. (1988). Clinical trials of immunosuppression and immunomodulation in multiple sclerosis. *J NeuroImmunol* **20,** 261-268.

KELLY, D. (1966). Frequency doubling in visual responses. *J Opt Soc Am* **56,** 1628-1633.

KELLY, D. (1981). Nonlinear visual responses to flickering sinusoidal gratings. *J Opt Soc Am* **71,** 1051-1055.

KEMPSTER, P., IANSEK, R., BALLA, J., DENNIS, P. & BIEGLER, B. (1987). Value of visual evoked response and oligoclonal bands in cerebrospinal fluid in diagnosis of spinal multiple sclerosis. *Lancet* **8536,** 769-771.

KESSELRING, J. & KLEMENT, U. (2001). Cognitive and affective disturbances in multiple sclerosis. *J Neurol* **248,** 180-183.

KIKUCHI, Y., YOSHI, M., YANASHIMA, K., ENOKI, T., IDE, T., SAKEMI, F. & OKISAKA, S. (2002). Multifocal visual evoked potential is dependent on electrode position. *Jpn J Ophthalmol* **46,** 533-539.

KJAER, M. (1980). Visual evoked potentials in normal subjects and patients with multiple sclerosis. *Acta Neurol Scand* **62,** 1-13.

KLEIN, S. (1992). Optimizing the estimation of nonlinear kernels. In *Nonlinear vision: determination of neural receptive fields, function, and networks*. ed. PINTER, R. & NABET, B., pp. 109-170. CRC Press, Ann Arbor.

KLISTORNER, A., GRAHAM, K., GRIGG, J. & BILLSON, F. (1998a). Multifocal topographic visual evoked potential: improving objective detection of local visual field defects. *Invest Ophthalmol Vis Sci* **39,** 937-950.

KLISTORNER, A., GRAHAM, K. & MARTINA, A. (2000). Multifocal pattern electroretinogram does not demonstrate localised field defects in glaucoma. *Doc Ophthalmol* **100,** 155-165.

KLISTORNER, A. & GRAHAM, S. (1999). Multifocal pattern VEP perimetry: analysis of sectoral waveforms. *Doc Ophthalmol* **98,** 183-196.

KLISTORNER, A. & GRAHAM, S. (2001). Electroencephalogram-based scaling of multifocal visual evoked potentials: effect on intersubject amplitude variability. *Invest Ophthalmol Vis Sci* **42,** 2145-2452.

KLISTORNER, A., GRAHAM, S., GRIGG, J. & BILLSON, F. (1998b). Electrode position and the multi-focal visual-evoked potential: role in objective visual field assessment. *Aust N Z J Ophthalmol* **26(Suppl.),** 91-94.

KONDO, M., MIYAKE, Y., HORIGUCHI, M., SUZUKI, S. & TANIKAWA, A. (1998). Recording multifocal electroretinogram on and off responses in humans. *Invest Ophthalmol Vis Sci* **39,** 574-580.

KORTH, M. (1983). Pattern-evoked responses and luminance-evoked responses in the human electroretinogram. *J Physiol* **337,** 451-469.

KREMLACEK, J., KUBA, M. & HOLCIK, J. (2002). Model of visually evoked cortical potentials (thesis). In *Pathological Physiology, Medical Faculty*. Charles University, Hradec Kralove.

KREMLACEK, J., KUBA, M., KUBOVA, Z. & VIT, F. (1999). Simple and powerful visual stimulus generator. *Comp Methods and Progr in Biomed* **58,** 175-180.

KULIKOWSKI, J. (1974). Human averaged occipital potentials evoked by pattern and movement. *J Physiol* **242,** 70-71P.

KULIKOWSKI, J. (1978). Pattern and movement detection in man and rabbit: separation and comparison of occipital potentials. *Vision Res* **18,** 183-189.

KULIKOWSKI, J., ROBSON, A. & MURRAY, T. (2002). Scalp VEPs and intra-cortical responses to chromatic and achromatic stimuli in primates. *Doc Ophthalmol* **105,** 243-279.

KURTZKE, J. (1985). Optic neuritis and multiple sclerosis. *Arch Neurolog* **42,** 704-710.

LANDERS, J., GOLDBERG, I. & GRAHAM, S. (2002). Analysis of risk factors that may be associated with progression from ocular hypertension to primary open angle glaucoma. *Clin Exper Ophthalmol* **30,** 242-247.

LEE, Y. & SCHETZEN, M. (1965). Measurement of the kernels of a nonlinear system by cross-correlation. *Int J Control* **2,** 237-254.

LEOCANI, L., LOCATELLI, T., MARTINELLI, V., ROVARIS, M., FALAUTANO, M., FILIPPI, M., MAGNANI, G. & COMI, G. (2000). Electroencephalographic coherence analysis in multiple sclerosis: correlation with clinical, neuropsychological, and MRI findings. *J Neurol Neurosurg Psychiatry* **69,** 192-198.

LESKE, C. M. (1983). The epidemiology of open-angle glaucoma, a review. *Am J Epidemiol* **118,** 166-191.

LOPES DE FARIA, J., KATSUMI, O., ARAI, M. & HIROSE, T. (1998). Objective measurement of contrast sensitivity function using contrast sweep visual evoked responses. *Br J Ophthalmol* **82,** 168-173.

LUND, J., LUND, R., HENDRIKSON, A., BUNT, A. & FUCHS, A. (1975). The origin of efferent pathways from the primary visual cortex, area 17, of the macaque

monkey as shown by retrograde transport of horseradish peroxidase. *J Comp Neurol* **164,** 287-304.

MADDESS, T. (1989). Method and apparatus for use in diagnosis of glaucoma; USA Patent No. 5,065,767.

MADDESS, T. (1991). Method and apparatus for use in diagnosis of glaucoma; Australia Patent No. 611,585.

MADDESS, T., BEDFORD, S., JAMES, A. & ROSE, K. (1997). A multiple - frequency, multiple-region pattern electroretinogram investigation of non-linear retinal signals. *Aust Nz J Ophthalmol* **25,** 94-97.

MADDESS, T., GOLDBERG, I., WINE, S., DOBINSON, J., WELSH, A. H. & JAMES, A. C. (1999). Testing for glaucoma with the spatial frequency doubling illusion. *Vision Res* **39,** 4258-4273.

MADDESS, T., HEMMI, J. & JAMES, A. (1998). Evidence fort spatial aliasing effects in the Y-like cells of the magnocellular visual pathway. *Vision Res* **38,** 1843-1859.

MADDESS, T. & JAMES, A. (1998). Simultaneous binocular assessment of multiple optic nerve and cortical regions in diseases affecting nerve conduction; USA Patent No. 6,315,414.

MADDESS, T., JAMES, A., GOLDBERG, I., WINE, S. & DOBINSON, J. (2000a). Comparing a parallel PERG, automated perimetry, and frequency-doubling thresholds. *Invest Ophthalmol Vis Sci* **41,** 3827-3832.

MADDESS, T., JAMES, A., GOLDBERG, I., WINE, S. & DOBINSON, J. (2000b). A spatial frequency - doubling illusion -based pattern electroretinogram for glaucoma. *Invest Ophthalmol Vis Sci* **41,** 3818-3826.

MADDESS, T. & SEVERT, W. (1999). Testing for glaucoma with the frequency-doubling illusion in the whole, macular and eccentric visual fields. *Aust N Z J Ophthalmol* **27,** 194-196.

MAFFEI, L. & FIORENTINI, A. (1982). Electroretinographic response to alternating gratings in the cat. *Expl Brain Res* **48,** 327-334.

MAFFEI, L., FIORENTINI, A., BISTI, S. & HOLLANDER, H. (1985). Research note: Pattern ERG in the monkey after section of the optic nerve. *Expl Brain Res* **59,** 423-425.

MAIER, J., DAGNELIE, G., SPEKREIJSE, H. & VANDIJK, B. (1987). Principal components analysis for source localization ov VEPs in man. *Vision Res* **27,** 165-177.

MANAHILOV, V., RIEMSLAG, F. & SPEKREIJSE, H. (1992). The Laplacian analysis of the pattern onset response in man. *Electroencephalogr Clin Neurophysiol* **82,** 220-224.

MANCINI, M., MADDEN, B. & EMERSON, R. (1990). White noise analysis of temporal properties in simple receptive fields of cat cortex. *Biol Cybern* **63,** 209-219.

MARMARELIS, P. & NAKA, K. (1973b). Nonlinear analysis and synthesis of receptive field responses in the catfish retina. III. Two-input white-noise analysis. *J Neurophysiol* **36,** 634-648.

MARMOR, M., TAN, F., SUTTER, E. & BEARSE, M. (1999). Topography of cone electrophysiology in the enhanced S cone syndrome. *Invest Ophthalmol Vis Sci* **40,** 1866-1873.

MARMOR, M. & ZRENNER, E. (1999). Standard for clinical electroretinography (1999 update). *Doc Ophthalmol* **97,** 143-156.

MARROCCO, R., MCCLURKIN, J. & YOUNG, R. (1982). Spatial summation and conduction latency classification of cells of the lateral geniculate nucleus of macaques. *J Neuroscie* **2,** 1275-1291.

MARTINELLI, V., COMI, G., LOCATELLI, T., DELLA SALA, S. & SOMAZZI, L. (1987). Assessment of visual function in MS patients: comparative study of some diagnostic tests. *Ital J Neurol Sci* **Suppl,** 121-124.

MARTINEZ, A., DI RUSSO, F., ANLLO-VENTO, L., SERENO, M., BUXTON, R. & HILLYARD, S. (2001). Putting spatial attention on the map: timing and localization of stimulus selection processes in striate and extrastriate visual areas. *Vision Res* **41,** 1437-1457.

MATTHEWS, W. & SMALL, M. (1983). Prolonged follow-up of abnormal visual evoked potentials in multiple sclerosis: evidence for delayed recovery. *J Neurol Neurosurg Psych* **46,** 639-642.

MCDONALD, W., COMPSTON, A., EDAN, G., GOODKIN, D., HARTUNG, H., LUBLIN, F., MAFARLAMD, H., PARTY, D., POLMAN, C., REINGOLD, S., SANDBERG-WOLLHEIM, M., SIBLEY, W., THOMPSON, A., VAN DEN NOORT, S., WEINSHENKER, B. & WOLINKSY, J. (2001). Recommended diagnostic criteria for multiple sclerosis: guidelines from the international panel on the diagnosis of multiple sclerosis. *Ann Neurol* **50,** 121-127.

MCMILLAN, S., MCDONNELL, G., DOUGLAS, J. & HAWKINS, S. (2000). Evaluation of the clinical utility of cerebrospinal fluid (CSF) indices of inflammatory markers in multiple sclerosis. *Acta Neurol Scand* **101,** 239-243.

MIETZ, H., SCHLOOTZER-SCHREHARDT, U., STRASSFELD, C. & KRIEGLSTEIN, G. (2001). Effect of latonoprost and timolol on the histopathology of the rabbit conuctivita. *Invest Ophthalmol Vis Sci* **42,** 679-687.

MILLER, A. (1997). Current and investigational therapies to alter the course of multiple sclerosis. *South Med J* **90,** 367-375.

MILLER, R. (1973). Role of K+ in generation of b-wave of electroretinogram. *J Neurophysiol* **36,** 28-35.

MILLER, R. & DOWLING, J. (1970). Intracellular responses of the Müller (glial) cells of the mudpuppy retina: their relation to the b-wave of the electroretinogram. *J Neurophysiol* **33,** 323-341.

MUSCAT, S., PARKS, S., KEMP, E. & KEATING, D. (2002). The wide-field multifocal electroretinogram in the assessment of choroidal nevi and melanomas (abstract). In *Recent Developments in Ophthalmic Electrophysiology*, pp. 4.

MUSHLIN, A., DETSKY, A., PHELPS, C., O'CONNOR, P., KIDO, D., KUCHARZYK, W., GIANG, D., MOONEY, C., TANSEY, C. & HALL, W. (1993). The accuracy of magnetic resonance imaging in patients with suspected multiple sclerosis. The Rochester-Toronto magnetic resonance study group (abstract). *JAMA* **269,** 3146-3151.

NAKAYAMA, K. & MACKEBEN, M. (1982). Steady state visual evoked potentials in the alert primate. *Vision Res* **22,** 1261-1271.

NARAYANAN, S., DE STEFANO, N., FRANCIS, G., ARANAOUTELIS, R., CARAMANOS, Z., COLLINS, D., PELLETIER, D., ARNASON, B., ANTEL, J. & ARNOLD, D. (2001). Axonal metabolic recovery in multiple sclerosis patients treated with interferon b-1b. *J Neurol* **248,** 979-986.

NEIMA, D. & REGAN, D. (1984). Pattern visual evoked potentials and spatial vision in retrobulbar neuritis and multiple sclerosis. *Arch Neurolog* **41,** 198-201.

NEWMAN, E. (1980). Current source density analysis of the b-wave of frog retina. *J Neurophysiol* **43,** 1355-1366.

NICHOLSON, C. & FREEMAN, J. (1975). Theory of current source-density analysis and determination of conductivity tensor for anuran cerebellum. *J Neurophysiol* **38,** 356-368.

NOVAK, G., WIZNITZER, M., KURTZBERG, D., GIESSER, B. & VAUGHAN, H. (1988). The utility of visual evoked potentials using hemifield stimulation and several check sizes in the evaluation of suspected multiple sclerosis. *Electroencephalogr Clin Neurophysiol* **71,** 1-9.

NUWER, M. (1997). Fundamentals of evoked potentials and common clinical application today. *Electroencephalogr Clin Neurophysiol* **106,** 142-148.

ODOM, J., BACH, M., BARBER, M., BRIGELL, M., MARMOR, M. & TORMENE, A. (2003). Visual evoked potentials standard, 2004, Nagoya, ISCEV.

OKA, S., VAN TONDER, G. & EJIMA, Y. (2001). A VEP study on visual processing of figural geometry. *Vision Res* **41,** 3791-3803.

ONOZU, H. & YAMAMOTO, S. (2003). Oscillatory potentials of multifocal electroretinogram in diabetic retinopathy. *Doc Ophthalmol* **106,** 327-332.

OOSTENBRINK, J., RUTTEN-VAN MOLKEN, M. & OPDENOORDT, T. (2000). The treatment of newly diagnosed patients with glaucoma or with ocular hypertension in the Netherlands: an observational study of costs and initial treatment success based on retrospective chart review. *Doc Ophthalmol* **98,** 285-299.

PADMOS, P., HAAIJMAN, J. & SPEKREIJSE, H. (1973). Visually evoked cortical potentials to patterned stimuli in monkey and man. *Electroencephalogr Clin Neurophysiol* **35,** 153-133.

PADNICK, L. & LINSENMEIER, R. (1999). Properties of the flash visual evoked potential recorded in the cat primary cortex. *Vision Res* **39,** 2833-2840.

PARANHOS, F., KATSUMI, O., ARAI, M., NEHEMY, M. & HIROSE, T. (1999). Pattern reversal visual evoked response in retinitis pigmentosa. *Doc Ophthalmol* **96,** 321-331.

PARDUE, M., BALL, S., HETLING, J., CHOW, V., CHOW, A. & PEACHEY, N. (2001). Visual evoked potentials to infrared stimulation in normal cats and rats. *Doc Ophthalmol* **103,** 155-162.

PARISI, V., MANNI, G., CENTOFANTI, M., GANDOLFI, S., OLZI, D. & BUCCI, M. (2001). Correlation between optical coherence tomography, pattern electroretinogram, and visual evoked potentials in open-angle glaucoma patients. *Ophthalmol* **108,** 905-912.

PARKER, D., SALZEN, E. & LISHMAN, J. (1982). Visual evoked responses elicited by the onset and offset of sinusoidal gratings: latency, waveform, and topographic characteristics. *Invest Ophthalmol Vis Sci* **22,** 675-680.

PAUPOO, A., MAHROO, O., FRIEDBURG, C. & LAMB, T. (2000). Human cone photoreceptor responses measured by the electroretinogram a-wave during and after exposure to intense illumination. *J Physiol* **529,** 469-482.

PEACHEY, N. & BALL, S. (2003). Electrophysiological analysis of visual function in mutant mice. *Doc Ophthalmol* **107,** 13-26.

PERLMAN, I. (1983). Relationship between the amplitudes of the b wave and a wave as a useful index for evaluating the electroretinogram. *Br J Ophthalmol* **67,** 443-448.

PERRY, V. & COWEY, A. (1985). The ganglion cell and cone distribution in the monkey's retina: implications for central magnification factors. *Vision Res* **25,** 1795-1810.

POLOSCHEK, C. & SUTTER, E. (2002). The fine structure of multifocal ERG topographies. *J Vis* **2,** 577-587.

PORCIATTI, V. & SARTUCCI, F. (1996). Retinal and cortical evoked responses to chromatic contrast stimuli. Specific losses in both eyes of patients with multiple sclerosis and unilateral optic neuritis (abstract). *Brain* **119,** 723-740.

PORCIATTI, V., DI BARTOLO, E., NARDI, M. & FIORENTINI, A. (1997). Responses to chromatic and luminance contrast in glaucoma: a psychophysical and electrophysiological study. *Vision Res* **37,** 1975-1987.

POSER, C. (2000). The pathogenesis of multiple sclerosis: a commentary. *Clin Neurol Neurosurg* **102,** 191-194.

POSER, C. & BRINAR, V. (2002a). Multiple sclerosis 2001. *Clin Neurol Neurosurg* **104,** 15-167.

POSER, C. & BRINAR, V. (2002b). The symptomatic treatment of multiple sclerosis. *Clin Neurol Neurosurg* **104,** 231-235.

PRINEAS, J., BARNARD, R., REVESZ, T., KWON, E., SHARERT, L. & CHO, E. (1993). Multiple sclerosis. Pathology of recurrent lesions. *Brain* **116,** 681-693.

PUGLIATTI, M., SOTGIU, S. & ROSATI, G. (2002). The worldwide prevalence of multiple sclerosis. *Clinical Neurol and Neurosurg* **104,** 182-191.

ROBSON, A., EL-AMIR, A., BAILEY, C., EGAN, C., FITZKE, F., WEBSTER, A., BIRD, A. & HOLDER, G. (2003). Pattern ERG correlated of abnormal fundus autofluorescence in patients with retinitis pigmentosa and normal visual acuity. *Invest Ophthalmol Vis Sci* **44,** 3544-3550.

ROCKLAND, K. & PANDYAB, D. (1979). Laminar origins and terminations of cortical connections of the occipital lobe in the rhesus monkey*1. *Brain Res* **179,** 3-20.

RODER, H. (1991). [VEP in the determination of multiple lesions in the visual system in patients with multiple sclerosis]. *EEG EMG Z Elektroenzephalogr Elektromyogr Verwandte Geb* **22,** 234-238.

RODIECK, R. & BRENING, R. (1983). Retinal ganglion cells: properties, type, genera, pathways and trans-species comparisons. *Brain Behav Evol* **23,** 121-164.

ROMANI, A., CAPUTO, G., CALLIECO, R., SCHINTONE, E. & COSI, V. (1999). Edge detection and surface "filling-in" as shown by texture visual evoked potentials. *Clin Nerophysiol* **110,** 86-91.

ROVARIS, M., AGOSTA, F., SORMANI, M., INGLESE, M., MARTINELLI, V., COMI, G. & FILIPPI, M. (2003). Conventional and magnetization transfer MRI predictors of clinical evolution: a medium-term follow-up study. *Brain* **126,** 2323-2332.

SADOVNICK, A. (2002). The genetics of multiple sclerosis. *Clin Neurol Neurosurg* **104,** 199-202.

SAKAI, H., NAKA, K. & KORENBERG, M. (1988). White-noise analysis in visual neuroscience. *Visual Neurosci* **1,** 287-296.

SALA, A., COMI, G., MARTINELLI, V., SOMAZZI, L. & WILKINS, A. (1987). The rapid assessment of visual dysfunction in multiple sclerosis. *J Neurol Neurosurg Psych* **50,** 840-846.

SAMPLE, P. & WEINREB, R. (1990). Color perimetry for assessment of primary open-angle glaucoma. *Invest Ophthalmol Vis Sci* **31,** 1869-1871.

SAND, T., SJAASTAD, O., ROMSLO, I. & SULG, I. (1990). Brain-stem auditory evoked potentials in multiple sclerosis: the relation to VEP, SEP and CSF immunoglobulins. *J Neurol* **237,** 376-378.

SAND, T. & SULG, I. (1990). Evoked potentials and CSF-immunoglobulins in MS: relationship to disease duration, disability, and functional status. *Acta Neurol Scand* **82,** 217-221.

SANO, M., TAZAWA, Y., NABESHUIMA, T. & MITA, M. (2002). A new wavelet in the multifocal electroretinogram, probably originating from ganglion cells. *Invest Ophthalmol Vis Sci* **43,** 1666-1672.

SARTUCCI, F., MURRI, L., ORSINI, C. & PORCIATTI, V. (2001). Equiluminant red-green and blue-yellow VEPs in multiple sclerosis. *J Clin Neurophysiol* **18,** 583-591.

SASTRE-GARRIGA, J., TINTORE, M., ROVIRA, A., GRIVE, E., PERICOT, I., COMABELLA, M., THOMPSON, A. & MONTALBAN, X. (2003). Conversion to multiple sclerosis after a clinically isolated syndrome of the brainstem: cranial magnetic resonance imaging, cerebrospinal fluid and neurophysiological findings (abstract). *Mult Scler* **9,** 39-43.

SCAIOLI, V., RUMI, V., CIMINO, C. & ANGELINI, L. (1991). Childhood multiple sclerosis (MS): multimodal evoked potentials (EP) and magnetic resonance (MRI) comparative study (abstract). *Neuropediatric* **22,** 15-23.

SCHEIN, S. & DE MONASTERIO, F. (1987). Mapping of retinal and geniculate neurons onto striate cortex of macaque. *J Neuroscie* **7,** 996-1009.

SCHILLER, P. & MALPELI, J. (1977). Properties and tectal projections of monkey retinal ganglion cells. *J Neurophysiol* **40,** 428-445.

SCHIMITI, R., AVELINO, R., KARA-JOSE, N. & COSTA, V. (2002). Full-threshold versus Swedish interactive threshold algorithm (SITA) in normal individuals undergoing automated perimetry for the first time. *Ophthalmol* **109,** 2084-2092.

SCHROEDER, C., TENKE, C., GIVRE, S., AREZZO, J. & VAUGHAN, H. (1991). Striate cortical contribution to the surface-recorded pattern-reversal VEP in the alert monkey. *Vision Res* **31,** 1143-1157.

SEKHAR, G., NADUVILATH, T., LAKKAI, M., JAYKUMAR, A., PANDI, G., MANDAL, A. & HONAVAR, S. (2000). Sensitivity of Swedish interactive threshold algorithm compared with standard full threshold algorithm in Humphrey visual field testing. *Ophthalmol* **107,** 1303-1308.

SENA, A., PEDROSA, R. & GRACA MORAIS, M. (2003). Therapeutic potential of lovastin in multiple sclerosis. *J Neurol* **250,** 754-755.

SHAPLEY, R. & PERRY, V. (1986). Cat and monkey retinal ganglion cells and their visual functional roles. *Trends Neurosci* **9,** 229-235.

SHAPLEY, R. & VICTOR, J. (1978). The effect of contrast on the transfer properties of cat retinal ganglion cells. *J Physiol* **285,** 275-298.

SHAPLEY, R. & VICTOR, J. (1980). The effect of contrast on the non-linear response of the Y cell. *J Physiol* **302,** 535-547.

SHAWKAT, F. & KRISS, A. (2000). A study of the effects of contrast change on pattern VEPs, and the transition between onset, reversal and offset modes of stimulation. *Doc Ophthalmol* **101,** 73-89.

SHORSTEIN, N., DAWSON, W. & SHERWOOD, M. (1999). Mid-peripheral pattern electrical retinal responses in normals, glaucoma suspects, and glaucoma patients. *Br J Ophthalmol* **83,** 15-23.

SICOTTE, N., VOSKUHL, R., BOUVIER, S., KLUTCH, R., COHEN, M. & MAZZIOTTA, J. (2003). Comparison of multiple sclerosis lesions at 1.5 and 3.0 Tesla. *Invest Radiol* **38,** 423-427.

SILVEIRA, L., PICANCO-DINIZ, C., SAMPAIO, L. & OSWALDO-CRUZ, E. (1989). Retinal ganglion cell distribution in the cebus monkey: a comparison with the cortical magnification factors. *Vision Res* **29,** 1471-1483.

SLOTNICK, S., KLEIN, S., CARNEY, T., SUTTER, E. & DASTMALCHI, S. (1999). Using multi-stimulus VEP source localization to obtain a retinotopic map of human primary visual cortex. *Clin Neurophysiol* **110,** 1793-1800.

SNEPVANGERS, C. & VAN DEN BERG, T. (1990). Blue-yellow perimetry in the detection of early glaucomatous damage. *Doc Ophthalmol* **75,** 303-314.

SPEKREIJSE, H., VAN DER TWEEL, L. & ZUIDEMA, T. (1973). Contrast evoked responses in man. *Vision Res* **13,** 1577-1601.

STEWART, W., SHIELDS, M. & OLLIE, A. (1988). Peripheral visual field testing by automated kinetic perimetry in glaucoma. *Arch Ophthalmol* **106,** 202-206.

SUTTER, E. (1991). The fast m-transform: a fast computation of cross-correlations with binary m-sequences. *Soc Ind Appl Math* **20,** 686-694.

SUTTER, E. (1992). A deterministic approach to nonlinear systems analysis. In *Nonlinear vision: determination of neural receptive fields, function, and networks*. ed. PINTER, R. & NABET, B., pp. 171-220. CRC Press, Ann Arbor.

SUTTER, E. (2000). The interpretation of multifocal binary kernels. *Doc Ophthalmol* **100,** 49-75.

SUTTER, E. (2001). Imaging visual function with the multifocal m-sequence technique. *Vision Res* **41,** 1241-1255.

SUTTER, E. & BEARSE, M. (1999). The optic nerve head component of the human ERG. *Vision Res* **39,** 419-436.

SUTTER, E. & TRAN, D. (1992). The field topography of ERG components in man - I. The photopic luminance response. *Vision Res* **32,** 433-446.

SUTTLE, C., BANKS, M. & CANDY, T. (2000). Does a front-end nonlinearity confound VEP acuity measures n human infants? *Vision Res* **40,** 3665-3675.

SUTTLE, C. & HARDING, F. (1999). Morphology of transient VEPs to luminance and chromatic pattern onset and offset. *Vision Res* **39,** 1577-1584.

SWANK, R. & DUGAN, B. (1987). *The multiple sclerosis diet book. A low-fat diet for the treatment of MS*. Doubleday, New York.

THIENPRASIDDHI, P., GREENSTEIN, V., CHEN, C., LIEBMANN, M., RITCH, R. & HOOD, D. (2003). Multifocal visual evoked potential responses in glaucoma patients with unilateral hemifield defects. *Am J Ophthalmol* **136,** 34-40.

THOMAS, M. & LAMB, T. (1999). Light adaptation and dark adaptation of human rod photoreceptors measured from the a-wave of the electroretinogram. *J Physiol* **518,** 479-496.

TOWLE, V., WITT, J., NADER, S., REDER, A., FOUST, R. & SPIRE, J. (1991). Three-dimensional human pattern visual evoked potentials. II. Multiple sclerosis patients. *Electroencephalogr Clin Neurophysiol* **80,** 339-346.

TYLER, C., APKARIAN, P. & NAKAYAMA, K. (1978). Multiple spatial frequency tuning of electrical responses from the human visual cortex. *Exp Brain Res* **33,** 535-550.

VAN DER MEI, I., PONSONBY, A., BLIZZARD, L. & DWYER, T. (2001). Regional variation in multiple sclerosis. Prevalence in Australia and its association with ambient ultraviolet radiation. *Neuroepidemiology* **20,** 168-174.

VAN DIEMEN, H., LANTING, P., KOETSIER, J., STRIJERS, R., VAN WALBEEK, H. & POLMAN, C. (1992). Evaluation of the visual system in multiple sclerosis: a comparative study of diagnostic tests. *Clin Neurol Neurosurg* **94,** 191-195.

VERMA, L., PRAKASH, G., TEWARI, H., GUPTA, S., MURTHY, G. & SHARMA, N. (2003). Screening for diabetic retinopathy by non-ophthalmologists: an effective public health tool. *Doc Ophthalmol* **81,** 373-377.

VESTI, E., JOHNSON, C. & CHAUBAN, B. (2003). Comparison of different methods for detecting glaucomatous visual field progression. *Invest Ophthalmol Vis Sci* **44,** 3873-3879.

VICTOR, J. (1988). The dynamics of the cat retinal Y cell subunit. *J Physiol* **405,** 289-320.

VICTOR, J. (1992). Nonlinear systems analysis in vision: overview of kernel methods. In *Nonlinear vision: determination of neural receptive fields, function, and networks*. ed. PINTER, R. & NABET, B., pp. 1-34. CRC Press, Ann Arbor.

VICTOR, J. & KNIGHT, B. (1979). Nonlinear analysis with an arbitrary stimulus ensemble. *Quaterly of Applied Mathematics* **XXXVII,** 114-136.

VICTOR, J. & SHAPLEY, R. (1979a). The nonlinear pathway of Y ganglion cells in the cat retina. *J Physiol* **74,** 671-689.

VICTOR, J. & SHAPLEY, R. (1979b). Receptive field mechanism of cat X and Y retinal ganglion cells. *J Physiol* **74,** 275-298.

VICTOR, J., SHAPLEY, R. & KNIGHT, B. (1977). Nonlinear analysis of cat retinal ganglion cells in the frequency domain. *Neurobiol* **74,** 3068-3072.

VISWANATHAN, S., FRISHMAN, L. & ROBSON, J. (2000). The uniform field and pattern ERG in macaques with experimental glaucoma: removal of spiking activity. *Invest Ophthalmol Vis Sci* **41,** 2797-2810.

WALL, M., NEAHRING, R. & WOODWARD, K. (2002). Sensitivity and specificity of frequency doubling perimetry in neuro-ophthalmic disorders: a comparison with conventional automated perimetry. *Invest Ophthalmol Vis Sci* **43,** 1277-1283.

WALSH, T. (1990a). Automated perimetry in glaucoma. In *Visual fields. Examination and interpretation*. ed. WALSH, T. American Academy of Ophthalmology, San Francisco.

WALSH, T. (1990b). Optic nerve field defects. In *Visual fields. Examination and interpretation*. ed. WALSH, T. American Academy of Ophthalmology, San Francisco.

WALSH, T. (1990c). *Visual fields. Examination and interpretation*. American Academy of Ophthalmology, San Francisco.

WANDELL, B. (1995a). The cortical representation. In *Foundations of vision*, pp. 13-43. Sinauer Associates, Inc., Sunderland.

WANDELL, B. (1995b). Image formation. In *Foundations of vision*, pp. 13-43. Sinauer Associates, Inc., Sunderland.

WANG, C., TOW, S., AUNG, T., LIM, S. & CULLEN, F. (2001). The presentation, aetiology, management and outcome of optic neuritis in an Asian population. *Clin Exper Ophthalmol* **29,** 312-315.

WASSLE, H. & BOYCOTT, B. (1991). Functional architecture of the mammalian retina. *Physiol Rev* **71,** 447-480.

WASSLE, H., GRUNERT, U., ROHRENBECK, J. & BOYCOTT, B. (1989). Cortical magnification factor and the ganglion cell density of the primate retina. *Nature* **341,** 643-646.

WASSLE, H., GRUNERT, U., ROHRENBECK, J. & BOYCOTT, B. (1990). Retinal ganglion cell density and cortical magnification factor in the primate. *Vision Res* **30,** 1897-1911.

WASSLE, H., LEVICK, W. & CLELAND, B. (1975). The distribution of the alpha type of ganglion cells in the cat's retina. *J Comp Neurol* **159,** 419-439.

WAXMAN, S. (1983). The demyelinating diseases. *Clinical Neurosci* **1,** 609-643.

WEINSHENKER, B., ISSA, M. & BASKERVILLE, J. (1996). Meta-analysis of the Placebo treated groups in clinical trials of progressive multiple sclerosis. *Neurology* **46,** 1613-1619.

WELSH, R. (1961). Finger counting in the four quadrants as a method of visual field gross screening. *Arch Ophthalmol* **66,** 678-679.

WIENER, N. (1935). The homogenous chaos. *Am J Math* **60,** 897-936.

WILENSKY, J., MERMELSTEIN, J. & SIEGEL, H. (1986). The use of different-sized stimuli in automated perimetry. *Am J Ophthalmol* **101,** 710-413.

WILHELM, H., NEITZEL, J., WILHELM, B., BEUEL, S., LUDTKE, H., KRETSCHMANN, U. & ZRENNER, E. (2000). Pupil perimetry using M-sequence stimulation technique. *Invest Ophthalmol Vis Sci* **41,** 1229-1238.

WONG, A. & SHARPE, J. (2000). A comparison of tangent screen, Goldmann, and Humphrey perimetry in the detection and localization of occipital lesions. *Ophthalmol* **107,** 527-544.

XU, S., MEYER, D., YOSER, S., MATHEWS, D. & ELFERVIG, J. (2001). Pattern visual evoked potential in the diagnosis of functional visual loss. *Ophthalmol* **108,** 76-81.

YU, M. & BROWN, B. (1996). Variation of topographic visually evoked potentials across the visual field. *Ophthalmol Physiol Opt* **17,** 25-31.

ZHANG, X., HOOD, D., CHEN, C. & HONG, J. (2002). A signal-to-noise analysis of multifocal VEP responses: an objective definition for poor records. *Doc Ophthalmol* **104,** 287-302.

ZRENNER, E. (1990). The physiological basis of the pattern electroretinogram. In *The pattern electroretinogram.* ed. OSBORNE, N. & CHADER, G. Pergamon Press, Oford.

ZRENNER, E., BAKER, C., HESS, R. & OLSEN, B. (1986). Current source density analysis of linear and nonlinear components of the primate electroretinogram. *Invest Ophthalmol Vis Sci* **Suppl.,** R82.

CHAPTER I

Effect of Sparseness and Dichoptic Presentation upon Multifocal Visual Evoked Potentials

Abstract

Purpose. To examine multifocal VEPs (mfVEPs) obtained to the different levels of temporal sparseness.

Methods. mfVEP responses were obtained for 9 test conditions including three degrees of temporal sparseness: Binary, $Sparse_4$ and $Sparse_{16}$, and dichoptic versus monocular viewing conditions. Spatially the stimulus consisted of 8 cortically scaled checkerboard stimuli per eye. The Binary stimuli provided pseudorandom contrast reversals of the checkerboard stimuli as is typical mfVEP methods to date. The $Sparse_4$ and $Sparse_{16}$ stimuli were ternary, thus including non-stimuli in their video stimulus sequences where a given test region had 0 contrast.

Results. A multiple regression model showed that responses to the $Sparse_{16}$ stimulus were 4.00 times larger than for the conventional binary stimulus. For dichoptic presentation $Sparse_{16}$ responses were 5.53 times larger. Binocular suppression was greatest for the Binary stimulus. Responses to the dichoptic $Sparse_{16}$ stimulus were about 20% smaller in the superior visual field locations.

Conclusions. Consideration of the signal to noise ratios indicated to achieve a given level of reliability Binary stimulation would require 40% longer trials. For the dichoptic case binary stimuli would require 300% more time.

Introduction

Visual evoked potentials (VEPs) recorded in response to contrast reversing checkerboard stimuli have been used to evaluate optic neuritis, optic tumours, glaucoma, retinal disorders and demyelinating diseases such as multiple sclerosis (Sand *et al.*, 1990; Sand & Sulg, 1990; Stenager & Jensen, 1990; Andersson & Siden, 1991; Andersson *et al.*, 1991; Jones, 1993; Hood & Zhang, 2000; Hood *et al.*, 2000b). In the present study VEPs were recorded in response to a multifocal stimulus in which many visual stimuli are presented concurrently. Sutter introduced m-sequence stimuli for multifocal recording (e.g. Sutter, 1992), and has done much to popularise multifocal ERG (mfERG) analysis. More recently others (Klistorner *et al.*, 1998b; Klistorner & Graham, 1999; Goldberg *et al.*, 2002) have used multifocal VEPs (mfVEPs) to quantify the localized visual-field defects of glaucoma.

We recorded mfVEPs obtained for multifocal stimuli having eight different visual field regions per eye and three classes of temporal modulation. Preliminary experiments (James & Maddess, 2000; James *et al.*, 2000) indicated that temporally *sparse* stimuli produce large responses. Therefore we have sought to compare sparse stimuli with more conventional contrast reversing multifocal stimuli. We also compared responses to monocular (left or right) and dichoptic viewing conditions for each temporal stimulus variant. Nonlinear binocular summation is expected for dichoptic viewing (e.g. Regan & Regan, 1989). At issue is whether binocular suppression is so large as to rule out use of dichoptic presentation. In principle dichoptic stimulation permits a better statistical basis for between eye comparisons. Such comparisons have been shown to have diagnostic value (Atkin *et al.*, 1980; Maddess & James, 1998; Maddess & Severt, 1999; Hood *et al.*, 2000b).

Methods

Stimuli

Visual stimuli were presented on a model CCID 7551 monitor (Barco, Kortrjk, Belgium), mean luminance 45 cd/m^2. A program running on an AT Vista graphics board (Truevision, Shadeland Station, IN) controlled the stimulus display. Software for data acquisition, analysis and display was written in Matlab (Matlab; The MathWorks, Natick, MA). The image was 512 by 436 pixels and the non - interlaced refresh rate of the monitor was 101.5 Hz. Subjects viewed the monitor from 30 cm providing the stimulus layout illustrated in Figure 1.1.

The visual stimuli presented to each eye had eight visual regions. The check sizes within each region were scaled so that each check stimulated an approximately equal area of the striate visual cortex. A 0.75 deg square, red, fixation spot was presented at the screen's centre. The contrast of the eight regions was independently modulated in time with binary or ternary noise sequences as illustrated by Figure 1.2. Contrast, C, can most generally be defined as the difference between the brightness at each image point, B, and the mean or background brightness, M, divided by M: C= (B - M)/M. Notice that the mean brightness has contrast = 0, and objects that are brighter or darker than the mean by an amount of M (*i.e.* B= 2M or 0) have contrasts 1 and -1 respectively. The checks illustrated in Figure 1.1 had contrasts ±1 or 0. Three different types of temporal sequences were examined (Fig. 1.2):-

1. Binary or "contrast reversing", when the probability of a checkerboard of either sign appearing was ½, hence the stimulus is binary, i.e. check contrast could take the values {-1, 1} (Fig. 1.2a).

2. $Sparse_4$, when the probability of a checkerboard appearing in one sign or the other was ¼; hence the stimulus was ternary, i.e. check contrast took the values {-1, 0, 1} (Fig. 1.2b).

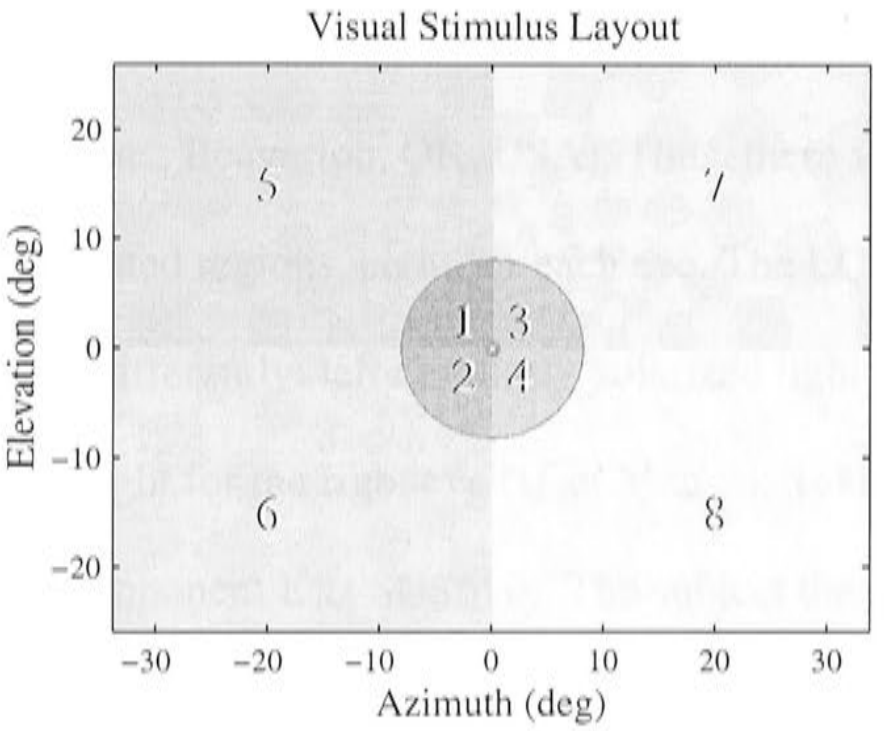

Figure 1.1 Illustration of the spatial layout of the visual stimulus. The numbers (1…8) are the indices to the eight different regions for the left or right eye. The differing grey levels of each region are presented to assist the reader to visualize the regions. In practice the M-scaled checks had contrasts ± 1 or 0 (i.e. black, white or grey).

3. $Sparse_{16}$, when the probability of a checkerboard appearing in one sign or the other was 1/16. Again the stimulus was ternary; check contrast taking the values {-1, 0, 1} (Fig. 1.2c).

Visual stimuli were presented in both monocular and dichoptic viewing conditions. To produce dichoptic stimulation, we generated two images and presented them separately to each eye on successive video frames. The interleaving of the images for the left and right eyes was achieved by means of a liquid crystal (LQ) stereoscopic modulator (or shutter) (Tektronix, Inc., Beaverton, OR, USA). Thus, there were actually 16 independently modulated regions, eight for each eye. The LQ shutter encodes each of the alternate images differently: left circularly polarized light for the left eye, and right circularly polarized light for the right eye (User Manual, Tektronix, Stereoscopic Graphics Display Component Kits SGS610). The subject then wears passive spectacles. Each eyepiece of the spectacles contains a sandwich of a quarter wave plate and a linear polariser. The quarterwave plate transforms the circular polarised light to vertical or horizontal linearly polarise light and the polarising material acts as an analyser. Monocular stimulation was achieved through the use of an eye-patch, all other stimulus conditions being identical to the dichoptic case. The shutter and spectacles reduced the initial mean luminance of the monitor from 45cd/m^2 to 7.6 cd/m^2.

Recording

We recorded Visual Evoked Potentials (VEPs) using gold cup electrodes (diameter = 8 mm) placed on the scalp by using the conductive gel EEG Ten20 (D.O.Weaver and Co, Aurora, LO). Electrodes were attached 3 cm above and 4 cm below the inion. This

configuration has been shown to increase the response obtained for the superior visual field (Klistorner *et al.*, 1998a). An earth electrode was attached to the right ear lobe. Signals were amplified 50,000 times and initially band pass filtered between 1.6 and 200 Hz (6 dB/octave attenuation).

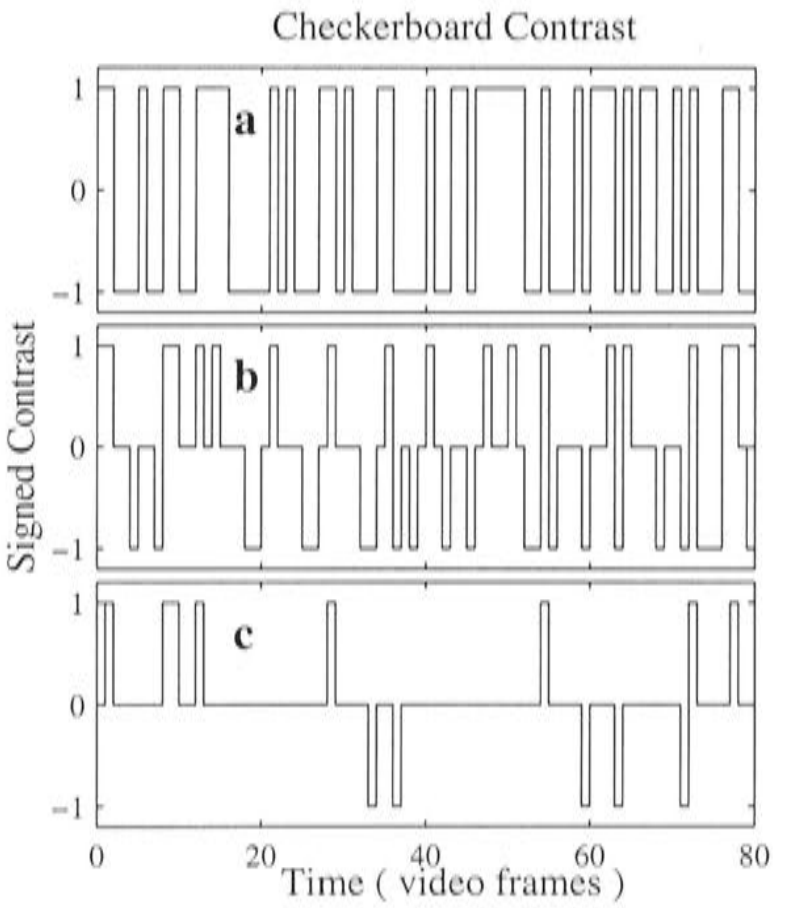

Figure 1.2 Examples of the temporal modulation of a single region. **a)** Temporal stimulus density for the Binary (contrast reversing) condition (probability of ½ that check contrast could take the values –1 or 1). b) $Sparse_4$ (or intermediate) stimulus, when the probability of a checkerboard appearing in one sign of the other was ¼; check contrast took the values {-1, 0, 1}). **c)** $Sparse_{16}$ (sparse), when the probability of a checkerboard appearing in one sign of the other was 1/16. As for $Sparse_4$ the stimulus was ternary; checkerboard contrast took the values {-1, 0, 1}. The duration of one video frame (*Time* axis) is 9.85 ms.

Subsequent forward and backward, zero phase shift, digital filtering (Chebychev type 2) further attenuated signals below 2 Hz (4^{th} order filter) and above 80 Hz (16^{th} order filter). Each trial lasted 40.4 s (4096 frames). The test was repeated eight times for each stimulus and each viewing condition. Subjects were required to attend two recording sessions, four records for each condition being obtained in each session. Blocks of four repeats of each stimulus were presented in a randomised order.

Subjects

VEPs were recorded from 13 normal subjects (nine men and four women, age range 22 to 44, with normal or corrected to normal (6/9) refraction). A Frequency Doubling Technology (FDT) perimeter (Humphrey, San Leandro, CA) was used to test subjects' visual fields before the first test session. Each subject was first given the C-20 screening test, followed by the Full Threshold C-20 program of the FDT. The research followed the tenets of the Declaration of Helsinki, under the Australian National University's Human Experimentation Ethics Committee under protocol M9901. Informed written consent was obtained from the subjects after the nature and possible consequences of the study were explained to them.

Data Analysis

Non-linear systems identification is now commonly applied in vision research. One of the best known of these methods is so called Wiener decomposition (Lee & Schetzen, 1965; Sutter, 1992). The Wiener method is able to characterise a system's response by a set of *kernels*, each of which describes progressively higher order polynomial

components of the response system's behaviour over the particular epoch, or memory length, of interest. The first order kernel, K_1, summarises the linear response and is equivalent to the impulse response (Bracewell, 1986) of a linear system. The first order kernel convolved with the stimulus thus predicts the linear response $R(t)$ to the stimulus $S(t)$: $R(t) = K_1 * S(t)$, where * is a convolution. The second order kernel, K_2, characterises quadratic non-linear responses between the stimulus and itself. The estimated quadratic nonlinear response is obtained from K_2 and the stimulus by a modified convolution procedure (e.g. James, 1992). The full estimate of the response up to second order is then the sum of the predicted components.

K_2 is a two-dimensional matrix of coefficients, its diagonal elements characterising responses to products between the stimulus and itself at various delays, from no delay to the maximum memory length of the system. These diagonal elements of the K_2 matrix are often called *slices*: the main diagonal being called $K_{2,0}$, and successive slices $K_{2,1}$, $K_{2,2}$, and so on (Fig. 1.3b). In the present case $K_{2,0}$ describes the response to squared contrast that might arise from a process such as response rectification, while $K_{2,1}$, and $K_{2,2}$, quantify similar quadratic non-linear contributions, but for those occurring for particular delays. In the present case the K_2 slices are separated by delays equal to two video frame times or 0.0197 s. Since the sixteen (8 per eye) different visual regions had temporally independent stimuli, separate kernels could be computed for each region. The kernel slices were estimated by the regressive method of James (2003). Since squaring the response is related to rectification, K_2 in effect tells us about rectifying or ON-OFF style response components, and for the purposes of this study can be thought of as the first order response to contrast reversal.

In the case of binary stimuli we estimated K_1 and the first two off-diagonal slices of $K_{2,1}$ and $K_{2,2}$, as $K_{2,0}$ cannot be estimated for Binary stimuli (Klien, 1992; Sutter, 1992). In the case of $Sparse_4$ and $Sparse_{16}$ stimuli we estimated K_1, $K_{2,0}$ and $K_{2,1}$. In all

cases K_1 was near zero (dotted line Fig. 1.3a) indicating good balance between on- and off-pathways, further justifying analysis of the major K_2 components. Thus, except for Figure 3, we only consider the slices: $K_{2,1}$ for binary stimuli and $K_{2,0}$ for the $Sparse_4$ and $Sparse_{16}$ stimuli. To simplify matters we will henceforth refer to these kernel components as *responses*. These responses represent the largest components of the second order kernel and so they summarise the response to contrast exchange well.

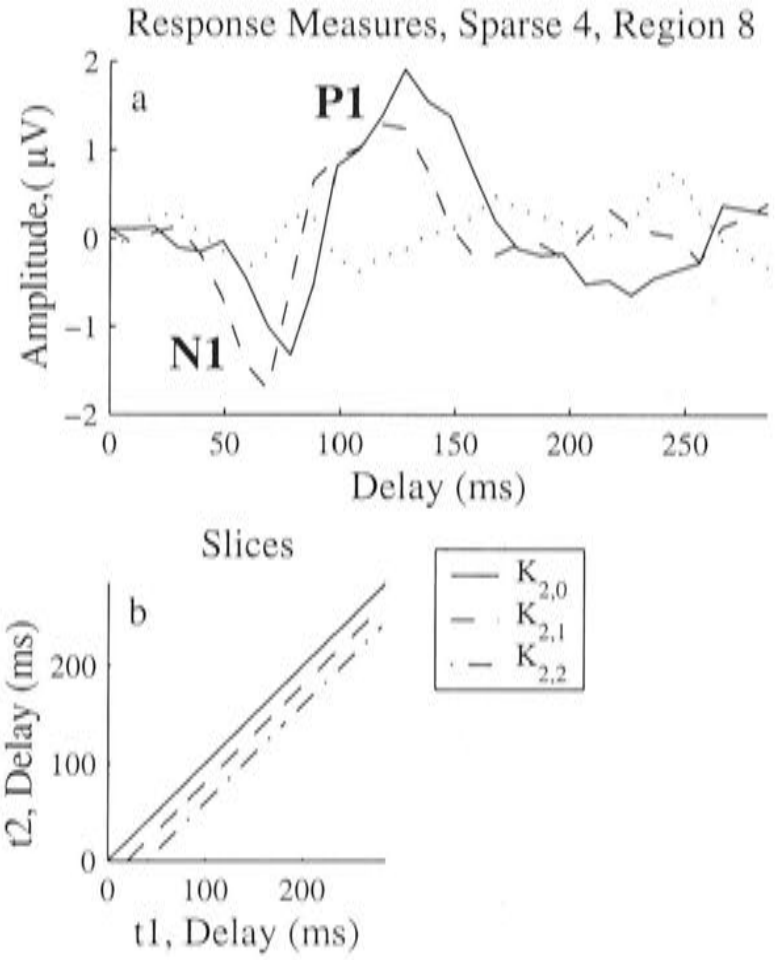

Figure 1.3 Response nomenclature. **a)** Averaged responses across subjects for the $Sparse_4$ condition, left eye only, region 8 (see Fig. 1.1): the dotted trace is K_1, other traces as per legend of panel **b**. **b)** Kernel slices shown in relation to the domain of the full second order expressed in the in the t1- and t2-delays. The second order kernel is two-dimensional, its diagonal elements characterising interactions between the stimulus and itself at various delays. These diagonal kernel elements are often called *slices*: the main diagonal being called $K_{2,0}$, and successive slices $K_{2,1}$, $K_{2,2}$, and so on. $K_{2,0}$ presents the response to squared contrast that might arise from a process such as response rectification, while $K_{2,1}$, and $K_{2,2}$, describe similar non-linear contributions but for those occurring for particular delays. Notice that the 2D form of K_2 leads to an apparent earlier onset for $K_{2,1}$ than for $K_{2,0}$ when shown in the 1D plot of **a**.

Within each response the two periods 59.1 to 95.8 ms and 108 to 158 ms contained the first two peaks of all the responses (e.g. Fig. 1.8). The first peak can be considered to be negative with respect to the surface of the cortical sheet, the curvature of the calcarine sulcus effecting an inversion of responses from the inferior visual field for scalp recordings (cf. Fig. 1.1 and Figs. 1.4, 1.5). Since these two time windows contained the first negativity and the first positivity, the peaks and their associated temporal windows are referred to as the N1 and P1 (Fig. 1.3a) peaks and windows. Coincidently this is similar to the nomenclature of the peaks of the mfERG recorded with respect to the cornea. Before finding the maximum or mean deflection in the N1 and P1 regions the kernels were, if necessary, inverted to make the first peak negative. This was done according to a schedule derived from the averages obtained across subjects.

Multivariate Linear Regression

Generalized regression was used to quantify the major effects determining the responses. The multivariate linear regression model (Johnson & Wichern, 1992) can be given as

$$\underset{(n*m)}{Y} = \underset{(n*r)}{Z}\,\underset{(r*m)}{\beta} + \underset{(n*m)}{\varepsilon} \qquad (1.1)$$

where Z is the design matrix. Each column of Z consists of the n values of the corresponding variable, for m observations. In the present case $m=1$, and r is the number of fitted coefficients. In our case Y was derived from the response data: we examined both response amplitudes and means from the N1 and P1 windows. β is a vector of model parameters characterising the data that are to be estimated. One of the objectives of regression analysis is to develop an equation that will predict the response

for given values of the predictor variables. So, we need to determine the values for a parsimonious set of regression coefficients β, and the error variance (the residuals), that are most consistent with data. The regression coefficients were examined for the degrees of temporal sparseness, monocular and dichoptic viewing conditions, visual field location (e.g. superior, left, nasal, peripheral) and possible interactions between these variables.

T-statistics

The above description of multivariate regression introduced some terms that are useful for describing an alternative representation of the responses that we have employed. In the regressive response estimation method (James, 2003) each point in the response is an estimate coefficient β and therefore has an associated standard error SE(β). These SE(β) were very useful in determining the signal to noise ratios (SNRs) for the N1 and P1 responses. The SE(β) also provide another opportunity.

In addition to presenting the slices with units of μV we sometimes present them where each coefficient of the response is given as a t-statistic (Eq. 1.2). The purpose of t-statistics is to provide and indication of the significance of the response elements. Since the responses were estimated by a regression method, where the slice coefficients correspond to β of Eq.1.1 we can write:

$$\frac{\beta}{SE(\beta)} \approx t(n-r), \quad t_{\partial f = n-r} \tag{1.2}$$

n being the number of samples in the 40s recording, and r the number of response coefficients. Since $(n - r)$ is very large so the obtained t-statistics could be considered as z-scores.

Results

We recorded mfVEPs for three viewing conditions (dichoptic, and monocular left or right eye), for each sparseness (Binary, $Sparse_4$ and $Sparse_{16}$). Thus, for each of the 16-stimulus regions (eight per eye) we obtained eight repeats of nine response data sets. The results for the subject having the largest responses are shown in the Figure 1.4. The left panel, Figure 4a, represents the responses for the Binary stimulus, and the right, Figure 4b, panel represents responses to $Sparse_{16}$. Stimuli were presented dichoptically in both cases and the plotted responses are averages from randomly interleaved trials. The multifocal responses to the Binary stimulus are about 5 times smaller than those obtained for the $Sparse_{16}$ stimulus. Aside from the differences in response amplitude the figure illustrate that even in the case of our best recording conditions the shapes of the $Sparse_{16}$ responses are more consistent across visual field regions than are the responses to the Binary stimulus.

Figure 1.5 demonstrates the averaged responses across the 13 subjects for dichoptic viewing. The left panel shows responses for the Binary stimulus and the left panel responses for the $Sparse_{16}$ stimulus. We see, that the mean amplitudes for the Binary stimuli are significantly smaller than the $Sparse_{16}$ responses (see also Table 1.1). As with the subject of Figure 1.4 the average responses to the $Sparse_{16}$ stimulus are of a more consistent size and shape across visual field locations.

Means and Standard Deviations

We averaged the response waveforms across subjects and test regions for monocular and dichoptic stimuli, and calculated the population standard deviations for each response coefficient. Figures 1.6 and 1.7 show the averages for monocular and dichoptic

viewing respectively. The rows of Figures 1. 6 and 1.7 correspond, from top to bottom, to the Binary, Sparse 4 and Sparse 16 stimuli.

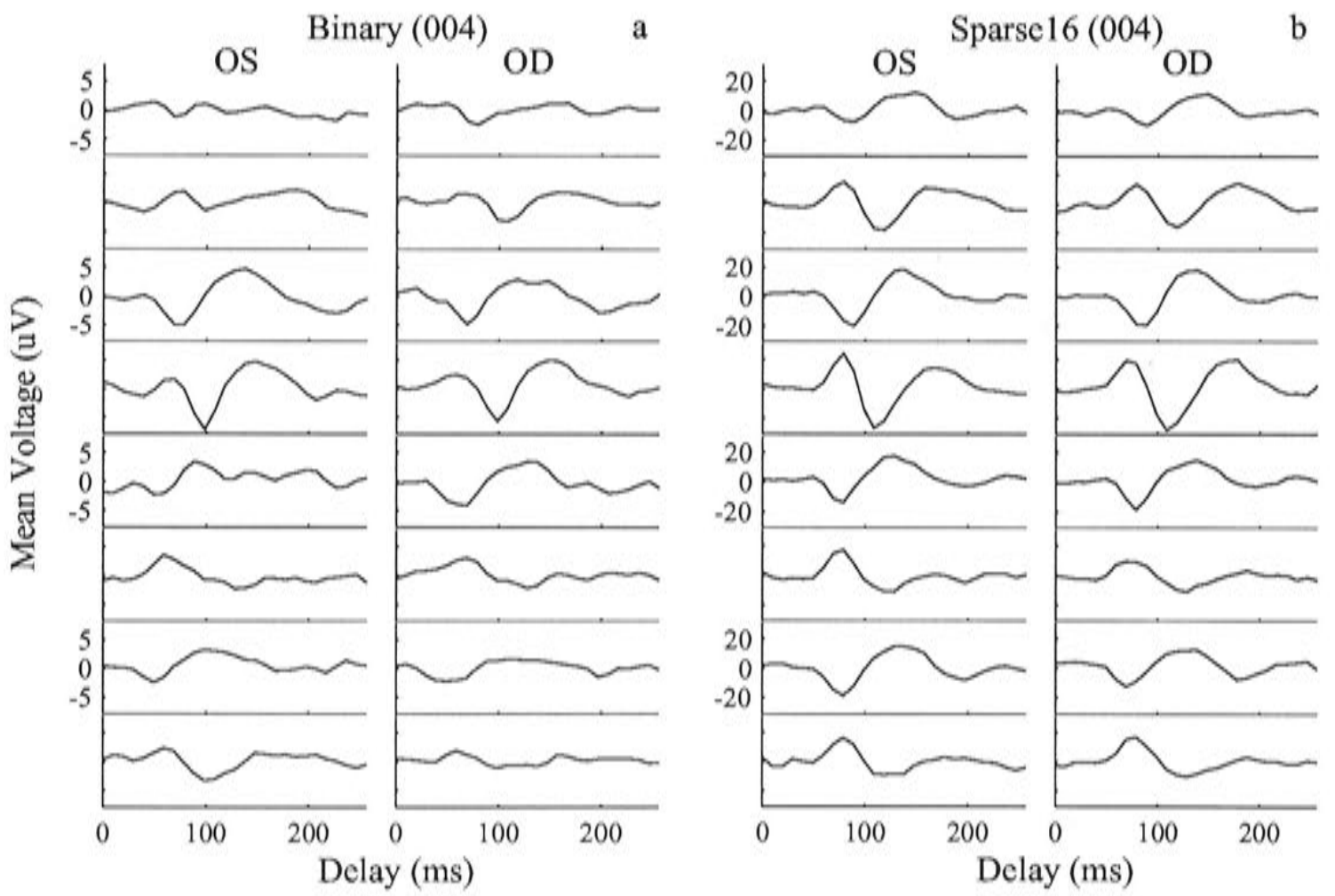

Figure 1.4 Large multifocal responses (in μV) were obtained for subject 004. **a)** These two panels on the left (Binary (004)) represent the multifocal responses for the left (OS) and for the right (OD) eye. **b)** The right two panels ($Sparse_{16}$ (004)) show the Sparse 16 multifocal responses for the left (OS) and for the right (OD) eye, for the eight visual field regions (see Fig.1). The eight rows of responses in each vertical panel represent responses from regions 1 to 8, where region 1 is at the top and 8 the response in the bottom row. Thus, the top 4 rows are responses to central stimuli (1 to 4), and the bottom 4 rows are responses to peripheral stimuli (5 to 8), odd rows correspond to stimuli presented to the superior visual field, even to inferior. Note the inversion of responses in the inferior field. Even in this very good result the Binary responses appear more variable, both individually and across visual field regions.

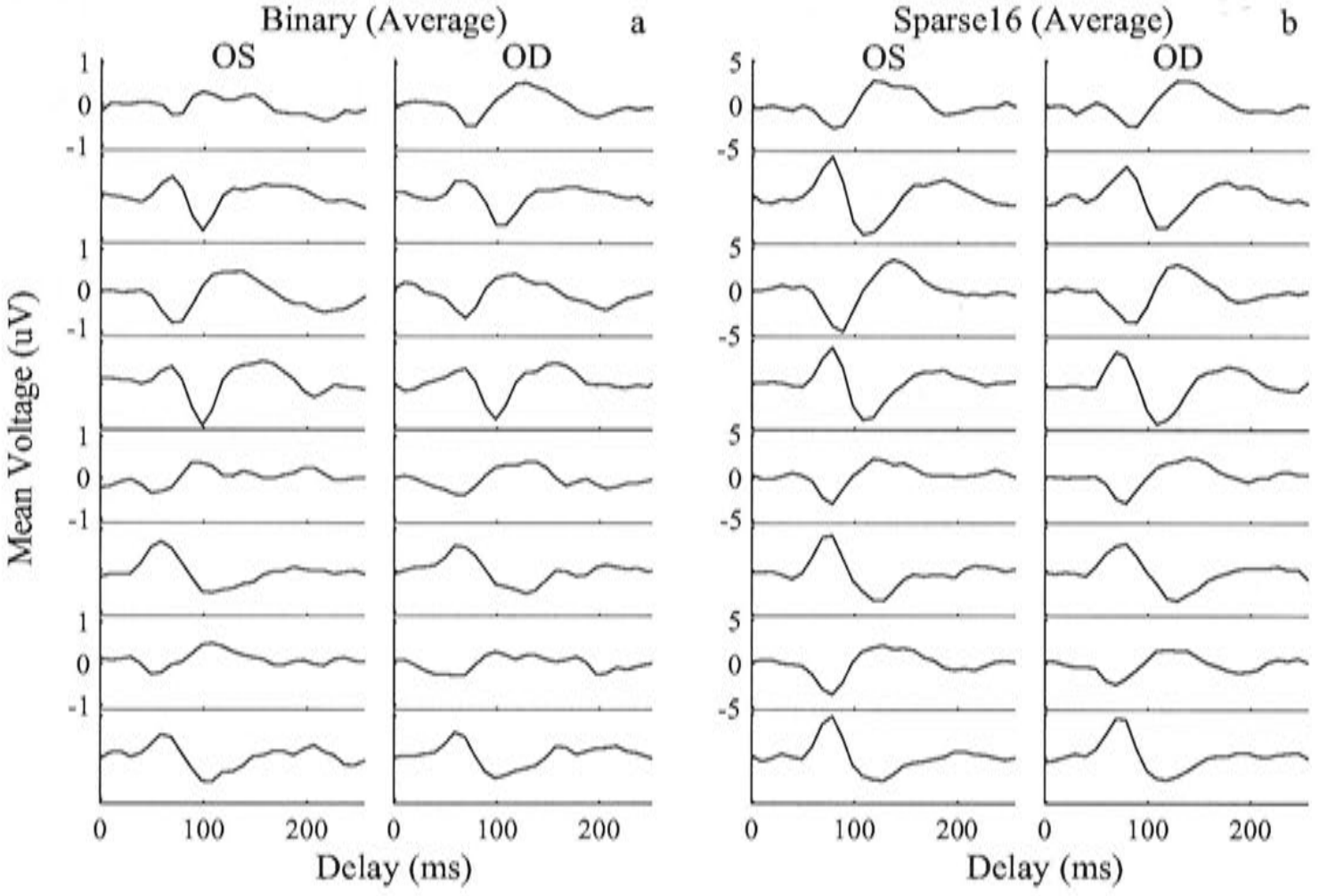

Figure 1.5 Averaged multifocal responses (mean voltage) across 13 subjects. **a)** Binary (Average) shows the averaged multifocal responses for the left (OS) and for the right (OD) eye. **b)** $Sparse_{16}$ (Average) shows the averaged $Sparse_{16}$ multifocal responses for the left (OS) and for the right (OD) eye, for eight regions (Fig.1). The axis conventions are the same as in Figure 4. Even when responses are averaged across subjects the Binary responses are more variable in time and across visual field location than $Sparse_{16}$, as in Figure 1.4.

Figures 1.6a–c show the mean voltages of the averaged data for the monocular viewing condition. The horizontal dashed lines in Figures 1.6a-c show the average standard error (SE) from the regression estimates of the responses multiplied by 2.5. A parallel study of different methods for estimating the significance of the responses indicates that 2.5 SE is a conservative estimate of the 95% confidence level (James, 2003). The grey waveforms bracketing the mean voltage responses are of Figure 1.6a-c are ±1 population standard deviation (SD) of the averaged slice data. The right columns (Fig. 1.6d-f) show mean of the absolute values of the t-statistics for the same data set. The mean of the t-statistics is shown with solid lines, and ± SE in grey lines.

Figure 1.7 presents the mean voltages (Fig.1.7a-c) and mean t-statistics (Fig.1.7d-f) for data recorded under the dichoptic viewing condition. The axis conventions are same as in the Figure 1.6. The × symbol (Fig. 1.7a) shows the mean N1 peak amplitude minus one population SD, thus providing the typical significance of the Binary multifocal responses. Notice that the × does not exceed the 95% confidence level (dashed horizontal line), thus only about the upper 15 percentile of N1 responses are significant. The + symbol in Figure 1.7c, indicates the lower 15% bound of the N1 responses to the $Sparse_{16}$ stimulus. Its position indicates that about 90% of the $Sparse_{16}$ N1 peaks exceed the 95% confidence level.

To provide an alternative measure of significance we can convert the elements of each response from voltages to t-statistics *(Methods)* (Figs, 1.6d-f, 1.7d-f). In the present example the absolute values of the t-statistics were taken before averaging across subjects and stimulus regions. The results indicate that the N1 peak is particularly affected by dichoptic viewing, especially for the Binary visual stimulus (cf. Figs. 1.6d and 1.7d). Overall, both the voltage and t-statistic averages indicate that the $Sparse_4$ visual stimulus rarely produces significant responses.

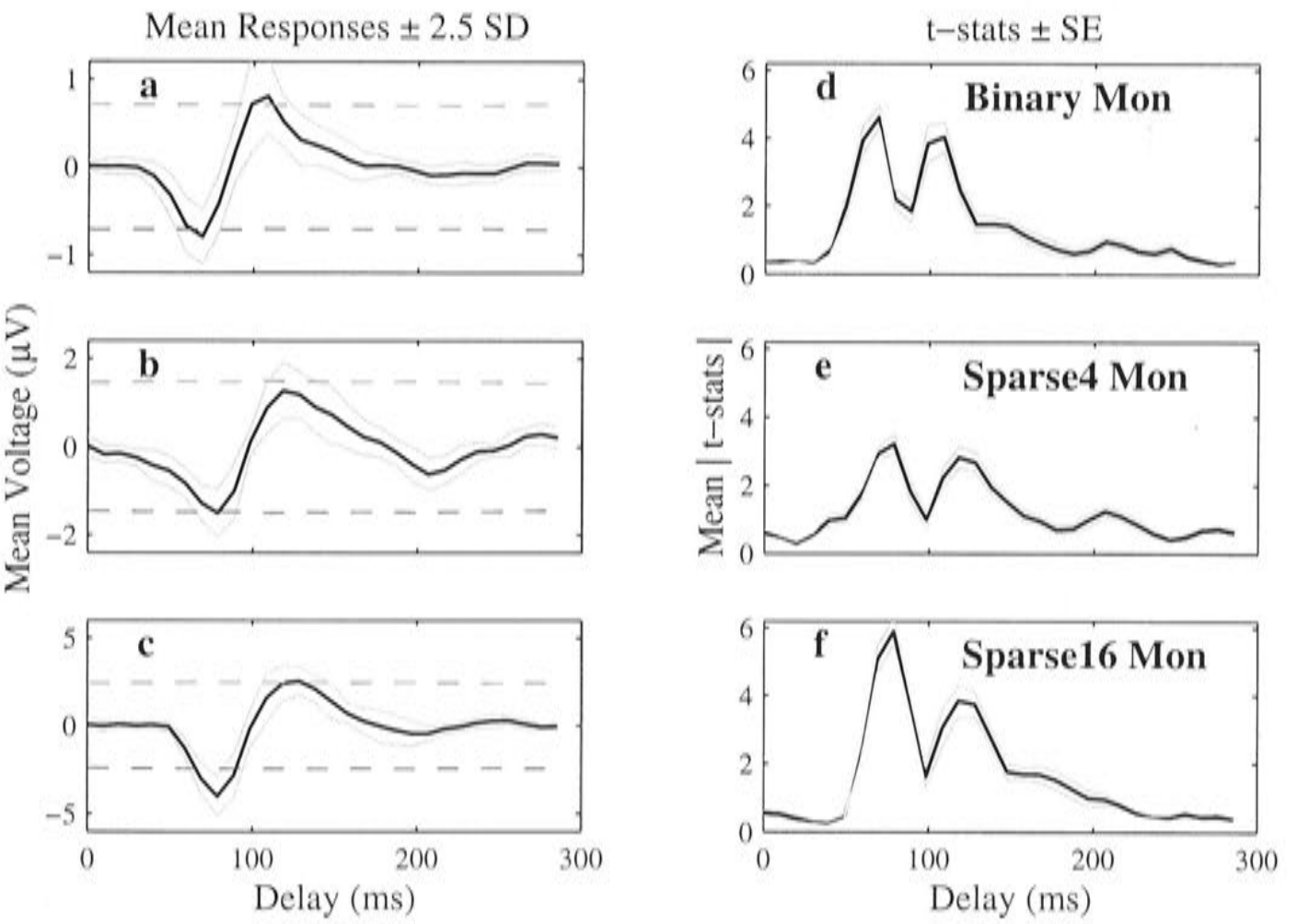

Figure 1.6 Averaged multifocal responses across all eight regions and 13 subjects for the monocular viewing condition. The left column shows the mean voltages for the Binary, $Sparse_4$ and for $Sparse_{16}$ condition (rows). The right column represents t-statistics for the rectified kernel data (the same sparseness as in the left column). Solid waveforms symbolise the averaged kernel data. Grey waveforms in the left column are ± standard deviations (in the right column - ±SE). The horizontal dashed lines in the left column symbolize 2.5 standard errors from the regression process estimating the slices (representing the 95% confidence level). See text for explanation of the symbols.

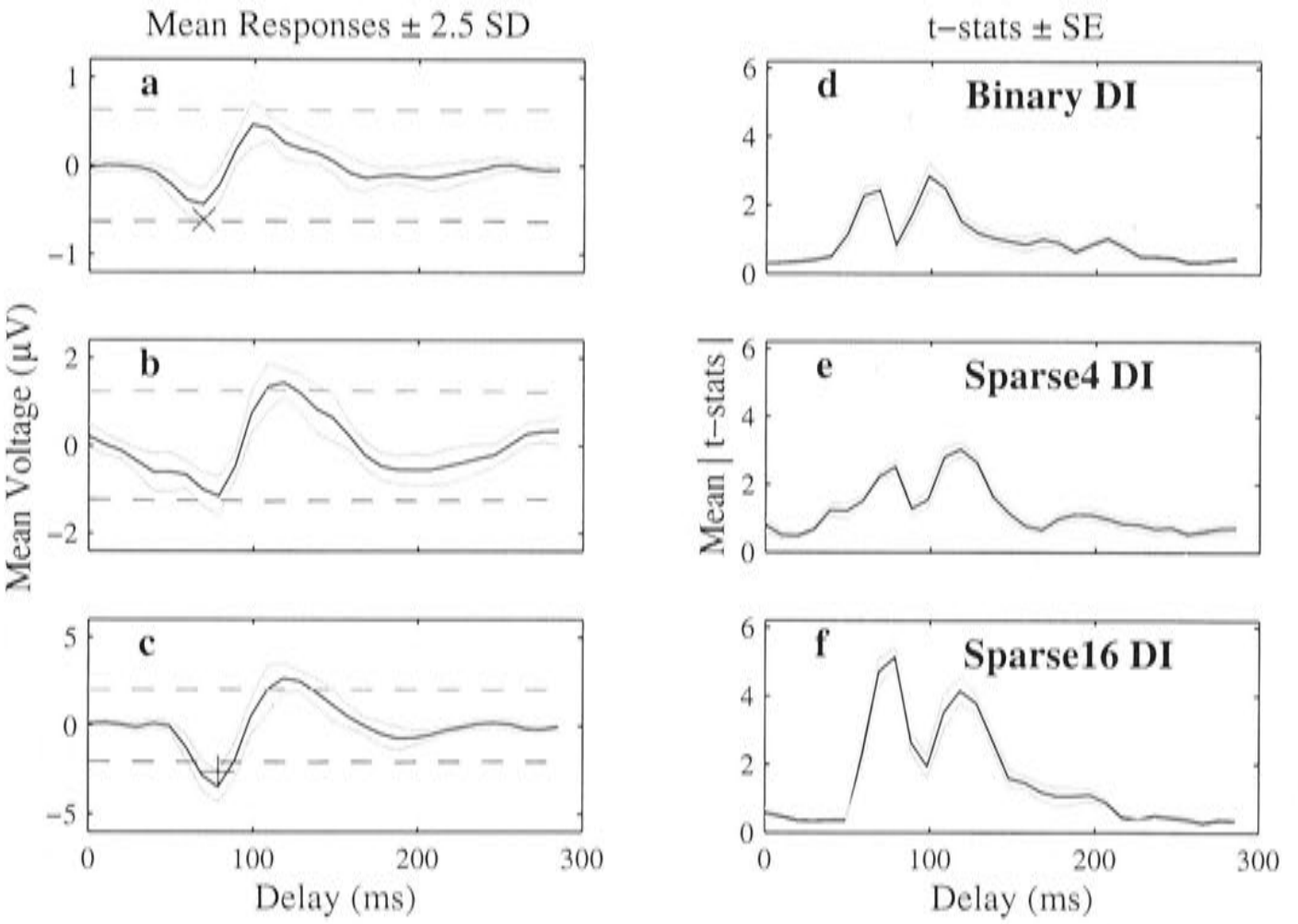

Figure 1.7 Averaged multifocal responses across all eight regions and 13 subjects for the dichoptic viewing condition. The axis conventions are the same as in Figure 6. **a)** Binary response significance. Only about 15% of all responses are significant (the '**x**' marker on the standard deviation line). **c)** Represents the $Sparse_{16}$ response significance (the '**+**' marker on the standard deviation line, when ~90% reaches the confidence level). T-statistics (the left column of the figure) show the strongest response to the $Sparse_{16}$ visual stimulus, however the responses are stronger for monocular viewing.

We have also found that for all sparseness the inferior – central regions 2 and 4 tended to provide more transient, triphasic, responses for all test conditions (Fig.1.8). Regions 2 and 4 can thus be called "fast" responses, as their N1 peaks appear ~16.7 ms earlier than the responses from other regions. The fast responses are presented in a picture as black waveforms.

Regions and Responses

Our stimulus was partitioned into eight different visual field regions (Fig.1.1). Figure 1.9 shows N1 mean responses, averaged across subjects, presented in an image format, where the stimulus regions are colour according to the average N1 response for that region. The rows of panels in Figure 1.9 represent Binary, $Sparse_4$ and $Sparse_{16}$ stimuli. The central two columns indicate average responses to monocular stimuli, and the outer two columns responses to dichoptic viewing conditions. Light colours represent higher amplitudes, and darker regions - lower amplitudes for the N1 means respectively. Notice that the rows have separate grey-level calibrations (vertical scale bas at right of each row). Here the relatively greater suppression of responses to dichoptic binary stimuli relative to dichoptic $Sparse_{16}$ stimuli is very evident. Variances (not shown) for the same data scale linearly with the response means.

Model Fit and Regression Analysis

In an attempt to quantify the picture presented in Figure 1.9 we examined the independent effects generating that picture through a generalized regression analysis

(see *Methods* section). Data are presented here for mean responses for the N1 window. A parsimonious model of the data is provided by (simultaneously) fitting N1 values for each sparseness (Binary, $Sparse_4$ or $Sparse_{16}$), an interaction between $Sparse_{16}$ sparseness and Superior visual fields, and interaction between the Binary and $Sparse_{16}$ stimuli and Dichoptic viewing. The fitted values are shown in Table 1.1. The regression statistics for the overall model were $F=114.6_{18,1230}$, $p = 0.0000$. The goodness of fit was $r^2 = 0.68$.

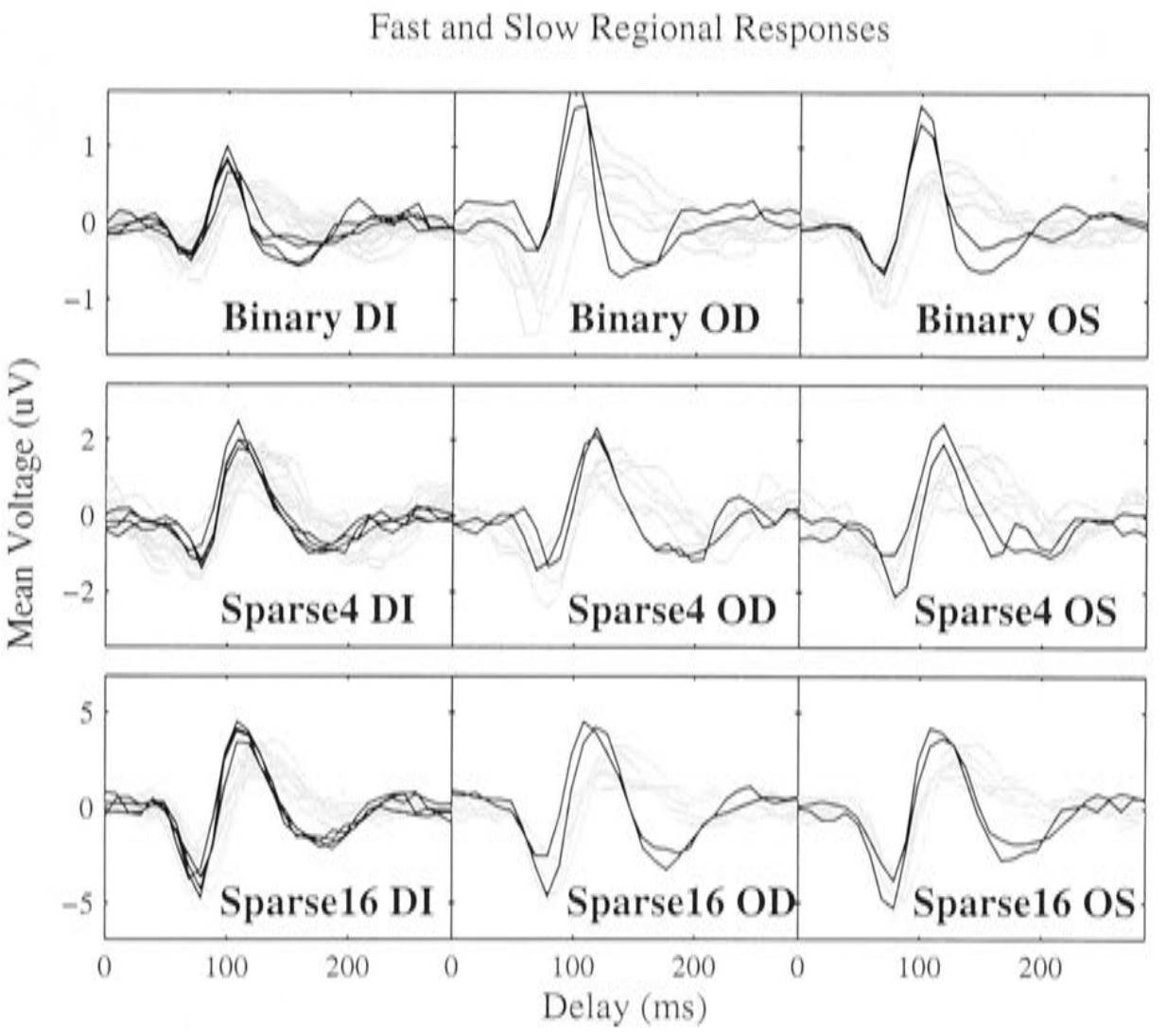

Figure 1.8 Fast and slow regional responses. Each panel represents the averaged responses across the 13 subjects, according to the viewing condition (columns dichoptic, monocular left and right); as well to the sparseness (rows Binary, $Sparse_4$ and $Sparse_{16}$). The black coloured waveforms represent responses of the inferior central stimuli (region 2 and 4), which appear faster than the other (grey waveforms).

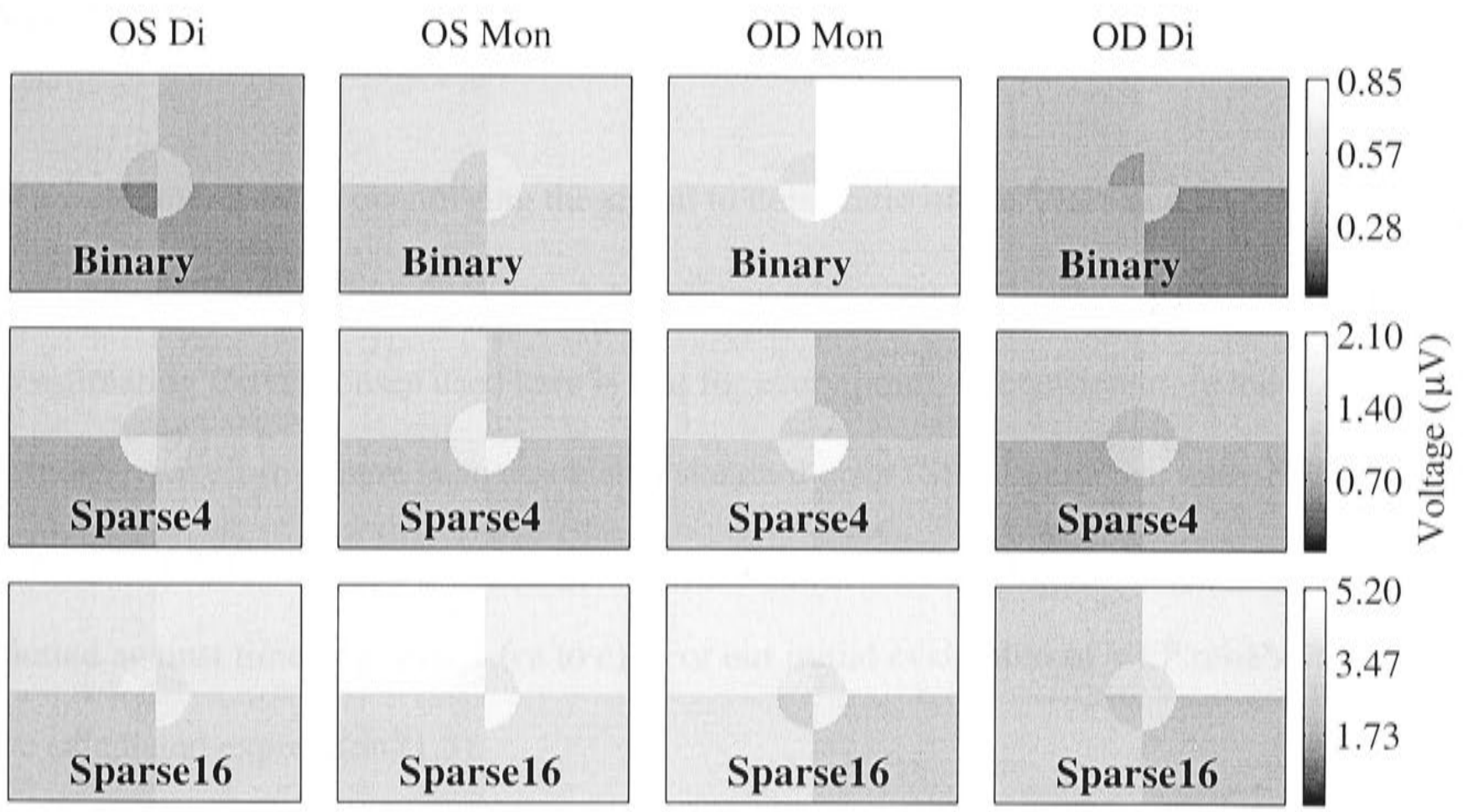

Figure 1.9 Monocular data versus dichoptic. The left columns represent voltage responses averaged across subjects for the eight regions of the left eye (OS), dichoptic (DI) and monocular (Mon) viewing condition. The three rows correspond to the sparsenesses: Binary, $Sparse_4$ and $Sparse_{16}$. Lighter colors represent higher voltages. The right columns (OD Mon and OD Di) represent responses averaged across subjects for the eight regions of the right eye (OD), dichoptic (DI) and monocular (Mon) viewing conditions. There is an obvious effect of dichoptic viewing, for the OS Di and OD Di. The right – most colorbar represents amplitudes (in μV) for three temporal stimuli.

There was more suppression for dichoptic viewing for $Sparse_{16}$ stimulus in the superior field. The fitted parameters reflect the situation shown in the average data (Fig. 1.9). Peak N1 responses provided very simular results (not shown).

Signal vs. Noise

We were interested in quantifying the signal to noise ratio of the VEPs and its implications for recording duration. A significant advantage of the regressive approach to estimating the responses used here is that for every point, or coefficient, in the response waveforms there is an associated standard error (SE). In practice these SE are very similar for each coefficient and therefore they appear as horizontal lines when plotted against time (e.g. Fig. 1.6 a to c). For our initial evaluation of VEP reliability we calculated expression (1.3).

$$\log(SE) = \log(k) + z\log(M) \qquad (1.3)$$

that is equivalent to

$$SE = kM^z \qquad (1.3.1)$$

or

$$1/k = M^z/SE \qquad (1.3.2)$$

M and SE are the individual mean N1 and SE values within the N1 window (*Methods*). Recall that SE values are obtained for each response point via the regressive kernel estimation procedure. Since we are using mean N1 values within the N1 window, we also computed the mean SE values for the same response region. The factor 1/k can be thought of as signal to noise ratio, but only if $z=1$. If z differs from 1 then a single signal to noise ratio (SNR) is invalid. In general we found in regressive fits to Eq. 3 that z was significantly < 1 (Table 1.2), i.e. *the error grows more slowly than the mean peak*

amplitude. Hence the signal reliability improves nonlinearly as response amplitude increases.

Table 1.1 Summarized generalized regression results for each model parameter. The coefficients show the simultaneously fitted values for the conditions in the left-most column, which identifies the experimental conditions. The values for Binary, $Sparse_4$, $Sparse_{16}$ are the respective mean amplitude in the N1 window. Note that at 5.33 ± 0.3 SE (μV) the $Sparse_{16}$ responses are about four times the Binary ones for all viewing conditions. The row labeled Bin * Dich describes an interaction for the Binary stimulus indicating a suppression of those responses by 0.49 ± 0.22 SE μV for dichoptic viewing. The corresponding binocular suppression for the $Sparse_{16}$ stimulus (Sp_{16}*Dich) is 0.69 ± 0.22 SE μV. There was no significant binocular interaction for $Sparse_4$. The Sup* Sp_{16} interaction indicates that 1.06 ± 0.22 SE μV needs to be subtracted from responses obtained for the superior visual field for $Sparse_{16}$ stimuli in the dichoptic viewing condition.

Condition	Coefficient (μV)	SE	t	p
Binary	1.33	0.27	4.84	0.0000
$Sparse_4$	1.91	0.25	7.61	0.0000
$Sparse_{16}$	5.33	0.30	18.18	0.0000
Sup* Sp_{16}	-1.06	0.22	4.73	0.0000
Bin*Dich	-0.49	0.22	2.20	0.0302
Sp_{16}*Dich	-0.69	0.22	3.05	0.0025

Figure 1.10 summarises the relationship between the N1 means and their standard errors. Figure 1.10a shows raw data for the $Sparse_4$ dichoptic stimulus, and a fitted curve computed according Eq. 1.3. Since a single SNR is invalid it makes sense to consider the individual SNR_i for each response waveform measured

$$SNR_i = M_i / SE_i \qquad (1.4)$$

Here the M refers to the mean response value within the N1 window. The two histograms of Figure 1.10b show the frequency of occurrences of the SNR_i for dichoptic Binary stimuli (black bars) and dichoptic $Sparse_{16}$ stimuli (white bars), again for the N1 means. Consistent with the finding of $z < 1$ from the fit, the values SNR_i are only somewhat larger for the Sparse 16 stimulus. Since the fits to Eq. 1.3 appear to be born out by the SNR_i it makes sense to derive an expression that shows how the SNR improves with M. This is accomplished by substituting Eq. 1.3.1 into Eq. 1.4 to obtain

$$SNR = \frac{M}{SE} = \frac{M}{kM^{z}} = \frac{1}{k} M^{(1-z)} \qquad (1.5)$$

Figure 1.10c illustrates how the fitted SNR (Eq. 1.5) for Binary (dotted line) and $Sparse_{16}$ (solid line) changes over the range of observed N1 (M) values. The solid and open circle markers on the dotted line shows the SNR values computed for the median and mean (respectively) N1 values for the Binary stimulus (Table 1.2). Similarly the solid and open pentagram markers on the solid line indicate the median and mean SNR values for the $Sparse_{16}$ stimulus. Notice that the tabulated values of SNR_i, and the computed SNR values of the symbols of Figure 1.10 are in good agreement. Since the SNR_i values in Table 1.2A are medians we compare them with the predicted SNR values from Eq. 1.5 obtained for the median N1 values (closed symbols of Fig. 1.10c). For the Binary stimulus (dichoptic) the tabulated value is 2.93 ± 0.22, while the SNR

from the fitted function is 2.18. For the Sparse_{16} stimulus the tabulated value is 5.13 ± 0.31, while the predicted value from the fit is 4.20.

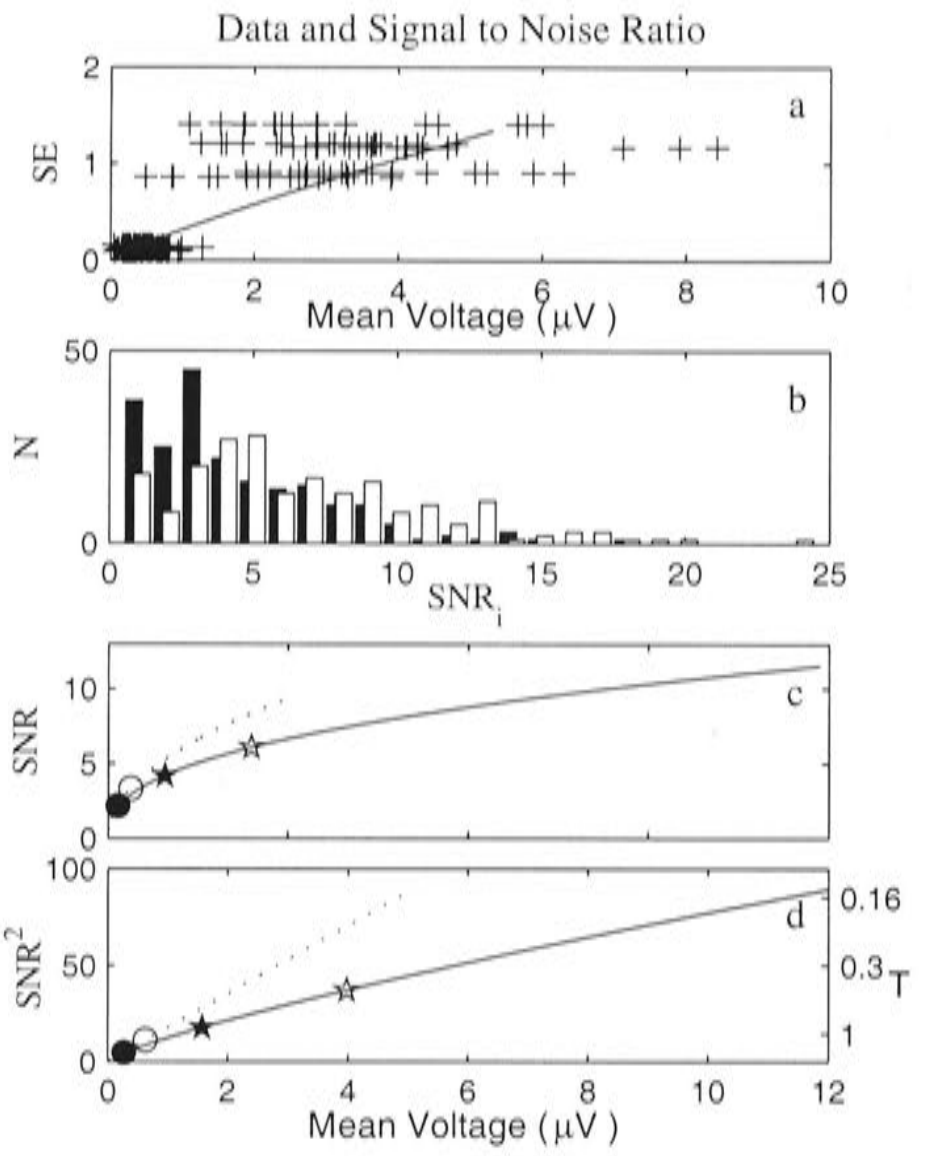

Figure 1.10 Signal versus noise. **a)** Raw N1 data for the dichoptic $Sparse_4$ stimulus across all the subjects. Each point represents the mean response for a region and subject within the N1 window (abscissa), plotted against the mean SE values for those N1 response coefficients (ordinate). The solid line shows the fitted curve for Eq. 3. As shown in Table 2 the $Sparse_4$ conditions had the closest approach to a linear response between SE and M. **b)** Distribution of Binary and $Sparse_{16}$ SNR_i. The black bars represent the number of occurrences (N) for the Binary stimulus; the white bars are the histogram for the $Sparse_{16}$ stimulus. SNR values are larger for $Sparse_{16}$ stimulus. **c)** SNR for the dichoptic Binary and $Sparse_{16}$ stimuli, computed as in Eq. 1.5 for N1 data. The short dashed curve represents the Binary N1 data, and the long solid curve stands for the $Sparse_{16}$ N1 fit. In both cases curve length reflects the range of the observed N1 data in each case. The solid circle on the dotted line is the SNR obtained for the median Binary N1 value (Median N1 = 0.27μV, SNR(Median) = 2.18), the open circle indicates the SNR for the mean N1 value (Mean = 0.63μV, SNR(Mean) = 3.33). The solid and open pentagrams on the solid line show SNRs obtained for the median and mean $Sparse_{16}$ N1 values (Median N1 = 1.58μV, SNR(Median) = 4.20; Mean = 3.98 μV, SNR(Mean) = 6.08) . **d)** SNR^2. The conventions for the lines and symbols are as in **c**. The right ordinate axis shows how the relative recording time to achieve a criterion response, T, changes with respect to the SNR^2. Here the criterion is the time to achieve the mean Binary N1 response. This indicates the same SNR would be achieved for the Sparse 16 stimulus in 0.30 of the time.

The predicted values obtained for the mean N1 values (open symbols Fig. 1.10c) are a little higher at 3.33 and 6.08 for the Binary and $Sparse_{16}$ cases. Thus, the two methods give typical SNRs of about 3 and 5 for the Binary and $Sparse_{16}$ stimuli in the dichoptic viewing condition.

Figure 10d represents the SNR^2 for Binary and $Sparse_{16}$ visual stimuli in the dichoptic case. Since the fitted values of z are close to 0.5 (Table 1.1) this means the relationship between the N1 values and the SNR^2 is nearly linear (since $1\text{-}z \approx 0.5$, Eq. 1.5). The SNR^2 is proportional to the required recording time to achieve a given accuracy. We can therefore compute the relative recording time improvement (IMP) as the ratio of the SNR for different conditions.

$$IMP = \left(\frac{SNR_{Sparse16}}{SNR_{Binary}} \right)^2 \tag{1.6}$$

The last two rows of each of Tables 1.2A,B show the expected recording time improvement (IMP, Eq. 1.6) for $Sparse_{16}$ relative to Binary stimuli. The IMP values based on Mean or Median SNRs are shown in the Mean and Median N1 columns respectively. We expect about a 40% reduction for monocular viewing, and a 300% reduction for dichoptic presentation. The figure of 300% may also be interpreted as meaning that the effects of dichoptic viewing are so deleterious for Binary stimuli that 3 times more recording time would be required to obtain the accuracy found for the $Sparse_{16}$ stimulus, resented here in 8 repeats of 40 s, or 5.3 min. The right ordinate of Figure 1.10d shows the inverse of IMP (T).

Table 1.2 Tables A and B present data for mean amplitudes computed in the N1 and P1 window (Methods). In each table the mean, median (Md), and median signal to noise ratio, $SNR_i \pm SE$ (Eq.1.5) are given in the left three data columns. Mean SNR_i (not shown) were 1.19 ± 0.08 SE larger than the median values. Fitted values from Eq. 1.3 are given in the 3 rightmost columns. Row labels in the leftmost column having the suffix *Dich* represent dichoptic stimulation, while those with the suffix *Mon* represent the mean of left and right eye data for monocular conditions. The exponents, z, are all significantly < *1*. The IMP values shown in the bottom 2 rows are dimensionless and represent the relative improvement in recording time for using $Sparse_{16}$ rather than Binary stimuli in the dichoptic case. They are presented in the Mean and Median columns because there are based on Mean and Median SNRs. The reader may confirm the median N1 and P1 IMP values by taking the ratio of the squares of the appropriate values in the SNR_i Md columns.

A. N1 Values

N1	Mean (μV)	Md (μV)	SNR_iMd ± SE	log(k) ± SE	1/k	z ± SE
Binary Mon	1.13	0.40	5.37 ± 0.43	-1.35 ± 0.08	3.90	0.63 ± 0.04
Binary Dich	0.64	0.27	2.93 ± 0.22	-1.45 ± 0.08	4.20	0.49 ± 0.05
$Sparse_4$ Mon	1.87	0.76	3.74 ± 0.29	-0.94 ± 0.06	2.55	0.79 ± 0.04
$Sparse_4$ Dich	1.55	0.65	3.25 ± 0.13	-1.14 ± 0.06	3.10	0.86 ± 0.05
$Sparse_{16}$ Mon	4.67	1.81	6.44 ± 0.54	-0.90 ± 0.06	2.45	0.59 ± 0.04
$Sparse_{16}$ Dich	3.98	1.58	5.13 ± 0.31	-1.26 ± 0.07	3.50	0.63 ± 0.05
IMP Mon	1.38	1.44				
IMP Dich	2.67	3.06				

B. P1 Values

	Mean (μV)	Md (μV)	SNR_iMd ± SE	log(k) ± SE	1/k	z ± SE
Binary Mon	1.18	0.38	5.02 ± 0.48	-1.28 ± 0.07	3.85	0.66 ± 0.04
Binary Dich	0.67	0.28	3.14 ± 0.25	-1.43 ± 0.08	4.17	0.54 ± 0.05
$Sparse_4$ Mon	2.00	0.77	3.82 ± 0.28	-1.00 ± 0.06	2.72	0.85 ± 0.05
$Sparse_4$ Dich	1.96	0.70	4.08 ± 0.15	-1.30 ± 0.06	3.70	0.84 ± 0.05
$Sparse_{16}$ Mon	3.94	1.55	5.15 ± 0.46	-0.87 ± 0.06	2.38	0.65 ± 0.05
$Sparse_{16}$ Dich	3.69	1.43	4.94 ± 0.29	-1.21 ± 0.06	3.35	0.64 ± 0.05
IMP Mon	1.00	1.05				
IMP Dich	2.02	2.48				

Discussion

General Findings

Multifocal VEPs were recorded for nine different test conditions including three degrees of temporal sparseness, and monocular and dichoptic viewing. The mean N1 amplitudes for Binary are significantly smaller rather than for the $Sparse_{16}$ stimuli (Tables 1.1, 1.2). Multivariate linear regression provided estimates of the average N1 amplitudes and the effects of binocular suppression. We also examined P1, but found it had greater variance. Adding P1 to N1, while achieving a greater average amplitude, similarly increased variance. Hence we concentrated on N1 here. Binocular suppression was only significant for the Binary and $Sparse_{16}$ dichoptic stimuli, these effects appearing in the regression model as the interactions Bin*Dich and Sp_{16}*Dich (Table 1.2). The effects are additive so the ratio of responses measured for Binary and Sparse 16 stimuli in the dichoptic viewing condition is

$$\frac{\text{Sparse16} + \text{Sp16} * \text{Dich}}{\text{Binary} + \text{Bin} * \text{Dich}} = 5.53. \qquad (1.7)$$

This estimate from the regression model is in good agreement with the ratios of the mean or median N1 responses for dichoptic viewing at 6.21=3.98/0.64 and 3.95=1.58/0.4 respectively (figures from Table 1.2A).

The relative binocular suppressive effect was 0.33/0.13 = 2.53 times larger for Binary stimuli since

$$\frac{Bin * Dich}{Binary} < \frac{Sp16 * Dich}{Sparse16} = -\frac{0.49}{1.33} < -\frac{0.69}{5.33} = -0.33 < -0.13. \qquad (1.8)$$

These effects are readily observable when the average N1 data are presented as images (Fig. 1.9).

Signal Quality

The $Sparse_{16}$ responses are more consistent across visual field regions than the responses to Binary stimulus (cf. Fig. 1.4a, with 1.4b, and 1.5a with 1.5b). A possible contributing factor that has been suggested to us is the presence of following eye movements evoked by illusory motion effects between regions that are possibly greater for the Binary stimulus. We did not monitor eye movements but the large stimulus regions used would mitigate against this effect. Also large illusory motion effects were not observed, especially for dichoptic presentation where contrary motions were more likely. This logic would predict more stable responses in the dichoptic case and this seems to be true. This conclusion arises from examining the *variances* in the SNR_i. All dichoptic SNR_i variances were smaller than their monocular companions (not shown). Since the mean and median N1 and P1 responses are always smaller in the dichoptic case, and since the voltage data appear heteroskadastic, we scaled the dichoptic variances upward by the ratio of the appropriate dichoptic/monocular mean (or median) responses. Although this scaling made the dichoptic variances more similar to the larger monocular variances they were still significantly smaller whether scaled by the mean responses ($p=0.0030$) or the median responses ($p=0.0038$).

The relative reliability of responses obtained to Sparse stimuli suggested by Figures 1.4 to 1.7 was reflected in the signal to noise ratios (SNRs). Since the responses were estimated using a regressive method we could obtain SE for every point in every response waveform. We could thus compute both average responses amplitudes, and average SE, within the N1 and P1 time windows. These summary statistics for these individual SNR_i, calculated for all test conditions, are given in Table 1.1.

We also fit the N1 versus SE data to Eq. 1.3. Since the fitted exponents, z, were significantly < 1 (Table 1.2) a single SNR for each test condition is not valid, instead

SNR grows nonlinearly with response amplitude. Typical SNRs predicted by the model matched median and mean SNR_i values well. The similar values of z and k for Binary and $Sparse_{16}$ stimuli permit us to conclude a definite SNR advantage for the larger responses obtained to $Sparse_{16}$ stimuli.

SNR^2 is proportional to the time required for an experiment to achieve a criterion level of accuracy. Because the values of z obtained for all Binary and Dichoptic conditions were close to 0.5 (Table 1.2) this means that SNR^2 rises nearly linearly with N1 amplitude (Fig. 1.10d). In the dichoptic case Binary stimuli will therefore require about 3 times longer recording time (about 15 min.) to achieve the same level of accuracy as obtained for the $Sparse_{16}$ stimulus here. For monocular recording about a 40% improvement is predicted for $Sparse_{16}$ stimuli.

Another way of looking at this is the proportion of responses that reach significance within our test time of 8 repeated 40s stimuli. In the dichoptic case about 90% of responses were significant (2.5 SE) with $Sparse_{16}$ stimuli, while only about 15% of responses to Binary stimuli reached this level (Fig. 1.7).

Regional Effects

The entry labeled Sup* Sp_{16} in Table 1.2 is an interaction indicating that the 4 superior visual field regions are suppressed by 1.06 ± 0.22 SE μV for the $Sparse_{16}$ stimulus (Eq. 1.4). Another regional effect was that illustrated in Figure 1.8 where the responses from the inner 2 inferior regions 2 and 4 (Fig. 1.1) were more transient in our study for all stimuli and viewing conditions. Those responses could be so called fast because the N1 peak appears ~17 ms earlier than other responses. Such triphasic responses have been reported for transient VEP stimuli presented to the lower visual field (Jeffreys, 1971; Jeffreys & Axford, 1972). Triphasic responses in the lower central visual field have also

been reported for a 60 region Sparse mfVEP stimulus (James, 2003). We have subsequently re-estimated the kernels using the same number of slices for each stimulus type. This did not affect the conclusions of this study.

Larger Responses

Why were response amplitudes greater to the transient but infrequent $Sparse_{16}$ stimulus? The effect may in part be caused by a retinal gain control mechanism. Retinal ganglion cells that project to the magnocellular layers of the dorsal lateral geniculate nucleus (M-cells) have a strong luminance contrast gain control. The retinal gain control system acts so that responses to transiently presented visually large-scale (low spatial frequency) stimuli are enhanced (Victor *et al.*, 1977; Victor & Shapley, 1979a, b; Benardete *et al.*, 1992). For example, in response to a step change in contrast over time, the initial neural response of the M-cells to the initial response is greatly amplified (Victor, 1988). An increase in VEP response, and also in apparent contrast, for periodically presented transient, but infrequent, stimuli has been reported previously (Kulikowski, 1992). Interestingly, when low spatial frequency sinusoidal grating patterns are presented transiently at low contrasts their spatial frequency appears to be doubled . The spatial frequency doubling (FD) illusion has also been attributed to the same M-pathway gain control (Bedford *et al.*, 1997; Maddess *et al.*, 1997; Maddess *et al.*, 1998). Glaucoma patients see the FD illusion poorly (Maddess & Henry, 1992; Maddess *et al.*, 1999; Maddess & Severt, 1999; Maddess *et al.*, 2000a, b) and this is the basis (Maddess, 1989) for the quite successful FDT perimeter (for short reviews see Alward, 2000; Maddess, 2000).

The larger responses observed here should not be confused with the responses obtained in conventional VEPs in response to slow alternations of contrast. Waveforms

obtained for those slow stimuli do not invert for stimuli presented in the inferior visual field (e.g. Fortune *et al.*, 2002) as observed here and elsewhere for mfVEPs (Hood & Zhang, 2000; Hood *et al.*, 2000b; Goldberg *et al.*, 2002; James, 2003). The large, non-inverting responses observed for slow VEPs may have an extrastriate cortical origin.

James (2003) also used a form of sparse stimulation and simultaneously measured mfVEP responses to a 60 region stimulus at 30 scalp locations. In one subject he compared responses to Binary and Sparse stimuli showing that the distribution and shape of the responses recorded for every visual field and scalp location were very similar for the Binary and Sparse stimuli, differing principally in scale. In that case the sparse stimuli generated 15 times larger responses. In James (2003) the Sparse stimuli were delivered at a slower rate than here, and the pulse duration was 1.33 times longer. Unpublished studies indicate these factors explain the differences in amplitude reported in that study and the present one.

Clinical Implications

Multifocal stimulation is effective in characterising multiple sclerosis (Hood *et al.*, 2000a; Hood & Zhang, 2000; Hood *et al.*, 2000b). Since the optic nerve is somewhat retinotopically organised (Walsh, 1990) using several fairly large stimuli could characterise demyelination localized within relatively large confluent parts of the optic nerve. Smaller stimulus regions might be less effective as the relatively poor retinotopicity would result in cross-talk between the responses for damage to a single optic nerve location. Multifocal methods also appear to be useful for early detection of glaucoma (Klistorner *et al.*, 1998b; Klistorner & Graham, 1999; Hood & Zhang, 2000; Hood *et al.*, 2001; Goldberg *et al.*, 2002), diabetic retinopathy (Palmowski *et al.*, 1997; Fortune *et al.*, 1999; Greenstein *et al.*, 2000), and macular degeneration (Palmowski *et*

al., 1999). If the enhanced responses seen for Sparse stimuli reflect the same retina mechanisms as drive the FD illusion then we may expect Sparse stimuli to perform very well in the characterisation of glaucomatous visual field loss. For any disease process the reduced recording time obtained Sparse stimuli would sit well with patients. Dichoptic recording would assist even further and permits quantitative comparison of responses from the two eyes (Atkin *et al.*, 1980; Maddess & James, 1998; Maddess & Severt, 1999; Hood *et al.*, 2000b).

Bibliography

ALWARD, W. L. M. (2000). Editorial: Frequency doubling perimetry for the detection of glaucomatous field loss. *Am J Ophthalmol* **129,** 376-378.

ANDERSSON, T. & SIDEN, A. (1991). Multimodality evoked potentials and neurological phenomenology in patients with multiple sclerosis and potentially related conditions. *Electromyogr Clin Neurophysiol* **31,** 109-117.

ANDERSSON, T., SIDEN, A. & PERSSON, A. (1991). A comparison of clinical and evoked potential (VEP and median nerve SEP) evolution in patients with MS and potentially related conditions. *Acta Neurol Scand* **84,** 139-145.

ATKIN, A., WOLKSTEIN, M., BODIS-WOLLNER, I., ANDERS, M., KELS, B. & PODOS, S. M. (1980). Interocular comparison of contrast sensitivities in glaucoma patients and suspects. *Br J Ophthalmol* **64,** 858-862.

BEDFORD, S., MADDESS, T., ROSE, K. A. & JAMES, A. C. (1997). Correlations between observability of the spatial frequency doubled illusion and a multi-region PERG. *Aus NZ J Ophthalmol.* **25,** 91-93.

BENARDETE, E., KAPLAN, E. & KNIGHT, B. (1992). Contrast gain control in the primate retina: P cells are not X-like,some M cells are. *Visual Neurosci* **8,** 483-486.

BRACEWELL, R. N. (1986). Chapter 10. Sampling and series. In *The Fourier transform and its applications*, pp. 189-218. McGraw-Hill, New York.

FORTUNE, B., HOOD, D. & JOHNSON, C. (2002). Comparison of conventional and multifocal VEPs. In *ARVO*, pp. 2126, Ft. Lauderdale.

FORTUNE, B., SCHNECK, M. E. & ADAMS, A. J. (1999). Multifocal electroretinogram delays reveal local retinal dysfunction in early diabetic retinopathy. *Invest Ophthalmol Vis Sci* **40,** 2638-2651.

GOLDBERG, I., GRAHAM, S. & KLISTORNER, A. (2002). Multifocal objective perimetry in the detection of glaucomatous field loss. *Am J Ophthalmol* **133,** 29-39.

GREENSTEIN, V. C., HOLOPIGIAN, K., HOOD, D. C., SEIPLE, W. & CARR, R. E. (2000). The nature and extent of retinal dysfunction associated with diabetic macular edema. *Invest Ophthalmol Vis Sci* **41,** 3643-3654.

HOOD, D., BEARSE, M., SUTTER, E., VISWANATHAN, S. & FRISHMAN, L. (2001). The optic nerve head component of the monkey's (Macaca mulatta) multifocal electroretinogram (mERG). *Vision Res* **41,** 2029-2041.

HOOD, D., ODEL, J. & ZHANG, X. (2000a). Tracking the recovery of local optic nerve function after optic neuritis: a multifocal VEP study. *Invest Ophthalmol Vis Sci* **41,** 4032-4038.

HOOD, D. & ZHANG, X. (2000). Multifocal ERG and VEP responses and visual fields: comparing disease - related changes. *Doc Ophthalmol* **100,** 115-137.

HOOD, D., ZHANG, X., GREENSTEIN, V., KANGOVI, S., ODEL, J., LIEBMANN, M. & RITCH, R. (2000b). An interocular comparison of the multifocal VEP: a possible technique for detecting local damage to the optic nerve. *Invest Ophthalmol Vis Sci* **41,** 1580-1587.

JAMES, A. (1992). Nonlinear operator network models of visual processing. In *Nonlinear vision: determination of neural receptive fields, function, and networks*. ed. PINTER, R. & NABET, B., pp. 31-74. CRC Press, Ann Arbor.

JAMES, A. (2003). The pattern pulse multifocal visual evoked potential. *Invest Opthalmol Vis Sci*, 2003;44:879-890.

JAMES, A. & MADDESS, T. (2000). Method and apparatus for assessing neural function by sparse stimuli; Australia Patent No. Patent App. PQ 6465-00.

JAMES, A., MADDESS, T., PRICE, N. & YE, N. (2000). Dichoptic multiregion VEP kernels from short binary and ternary sequences. In *ARVO*, vol. 41, pp. S490. Invest Opthalmol Vis Sci, Florida, USA.

JEFFREYS, D. (1971). Cortical source locations of pattern-related visual evoked potentials recorded from the human scalp. *Nature* **229,** 502-504.

JEFFREYS, D. & AXFORD, J. (1972). Source locations of pattern-specific components of human visual evoked potentials. I.Component of striate cortical origin. *Exp Brain Res* **16,** 1-21.

JOHNSON, R. & WICHERN, D. (1992). *Applied multivariate statistical analysis*. Prentice-Hall, Inc.

JONES, S. (1993). Visual evoked potentials after optic neuritis. Effect of time interval, age and disease dissemination. *J Neurol* **240,** 489-494.

KLIEN, S. (1992). Optimizing the estimation of nonlinear kernels. In *Nonlinear vision: determination of neural receptive fields, function, and networks*. ed. PINTER, R. & NABET, B., pp. 31-74. CRC Press, Ann Arbor.

KLISTORNER, A. & GRAHAM, S. (1999). Multifocal pattern VEP perimetry: analysis of sectoral waveform. *Doc Ophthalmol* **98,** 183-196.

KLISTORNER, A., GRAHAM, S., GRIGG, J. & BILLSON, F. (1998a). Electrode position and the multi-focal visual-evoked potential: role in objective visual field assessment. *Aust Nz J Ophthalmol* **26(Suppl.),** 91-94.

KLISTORNER, A., GRAHAM, S., GRIGG, J. & BILLSON, F. (1998b). Multifocal topographic visual evoked potential: improving objective detection of local visual field defects. *Invest Ophthalmol Vis Sci* **39,** 937-950.

KULIKOWSKI, J. (1992). Contrast and contrast constancy: sustained and transient components. *Irish J PsychoL* **13,** 473-493.

KULIKOWSKI, J. J. (1975). Apparent fineness of briefly presented gratings: balance between movement and pattern channels. *Vision Res* **15,** 673-680.

LEE, Y. & SCHETZEN, M. (1965). Measurement of Wiener kernels of a non-linear system by cross-correlation. *Int J Control* **2,** 237-254.

MADDESS, T. (1989). Method and apparatus for use in diagnosis of glaucoma; USA Patent No. 5,065,767.

MADDESS, T. (2000). Perspectives on the use of frequency doubling and short wavelength perimetry for the diagnosis of glaucoma. *Clinical Exp Ophthalmol* **28,** 245-247.

MADDESS, T., BEDFORD, S., JAMES, A. & ROSE, K. (1997). A multiple - frequency, multiple-region pattern electroretinogram investigation of non-linear retinal signals. *Aust Nz J Ophthalmol* **25,** 94-97.

MADDESS, T., GOLDBERG, I., WINE, S., DOBINSON, J., WELSH, A. H. & JAMES, A. C. (1999). Testing for glaucoma with the spatial frequency doubling illusion. *Vision Res.* **39,** 4258-4273.

MADDESS, T., HEMMI, J. & JAMES, A. C. (1998). Evidence for spatial aliasing effects in the Y-like cells of the magnocellular visual pathway. *Vision Res.* **38,** 1843-1859.

MADDESS, T. & HENRY, G. H. (1992). Nonlinear visual responses and visual deficits in ocular hypertensive and glaucoma subjects. *Clin Vis Sci* **7,** 371-383.

MADDESS, T. & JAMES, A. (1998). Simultaneous binocular assessment of multiple optic nerve and cortical regions in diseases affecting nerve conduction; USA Patent No. 6,315,414.

MADDESS, T., JAMES, A., GOLDBERG, I., WINE, S. & DOBINSON, J. (2000a). Comparing a parallel PERG, automated perimetry, and frequency-doubling thresholds. *Invest Ophthalmol Vis Sci* **41,** 3827-3832.

MADDESS, T., JAMES, A., GOLDBERG, I., WINE, S. & DOBINSON, J. (2000b). A spatial frequency - doubling illusion -based pattern electroretinogram for glaucoma. *Invest Ophthalmol Vis Sci* **41,** 3818-3826.

MADDESS, T. & SEVERT, W. (1999). Testing for glaucoma with the frequency-doubling illusion in the whole, macular and eccentric visual fields. *Aust N Z J Ophthalmol* **27,** 194-196.

PALMOWSKI, A. M., SUTTER, E. E., BEARSE, M. A., JR. & FUNG, W. (1997). Mapping of retinal function in diabetic retinopathy using the multifocal electroretinogram. *Invest Ophthalmol Vis Sci* **38,** 2586-2596.

PALMOWSKI, A. M., SUTTER, E. E., BEARSE, M. A., JR. & FUNG, W. (1999). [Multifocal electroretinogram (MF-ERG) in diagnosis of macular changes. Example: senile macular degeneration]. *Ophthalmologe* **96,** 166-173.

REGAN, M. & REGAN, D. (1989). Objective investigation of visual function using a nondestructive zoom-FFT technique for evoked potential analysis. *Can J Neurol Sci* **16,** 168-179.

SAND, T., SJAASTAD, O., ROMSLO, I. & SULG, I. (1990). Brain-stem auditory evoked potentials in multiple sclerosis: the relation to VEP, SEP and CSF immunoglobulins. *J Neurol* **237,** 376-378.

SAND, T. & SULG, I. A. (1990). Evoked potentials and CSF-immunoglobulins in MS: relationship to disease duration, disability, and functional status. *Acta Neurol Scand* **82,** 217-221.

STENAGER, E. & JENSEN, K. (1990). Multiple sclerosis: symptom equivalent to delayed visual evoked potential latency. *Acta Ophthalmol Copenh* **68,** 587-590.

SUTTER, E. (1992). A deterministic approach to nonlinear systems analysis. In *Nonlinear vision: determination of neural receptive fields, function, and networks*. ed. PINTER, R. B. & NABET, B., pp. 31-74. CRC Press, Ann Arbor.

VICTOR, J. & SHAPLEY, R. (1979a). The nonlinear pathway of Y ganglion cells in the cat retina. *J PHYSIOL* **74,** 671-689.

VICTOR, J. & SHAPLEY, R. (1979b). Receptive field mechanism of cat X and Y retinal ganglion cells. *J Physiol* **74,** 275-298.

VICTOR, J., SHAPLEY, R. & KNIGHT, B. (1977). Nonlinear analysis of cat retinal ganglion cells in the frequency domain. *Neurobiol* **74,** 3068-3072.

VICTOR, J. D. (1988). The dynamics of the cat retinal Y cell subunit. *J Physiol***405,** 289-320.

WALSH, T. (1990). The fields of vision. In *Visual fields, examination and interpretation.* ed. WALSH, T., pp. 1-29. American Academy of Ophthalmology, La Jolla.

CHAPTER II

Sparse Multifocal Stimuli for the Detection of Multiple Sclerosis

Abstract

Purpose. To compare the diagnostic capabilities of contrast reversing and Sparse multifocal visual evoked potentials (mfVEPs) in Normal subjects and Multiple Sclerosis (MS) patients.

Methods. Dichoptic multifocal VEPs were recorded with 8 stimuli per eye. Four levels of temporal sparseness: Binary, $Sparse_4$, $Sparse_{16}$ and Pattern Pulse were examined. Multifocal responses were obtained from 27 Normal subjects and 50 MS patients, 26 of whom had experienced Optic Neuritis (ON). We employed multiple regression, principal components (PCA) and discriminant analysis to quantify any differences between the Normal and MS study groups in terms of response sizes, waveform shape and latencies.

Results. Compared to Normal subjects the MS patients had delayed VEP waveforms (mean delays of 26.15 ± 1.24 ms). The responses of MS subjects were also smaller than those of Normal subjects for temporally sparse stimuli. A classification model, containing the maximum fitted latencies (NT_F) to Pattern Pulse stimulus, gave the best performance at 100% sensitivity and 100% specificity for Normal versus MS subjects with ON. This model was also able to classify 100% of the MS subjects, who had not experienced ON. Bootstrap estimates of performance on earlier stage patients indicated sensitivities of 92% ± 3.3 SE at 100% specificity (0% False Positive rate) for the Pattern Pulse stimulus. By contrast at 92% sensitivity the Binary stimulus would misdiagnose more than 20% of the Normal population.

Conclusions. Multifocal VEPs recorded using temporally sparse stimuli are a useful tool with which to diagnose MS and ON patients.

Introduction

Visual evoked potentials (VEPs) to checkerboard stimuli are often recorded to evaluate the functional visual nervous system from the eye to brain (Weinstein *et al.*, 1991). In particular, various types of VEPs have been used to detect multiple sclerosis (MS) (Chiappa, 1983; Andersson *et al.*, 1991; Towle *et al.*, 1991; Hood *et al.*, 2000). MS is a central nervous system (CNS) disease, characterized by multiple areas of demyelination (Robinson & Rudge, 1977; Waxman, 1983; Prineas *et al.*, 1993; Brinar, 2002; Chamczuk *et al.*, 2002; De Stefano *et al.*, 2003; Barnett & Prineas, 2004). It has its onset in the third or fourth decade of life, and the risk reaches its peak at about age 30 years. It is also known, that MS is between 1.4 and 2 times more common in women than in men (Waxman, 1983).

MS patients initially report motor symptoms such as "weakness" or sensory symptoms like "burning" or "pressure". Abnormalities of vision are present in many patients as well. These abnormalities are the result of lesions of the optic nerve; resulting from optic neuritis (ON). Patients with ON can have "blurred vision", or "haziness", which can progress to complete loss of vision. There is often some loss of visual acuity as well (Waxman, 1983).

Previous studies report abnormal VEPs in MS patients (Chiappa, 1983; Andersson *et al.*, 1991; Towle *et al.*, 1991; Hood *et al.*, 2000). The aberrant waveforms found are thought to be caused by differential demyelination of components of the optic nerve (Waxman, 1983). Thus MS subjects' VEP responses can consist of the sum of one or more differently delayed waveforms, a concept we will deal with here.

Multifocal stimulation is effective in detecting MS (Hood *et al.*, 2000). Retinotopic mapping (Wandell, 1995) allows abnormality in the visual field to be traced to a lesion at a set of points along the visual pathway. Large multifocal stimuli could

characterize demyelination localized within parts of the roughly retinotopic optic nerve with relatively little cross-talk. Hence, abnormal responses from particular parts of visual field can tell us about differential demyelination of sub-sections of the optic nerve. Previous multifocal experiments have shown (James, 2003; James *et al.*, 2004) that sparser stimuli produced larger responses with higher signal to noise ratios than traditional contrast reversing stimuli in Normal subjects. We therefore decided to examine mfVEPs of MS patients obtained to different levels of temporal sparseness. We further attempted to decompose the mfVEP responses into one or more delayed versions of the average normal VEPs. Classification models based on a range of response measures were constructed to discriminate normal subjects from those with ON. These classification models were then applied to MS patients who showed no previous ON. Sensitivities and specificities for both patient groups were compared.

Methods

Stimuli

The multifocal stimuli used are described in more detail in earlier studies (James, 2003), (James *et al.*, 2004) and CHAPTER I.. Subjects viewed the monitor from a distance of 30 cm providing the stimulus layout illustrated in Figure 2.1. A bright red fixation cross was presented at the screen's centre.

Visual stimuli were presented dichoptically. We used a single monitor and interleaved the images for the left and right eyes on alternate video frames. This was achieved by means of a liquid crystal stereoscopic modulator (or shutter) (Tektronix, Inc., Beaverton, OR, USA). The non-interlaced frame rate of the monitor was 101.5 Hz, producing 50.75 images/eye following the shutter. A detailed description of the dichoptic set-up is given in James *et al.* (2004).

The temporal contrast modulation of the cortically scaled checkerboard regions illustrated in Figure 2.1 could take the values ±1 or 0, each region, being independently modulated in time with binary or ternary noise sequences as illustrated by Figure 2.2. A contrast of 0 corresponded to a region being blank at the mean luminance. Bright and dark checks had contrasts 1 and -1 respectively.

We examined four different densities of temporal contrast modulation sequences (Fig. 2.2). Three of them (Binary, $Sparse_4$ and $Sparse_{16}$) were used in our previous experiments (James *et al.*, 2004) on Normal subjects. In the Binary case contrast reversal occurred at a mean rate of 25.4 rev/s/eye. A mean rate of 25.4 presentations/s/eye occurred in the $Sparse_4$ condition. In the $Sparse_{16}$ sequence non-null stimuli appeared at a mean rate of 6.34 presentations/s/eye.

We also used the Pattern Pulse stimulus (James, 2003), which is a *very sparse* stimulus, given that the non-null stimuli appeared at a mean rate of 4/3 presentations/s/eye. For the Pattern Pulse stimulus two consecutive presentations in a

given region were separated by an interval uniformly distributed between 400 and 600ms. Each presentation could be left-eye, right-eye, or binocular, with equal probability. Thus each of left-eye, right-eye and binocular stimuli appeared at a mean rate of 2/3 per second (James, 2003) (Fig. 2.2d).

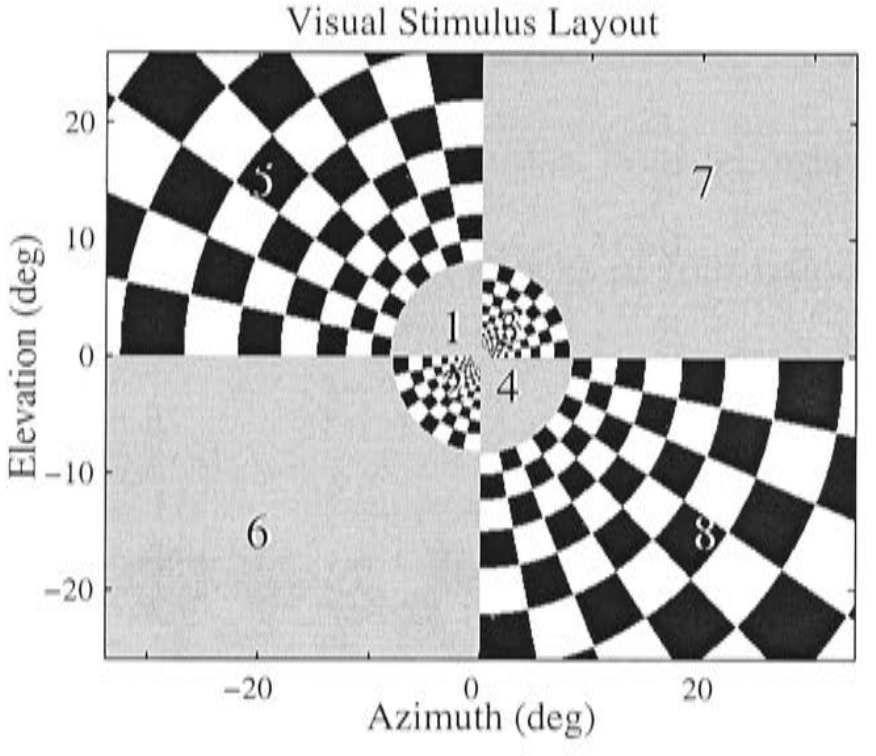

Figure 2.1 Illustration of the visual stimulus presented to each eye. Dichoptic stimulation provided 8 independent stimuli per eye. The numbers (1…8) are indices to the eight different regions. The figure shows a possible frame of a Sparse ternary sequence (*Methods*).

Recording

Multifocal Visual Evoked Potentials (mfVEPs) were recorded by using gold cup electrodes (diameter = 8 mm) secured on the scalp by the conductive paste EEG Ten20 (D.O.Weaver and Co, Aurora, LO). Electrodes were attached 3 cm above and 4 cm below the inion (Klistorner *et al.*, 1998). An earth electrode was attached to the right ear lobe. Signals were amplified 50 000 times and filtered between 1.6 and 40 Hz. Each stimulus sequence lasted 40.4 s, or 4096 video frames. Four records for each test condition were obtained during the experiment. Blocks of four repeats were presented in a randomized order.

Subjects

The diagnosis of MS requires a number of clinically recognizable attacks and objective lesions. We employed the latest MS diagnostic criteria(McDonald *et al.*, 2001) to classify our subjects. The MS study group contained 50 subjects (8 men and 42 women, age range 25 to 64 (mean of 45 ± 15.2 year)), with normal or corrected to 6/9 refraction. Twenty-six patients had suffered optic neuritis (ON). Eight of twenty-six ON patients had remyelination (as evidenced by their clinical history) of the optic nerve. MS type was Relapsing Remitting (RR) for all MS patients. The Normal study group contained 27 subjects (12 men and 15 women, age range 22 to 69 (mean of 43.1 ± 12.14 year)), with normal or corrected to normal refraction. The subjects' data are summarized in Table 2.1. All diagnoses were confirmed by the same neurologist.

A Frequency Doubling Technology (FDT) perimeter (Humphrey, San Leandro, CA) was used to test subjects' visual fields before the first test session. Each subject was first given the C-20 screening test followed by the Full Threshold C-20 program of

the FDT. The research followed the tenets of the Declaration of Helsinki, under the Australian National University's Human Experimentation Ethics Committee under protocol M9901. Informed written consent was obtained from the subjects after the nature and possible consequences of the study were explained to them.

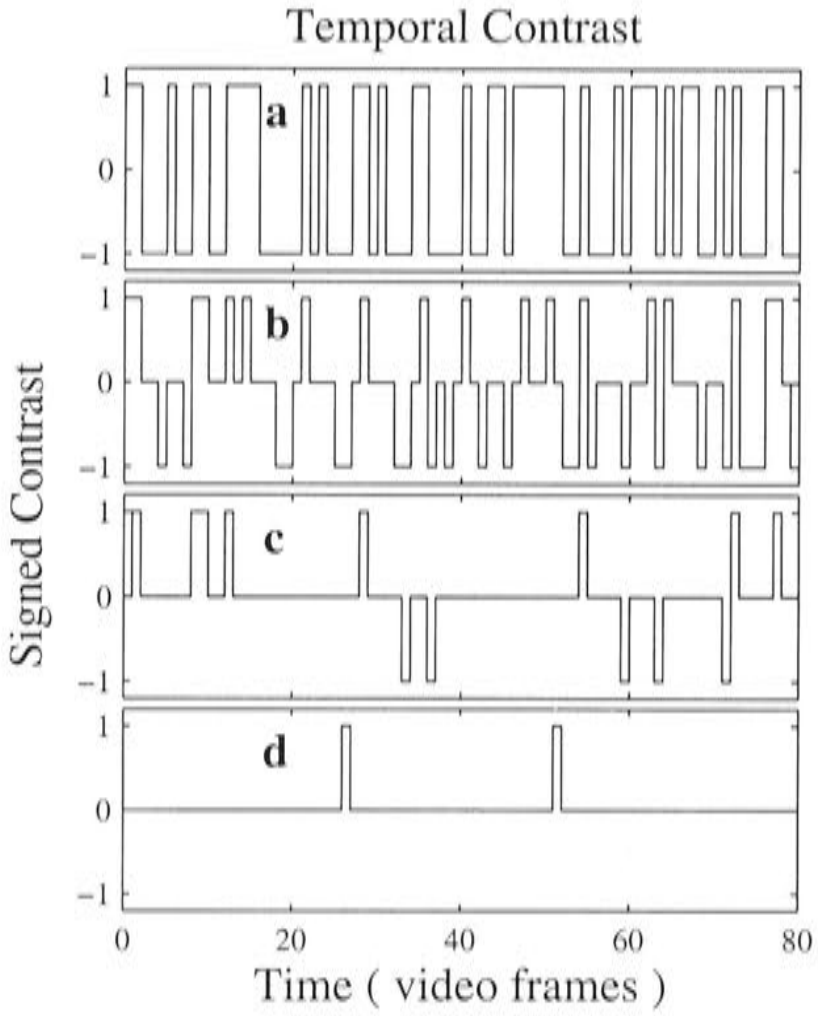

Figure 2.2 Example of the temporal contrast modulation, *c(t)*, applied to a single stimulus region. **A)** Temporal contrast modulation for the Binary stimulus having probability of ½ that the temporal contrast modulation function, *c(t)*, takes the values –1 or 1. **B)** $Sparse_4$ stimulus, when the probability of *c(t)* taking the value –1 or 1 on a given frame was ¼. **C)** $Sparse_{16}$, when the probability of *c(t)* taking the value –1 or 1 was 1/16. **d)** Pattern Pulse when the probability of *c(t)* taking the value 1 at a given frame was about 1/39. The stimuli in **b), c)** and **d)** are ternary; the check contrast taking the values {-1, 0, 1}. The minimum duration of the stimuli (*Time* axis) is 9.9 ms.

Table 2.1 Subject data. The two columns at the left indicate the study groups (MS, ON and Normal) and the number of subjects who participated in the experiments. 26 subjects had optic neuritis (*ON* row) and for 16 of them a CSF Oligobanding test was positive (*CSF*).

Study group	N	Age ± SE (yr)	Sex (M/F)	Duration of MS (yr)	N of attacks	ON	CSF	MS type
MS	24	43 ± 15.2	6/18	8.65 ± 6.6	9.49 ± 4.8	NO	7	RR
ON	26	42 ± 16.3	2/24	8.12 ± 7.6	10.1 ± 5.6	YES	9	RR
Normals	27	43.1 ± 12.1	12/15	NA	NA	NA	NA	NA

Data Analysis

The regression method used to estimate the multifocal responses (James, 2003; James *et al.*, 2004) provides a standard error (SE_i) for each point, or coefficient β_i in the response. SE_i were also useful in determining the signal to noise ratio (SNRs) for the responses because the SE_i allowed us to calculate *running* t-statistics (β_i/SE_i), which give an indication of the significance of the response at each time point (James *et al.*, 2004).

Within each response we analysed two time periods. For the Normal study group the first two peaks of all the responses were contained in the temporal windows 59.4 to 99 ms and 100 to 158 ms. By inspecting Figures 2.1 and 2.3 we can see that responses of Normal subjects were inverted for the superior field. We therefore flipped the sign of superior field responses so that for Normal subjects the first peak was negative (N1) and the later peak was positive (P1). This inversion makes sense given that the first peak is negative with respect to the surface of the cortical sheet, the curvature of the calcarine sulcus effecting an inversion of responses from the inferior visual field scalp recordings (Slotnick *et al.*, 1999),(Di Russo *et al.*, 2001). The nomenclature for the peaks is thus similar to that for the peaks of the multifocal ERG when recorded with respect to the cornea.

It was more complicated to find N1 and P1 values for the MS study group as these peaks could be found anywhere along entire length of response from 40 to 300 ms. Before looking for peaks the responses of the inferior regions were first inverted as for Normal subjects. To determine the implicit times of the N1 and P1 peaks, we examined the minimums and maximums of the *running* t-statistics. The threshold levels for N1 and P1 were –1.45 and 1.45 t-units respectively. The N1 and P1 implicit times are referred to as NT and PT.

TEMPLATE Method

We tried to decompose the aberrant waveforms of the patients into a few delayed versions of response waveforms of Normal subjects. To do that we developed the TEMPLATE algorithm, based on multiple linear regression. The TEMPLATE model allowed us to regress the individual waveforms of MS patients onto templates consisting of delayed versions of the average response waveforms for each stimulus region of the Normal subjects. The regression coefficients thus found, described weights (ω_i) between the TEMPLATE waveforms and those of the MS subjects. Thus, if the responses from MS subjects were delayed by a certain amount of time, they should fit the sum of one or more delayed and scaled (by ω_i) waveforms of the TEMPLATE. We examined up to the two most significant fitted delays ($p<0.05$) for each subject.

Principal Component Analysis

Principal Component Analysis (PCA) is a decorrelation method that finds a linear transformation W given the data x so that the output vectors u are uncorrelated, the basis vectors of W are orthogonal to each other and the eigenvalues are obtained from W.

$$u = Wx \tag{2.1}$$

We applied PCA to Normal and MS mfVEP response waveforms. We extracted the communalities for each response for a two principal component model (Reyment & Joreskog, 1996). We also examined the proportion of variance accounted for by each component across the responses of each subject.

Discriminant Analysis

The objective of this analysis was to determine whether the structure of the data permitted our subjects to be classified as being from the Normal or MS groups. We employed two types of discriminant analysis: Linear (LDA) and Quadratic discriminant analysis (QDA) (Johnson & Wichern, 1992). See Maddess *et al.*(1999) on the use of LDA and QDA to discriminate patients from Normal subjects. Sensitivities and specificities were estimated from Receiver Operator Characteristic plots (ROCs) (Egan, 1975). Standard errors for the ROC plots were estimated by a bootstrap method.

Results

General Findings

Multifocal VEPs were recorded in response to dichoptically presented stimuli, using four different degrees of sparseness for Normal and MS subjects' groups. We obtained four repeats for each of the four experiments. Examples of response waveforms for each of the 16-stimulus regions (eight per eye) are shown in Figure 2.3. Figure 2.3a represents typical (i.e. the subject closest to the population median) Pattern Pulse responses of Normal subjects, and Figure 2.3b - typical responses to the same stimulus for a ON patient. The ON responses are smaller than the Normal responses and they contain abnormal waveforms.

Figure 2.4 illustrates some other samples of mfVEP responses recorded to the Pattern Pulse stimulus from MS patients. Figure 2.4a shows the waveforms of the MS Patient 11; Figure 2.4b represents the signals obtained from the patient 15. The responses of the MS patient 26 and 46 are shown in the Figure 2.4c and 2.4d respectively. The mfVEPs for different patients had strangely looking waveforms; their amplitudes and delays differed as well.

Main Effects

Table 2.2 summarizes regression results contrasting the response amplitudes of Normal and MS subjects. The effects of the fitted factors were multiplicative, thus the N1 was transformed to dB, $N1_{dB} = 20\log_{10}(N1)$, to allow an additive regression model to be fitted and to stabilize the variance. The *Multiplier* column indicates the multiplicative factor corresponding to each dB gain or suppression. Table 2.2A indicates regression results for the simultaneously fitted N1 voltages from the Normal and MS study groups. The variance accounted for the total model was $r^2 = 0.81$. The reference condition (-9.97

dB) corresponds to the N1 of *Normal* subjects for the *Binary* stimulus, the mean value of which was 0.31 μV (*Multiplier* column). The coefficients for the $Sparse_4$ (6.92 dB, 95% CI, 2.00 & 2.45), $Sparse_{16}$ (15.12 dB, 95% CI, 5.17 & 6.29) and *Pattern Pulse* (20.74 dB, 95% CI, 10.02 & 11.84) conditions correspond to significant differences of the responses for both Normal and MS subjects compared to responses to Binary stimulus. The interactions $Sparse_4$ * *MS* (-2.03 dB, 95% CI, 0.73 & 0.85 dB), $Sparse_{16}$ * *MS* (-3.11 dB, 95% CI, 0.64 & 0.75 dB) and *Pattern Pulse* * *MS* (-1.68 dB, 95% CI, 0.75 & 0.89 dB) correspond to significant *(p= 0.0000)* suppression of

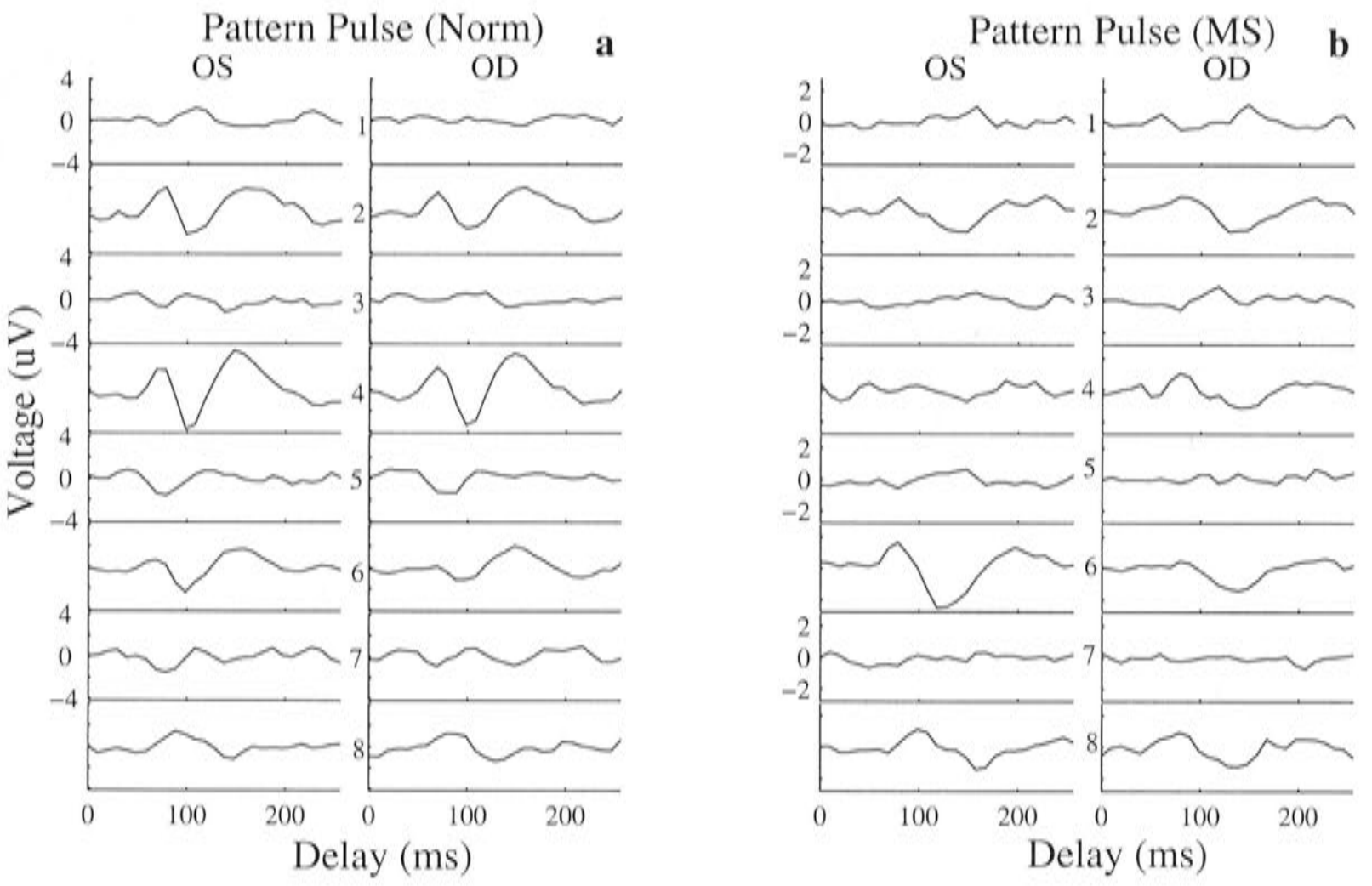

Figure 2.3 Typical multifocal responses for Normals and MS subjects in response to the Pattern Pulse stimulus. **a)** The two columns on the left (Pattern Pulse (Norm)) show multifocal responses from the left (OS) and for the right (OD) eye of a Normal subject. **b)** The two right columns (Pattern Pulse (MS)) show responses for an MS patient. The numbers 1 to 8 situated between the left and right columns of **a** and **b** indicate the region numbers (*cf.* Fig.2.1). In general responses from MS patients were significantly smaller (*cf.* Table 2.2A) than responses obtained from Normal subjects and contained abnormally shaped and/or delayed waveforms (*cf.* Table 2.2C).

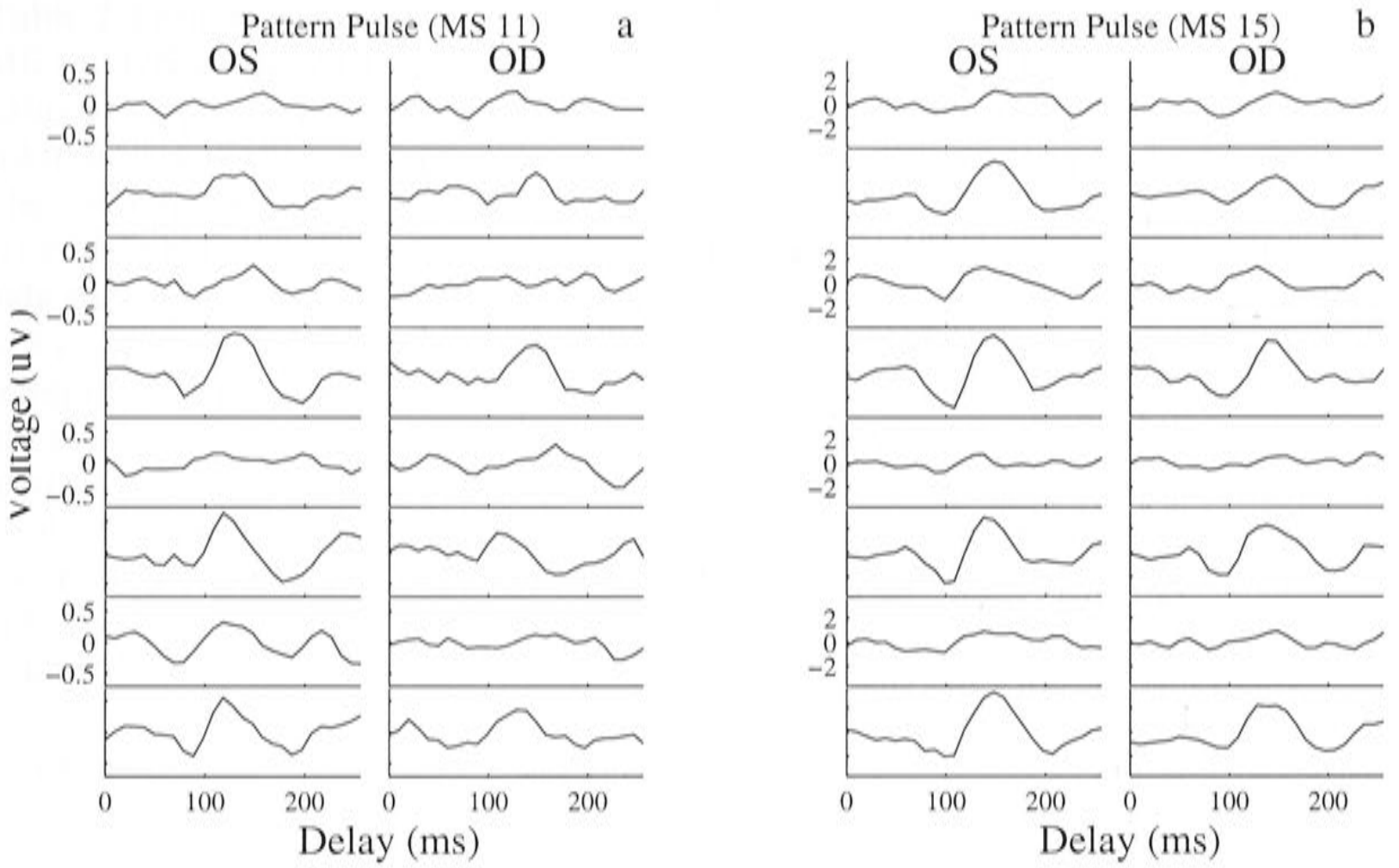

Figure 2.4 Four exemplary multifocal responses for MS patients in response to the Pattern Pulse stimulus. A description of the layout of the figure is given in the legend of Figure 2.6.

Table 2.2 Summarized multivariate regression results for the responses from Normal vs. MS and ON study groups. The coefficients (column 2) show the simultaneously fitted dB gains or suppressions for the factors in the left-most column (*Condition*). The *Multiplier* column indicates the multiplicative factor corresponding to each dB gain or suppression. The column labeled *Condition* indicates the fitted factors. The reference condition was the N1 of *Normal (N)* subjects for the Binary stimulus. The *–95% CI* and *+95% CI* columns indicate the (asymmetric) confidence limits of the coefficients. The coefficients for the factors $Sparse_4$, $Sparse_{16}$ and *Pattern Pulse* illustrate the differences from the reference condition for the respective visual stimuli in all subjects. Hence the *p* - values for these rows illustrate the significance of those differences. The interactions *Binary * MS*, *Sparse4 * MS*, $Sparse_{16}$ * *MS* and *Pattern Pulse * MS* indicate the additive effect of MS for each stimulus. The *Superior VF* condition represents response suppression in superior visual field regions for all subjects generally. A) are the fitted values of the N1 voltages, obtained from Normal and MS subjects. B) shows the results for N1 SNR, while C) indicates the fitted values for N1 implicit times (NT). Here the fitted coefficients are given in ms, and the *Multiplier* column is not required as there was no initial *log* transformation.

A. Normals versus MS, N1, Voltages

Condition	Coefficient (dB)	SE(dB)	t	p	Multiplier (times)	-95%CI	+95%CI
Ref = Binary * N	-9.97	0.71	-13.90	0.0000	0.31	0.26	0.37
$Sparse_4$	6.92	0.44	15.61	0.0000	2.22	2.00	2.45
$Sparse_{16}$	15.12	0.43	34.84	0.0000	5.70	5.17	6.29
Pattern Pulse	20.74	0.37	56.04	0.0000	10.89	10.02	11.84
Binary * MS	-0.33	0.38	-0.85	0.4041	0.96	0.88	1.05
$Sparse_4$ * MS	-2.03	0.34	-5.97	0.0000	0.79	0.73	0.85
$Sparse_{16}$ * MS	-3.11	0.34	-9.13	0.0000	0.69	0.64	0.75
Pattern Pulse * MS	-1.68	0.38	-4.32	0.0000	0.82	0.75	0.89
Superior VF	-2.48	0.15	-16.39	0.0000	0.75	0.72	0.77

B. Normals versus MS, N1, SNR

Condition	Coefficient (dB)	SE(dB)	t	p	Multiplier (times)	-95%CI	+95%CI
Ref = Binary * N	11.68	0.62	18.82	0.0000	3.84	3.33	4.41
$Sparse_4$	-0.53	0.38	-1.39	0.1701	0.94	0.86	1.02
$Sparse_{16}$	3.75	0.37	9.99	0.0000	1.54	1.41	1.67
Pattern Pulse	3.06	0.32	9.56	0.0000	1.42	1.32	1.52
Binary * MS	-0.11	0.33	-0.34	0.7481	0.98	0.91	1.06
$Sparse_4$ * MS	-0.37	0.29	-1.28	0.2094	0.95	0.89	1.02
$Sparse_{16}$ * MS	-1.99	0.29	-6.75	0.0000	0.79	0.74	0.84
Pattern Pulse * MS	-2.43	0.33	-7.24	0.0000	0.75	0.70	0.81

C. Normals versus MS, NT

Condition	Coefficient (ms)	SE(ms)	t	p	-95%CI	+95%CI
Ref = Binary * N	82.02	2.77	29.57	0.0000	76.59	87.46
$Sparse_4$	-0.26	1.71	-0.15	0.7813	-3.63	3.09
$Sparse_{16}$	7.65	1.67	4.56	0.0000	4.37	10.94
Pattern Pulse	-1.29	1.43	-0.90	0.3805	-4.09	1.51
Binary * MS	20.03	1.50	13.34	0.0000	17.09	22.98
$Sparse_4$ * MS	18.19	1.31	13.79	0.0000	15.61	20.78
$Sparse_{16}$ * MS	14.95	1.31	11.33	0.0000	12.37	17.54
Pattern Pulse * MS	18.69	1.50	12.45	0.0000	15.75	21.64
Superior VF	-3.56	0.58	-6.07	0.0000	-4.71	-2.41

the responses of MS patients compared to those obtained from Normal subjects. The *Binary * MS* interaction was not significant *($p = 0.4041$)*, thus for the Binary stimulus the response amplitudes of MS patients did not differ from Normal subjects. The regression coefficient of –2.48 dB ± 0.15 SE for *Superior Visual Field (VF)* also shows a significant response decrease for all subjects in that hemifield of 0.75 times. The effects between peripheral vs. central, left vs. right and inner vs. outer visual fields were examined as well, but there were no significant response enhancements were found.

Table 2.2B represents regression results for the simultaneously fitted the N1 running SNRs (*Methods*) from Normal and MS study groups. The variance accounted for this model was $r^2 = 0.57$. As in Table 2.2A, SNRs obtained for sparser stimuli from MS subjects are often smaller than the SNRs of Normal subjects, i.e. the coefficient of -1.99 dB ± 0.29 for $Sparse_{16}$ and the coefficient of -2.43 dB ± 0.33 for *Pattern Pulse* stimulus indicate a significant (*$p=0.0000$*) SNR decrease. Notice, that in agreement with previous results for Normal subjects (James *et al.*, 2004), the SNRs are significantly higher for $Sparse_{16}$ and *Pattern Pulse* stimuli in all groups (Table 2.2B, rows 3 and 4).

Table 2.2C indicates the regression results for N1 implicit times (NT) of Normal and MS subjects. The variance accounted for was $r^2 = 0.61$. The table format is the same as the format of Tables 2.2A and B, except for the absence of a *Multiplier* column, since the delays were not converted to dB. The reference condition indicates the NT of the Normal subjects' responses to the *Binary* stimulus (82.02 ms ± 2.77 SE). The coefficient for $Sparse_{16}$ (7.65 ms, 95% CI, 4.37 & 10.94) stimulus represents a significant change of NT for that visual stimulus in all subjects. The coefficients for the *Binary * MS* (20.03 ms ± 1.50 SE), $Sparse_4$ * *MS* (18.19 ms ± 1.31 SE), $Sparse_{16}$ * *MS* (14.95 ms ± 1.31 SE) and *Pattern Pulse * MS* (18.69 ms ± 1.50 SE) conditions indicate the significant mean (*$p= 0.0000$*) additional delays of the implicit times of MS patients.

Principal Component Analysis

Principal components (Eq.2.1), formed from responses from all regions and eyes, for Normal and ON subjects are shown in Figure 2.5. Figure 2.5 a-b, d-e are the first two PCs for Normal and ON subjects for Binary and Pattern Pulse stimuli. The first component is shown as a solid waveform and the dashed waveform represents the second component. Figure 2.5c shows the proportion of variance accounted for by the first eight components for Normal subjects for Binary (solid lines) and Pattern Pulse (dashed-dotted lines) stimuli. Figure 2.5f indicates the proportion of variance of each PC for ON subjects. Overall the proportion of variance accounted for by the first component increases as sparseness increases but it is smaller for ON subjects.

The PCs also provided an amplitude-independent measure of similarity of waveform shape across subjects and visual fields locations (for ON and Normal subjects): the communalities, computed here as proportion of variance of *each response* explained by the first two PCs. The mean, median and STD of the communalities for both study groups are given in the Table 2.3. The median communalities are perhaps a more conservative measure than the mean value as it describes the typical similarity of waveforms across all subjects. Both the mean and median communalities for Normal subjects rose with increasing sparseness (Table 2.3). The median communalities were lower for ON subjects. Thus, in the Pattern Pulse case for Normal subject, the typical response has 72% of its variance explained by the first two PCs (and mostly from the first), while the typical response from an ON patient has only 43% of its variance explained by the first two PCs (Table 2.3). Lower communalities mean that smaller components, such as noise components, contribute more to the waveform shape, i.e. the waveforms are more irregular.

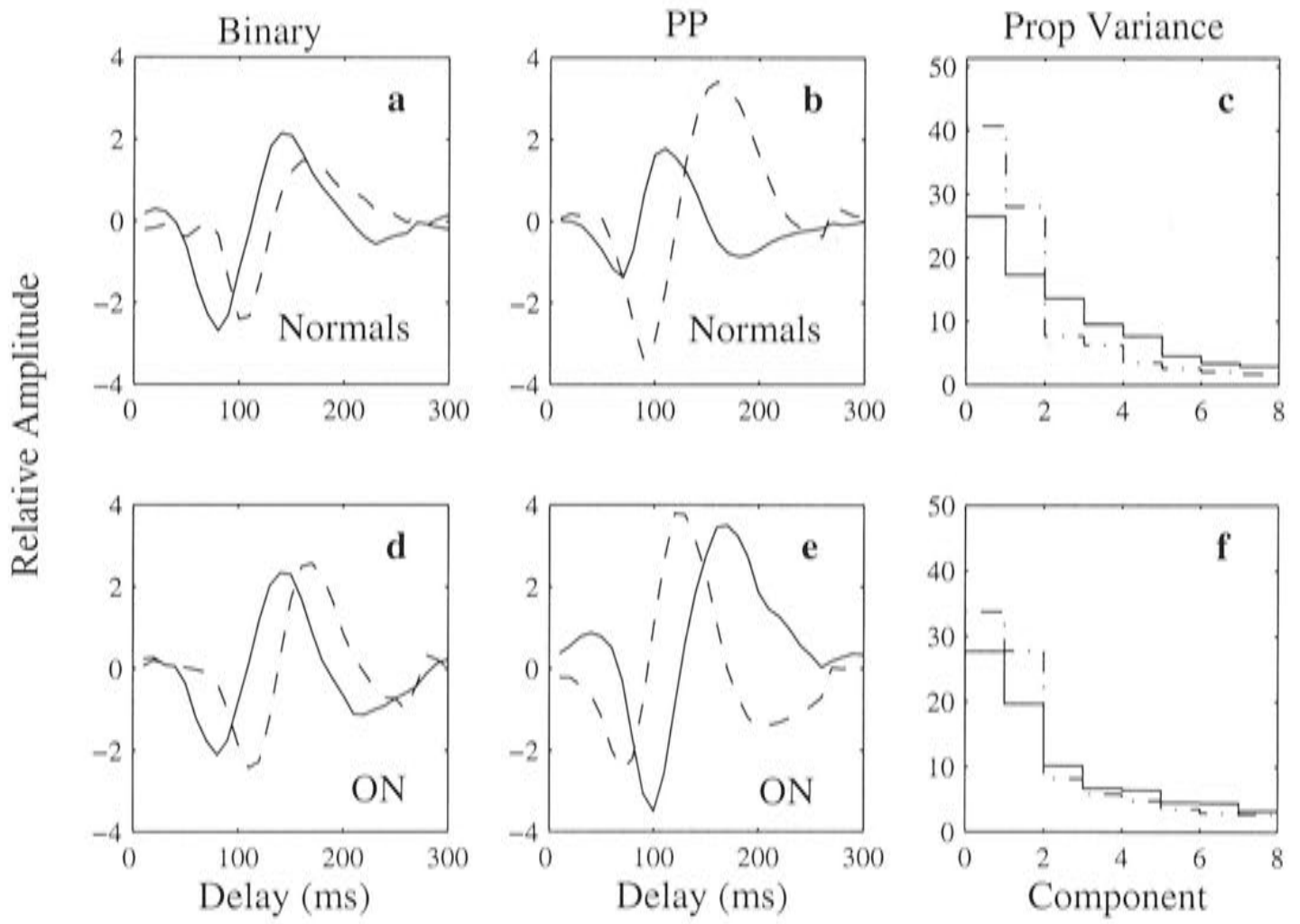

Figure 2.5 Principal Components Analysis (PCA) of responses from the Normal and ON study groups. In panels **a**, **b**, **d** and **f**, the first PC is shown as a solid waveform, the second component is the dashed waveform. The panels **a** and **b** show PCs for the Normal study group, while the **d** and **e** are the PCs from the ON subjects. **a** and **d** represent PCs for Binary stimulation. **b** and **e** show the PCs obtained for Pattern Pulse stimulation. Panels **c** and **f** give the proportions of variance accounted for by the first 8 principal components, shown on abscissa (solid = Binary, dashed-dotted = Pattern Pulse).

Table 2.3 Mean, median and STD of the PCA communalities (the proportion of the variance within each response accounted for by the first 2 PCs) for the Normal (N) and ON (N=26) subjects. The *Condition* column describes the stimulus for which the PCA communalities were calculated.

Condition	Mean	Median	STD
Binary (N)	0.48	0.51	0.26
$Sparse_4$ (N)	0.53	0.54	0.22
$Sparse_{16}$ (N)	0.66	0.72	0.23
Pattern Pulse (N)	0.64	0.72	0.24
Binary (ON)	0.35	0.31	0.23
$Sparse_4$ (ON)	0.35	0.32	0.22
$Sparse_{16}$ (ON)	0.45	0.41	0.26
Pattern Pulse (ON)	0.44	0.43	0.26

Fitted Delays

In order to examine whether the responses of our MS patients consisted of sums several waveforms of different delays and amplitudes, we applied the multivariate TEMPLATE regression method described in the *Methods*. The TEMPLATE matrix of delayed responses from Normal subjects was regressed onto all the MS subjects' responses. The earliest significant ($p < 0.05$) delays, T_1, were estimated for all MS subjects. All ON responses were delayed by at least one video frame. The largest delays (3 video frames) were obtained for Pattern Pulse visual stimuli.

We also examined the second significant delay (T_2), if any. Our goal was to discover whether any MS subjects' responses had multiple delayed components. We found that 18/26 ON subjects had at least one second significant ($p < 0.05$) delay (T_2). Amongst those 18 subjects the second delay was found in regions 2, 4, 7 and 8 for the right eye. The averaged T_2 were: ~3.6 ± 0.52, 3.9 ± 0.38, 3.0 ± 0.4 and 4.2 ± 0.42 SE video frames for each sparseness respectively.

Fitted Delays vs. Implicit Times

To test whether the delays TEMPLATE model were reasonable, we compared the fitted delays with the implicit times for ON patients (the estimation of N1, NT, P1 and PT for all MS and ON patients is described under *Methods*). The implicit times of the first negativity (NT) were compared with the longest fitted delay T_F, which was either T_1 or T_2. That is if the response waveforms contained more than one significant fitted delay, the more delayed one was chosen. Since the T_1 and T_2 values were the *additional* delay compared to the templates, we added the average NT values of Normal subjects to derive the total fitted implicit times NT_F. Figure 2.6 presents histograms of all NT_F and

MS NT. The white bars indicate the implicit times NT, while the black bars are the fitted NT_F. Histograms are shown for each visual stimulus for the 50 MS and ON subjects. Table 2.4A indicates the correlation statistics between NT_F and the NT values for each sparseness for MS patients. The correlation was good for all stimuli, but was best for the Pattern Pulse stimulus ($r^2 = 0.81$).

Table 2.4B summarizes the major determining effects for the NT_F for Normal and MS subjects (at the variance accounted for $r^2 = 0.64$). The reference condition (*Binary * N*) 96.84 ms ± 3.57SE indicates the average NT_F for Normal subjects, for the *Binary* stimulus. The regression coefficients show the significant delays (ms) compared to the reference condition. Factors describing average differences from the delay of the reference condition and $Sparse_4$, $Sparse_{16}$ and *Pattern Pulse* in general for all responses are not significant. The interactions *Binary * MS*, $Sparse_4$ * *MS*, $Sparse_{16}$ * *MS* and *Pattern Pulse * MS* conditions represent the NT_F obtained from MS subjects for the particular stimuli. Those delays were overall longer and more similar across stimulus types than was the case for the implicit times (*cf.* Table 2.2C).

Table 2.4 A) correlations between the fitted NT_F and real NT by visual stimuli. *T*-values, and probabilities *p*, describe the significance of the correlations (*r2*). B) indicates the fitted values (in ms) of NT_F obtained from the responses of Normal and MS study groups. The table format is similar to the format of Table 2.2C).

A. Correlations between fitted NT_F and NT.

Condition	*t*	r^2	*p*
Binary	4.89	0.68	0.000
$Sparse_4$	6.74	0.63	0.000
$Sparse_{16}$	6.80	0.74	0.000
Pattern Pulse	6.37	0.81	0.000

B. Normals versus MS, NT_F

Condition	Coefficient (ms)	SE(ms)	t	p	-95%CI	+95%CI
Ref = Binary * N	96.84	3.57	27.12	0.0000	89.84	103.84
$Sparse_4$	-2.63	2.20	-0.73	0.2437	-6.95	1.69
$Sparse_{16}$	3.03	2.16	0.84	0.1684	-1.20	7.26
Pattern Pulse	1.94	1.84	0.54	0.3028	-1.66	5.55
Binary * MS	29.74	1.93	8.33	0.0000	25.95	33.53
$Sparse_4$ * MS	23.91	1.69	6.69	0.0000	20.59	27.24
$Sparse_{16}$ * MS	24.08	1.69	6.74	0.0000	20.75	27.40
Pattern Pulse * MS	26.88	1.93	7.53	0.0000	23.09	30.67
Superior VF	0.14	0.75	0.04	0.8130	-1.33	1.62

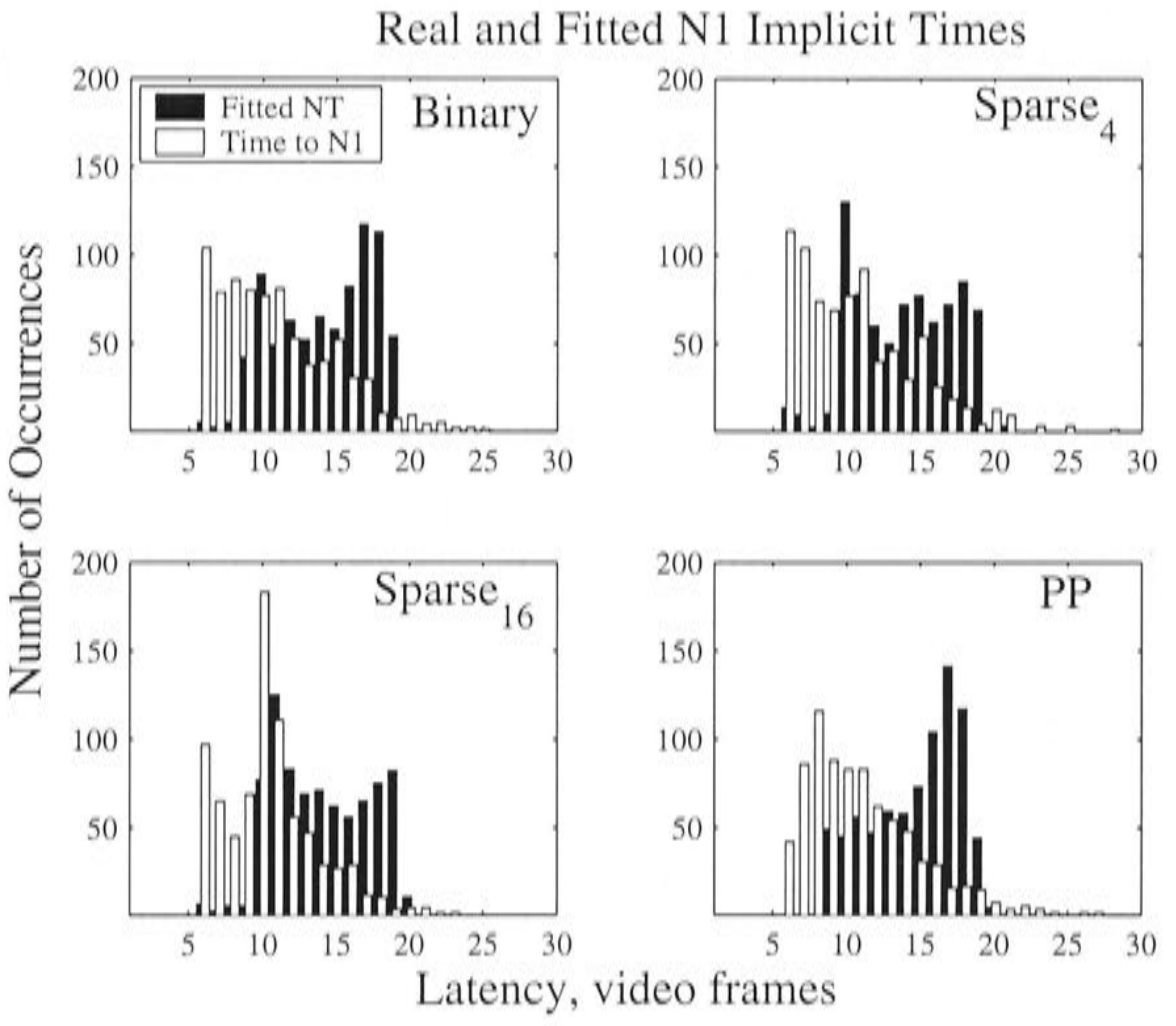

Figure 2.6 Histograms of the longest fitted N1 latencies (NT_F, black bars), and the N1 implicit times (NT, white bars) for MS patients. The histograms are presented for each visual stimulus: Binary, $Sparse_4$, $Sparse_{16}$ and Pattern Pulse (PP). The abscissas show the latencies in video frames. One video frame is equal to 9.9ms. The ordinate indicates the number of occurrences of each case.

Discriminant Analysis

We next examined the sensitivities and specificities for classifying the Normal and ON responses. We classified the MS patients without ON history by applying linear and quadratic (*Methods*) classification models obtained from the Normal subjects vs. ON patient comparisons. We first were interested whether the age and sex of our subjects could classify the subjects. To test this hypothesis we examined a discriminant model containing the age and sex of the Normal and ON subjects. The classification statistics were poor – sensitivities and specificities of 66% were achieved in both LDA and QDA. The poor classification performance was expected given no significant differences in the age groups (*cf.* Table 2.1).

We examined the classification performance of the waveforms' complexity, using the communalities from the PC analysis (see *Methods*). The performance of the LDA model containing the median communalities is shown in the Figure 2.7. We also examined the performance of measures such as the maximum communalities but we present results for the medians as they are similar and likely to be more robust. The left column in the Figure 2.7 displays the ROC plots for the Normal vs. ON patients. The right column shows the performance of these classification rules applied to the MS patients with no history of ON. The top row in the figure illustrates the ROC plots for the Binary stimulus, the second – for the $Sparse_4$, the third for the $Sparse_{16}$. The bottom row of panels represents the ROCs for the Pattern Pulse stimulus. The '*' symbol in each panel indicates the point of the simultaneously largest sensitivities and specificities, sometimes called the accuracy. The % value corresponding to these '*' accuracies, is also given in the lower right corner of each panel. Overall the figure clearly illustrates that classification accuracy improves with increasing sparseness of the

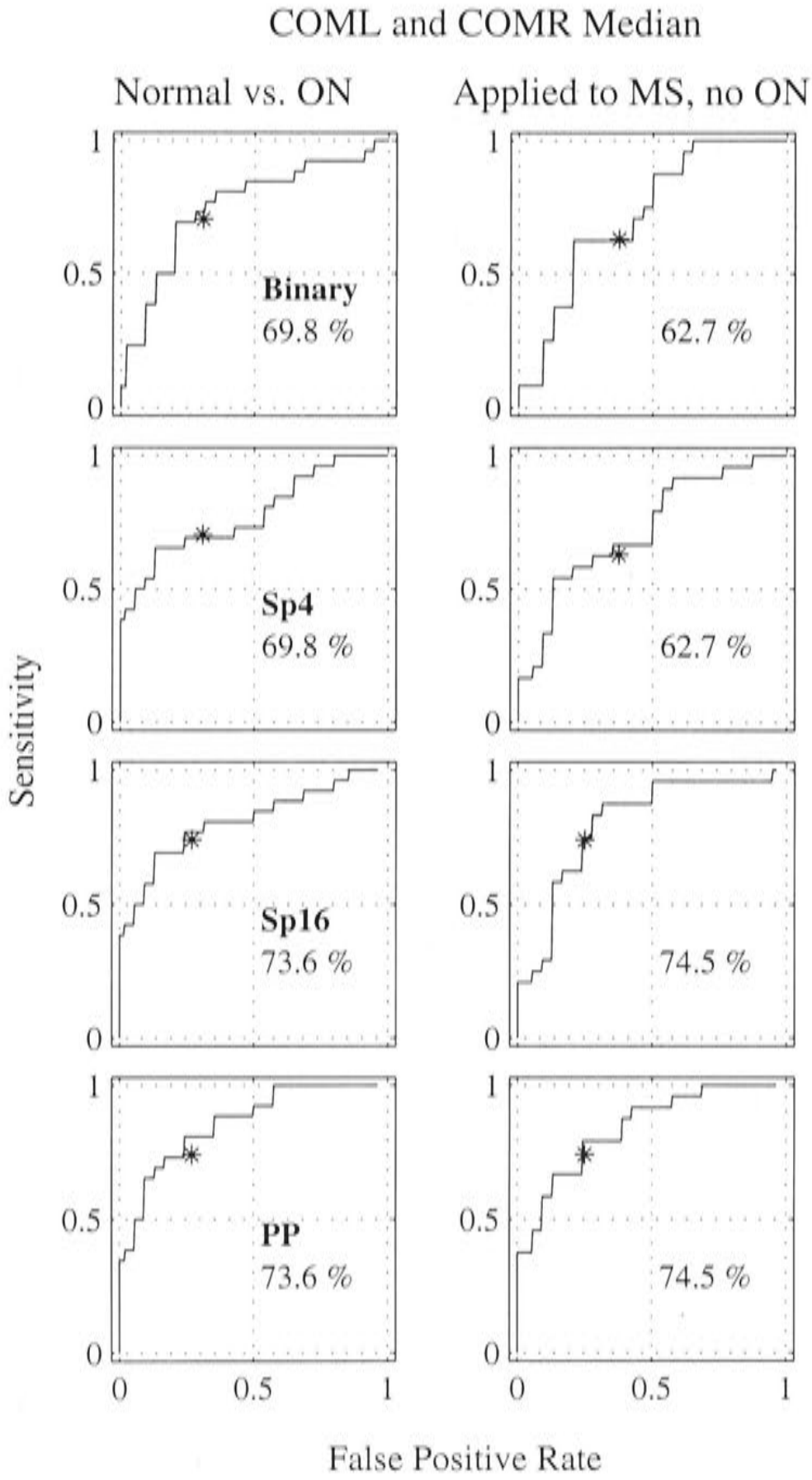

Figure 2.7 Receiver Operator Characteristic (ROCs) plots comparing sensitivities and specificities of PCA median communalities obtained from the left (COML) and right (COMR) eyes. The left column shows the ROCs for models constructed for the Normal subjects vs. ON patients for each stimulus type. The right column represents those classification models applied to the MS patients without ON. The curves are given for the Binary, $Sparse_4$, $Sparse_{16}$ and Pattern Pulse visual stimuli. The abscissa shows the false positive rates (1 – specificity). The ordinate indicates sensitivities of the model. The '*' symbol represents the point where the highest simultaneous sensitivity and specificity occurs. The mean of these values is, the accuracy, shown as a percentage at the bottom right corner of each panel.

stimuli. Communalities obtained for the Pattern Pulse stimulus had accuracies of 73.6% for ON patients and 74.5% MS for patients with no history of ON.

ROCs formed for response amplitude (N1, P1, N1 + P1 and RMS) displayed similarly improving performance with increasing stimulus sparseness (not shown). For example, the median N1 the performance gave poor sensitivity of 66.6% at specificity of 59.2% for LDA, and 58.3% at 62.9% for QDA, for the Pattern Pulse stimulus (the performance for the other visual stimuli was similarly poor). The performance of P1 median amplitudes increased the sensitivity and specificity to 83.3% at 81.4% both for LDA and QDA models for the Pattern Pulse stimulus.

We also examined LDA models based on the response latencies, NT and NT_F. The classification sensitivities for the NT_F medians are presented in Figure 2.8. High sensitivities and specificities of the model containing NT_F medians from the left (NFL) and the right eye (NFR) were achieved for the Pattern Pulse stimulus (> 95%).

In contrast to the median NT and NT_F for each subject and stimulus both the NT and the NT_F subject-wise maxima gave perfect discrimination for all visual stimuli (figure not shown).

A possible interpretation of the perfect performance of the maximal NT and NT_F is that the patient group had fairly advanced disease (Table 2.1). We can make some prediction of performance of the maximal delays for less advanced patients by using a bootstrap process. Here each subject's data is resampled randomly and with replacement. Thus, any of a subject's 16 regional delays, each with equal probability, could be selected to represent a subjects' data set. In this standard bootstrap method some delays can be repeated and some lost. Taking the maximum of these resampled delays, however, we can only obtain values that are smaller than or equal to the original delays. In this way we can realistically simulate patients, drawn from the present distributions, who have on average less advanced disease, providing evidence as to

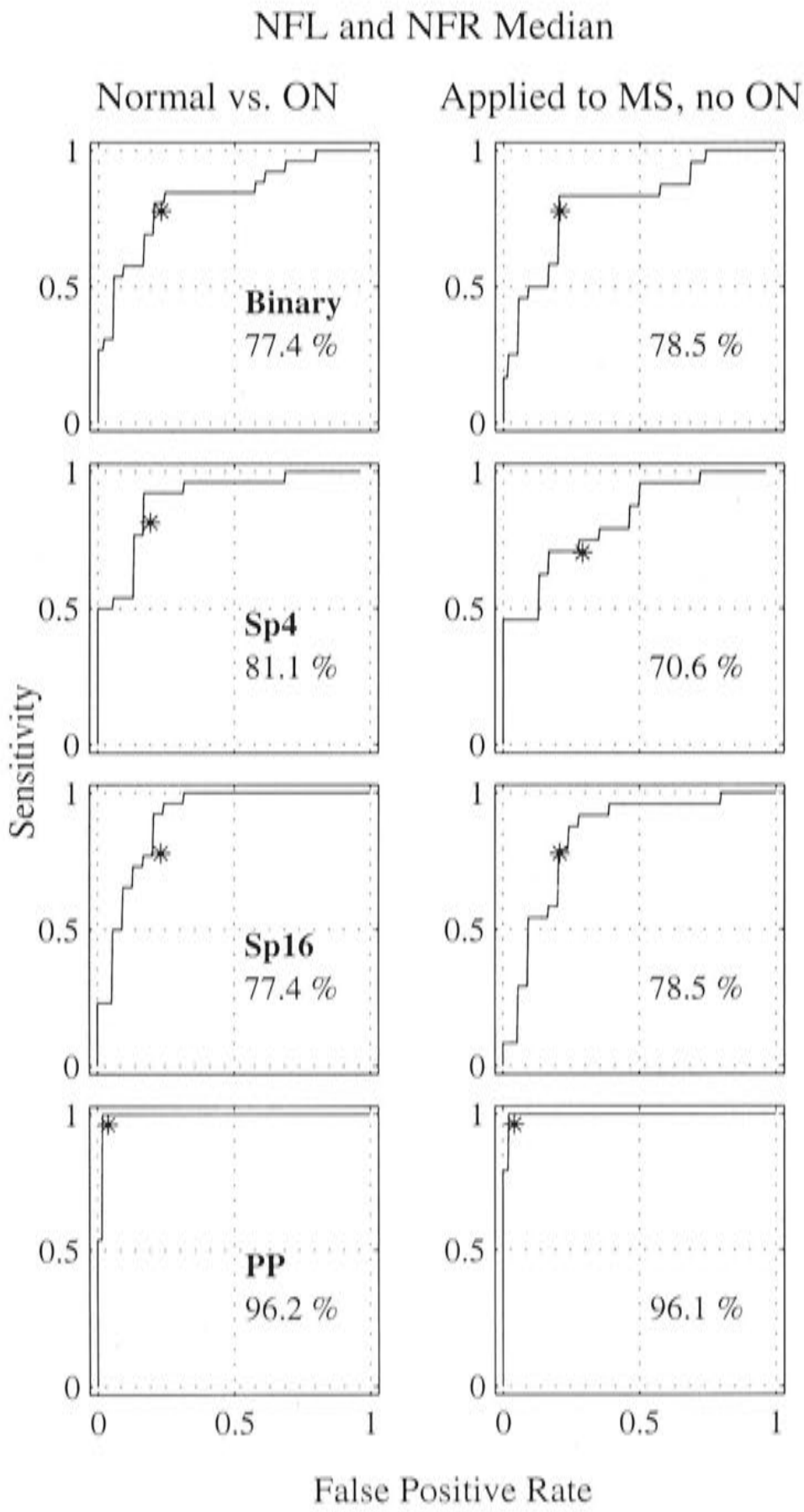

Figure 2.8 ROCs for the median fitted N1 delays (NT_F) obtained from the left (NFL) and right (NFR) eyes. A description of the layout of the figure is given in the legend of Figure 2.7.

which stimulus, if any, will perform best for less advanced patients. Figure 2.9 illustrates ROCs obtained to the bootstrapped NT_F values. We used 500 bootstrapped data sets and therefore obtained 500 bootstrapped ROCs. Clearly the Pattern Pulse stimulus behaved best on average.

The bootstrap method also permits estimates of the SE for the ROCs. Figure 2.10 illustrates the Mean ± SE of the bootstrapped ROCs for the NT_F maximums for MS patients with ON. The SEs are the standard deviations in the mean bootstrapped ROC. Thus, only the accuracy of the estimate of the SE, and not the magnitudes of the SE, are affected by the large N. Note that at 92% sensitivity the mean False Positive rate for the Pattern Pulse stimulus is 0%. By contrast at 92% sensitivity the Binary stimulus would misdiagnose more than 20% of the Normal population.

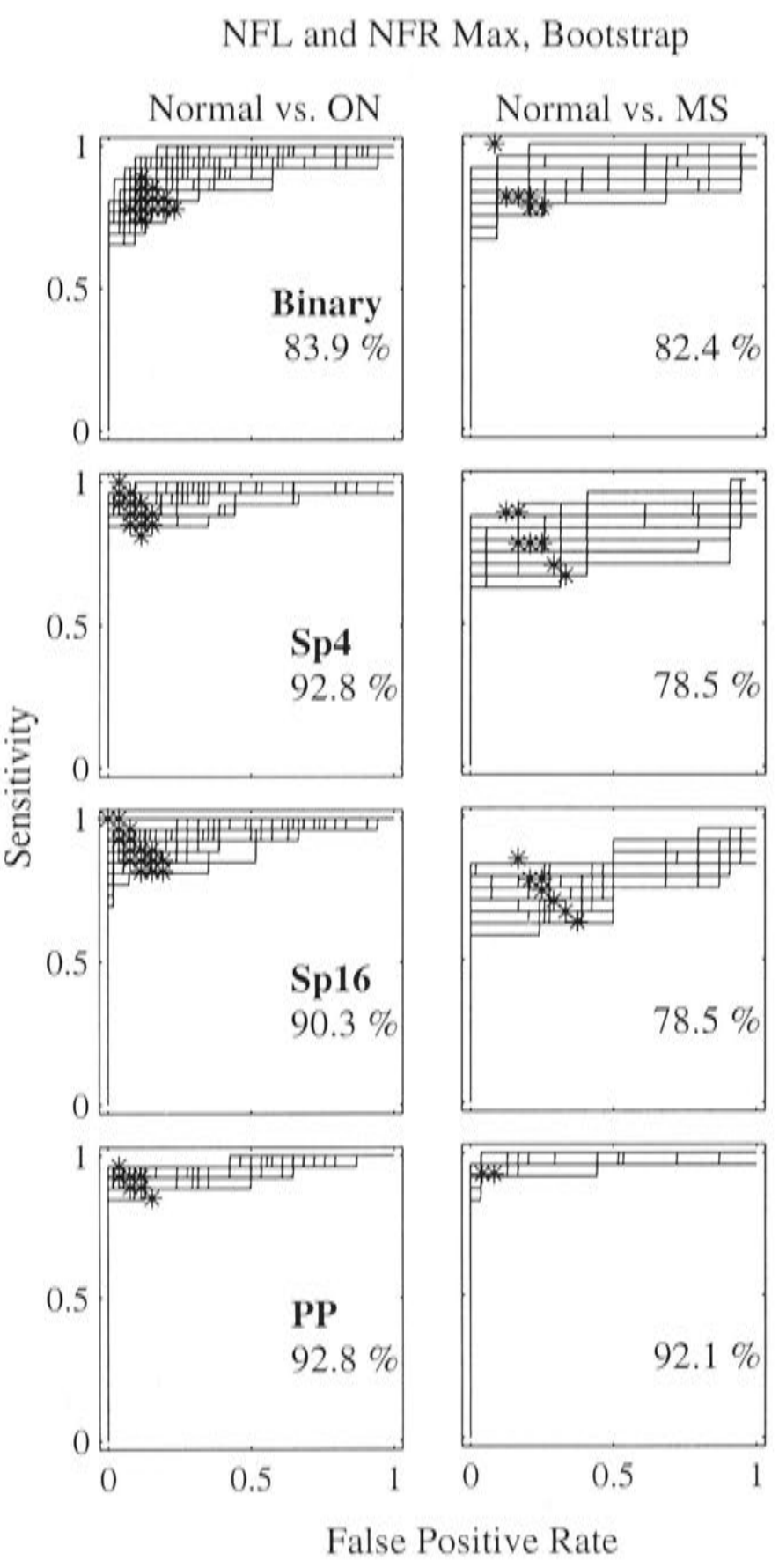

Figure 2.9 Bootstrapped ROC plots for the maximum of the fitted delays (NFL and NFR) obtained from the left and right eyes of each subject. There are 500 curves per panel. A description of the layout of the figure is given in the legend of Figure 2.6.

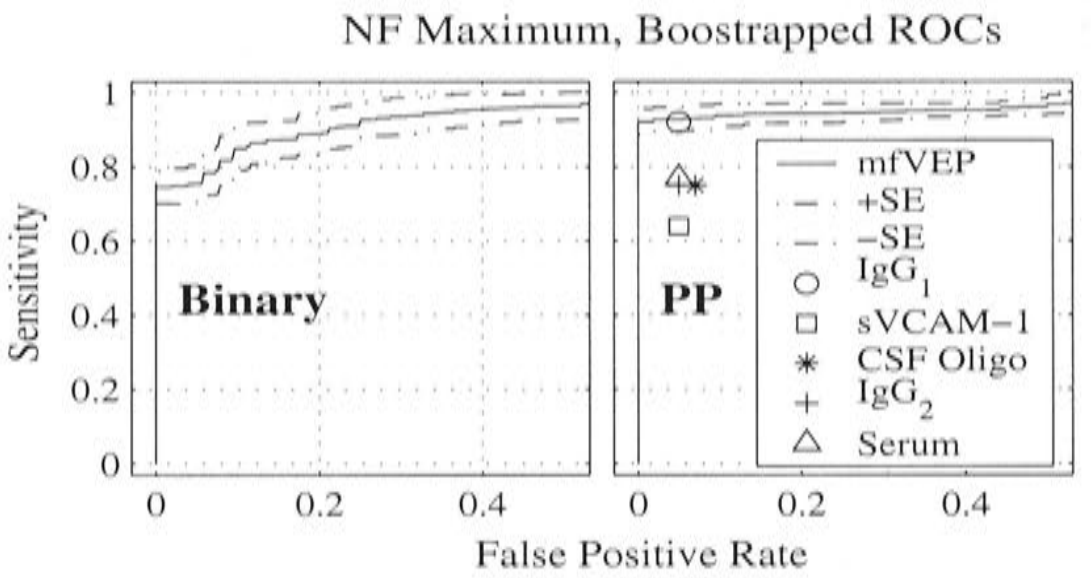

Figure 2.10 Mean ± SE of bootstrapped maximum NT_F (n =500) for Normal subjects and MS patients with a history of ON. The left panel indicates ROCs for the Binary stimulus, the right panel shows the ROCs obtained for the Pattern Pulse stimulus. Note, that sensitivities are much higher for the Pattern Pulse stimulus than the Binary at a False Positive rate of 0%. The legend also illustrates the performance of other MS diagnostic methods as reported in the literature(Brasher *et al.*, 1998; McMillan *et al.*, 2000; Chamczuk *et al.*, 2002). The 'o' symbol in the legend shows the sensitivity of 92% at a specificity of 95% for the immunoglobulin IgG index(McMillan *et al.*, 2000). The '□' symbol presents the sensitivity of 64% at a specificity of 95% of soluble vascular cell adhesion molecule-1 (sVCAM-1) (McMillan *et al.*, 2000). The '*' symbol in the legend indicates the sensitivity of 75% at a specificity of 92% of CSF Oligoclonal banding (Brasher *et al.*, 1998). The '+' symbol indicates the sensitivity of 75% at a specificity of 95% of immunoglobulin IgG index(Brasher *et al.*, 1998). The sensitivity of 77% at a specificity of cerebrospinal fluid (CSF) serum according to (Chamczuk *et al.*, 2002) is shown as 'Δ'.

Discussion

General Findings

We examined the differences between Normal and MS groups for 4 multifocal stimulus types. In general, responses of MS subjects are more delayed (Table 2.2C) and smaller (Table 2.2B) for Sparser visual stimuli. One subject, who had suffered from ON, had response amplitudes reduced almost by 10 times (compared to Normal sample responses). Axonal (Waxman, 1983; McDonald *et al.*, 2001) and grey matter loss (De Stefano *et al.*, 2003; Ukkonen *et al.*, 2003) associated with MS would be expected to reduce VEP amplitudes. Thus, in agreement with previous studies (Chiappa, 1983; Jones, 1993; Andersson & Siden, 1995; Hood *et al.*, 2000; Brusa *et al.*, 2001) the VEP waveforms of our MS patients are abnormal and delayed.

Signal Quality

We examined the Principal Components (PCs) of the responses of all subjects. The variance from Normal subjects is more loaded onto the first two components than occurs for ON responses (Fig.2.5). Thus, patients response waveforms were more complex possibly because ON patients have differential levels of demyelination. The deviation from simple forms of response signal waveform shapes were described by the communalities for the first two PCs. Lower communalities for two PCs indicate that the noise components contribute more to each waveform shape. The communalities were lower for ON subjects (Table 2.3). Thus, if we examine the median case, the first two PCs explain 31% of response variance in the Binary case for ON the typical response and 43% of the variance for Pattern Pulse. The higher communalities for the sparser stimuli seem to reflect the higher SNRs (Table 2.2B) for those stimuli, noise components contributing less to these responses. There was no overall significant SNR

improvement for the $Sparse_4$ stimulus in agreement with our previous work on Normal subjects (James *et al.*, 2004) and that of Hoffmann *et al.*(2003) who employed temporally similar multifocal stimulus.

Delays

According to new MS diagnostic criteria (McDonald *et al.*, 2001), abnormal VEPs, typical of MS, can be used to supplement information provided by clinical examination to provide objective evidence of a second lesion, provided that other clinically expressed lesions did not affect the visual pathways. Our findings confirm the above-mentioned criteria. We found that the VEPs for MS (especially ON) patients contained one or more components delayed by up to 24 ms compared to Normal subjects (Table 2.4B).

To estimate possible multiple delayed components within the responses of MS patients we employed a multivariate regression model (TEMPLATE). Multiple significant components for 18 ON subjects were found in regions 2, 4, 7 and 8. These correspond roughly to the regions with the largest responses. All other responses contained only one significant component. In summary, using relatively large multifocal stimuli is reasonable and compound waveforms, if any, can be recovered by a method like the TEMPLATE algorithm provided that SNRs are high enough. Large stimulus regions will also minimize the effects of minor losses of fixation.

We found good correlation between implicit times and fitted (TEMPLATE) delays for all stimuli (Table 2.4A); however, the variability of differences between NT and NT_F was large across the visual field regions. For the implicit times, NT, the delays grew with increasing sparseness (Table 2.2C). The larger implicit times for sparser stimuli may reflect the better SNRs obtained for those stimuli and the fact the NT is based upon a single data point. Thus, in the case of implicit times (NT and PT) noise

can provide erroneously early delays. By contrast, the TEMPLATE method is likely to be more robust than a threshold method since many data points are used to estimate the delay, rather than only 1. In agreement with this idea the NT_F were somewhat larger than the NT and had proportionally smaller SE, *cf.* Tables 2.2C, 2.4B. NT_F values for MS patients were also more similar across the stimulus types (*cf.* Tables 2.2C, 2.4B) and unlike NT there was no significant effect of superior visual field location for NT_F. If NT_F is actually more accurate this would mean that the response increases seen for sparser stimuli are not achieved by recruiting afferent inputs with shorter latencies, rather neurons with the same latency are having their gain modulated.

Discriminant Analysis

Other researchers (Frederiksen *et al.*, 1991; Andersson & Siden, 1995) have shown that conventional VEPs were useful in MS or ON diagnosis. Our discriminant models examined a set of mfVEP parameters that were possibly useful for diagnostic purposes. The best sensitivities and specificities (100%) were obtained for the Pattern Pulse stimulus and the maximums of the delays (NT and NT_F).

The quadratic discriminant (QDA) models examined had the capacity to quantify the value of between eye interactions, but in general QDA models provided with data from the two eyes separately, performed little better than their less complex LDA partners. Thus, at least for this data set, between eye comparisons, which QDA models could capture (Egan, *1975)*, had little value. A surprising result was that many models based upon responses of patients who had experienced ON, performed well for MS patients who had not experienced ON. The sparse stimuli produced better performance than sensitivities and specificities for IgG (Brasher *et al.*, 1998; McMillan *et al.*, 2000), sVCAM – 1 (McMillan *et al.*, 2000), CSF Oligoclonal bands, and serum antibodies to myelin (Chamczuk *et al.*, 2002) (Fig. 2.9). Bootstrapped ROC models

predicted excellent performance of sparser stimuli for less advanced patients. Taken together these findings suggest that discriminant models based on mfVEP latencies obtained to sparse stimuli can provide rapid and cost effective diagnosis and monitoring of multiple sclerosis. Including measures such as response amplitude and the communalities might provide accurate classification in early MS. A large scale retrospective study would be required to verify this. If the method has good reproducibility it could provide a cost effective monitoring and treatment.

Bibliography

ANDERSSON, T. & SIDEN, A. (1995). An analysis of VEP components in optic neuritis. *Electromyogr Clin Neurophysiol* **35,** 77-85.

ANDERSSON, T., SIDEN, A. & PERSSON, A. (1991). A comparison of clinical and evoked potential (VEP and median nerve SEP) evolution in patients with MS and potentially related conditions. *Acta Neurol Scand* **84,** 139-145.

BARNETT, M. & PRINEAS, J. (2004). Relapsing and remitting multiple sclerosis: pathology of the newly forming lesion. *Ann Neurol* **55,** 458-468.

BRASHER, G., FOLLENDER, A. & SPIEKERMAN, A. (1998). The clinical value of commonly used spinal fluid diagnostic studies in the evaluation of patients with suspected multiple sclerosis. *Am J Manag Care* **4,** 1119-1121.

BRINAR, V. (2002). The differential diagnosis of multiple sclerosis. *Clin Neurol Neurosurg* **104,** 211-220.

BRUSA, A., JONES, S. & PLANT, G. (2001). Long-term remyelination after optic neuritis. A 2-year visual evoked potential and psychophysical serial study. *Brain* **124,** 468-489.

CHAMCZUK, A., URSELL, M., O'CONNOR, P., JACKOWSKI, G. & MOSCARELLO, M. (2002). A rapid ELISA-based serum assay for myelin basic protein in multiple sclerosis. *J Immun Methods* **262,** 21-27.

CHIAPPA, K. (1983). Pattern shift visual evoked potentials: interpretation. In *Evoked potentials in clinical medicine*, pp. 63-104. Raven Press, New York.

DE STEFANO, N., MATTEHWS, P., FILIPPI, M., AGOSTA, F., DE LUCA, M., BARTOLOZZI, M., GUIDI, L., GHEZZI, A., MONTANARI, E., CIFELLI, A., FEDERICO, A. & SMITH, S. (2003). Evidence of early cortical atrophy in MS. Relevance to white matter changes and disability. *Neurology* **60,** 1157-1162.

DI RUSSO, F., MARTINEZ, A., SERENO, M., PITZALIS, S. & HILLYARD, S. (2001). Cortical sources of the early components of the visual evoked potential. *Hum Brain Mapping* **15,** 95-111.

EGAN, J. (1975). *Signal detection theory and ROC analysis*. Academic Press, Inc. Ltd., London.

FREDERIKSEN, J., LARSSON, H., OLESEN, J. & STIGSBY, B. (1991). MRI, VEP, SEP and biothesiometry suggest monosymptomatic acute optic neuritis to be a first manifestation of multiple sclerosis. *Acta Neurol Scand* **83,** 343-350.

HOFFMAN, M., STRAUBE, S. & BACH, M. (2003). Pattern-onset stimulation boosts central multifocal VEP responses. *J Vision* **3,** 432-439.

HOOD, D., ODEL, J. & ZHANG, X. (2000). Tracking the recovery of local optic nerve function after optic neuritis: a multifocal VEP study. *Invest Ophthalmol Vis Sci* **41,** 4032-4038.

JAMES, A. (2003). The pattern pulse multifocal visual evoked potential. *Invest Opthalmol Vis Sci* **44,** 879-890.

JAMES, A., RUSECKAITE, R. & MADDESS, T. (2004). Effect of temporal sparseness and dichoptic presentation upon multifocal visual evoked potential. *Vis Neurosci* **in revision**.

JOHNSON, R. & WICHERN, D. (1992). *Applied multivariate statistical analysis*. Prentice-Hall, Inc.

JONES, S. (1993). Visual evoked potentials after optic neuritis. Effect of time interval, age and disease dissemination. *J Neurol* **240,** 489-494.

KLISTORNER, A., GRAHAM, S., GRIGG, J. & BILLSON, F. (1998). Electrode position and the multi-focal visual-evoked potential: role in objective visual field assessment. *Aust N Z J Ophthalmol* **26(Suppl.),** 91-94.

MADDESS, T., GOLDBERG, I., DOBINSON, J., WINE, S., WELSH, A. & JAMES, A. (1999). Testing for glaucoma with the spatial frequency doubling illusion. *Vis Res* **39,** 4258-4273.

MCDONALD, W., COMPSTON, A., EDAN, G., GOODKIN, D., HARTUNG, H., LUBLIN, F., MAFARLAMD, H., PARTY, D., POLMAN, C., REINGOLD, S., SANDBERG-WOLLHEIM, M., SIBLEY, W., THOMPSON, A., VAN DEN NOORT, S., WEINSHENKER, B. & WOLINKSY, J. (2001). Recommended diagnostic criteria for multiple sclerosis: guidelines from the international panel on the diagnosis of multiple sclerosis. *Ann Neurol* **50,** 121-127.

MCMILLAN, S., MCDONNELL, G., DOUGLAS, J. & HAWKINS, S. (2000). Evaluation of the clinical utility of cerebrospinal fluid (CSF) indices of inflammatory markers in multiple sclerosis. *Acta Neurol Scand* **101,** 239-243.

PRINEAS, J., BARNARD, R., REVESZ, T., KWON, E., SHARER, L. & CHO, E. (1993). Multiple sclerosis. Pathology of recurrent lesions. *Brain* **116,** 681-693.

REYMENT, R. & JORESKOG, K. (1996). *Applied factor analysis in the natural sciences*. Cambridge University Press, Cambridge.

ROBINSON, K. & RUDGE, P. (1977). Abnormalities of the auditory evoked potentials in patients with multiple sclerosis. *Brain* **100,** 19-40.

SLOTNICK, S., KLEIN, S., CARNEY, T., SUTTER, E. & DASTMALCHI, S. (1999). Using multi-stimulus VEP source localization to obtain a retinotopic map of human primary visual cortex. *clinical Neurophysiol* **110,** 1793-1800.

TOWLE, V., WITT, J., NADER, S., REDER, A., FOUST, R. & SPIRE, J. (1991). Three-dimensional human pattern visual evoked potentials. II. Multiple sclerosis patients. *Electroencephalogr Clin Neurophysiol* **80,** 339-346.

UKKONEN, M., DASTIDAR, P., HEINONEN, T., LAASONEN, E. & ELOVAARA, I. (2003). Volumentric quantitation by MRI in primary progressive multiple sclerosis: volumes of plaques and atrophy correlated with neurological dissablity. *Eur J Neurol* **10,** 663-669.

WANDELL, B. (1995). Image formation. In *Foundations of vision*, pp. 13-43. Sinauer Associates, Inc., Sunderland.

WAXMAN, S. (1983). The demyelinating diseases. *Clinical Neurosci* **1,** 609-643.

WEINSTEIN, G., ODOM, J. & CAVENDER, S. (1991). Visually evoked potentials and electroretinography in neurologic evaluation. *Neurol Clin* **9,** 225-242.

CHAPTER III

Comparing Multifocal Frequency Doubling Illusion Visual Evoked Potentials and Automated Perimetry in Normal and Multiple Sclerosis Patients

Abstract

Purpose. To examine frequency doubling (FD) illusion based perimeter (FDT C- 20) and dischoptic FD multifocal visual evoked potentials (FD mfVEPs) in Normal subjects and Multiple Sclerosis (MS) patients.

Methods. Threshold testing was performed using a FDT perimeter, using a low spatial frequency (0.25 cyc/°) sinusoidal gratings that underwent rapid (25 Hz) counterphase flicker in 17 visual field regions. Dichoptic FD mfVEPs were recorded by concurrently stimulating 8 regions/eye, each region containing achromatic sinusoidal gratings at 95% contrast. Gratings in all mfVEP regions had horizontal stripes, the spatial frequencies of inner regions were 0.4 cyc/°, and those of the outer regions were 0.2 cyc/°. To compare the FDT C-20 thresholds with the FD mfVEP regional responses, we converted the FDT C-20 test regions via weighted sums, into the FD mfVEP stimulus dimensionality. Recordings were obtained from 19 Normal subjects, 26 Optic Neuritis (ON) patients and 24 MS patients without ON. We employed multiple regression to examine differences between the responses of Normal and MS subjects.

Results. The FD mfVEP amplitudes were smaller in the superior visual field regions for all subjects. The FDT results for ON and MS patients were significantly different from those of Normal subjects. The FDT data showed an enhancement of sensitivity for ON patients and a decrease of sensitivity for MS patients without ON. FD mfVEP amplitudes declined in both patient groups. A classification model, containing FDT C – 20 regional amplitudes performed at the specificity of 83.7% and sensitivity of 85.5%.

A classification model, containing the scaled FDT C – 20 thresholds and FD mf VEP amplitudes performed at 100% sensitivity and specificity in the MS patient group.

Conclusions. FDT C – 20 and FD mfVEPs obtained from Normal and ON subjects showed a significant diagnostic value in MS subjects.

Introduction

The frequency doubling technology (FDT) perimeter is a new technology designed for rapid and effective detection of visual field loss due to ocular diseases (Johnson *et al.*, 1998). FDT is based on the assumption that low spatial frequencies combined with high temporal frequencies will stimulate M-cell mechanisms, which are primarily involved in the detection of motion and rapid flicker or luminance change. This system enhances responses to large transient stimuli (Maddess & Hemmi, 1992; Johnson *et al.*, 1998). Spatial frequency doubling (FD) stimuli may provide us with important information about the variability of the retinal contrast gain control system (Maddess *et al.*, 2001).

The FD illusion occurs when a low-spatial frequency sinusoidal grating undergoes high-frequency counterphase flicker, giving the appearance of a spatial frequency twice that of the actual spatial frequency (Kelly, 1966; Tyler, 1974; Kelly, 1981; Maddess *et al.*, 2001). The diagnostic value of FD illusion has been demonstrated for FD based tests for glaucoma (Maddess, 1991; Johnson *et al.*, 1998; Maddess *et al.*, 1999; Maddess, 2000; Maddess *et al.*, 2000a; Wall *et al.*, 2002; White *et al.*, 2002). Other researches have shown that high contrast FD stimuli could provide highly accurate diagnosis of glaucoma when employed in a multi- region PERG (Maddess *et al.*, 2000b, a). FDT has been employed to detect Optic Neuritis (ON) (Fujimoto & Adachi-Usami, 2000) as well. Fujimoto (Fujimoto & Adachi-Usami, 2000) suggested that patients with resolved ON had a loss of M-cell function in the extrafoveal area. ON is a demyelinating disease of the optic nerve causing people to lose vision in particular visual regions (Frederiksen *et al.*, 1991a; Fujimoto & Adachi-Usami, 2000). A large number of ON patients also suffer from Multiple Sclerosis (MS) (Chiappa, 1983), the disease having a high risk of prevalence in the population of the Northern hemisphere (Waxman, 1983; Pugliatti *et al.*, 2002).

Apart from FDT, multifocal visual evoked potentials (mfVEPs) have previously detected scotomas and response delays in ON as well (Hood *et al.*, 2000). Conventional VEPs have been used in detection of MS and potentially related conditions in previous studies (Sand *et al.*, 1990; Andersson *et al.*, 1991; Brasil Neto, 1991; Roder, 1991). Conventional VEPs were also combined with MRI (Frederiksen *et al.*, 1991a; Frederiksen *et al.*, 1991b).

Tulunay-Keesey et al. (1993) showed that patients with MS and ON often exhibited reduced spatial contrast sensitivity. The spatial frequency ranges over which deficits occurred to tend to vary among patients. An orientation-specific reduction of sensitivity to low spatial frequencies in MS patients was also noticed. This again suggests that FD stimuli would be effective in characterizing MS.

Multifocal sparse VEPs (mfVEPs) were employed in our earlier study in which we examined 50 MS subjects and found good sensitivities and specificities (over 95%), provided by sparse mfVEPs (James *et al.*, 2004). To investigate the FD stimuli in MS we employed the following stimuli: 1) an FDT perimeter, 2) FD multifocal VEP (FD mfVEPs). In this study we sought to compare FDT and FD mfVEP data in Normal and ON subjects.

Methods

Stimuli

Frequency Doubling Technology Perimeter

Contrast threshold testing was performed using a FDT perimeter (FDT full threshold C-20 test, Humphrey, San Leandro, CA) (Johnson *et al.*, 1998). The FDT stimuli consisted of a low spatial frequency (0.25 cyc/°) sinusoidal gratings that underwent rapid (25 Hz) counterphase flicker. The test duration for the C-20 threshold procedure was approximately 4 minutes per eye. The FDT C-20 test determined minimum contrast (dB) necessary to detect the stimulus for each of the 17 target locations in the stimulus display (Fig. 3.1). The FDT full threshold C-20 screening test was given to each subject at the beginning of each experimental session. Subjects were seated in front of the FDT perimeter, with one eye occluded. Both eyes were tested.

Multifocal Frequency Doubling Visual Evoked Potentials

For VEP recording, the dichoptic FD visual stimuli were presented on a model CCID 7551 monitor (Barco, Kortrjk, Belgium). A program running on a Vista graphics board (Truevision, Shadeland Station, IN) controlled the stimulus display. Software for data acquisition, analysis and display was written in Matlab (Matlab; The MathWorks, Natick, MA). Subjects viewed the monitor at 30 cm providing the stimulus layout as illustrated in Figure 3.2.

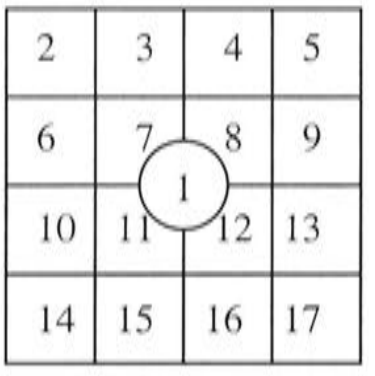

Figure 3.1 Illustration of the FDT C-20 stimulus regions. The visual field is divided into quadrants where each contains inner and outer visual field regions. During the experiment, frequency doubling illusion stimuli appeared randomly at each of the 17 regions until a contrast threshold is obtained in each region. The stimulus presentation pattern consists of four targets per quadrant each being 10 deg. square, and a central 5 deg. radius target.

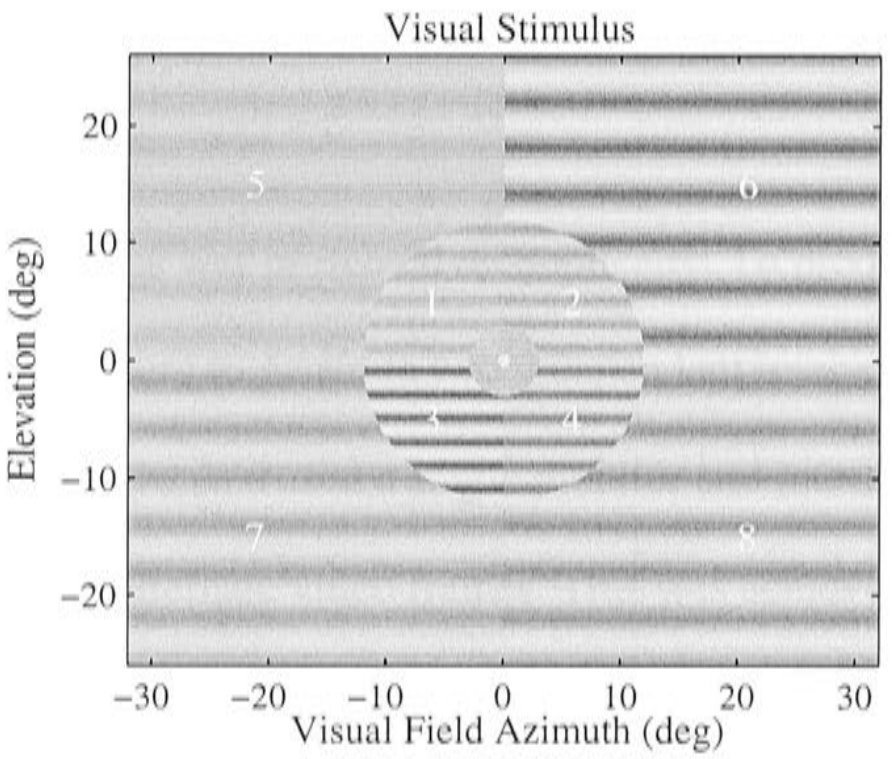

Figure 3.2 Illustration of the FD mfVEP stimulus appearance. The stimulus screen is divided into 8 simultaneously stimulated regions per eye. The regions 3, 4, 7, 8 are referred to inferior regions, the remaining are superior regions. Regions 1 to 4 are referred to as inner regions. Differences in contrast between regions are shown have to highlight boundaries between regions. Since the regions were modulated sinusoidally and asynchronously, this could represent a single frame of the stimulus sequence.

The face of the monitor was divided into eight different visual regions, which were presented simultaneously. A red fixation spot (0.75 °/square) was presented at the screen's centre. Each region contained an achromatic sinusoidal grating at 95% contrast. Gratings in all regions had horizontal stripes, the spatial frequencies of inner regions were 0.4 cyc/°, and the outer regions were 0.2 cyc/°. The contrast of each of the resultant 16 gratings stimuli was modulated sinusoidally with incommensurate temporal frequencies ranging from 15.45 to 21.51 Hz (Maddess *et al.*, 2000b). The spatial and temporal frequencies of the stimuli produced the FD illusion (Bedford *et al.*, 1997).

The visual stimulus was presented dichoptically. To produce dichoptic stimulation, it was necessary to generate two independent image sequences and present them separately to each eye. We used a single monitor and interleaved the images for the left and right eye on alternate video frames. This was achieved by means of a liquid crystal stereoscopic modulator (or shutter) (Tektronix, Inc., Beaverton, OR, USA) (James *et al.*, 2004). The shutter and spectacles reduced the initial mean luminance of the monitor from 45cd/m^2 to 7.6 cd/m^2. The noninterlaced refresh rate of the monitor was 101.5 Hz, producing a refresh rate of 50.75 Hz for each eye following the shutter.

Recording

FD mfVEPs were recorded using gold cup electrodes (diameter = 8 mm) placed on the scalp with the conductive paste EEG Ten20 (D.O.Weaver and Co, Aurora, LO). Electrodes were attached 3 cm above and 4 cm below the inion (Klistorner *et al.*, 1998). An earth electrode was attached to the right ear lobe. Each stimulus sequence lasted 40.4 seconds. Four records for each testing condition were obtained during the experiment. Blocks of four repeats were presented in a randomized order.

Subjects

The MS study group contained 50 subjects (eight men and 42 women, in the age range of 25 to 64 year). 26 subjects had experienced ON, 21 of them unilaterally. MS was diagnosed according to the latest MS diagnostic criteria (McDonald *et al.*, 2001). Subjects' medical history, including the number of MS attacks, MRI, CSF and other relevant details were collected from their neurologist. All MS subjects were classified as Relapsing Remitting (RR) (McDonald *et al.*, 2001). The Normal study group contained 19 subjects (12 men and seven women, in the age range of 22 to 44, with normal or corrected to normal refraction). A summary of all subjects' data is presented in Table 3.1A. The research followed the tenets of the Declaration of Helsinki, under the Australian National University's Human Experimentation Ethics Committee protocol M9901. Informed written consent was obtained from the subjects after the nature and possible consequences of the study were explained to them.

Table 3.1 A) Subject data. The three columns at the left show the three study groups (MS, ON and Normals) and the number of subjects who participated in the experiments. MS subjects had suffered from the disease on average 8.65 years (see *Duration of MS*), and during this time they had approximately 9.49 clinical attacks (see *N of attacks*). 26 subjects had optic neuritis and for 9 of them a CSF test was positive (*CSF*). MS type was Relapsing Remitting (RR) for all patients. Table 3.1B summarizes the number of significant response components (*Methods*). The *Study Group* column gives the name of study group, as in Table 3.1A. The *Total N of eyes* indicates the number of eyes used for our recordings. The three right most columns (*>95%, >93%* and *>90%*) indicate the number of eyes having 4 or more components at the level of significance for that column.

A. Subject data

Study group	N	Age ± SE (yr)	Sex (M/F)	Duration of MS (yr)	N of attacks	ON	CSF	MS type
MS	24	43 ± 15.2	6/18	8.65 ± 6.6	9.49 ± 4.8	NO	7	RR
ON	26	42 ± 16.3	2/24	8.12 ± 7.6	10.1 ± 5.6	YES	9	RR
Normals	19	31.2 ± 13.1	12/7	NA	NA	NA	NA	NA

B. Four significant response components

Study group	Total N of eyes	> 95%	> 93%	> 90%
MS	48	38	10	NA
ON	52	26	12	14
Normals	38	38	NA	NA

Data Analysis

FDT C-20 Data and FD mfVEPs

We compared FDT C-20 test data with the regional responses provided by the FD mfVEPs. The FDT C-20 test had 17 stimulated regions (Fig. 3.1) and FD mfVEP stimulus consisted from eight regions/eye stimulated simultaneously. To compare the FDT C-20 thresholds with the FD mfVEP regional responses it was necessary to equate the data. The regions of both stimuli overlapped, so we converted the FDT C-20 test regions into a mfVEP stimulus dimensionality.

The FD mfVEP regional areas were almost twice those of the FDT C-20 test quadrants. To transform the FDT C-20 stimulus dimensions, we averaged the dB thresholds of the FDT C-20 quadrant regions, weighted by a certain constant (Eq. 3.1). The weights were calculated according to the ratios of overlapping areas of the C-20 and mfVEPs stimulus regions.

$$R_{FDT} = \frac{\sum_{i=1}^{4}(r_i \times th_i)}{\sum_{i=1}^{4}(th_i)} \qquad (3.1),$$

R_{FDT} is thus the FDT threshold, transformed into the mfVEPs stimulus dimension; th_i (in dB) is the threshold of the C-20 test in the th_i region; r_i is the weight for th_i. The FDT C-20 full screening test thresholds (amplitudes) were given in decibels (dB). The FD mfVEPs' multifocal responses (in voltages) were transformed to decibels as well (Eq. 3.2). The log transformation had the additional effects of stabilizing the variance in the FD mfVEP data and permitting additive regression models to be fit to that data.

$$dB_{FD\ mfVEP} = 20 \log_{10}(\mu V_{FD\ mfVEP}) \qquad (3.2)$$

Multiple Linear Regression

Multiple linear regression (Johnson & Wichern, 1992) was used to quantify various independent effects from the averaged complex Fourier coefficients of the FD mfVEPs and the FDT C-20 thresholds. The regression analysis quantified the differences between the FDT C-20 and FD mfVEPs in the Normal and the ON/MS study groups. In all cases stimulus frequencies and subjects were fit as a nuisance variable.

FD mfVEP Phase Analysis

FD mfVEPs were analysed in both the amplitude and frequency domains. The Fast Fourier Transform (FFT) extracted the response components. The 40.4 s recording duration provided a temporal frequency resolution of 0.02 Hz. In order to employ FFT signal extraction, we needed to create an orthogonal design. Thus we had 16 stimulus frequencies (for eight stimulus regions and two eyes) – $f_1, f_2, \ldots f_{16}$, each containing an integer number of cycles over the 4096 video frames. Any two sinusoids with an integer number of cycles in the same interval are orthogonal. Because we were interested in the second harmonics, it was important none of the summed 240 frequencies $(f_i + f_j, i \neq j)$ should equal any of the 16-second harmonic frequencies. Such stimuli are said to be incommensurate (Maddess *et al.*, 2000b). We also arranged that none of the even order interactions between regions overlapped with the 16 2^{nd} harmonics to12th order (Victor & Shapley, 1979). The integer number of cycles was [735 739 744 750 757 767 781 793 801 820 841 870 900 935 968 1023].

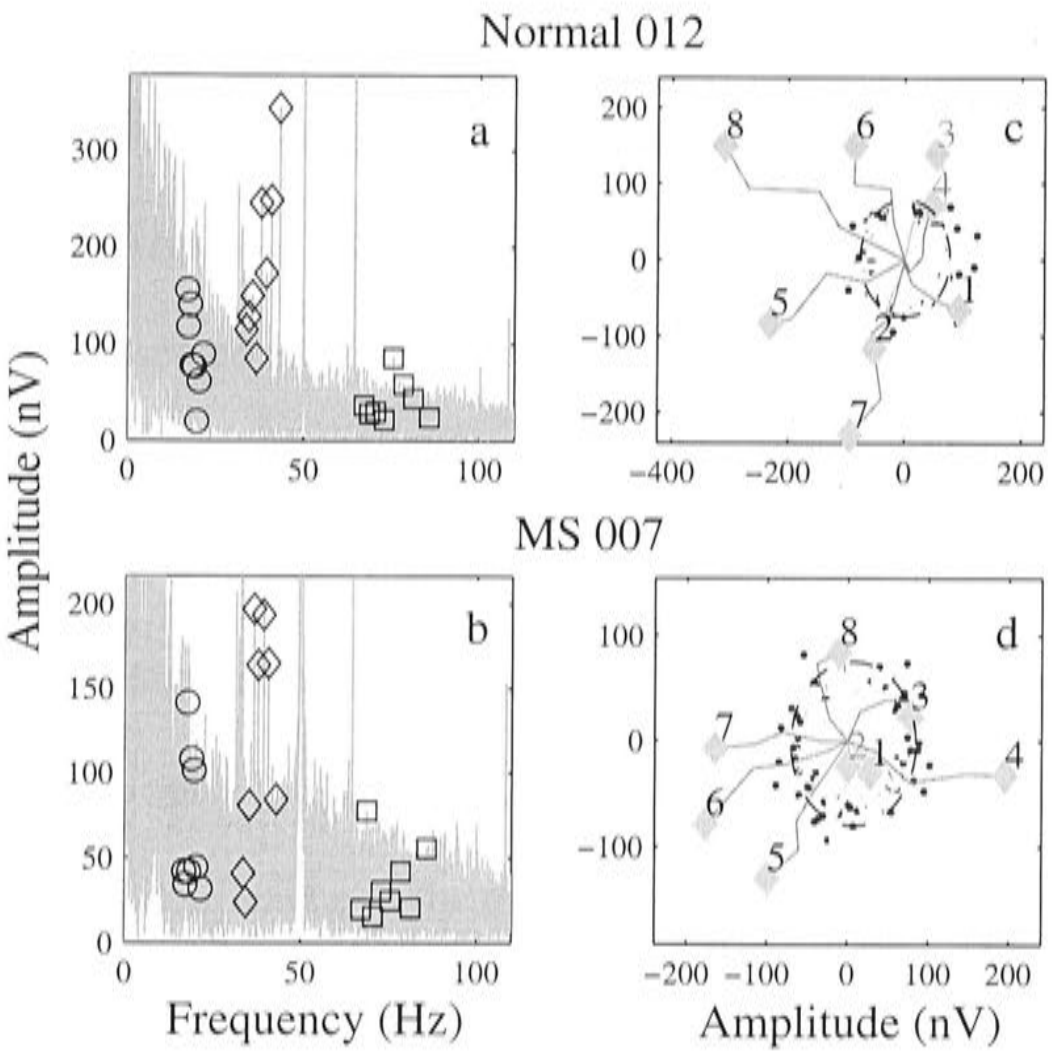

Figure 3.3 An example of FD mfVEP data. **a)** and **b)** represent amplitude spectra of exemplary Normal and MS subjects respectively. (○) the eight fundamentals, (◊) second and (□) fourth harmonics. **c)** and **d)** are Argand diagrams. The four segments of each trajectory show the gain and phase for each of the four trial responses, with overall gain scaled by 1/4, so that each trajectory is the vector mean, and its distance from the origin denotes the mean response amplitude. Regional interaction frequencies $f_i + f_j$ are shown as small black dots. Noise frequencies have random phases and therefore make random walks around the origin. The dashed oval is the 95% confidence limit computed from the resulting distribution of the noise frequencies. Vectors escaping from the dashed circle with increasing trial number are therefore significantly different from zero.

Figure 3.3 demonstrates graphically the output of the data acquisition program and the initial analysis. Figure 3.3a and 3.3b show examples of the amplitude spectra (in grey) highlighting the fundamental, second, and fourth harmonics (symbols) for the left eyes of a Normal and an MS subject. Figure 3.3c and 3.3d show the second harmonics for the left eye, numbered according to regions, 1 through 8, and some other frequencies in the complex plane (Argand diagrams (Maddess *et al.*, 2000b)). In the Fig. 3.3c, d frequencies were presented as vectors for which the length from the origin represents signal amplitude and the orientation represents phase lag. The vectors are jaggy as they are the vector sums of responses from 4 repeats divided by 4. Noise frequencies showed a random phase and so their vector sums circulated around the origin. The coefficients from the noise frequencies thus form a bivariate normal distribution and is used to measure the significance of the eight harmonics (Maddess *et al.*, 2000b). The noise frequency coefficients and regional interaction frequencies (f_i+f_j, $i \neq j$) were shown inside the circle representing the 95% confidence level (Maddess *et al.*, 2000b). Thus a given frequency is significant if its averaged vector lies outside the confidence limit circle.

We chose a notional criterion of at least 4 significant components per eye for each subject. 15 Normal subjects had more than 4 significant frequency components per eye under the limit of 95%. The remaining Normal subjects had 4 or more significant components under the confidence limit of 93%. Four per eye significant components (under the limit of 95%) were found in 19 MS and 13 ON patients. For the remaining 5 MS patients four significant responses per eye were achieved at 93% confidence. Data from 7 ON patients qualified the criterion of four significant components at the limit of 90%. Since the lower amplitudes could be due to damage due to MS (James *et al.*, 2004), we accepted these subjects. Table 3.1B summarizes the significance of the phase components in Normal, MS and ON study groups.

Note that the FD mfVEPs' phases would be expected to be relatively similar but rotated because at these frequencies small delays translate into large phase shifts. Thus, we examined the relative phase, calculated with respect to a reference phase. The reference phase was that of the frequency providing the most reliable signal across subjects. The phase from region 8 was the frequency providing the most reliable signal for all subjects (c.f. Fig. 3.6). To construct the relative phases for a given subject, we therefore subtracted the phase of region 8 from each of the eight regional FD mfVEP phases. This was achieved by rotation in the complex plane. The phase of region 8 was thus brought to 0 deg for all subjects while the phase lags and the leads of the other regional responses relative to that of region 8 were preserved. These relative phases had previously been shown to have diagnostic value (Maddess *et al.*, 2000b).

Discriminant Analysis

Discriminant analysis (Johnson & Wichern, 1992) was previously used to determine whether the structure of data could allow discriminating Normal subjects from those with glaucoma (Maddess *et al.*, 2000b). The objective of this analysis was to see if the structure of FD mfVEPs and FDT C-20 data permitted a method that was able to discriminate the Normal subjects from those having MS. The differing covariance of each data group suggested the use of quadratic discriminant data analysis (QDA) (Johnson & Wichern, 1992; Ruseckaite *et al.*, 2004). For comparison we also conducted linear discriminant data analysis (LDA) (Johnson & Wichern, 1992; Ruseckaite *et al.*, 2004). Diagnostic value was then assessed using ROC curves (Egan, 1975) constructed for the resulting discriminant models.

We used both unsorted and sorted measures in our discriminant models. The sorted measures were reminiscent of conventional perimetric practice where the worst N

regional results are often thought to be diagnostic. Therefore in these cases we sorted the regional response values and chose N to include in the discriminant models. This procedure means that regional information is lost thus precluding recognition of a particular region or set of regions (superior, central, peripheral) being highly diagnostic. Therefore we also used unsorted regional data to search for such possibilities. Scaled regional amplitudes (amplitudes, divided by the geometric mean of the Normal subjects FDT C-20 and FD mfVEPs data (in dB)) were considered as well.

Results

General Findings

Figure 3.4 summarizes the averaged FDT C-20 thresholds and FD mfVEPs regional amplitudes (dB) for the Normal (19 subjects), ON (26 patients) and MS (24 patients) study groups. The FDT C-20 thresholds are negative, but similar meaning in terms of sensitivity. The 8 FDT C-20 data/eye are computed as in Eq. 3.1 (*Methods*). In terms of sensitivity smaller dB values (vertical of each panel) indicate lower sensitivity for both data types. Visual inspection indicates that the pattern of responses was more similar across subject groups for the mfVEPs than for the C-20 test. Also, peripheral regions (5 to 8) had higher thresholds than inner.

To determine the major independent effects in the above-mentioned data, we used multivariate regression analysis. Table 3.2A summarizes the fitted effects for the FD mfVEP data (in nV) obtained from the Normal and MS (occluding ON) study groups. The regression model parameterisation set the responses from Normal subjects to be the reference condition. Thus, the *t - values* in Table 3.2 indicate the significance of the difference between the reference condition and the particular factor. The decrease of –0.52 nV ± 13.18 SE in the MS (without ON) subjects is not significantly different from the reference condition *($p = 0.0309$)*. The –24.84 nV ± 7.78 SE shows a significant decrease of amplitude in MS inner stimulated visual field

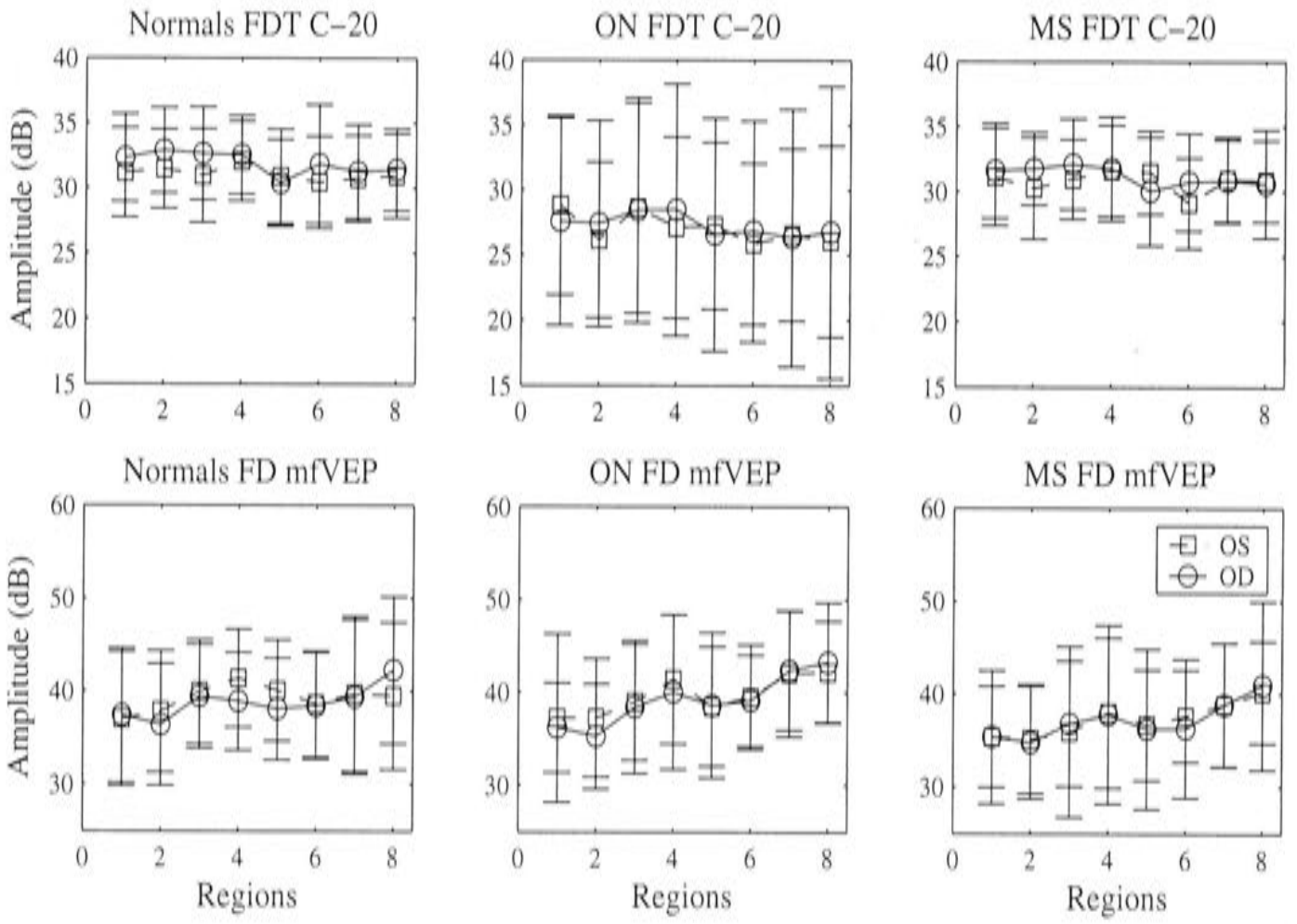

Figure 3.4 Averaged FDT C-20 and FD mfVEP data and their SDs. The top row shows the FDT C-20 thresholds, while the bottom represents the mfVEPs amplitudes. The left most column indicates the averaged Normal regional data; the middle column shows the ON averaged data. The right-most column represents the averaged MS responses. The averaged data are given for each of eight stimulated visual fields. Note that the FDT C-20 data are transformed into the eight-region convention (*Methods*) and are given as their absolute values.

Table 3.2 Tables A and B summarize multivariate linear regression results for the data from Normal versus MS and ON study groups. Multiple regression was performed on the FD mfVEP voltages. The coefficients show the simultaneously fitted values for the factors in the left-most column (*Condition*). The reference value (*Ref = Normals*) corresponding to the mean for Normal subjects, is given in nV at the top of the column (i.e. 117.9 nV). Table A) presents the fitted values for the Normal study versus MS, while B) gives the fitted values for the Normal versus ON data. The data of ON subjects gave a significant enhancement (8.7 ± 17.05 nV) in comparison to the data from Normals (cf. Fig. 3.6).

A. Normals versus MS. FD mfVEPs, Voltages

Condition	Coefficient (nV)	SE (nV)	t	p	-95%CL	+95%CL
Ref = Normals	117.90	4.89	24.10	0.0000	108.31	127.49
MS	-0.52	13.18	-0.39	0.0309	-26.36	26.32
MS superior	-12.38	7.78	-1.59	0.1178	-27.64	2.87
MS inner	-24.84	7.78	-3.19	0.0016	-40.10	-9.58
MS age > 40	-35.03	9.74	-3.59	0.0004	-54.13	-15.93
MS sex (male)	26.40	12.67	2.08	0.0399	1.52	51.24

B. Normals versus ON. FD mfVEPs, Voltages

Condition	Coefficient (nV)	SE (nV)	t	p	-95%CL	+95%CL
Ref = Normals	117.90	5.69	20.68	0.0000	106.73	129.07
ON	8.70	17.05	0.51	0.6275	-24.72	42.13
ON superior	-7.50	11.39	-0.65	0.5267	-29.84	14.83
ON inner	-28.51	11.39	-2.50	0.0135	-50.85	-6.17
ON age > 40	43.25	12.52	3.45	0.0006	18.70	67.80
ON sex (male)	-5.94	14.28	-0.41	0.6954	-33.94	22.04

regions. The decrease of –35.03 nV ± 9.74 SE amplitude was noticed in MS subjects older than 40 years (MS age). The variance accounted for by the model was $r^2 = 0.66$. Table 3.2B indicates multiple regression analysis results for the data (in nV) obtained from Normal and ON FD mfVEPs, the variance accounted for $r^2 = 0.68$. This model shows a non-significant amplitude increase between the reference condition and the ON responses (8.70 nV ± 17.05 SE).. The response increased by 43.24 nV ± 12.52 SE in those ON subjects, older than 40 years age. No significant effect of sex was noticed. These models had poorly stabilized variance but are presented to indicate approximately what happens to response amplitude.

As mentioned in the *Methods*, much better stability of variance was achieved by converting the mfVEP amplitude into decibels dB (Eq. 3.2, *Methods*). The transformation to decibels meant we could also fit the additive models for multiplicative effects; Table 3.3A, B summarizes the dB regression results. Table 3.3 has a similar format to the previous one, except for the *Multiplier* column, which indicates the multiplicative effect of each factor upon the reference condition (*Normal*). The –95% CI and +95% CI indicate the skewed confidence intervals for the given coefficient. For example, the FD mfVEPs (in dB) data from ON patients are significantly larger (1.24 dB ± 0.79 SE) than the data recorded from Normal subjects. When response voltage was fitted, the fits indicated significant suppression in ON superior and inner stimulated visual field regions rather in the remaining data. We found no significant effect of age in both the data of MS and ON patients; however the significant decrease of responses (-3.36 dB ± 0.80 SE) was found in MS patients, being older than age of 40 years. Responses of ON patients in the same age group increased by 2.75 dB ± 0.87 SE. The variance accounted for was $r^2 = 0.62$ in MS study group, and 0.64 in ON subjects.

Table 3.3 Tables A and B summarize multivariate linear regression results for the data obtained from Normal versus MS and ON subjects. Multiple regression was performed on the FD mfVEP amplitudes presented in decibels. The coefficients show the simultaneously fitted values for the factors in the left-most column (*Condition*). The *Multiplier* column indicates the scale value obtained when converting back to voltages from dB. –95% CI and + 95% CI indicate confidence intervals. The reference value (*Ref = Normals*) corresponds to the data of Normal subjects, is given in dB at the top of the column (i.e. 38.74 dB). Table A) shows the fitted values for the Normal study versus MS, while B) gives the fitted values for the Normal versus ON data. The values for the Reference *(Ref = Normals*), MS/ON, MS/ON superior and MS/ON inner visual fields' conditions are the respective responses or response enhancements in dB. The data of ON patients' gives a significant enhancement (1.24 ± 0.79 dB) from Normal data, while MS provides a barely significant suppression. The data of the ON patients, older than the age of 40 years are also larger by 2.75 dB ± 0.87 SE.

A. Normals versus MS. FD mfVEPs, Decibels

Condition	Coefficient (dB)	SE (dB)	t	p	Multiplier (x86.5)	-95%CL	+95%CL
Ref = Normals	38.74	0.40	95.33	0.0000	1	78.98	94.89
MS	0.58	0.64	0.91	0.6088	1.07	0.92	1.23
MS superior	-0.85	0.64	-1.31	0.1972	0.90	0.78	1.04
MS inner	-2.32	0.64	-3.62	0.0004	0.76	0.66	0.88
MS age > 40	-3.36	0.80	-4.15	0.0000	0.67	0.56	0.81
MS sex (male)	2.02	1.05	1.92	0.0580	1.26	1.25	1.27

B. Normals versus ON. FD mfVEPs, Decibels

Condition	Coefficient (dB)	SE (dB)	t	p	Multiplier (x86.5)	-95%CL	+95%CL
Ref = Normals	38.74	0.39	99.33	0.0000	1	79.16	94.68
ON	1.24	0.79	1.56	0.3080	1.15	0.96	1.38
ON superior	-0.64	0.79	-0.81	0.4315	0.92	0.77	1.11
ON inner	-2.32	0.79	-2.92	0.0038	0.76	0.64	0.91
ON age > 40	2.75	0.87	3.15	0.0018	1.37	1.12	1.67
ON sex (male)	-0.27	0.99	-0.27	0.7982	0.96	0.77	1.21

Table 3.4 Tables A and B summarize multivariate linear regression results for the FDT C-20 amplitudes in decibels of Normal versus MS and ON patients. The coefficients show the simultaneously fitted values for the factors in the left-most column (*Condition*). The table format is similar to the Table 3.3 format. The reference value (*Ref = Normals*) corresponds to the data of Normal subjects, is given in dB at the top of the column (i.e. 31.8 dB). Table A) shows the fitted values for the Normal study group versus MS, while B) gives the fitted values for the data of Normal versus ON study groups.

A. Normals versus MS. FDT C-20, Decibels

Condition	Coefficient (dB)	SE (dB)	t	p	Multiplier (x38.9)	-95%CL	+95%CL
Ref = Normals	31.80	0.20	159.1	0.0000	1	37.14	40.82
MS	-0.65	0.56	-1.15	0.2579	0.92	0.81	1.05
MS superior	-0.12	0.33	-0.36	0.7327	0.98	0.91	1.06
MS inner	0.85	0.33	2.58	0.0108	1.10	1.02	1.19
MS age > 40	-0.75	0.41	-1.81	0.0735	0.91	0.83	1.00
MS sex (male)	0.25	0.54	0.46	0.6576	1.02	0.91	1.16

B. Normals versus ON. FDT C-20, Decibels

Condition	Coefficient (dB)	SE (dB)	t	p	Multiplier (x38.9)	-95%CL	+95%CL
Ref = Normals	31.80	0.30	104.6	0.0000	1	36.35	41.70
ON	2.17	0.90	2.38	0.0185	1.28	1.04	1.57
ON superior	1.32	0.60	2.18	0.0313	1.16	1.01	1.33
ON inner	1.53	0.60	2.52	0.0128	1.19	1.04	1.36
ON age > 40	-3.52	0.66	-5.28	0.0000	0.66	0.57	0.77
ON sex (male)	-9.28	0.76	-12.19	0.0000	0.34	0.28	0.40

We also fitted the FDT C-20 data (in dB only). Table 3.4A shows the model fit between Normal and MS study groups, while Table 3.4B indicates the model fit between the Normal and ON subjects' FDT C-20 thresholds. The table format is the same as for Table 3.3. The reference condition is the FDT C-20 thresholds obtained from the Normal subjects. We found that the data from ON patients were enhanced by 2.17 dB ± 0.90 SE *($p< 0.05$),* but the thresholds significantly decreased in ON patients (women), older than the age of 40 years (-3.52 dB ± 0.66 SE). The variance accounted for was $r^2 = 0.67$ in MS study group, and 0.74 in ON subjects.

We compared the FDT C-20 thresholds and the FD mfVEPs (note that FDT C-20 thresholds were negative). Figure 3.5 illustrates the regression results for averaged regional values of the FDT C-20 and FD mfVEP data obtained from the Normal, ON and MS study groups. The regression coefficients $b \pm SE$ are given in dB for each study group. The dashed line indicates coefficients for the FD mfVEPs, while the solid line shows the coefficients for FDT C-20 thresholds. The effects of age and sex were considered as well. When dB values are fit this corresponds to different multiplication scaling of individuals results.

Discriminant Analysis

LDA and QDA (*Methods)* were performed on the regional FDT C-20 and FD mfVEP data amplitudes (in dB) and/or rotated mfVEP phases. Classifiers were based upon the data of the 26 ON subjects, and these were subsequently applied to the data of those MS patients without ON. The classification models described below were thus all computed using data from Normal subjects and ON patients. The performance of the best of these models on the 24 MS patients who had no visual symptoms is summarized in the section that follows.

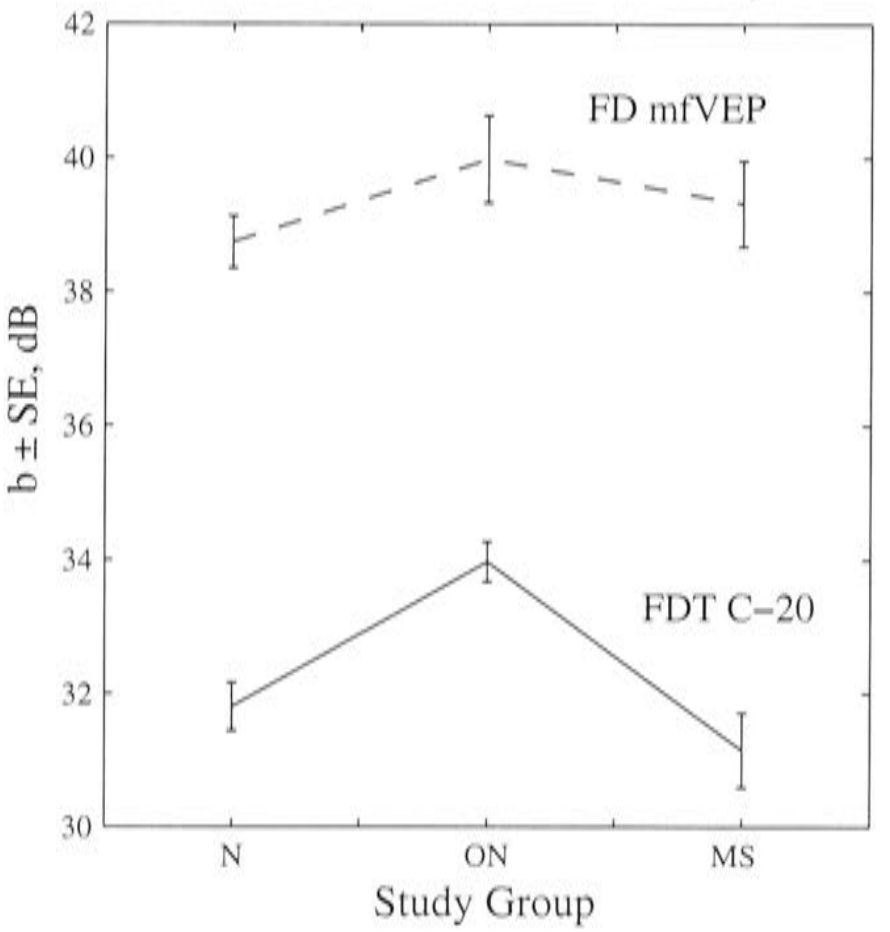

Figure 3.5 Multivariate regression coefficients and their SE for FDT C-20 and FD mfVEPs obtained from Normal (N), ON and MS patients. The dashed line represents FD mVEP regression coefficients, when the solid line illustrates the FDT C-20 regression coefficients. Note, that the data are averaged across all subjects in each group. These values are exclusive of the independent effects of age, sex, stimulus frequency which were fitted as well.

FDT C-20 and FD mfVEPs (Not Sorted and Sorted) Regional Amplitudes

The regional unsorted FDT C-20 thresholds and the mfVEPs were little of diagnostic use indicating that no particular region was diagnostic (*Methods*). Their sensitivities and specificities varied from 73% to 76% for LDA. QDA gave similarly poor performance. Thus we decided to sort the regional data from worst (lowest amplitudes) to best (highest amplitudes). The smaller threshold values presumably corresponded to more damaged visual regions. Sorting the data is similar to the practice in perimetry where a criterion number of damaged visual field locations are used for diagnosis. The sorted worst eight mfVEPs measures obtained from both eyes performed at specificity of 78.7% and sensitivity of 81.4 % for LDA model.

We were also interested to know how the FDT C-20 thresholds performed on their own. The performance of the eight worst thresholds obtained from both eyes was high; model performed at the specificity of 83.7% and sensitivity of 85.5% for LDA model. The performance of QDA was 100%. To increase the LDA classification performance we combined the measures from both tests. In this case the specificity and sensitivity for LDA increased to 95.3%, while the performance of QDA was 100%.

Relative FD mfVEP Phases

We were also interested to know how the relative phases (Maddess *et al.*, 2000b) would perform. Figure 3.6 illustrates the FD mfVEP amplitudes in voltages for the eight stimulated visual regions. For this purpose we took the relative phases of the four most significant regions, significant at least at 90%. The resulting discriminant model, based on the data from ON and Normal subjects gave a sensitivity of 83.3 %

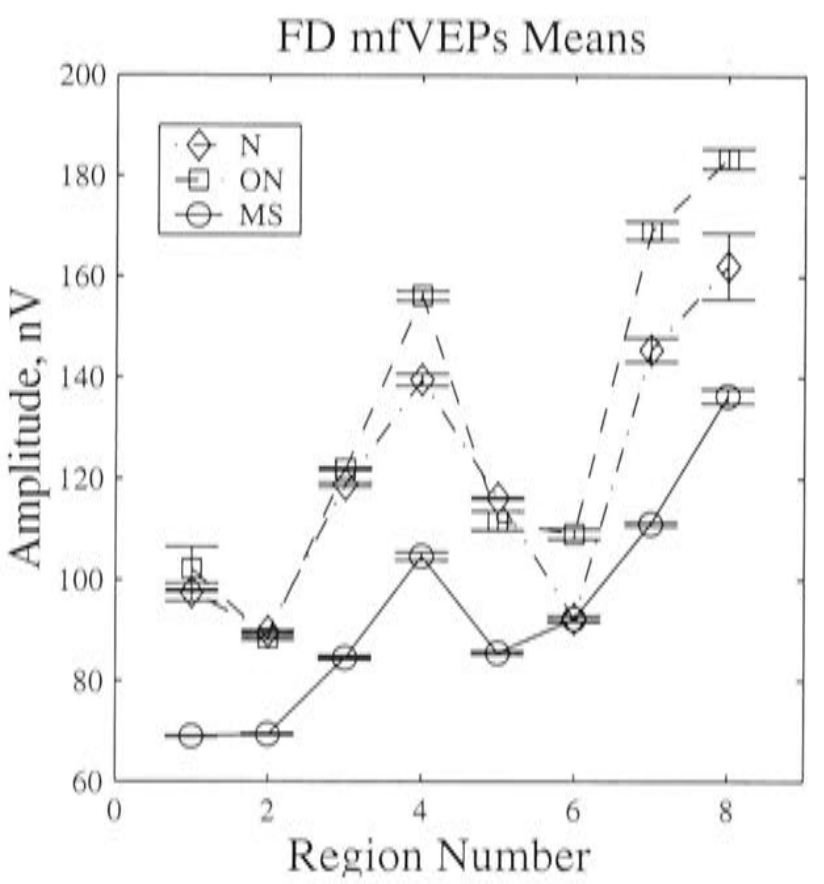

Figure 3.6 Regional FD mfVEP data of the second harmonics averaged across subjects, eyes and visual field locations. Averages are given for Normal subjects (N), ON group and MS subjects excluding those with ON. Error bars are SE. The amplitudes of region 8 were largest on average.

and specificity 78.94% for LDA, and for QDA was 100% and 94.7% respectively. To improve the performance of the discriminant analysis the relative phases were combined with the sorted FDT C-20 and FD mfVEPs' regional measures. Thus, the four worst sorted regional FDT C-20 and FD mfVEPs amplitudes (for both of the left and right eye) together with all FD mfVEPs relative phases were combined and examined. The current model performance improved to the sensitivity of 94.7% and the specificity of 97.7% for LDA. QDA increased to 100%. These models would be difficult to validate due to their complexity.

Sorted Amplitude Differences and Scaled Amplitudes

An other measure that gave a relatively good performance was sorted amplitude differences between the averaged data from Normal subjects and individual data sets. The eight (four from each eye) worst regional differences, combined with the four worst FDT C-20 thresholds and the four worst FD mfVEP data performed at the 94.7% sensitivity and 94.7% specificity levels for LDA.

One of the simplest measures, so-called scaled amplitudes, was the most reliable diagnostically, providing sensitivity and a specificity of 100% for LDA and QDA. To derive the scaled amplitudes we retrieved the four worst regional amplitudes for FDT C-20 and FD mfVEPs and divided them by the geometric mean of the data from Normal subjects (FDT C-20 and FD mfVEPs (in dB) respectively). Figure 3.7 illustrates the sensitivities and specificities for the above-described measures.

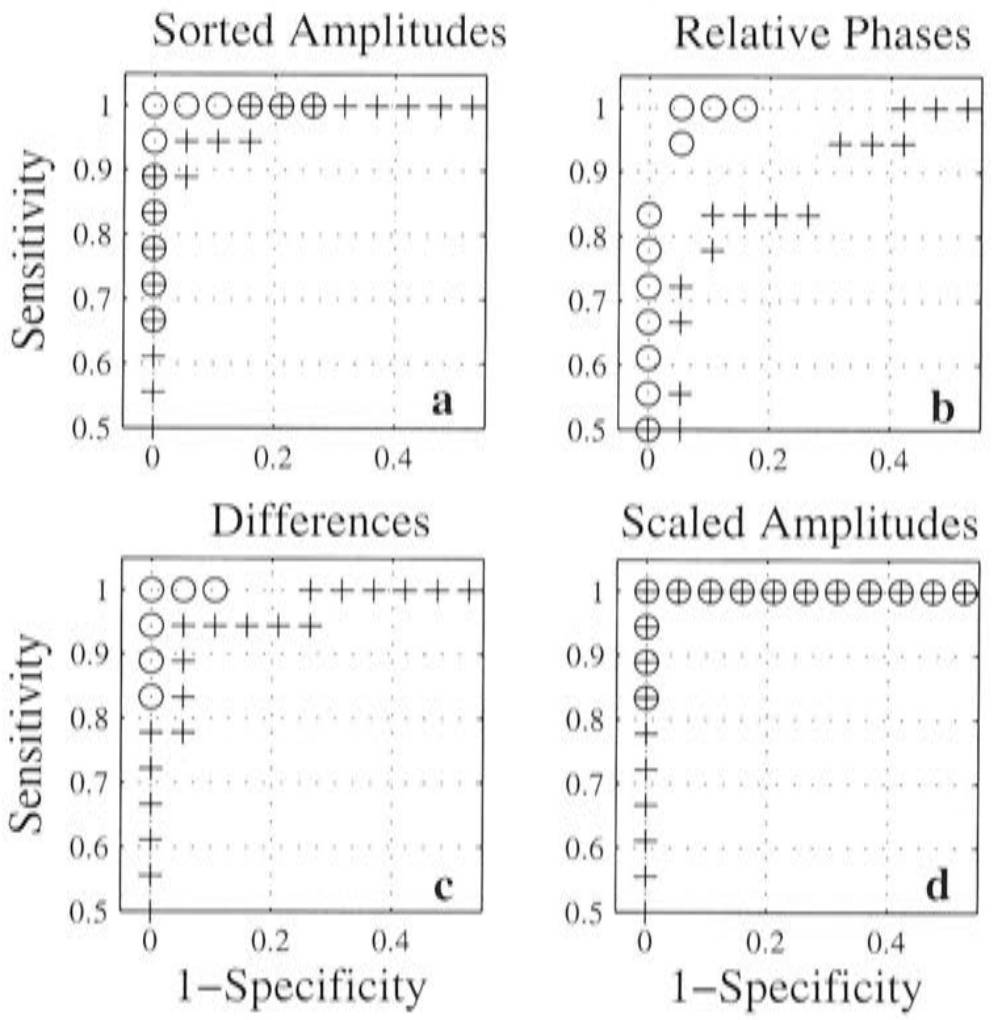

Figure 3.7 ROC curves comparing various LDA and QDA cases for ON patients. ROCs for LDA are shown as '+' symbols, QDA as 'o'. Only the upper left quadrant of a typical ROC plot is shown to permit the details to be seen. **a)** Sorted amplitudes for eyes, the FDT C-20 and mfVEP gave the sensitivities and specificities of 94.4% and 95.3% for LDA and 100% for QDA respectively. **b)** The mfVEPs' relative phases only gave poor performance at 83.3.2% and 78.96% for the LDA and the performances of 100% and 94.7% for QDA cases. **c)** Sorted amplitudes for eyes, the FDT C-20 and mfVEPs data and sorted differences gave the performances of 94.4% and 94.7% for LDA and 100% for QDA cases. **d)** Scaled and sorted FDT C-20 combined with the mfVEP amplitudes in both cases gave the performance of 100%.

Sparse mfVEPs and FD Stimuli

In our previous study (Ruseckaite *et al.*, 2004) we investigated the classification performance for the sparse multifocal stimuli obtained from the data recorded from Normal and ON study groups (James, 2003; James *et al.*, 2004). We examined different levels of temporal sparseness and found that VEPs, obtained from very sparse Pattern Pulse stimulus, gave very good performance for both LDA and QDA. To achieve this performance, we combined different VEPs measures: such as the first negativity (N1), the first positivity (P1), and their implicit times (N1 and P1). We also extracted the communalities of the first 2 principal components (PC), which were included in the discriminant analysis model.

The goal of the current experiment was to examine the performance of combined sparse VEPs, FDT C-20 and FD mfVEPs measures. We experimented with different models containing N1, P1, PCA Communalities and NT_F (for both eyes and all stimulated regions) recorded from the Pattern Pulse stimulus for the Normal and ON study groups. To reduce the complexity of classification models we decided to combine fewer measures, obtained from different stimuli. A classification model combining the scaled four FDT C-20 thresholds only, N1, P1 and NT_F gave the best performance: it increased to 100 % for both discrimination methods.

Classification of MS Patients

We then examined some of the above models formed on the data of Normals and ON subjects to classify the data of the 24 MS subjects (Table 3.5). The first 3 models M1 to M3 are based on the measures, extracted from the FDT C-20 and mfVEP tests.

Table 3.5 MS data classification models for Figure 3.8. Table presents 6 models, used for the classification of 24 MS patients. The first three models M1 – M3 contain the measures extracted from the FDT C-20 and FD mfVEPs tests. The models M4 - M6 incorporate the measures from the M1-M3 models and include the measures extracted from the Pattern Pulse mfVEP stimulus.

Model Name	Model Description
M1	Sorted 8 worst regional FDT C-20 thresholds from both eyes
M2	Sorted 4 worst regional FDT C-20 and 4 FD mfVEP amplitudes from both eyes
M3	Sorted 4 worst FDT C-20 and 4 FD mfVEP scaled amplitudes from both eyes
M4	The N1+ P1, PCA Communalities and NT_F for both eyes and all stimulated regions for the Pattern Pulse stimulus from Normals and ON study groups and sorted the 4 worst regions from the FDT C-20 and FD mfVEPs from both eyes
M5	The N1, NT, NT_F for both eyes and all stimulated regions for the Pattern Pulse stimulus from Normals and ON study groups and sorted 4 the worst regions from the FDT C-20 and FD mfVEPs from both eyes
M6	The N1, P1, NT_F for both eyes and all stimulated regions for the Pattern Pulse stimulus from Normals and ON study groups and the sorted 4 worst FDT C-20 scaled amplitudes from both eyes

Models M4 to M6 incorporate measures from M1 to M3 and measures from the Pattern Pulse stimulus.

Figure 3.8 illustrates the LDA classification statistics (specificity being 100%) for models M1 to M6. Black bars in the picture represent the percentage of correctly classified MS subjects. The M1 model correctly classified 62% MS patients. The rate of M2 and M3 was 58% and 61% respectively. The percentage of correctly classified subjects increased for M4 (95%), M5 (94%) and M6 (98%).

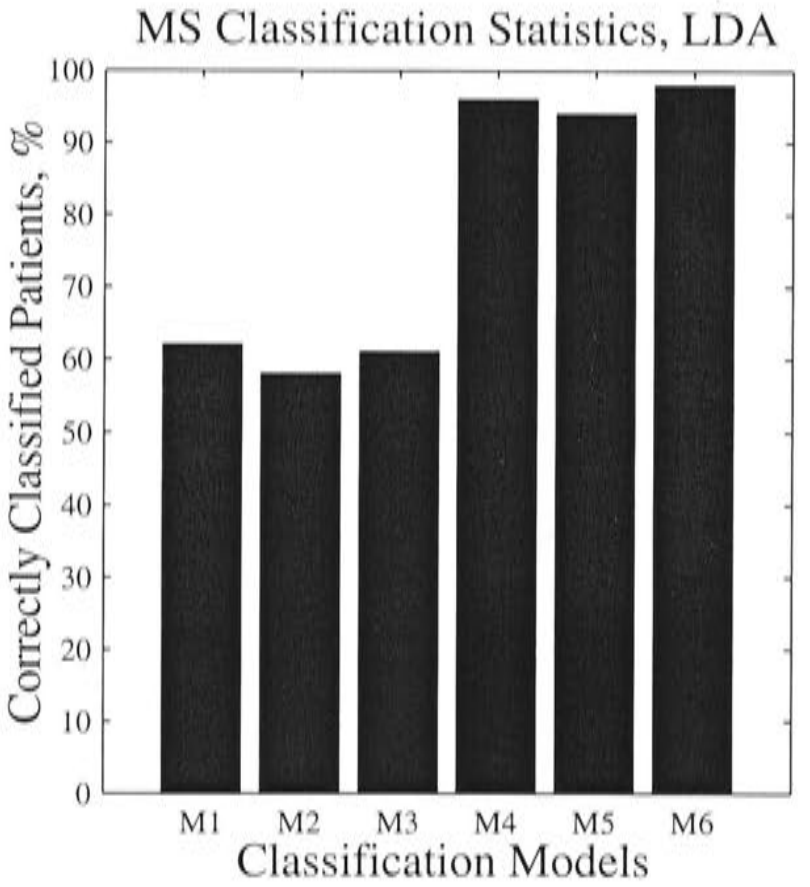

Figure 3.8 MS subjects classification statistics based on models developed for ON patients. The figure presents the percentage specificity for the 24 MS patients that were correctly classified (by LDA) at specificity of 100% using the FDT C-20 and FD mfVEP visual stimuli. The horizontal axis represents six classification models M1 – M6. A detailed description of each model is given in Table 3.5.

Discussion

General Findings

mfVEPs using super threshold FD stimuli were recorded from 24 MS, 26 ON and 19 Normal subjects. Their visual fields were examined with the FDT perimeter. We found that the FDT C-20 thresholds significantly differed between the Normal and ON study groups (*cf.* Table 3.4, Fig. 3.5). The FDT C-20 thresholds of the MS patients were smaller than for those of the Normal subjects by -0.65 dB ± 0.56 SE, and smaller by – 3.52 dB ± 0.66 SE in ON patients, older than 40 years of their age (Table 3.4). The top row of the Figure 3.4 illustrates this difference visually. Smaller responses for the ON and MS data illustrate the worst regions of visual field. Superior fields were also smaller, but probably due to electrode position (Ruseckaite *et al.*, 2004). The FDT results were also significantly different for Normal subjects and ON or MS patients. Interestingly, the mfVEPs of ON patients, older than 40 years of age, were larger than these of Normal subjects by 2.75 dB ± 0.87 SE (*cf.* Tables 3.3).

Discriminant Analysis

Discriminant analysis was performed on several parameters, including the regional FDT C-20 and mfVEP amplitudes, scaled amplitudes, also relative mfVEPs phases. High sensitivities and specificities were recorded for the more complex quadratic models, but some simpler models provided good performance. QDA models usually are much more complex and so would be difficult to validate but are suitable for where unequal variances occur in the patients and Normal groups. QDA models on one or two parameters like scaled amplitudes might be acceptable. LDA models with one ore more

parameters have definite clinical relevance (*i.e.* when mfVEP and FDT data are combined).

It was sensible to include a few of the worst regional amplitudes of the FDT C-20 and FD mfVEP data instead of using all amplitudes. The results showed good performance (specificity over 90% for LDA) for four the worst regional amplitudes of FDT C-20 and FD mfVEPs, selected from both eyes. The sorted amplitude differences (in decibels) also produced higher discrimination performance. One of the simplest measures was scaled amplitude, obtained by dividing the worst regional amplitudes by the geometric mean of the data from Normal subjects. In this case sensitivities and specificities increased to 100% for both LDA and QDA.

According to our previous study (Ruseckaite *et al.*, 2004), high discrimination performance was achieved when combining the N1, P1 and NT_F (*Methods*) from the sparse mfVEP stimulus. We were curious to create a model containing measures obtained from sparse mfVEPs and the FD illusion stimuli. Apparently, some less complex models based on the sparse mfVEP stimulus and the parameters such as sorted FDT C-20 and mfVEPs amplitudes were able to classify MS subjects even better than the complex ones. As proof of that, Figure 3.8 illustrates classification statistics for the models, described in Table 3.5. The percentage of correctly classified patients was above 90% for the models containing the N1, P1, NT_F, and sorted worst FDT C-20 and FD mfVEPs amplitudes. In comparison with the FD classification models M1 to M3, the percentage of the correctly classified MS patients increased to 98 % for the model based on the scaled amplitudes, N1, P1 and NT_F. Apparently relatively simply classification models can diagnose MS patients who have had no ON. This was also found in our earlier study using more conventional mfVEP study.

The FD illusion was studied by Fujimoto et al. (2000). Based on the knowledge, that patients with ON showed abnormalities of critical flicker frequency, contrast

sensitivity and contrast sensitivity, the researchers aimed to detect loss of magnocellular projecting cells (M_cells) in the extrafovea. They examined twelve ON patients using conventional Humphrey automated and FDT perimetry. Only FDT was able to find a depression in the extrafoveal area, related to a loss of M-cell function here.

Conventional automated perimetry and FDT was investigated in the study of Wall et al. (2002). This study was designed to determine the sensitivity and specificity of both tests in optic neuropathies. The researchers found that sensitivities and specificities of FDT and conventional perimetry were similar, being of [81.3% 76.2%] and [87.5% 81.0%] respectively.

Conventional VEPs combined with MRI were applied for ON diagnostics in the previous studies of Fredereksen et al. (1991a; 1991b) as well. Here the abnormalities revealed in 79% of patients, while our tests were able to classify more than 90% patients correctly. As a result of this we can state that mfVEP and FDT measures are powerful tool to classify the data of MS subjects, they are relatively inexpensive and might permit quantitave, cost effective management of treatment providing better quality of MS and ON patients life.

Bibliography

ANDERSSON, T., SIDEN, A. & PERSSON, A. (1991). A comparison of clinical and evoked potential (VEP and median nerve SEP) evolution in patients with MS and potentially related conditions. *Acta Neurol Scand* **84,** 139-145.

BEDFORD, S., MADDESS, T., ROSE, K. & JAMES, A. (1997). Correlations between observability of the spatial frequency doubled illusion, a multi-region PERG. *Aust N Z J Ophthalmol* **25,** 91-93.

BRASIL NETO, J. (1991). [Evoked potentials in multiple sclerosis: recent experience at the Locomotor System Diseases Hospital]. *Arq Neuropsiquiatr* **49,** 204-207.

CHIAPPA, K. (1983). Evoked potentials in clinical medicine.

EGAN, J. (1975). *Signal detection theory and ROC analysis*. Academic Press, Inc. Ltd., London.

FREDERIKSEN, J., LARSSON, H., OTTOVAY, E., STIGSBY, B. & OLESEN, J. (1991a). Acute optic neuritis with normal visual acuity. Comparison of symptoms and signs with psychophysiological, electrophysiological and magnetic resonance imaging data. *Acta Ophthalmol Copenh* **69,** 357-366.

FREDERIKSEN, J. L., LARSSON, H. B., OLESEN, J. & STIGSBY, B. (1991b). MRI, VEP, SEP and biothesiometry suggest monosymptomatic acute optic neuritis to be a first manifestation of multiple sclerosis. *Acta Neurol Scand* **83,** 343-350.

FUJIMOTO, N. & ADACHI-USAMI, E. (2000). Frequency doubling perimetry in resolved optic neuritis. *Invest Ophthalmol Vis Sci* **41,** 2558-2560.

HOOD, D., ODEL, J. & ZHANG, X. (2000). Tracking the recovery of local optic nerve function after optic neuritis: a multifocal VEP study. *Invest Ophthalmol Vis Sci* **41,** 4032-4038.

JAMES, A. (2003). The pattern pulse multifocal visual evoked potential. *Invest Opthalmol Vis Sci* **44,** 879-890.

JAMES, A., RUSECKAITE, R. & MADDESS, T. (2004). Effect of temporal sparseness and dichoptic presentation upon multifocal visual evoked potential. *Visual Neurosci* **submitted**.

JOHNSON, C., WALL, M., FINGERET, M. & LALLE, P. (1998). *A primer for frequency doubling technology*. Humphrey Systems, Dublin, CA, USA.

JOHNSON, R. & WICHERN, D. (1992). *Applied multivariate statistical analysis*. Prentice-Hall, Inc.

KELLY, D. (1966). Frequency doubling in visual responses. *J Opt Soc Am* **56,** 1628-1633.

KELLY, D. (1981). Nonlinear visual responses to flickering sinusoidal gratings. *J Opt Soc Am* **71,** 1051-1055.

KLISTORNER, A., GRAHAM, S., GRIGG, J. & BILLSON, F. (1998). Electrode position and the multi-focal visual-evoked potential: role in objective visual field assessment. *Aust N Z J Ophthalmol* **26(Suppl.),** 91-94.

MADDESS, T. (1991). Method and apparatus for use in diagnosis of glaucoma; Australia Patent No. 611,585.

MADDESS, T. (2000). Perspectives on the use of frequency doubling and short wavelength perimetry for the diagnosis of glaucoma. *Clinical Exp Ophthalmol* **28,** 245-247.

MADDESS, T., GOLDBERG, I., WINE, S., DOBINSON, J., WELSH, A. H. & JAMES, A. C. (1999). Testing for glaucoma with the spatial frequency doubling illusion. *Vision Res* **39,** 4258-4273.

MADDESS, T., JAMES, A., GOLDBERG, I., WINE, S. & DOBINSON, J. (2000a). Comparing a parallel PERG, automated perimetry, and frequency-doubling thresholds. *Invest Ophthalmol Vis Sci* **41,** 3827-3832.

MADDESS, T., JAMES, A., GOLDBERG, I., WINE, S. & DOBINSON, J. (2000b). A spatial frequency - doubling illusion -based pattern electroretinogram for glaucoma. *Invest Ophthalmol Vis Sci* **41,** 3818-3826.

MADDESS, T., SEVERT, W. & STANGE, G. (2001). Comparison of three tests using the frequency doubling illusion to diagnose glaucoma. *Clinical Exp Ophthalmol* **29,** 359-367.

MCDONALD, W., COMPSTON, A., EDAN, G., GOODKIN, D., HARTUNG, H., LUBLIN, F., MAFARLAMD, H., PARTY, D., POLMAN, C., REINGOLD, S., SANDBERG-WOLLHEIM, M., SIBLEY, W., THOMPSON, A., VAN DEN NOORT, S., WEINSHENKER, B. & WOLINKSY, J. (2001). Recommended diagnostic criteria for multiple sclerosis: guidelines from the international panel on the diagnosis of multiple sclerosis. *Ann Neurol* **50,** 121-127.

PUGLIATTI, M., SOTGIU, S. & ROSATI, G. (2002). The worldwide prevalence of multiple sclerosis. *Clinical Neurol and Neurosurg* **104,** 182-191.

RODER, H. (1991). [VEP in the determination of multiple lesions in the visual system in patients with multiple sclerosis]. *EEG EMG Z Elektroenzephalogr Elektromyogr Verwandte Geb* **22,** 234-238.

RUSECKAITE, R., MADDESS, T. & JAMES, A. C. (2004). Sparse multifocal stimuli for the detection of multiple sclerosis. *Visual Neurosci* **submitted**.

SAND, T., SJAASTAD, O., ROMSLO, I. & SULG, I. (1990). Brain-stem auditory evoked potentials in multiple sclerosis: the relation to VEP, SEP and CSF immunoglobulins. *J Neurol* **237,** 376-378.

TULUNAY-KEESEY, U., BROOKS, B., KUKULJAN, R. & VER HOEVE, J. (1993). Effect of orientation on spatiotemporal contrast sensitivity in multiple sclerosis. *Vision Res* **34,** 123-136.

TYLER, C. W. (1974). Observations on spatial-frequency doubling. *Perception* **3,** 81-86.

VICTOR, J. & SHAPLEY, R. (1979). Receptive field mechanism of cat X and Y retinal ganglion cells. *J Physiol* **74,** 275-298.

WALL, M., NEAHRING, R. & WOODWARD, K. (2002). Sensitivity and specificity of frequency doubling perimetry in neuro-ophthalmic disorders: a comparison with conventional automated perimetry. *Invest Ophthalmol Vis Sci* **43,** 1277-1283.

WAXMAN, S. (1983). The demyelinating diseases. *Clinical Neurosci* **1,** 609-643.

WHITE, A., SUN, H., SWANSON, W. & LEE, B. (2002). An examination of physiological mechanisms underlying the frequency-doubling illusions. *Invest Ophthalmol Vis Sci* **43,** 3590-3599.

CHAPTER IV

Comparing Multifocal Binocular Pattern Pulse Visual Evoked Potentials in Normal and Multiple Sclerosis Patients

Abstract

Purpose. To compare monocular and binocular Pattern Pulse multifocal visual evoked potentials (mfVEPs) in Normal subjects and Multiple Sclerosis (MS) patients.

Methods. Monocular and binocular mfVEPs were obtained by concurrently stimulating 8 regions of cortically scaled checkerboards to sparse Pattern Pulse visual stimulus. Multifocal responses were recorded from 19 Normal subjects, 50 MS patients, 26 of whom had Optical Neuritis (ON) and 24, who had no visual symptoms (MS). We employed multiple regression to examine the differences between the data from a monocular and binocular viewing. We examined the first response negativities (N1), positivities (P1) their implicit times NT and PT and fitted delays.

Results. Binocular mfVEP waveforms had larger amplitudes than monocular ones, but they were also smaller in MS and ON patients. The responses in any single eye and binocular condition were delayed in the patients' study group, but there was no significant difference between monocular and binocular latencies. We also found, that the binocular delays were intermediate between the best and the worst eye.

Conclusions. MfVEPs recorded to the Pattern Pulse stimulus in binocular viewing condition have larger amplitudes, but their latencies do not differ from the latencies in monocular responses.

Introduction

Previous studies have shown that visual evoked potentials (VEPs) obtained to both monocular and binocular summation stimuli are a useful tool in characterizing various ophthalmic diseases (Shea *et al.*, 1987; Leguire *et al.*, 1991; McKerral *et al.*, 1995; Amaya *et al.*, 1998; Di Summa *et al.*, 1999; Marshman *et al.*, 2001; Sloper *et al.*, 2001; Mizota *et al.*, 2003).

Shea et al. (1987) examined binocular VEP summation (the percentage by which the binocular VEP amplitude exceeded the mean of the two monocular VEP amplitudes) in infants and adults with abnormal binocular histories. In that study a significantly higher level of binocular VEP summation in infants produced much larger binocular VEP amplitudes, when monocular amplitudes were equivalent to those of stereo normal and stereo efficient adults. The results of Shea et al. (1987) study supported the hypothesis that VEP amplitude was mediated by two independent pools of monocular cortical neurons and that binocular VEP summation was not representative of the activation of binocular cortical neurons.

Amaya et al. (1998) investigated an effect of binocular summation of VEPs in normal tension glaucoma. They found a high spatial frequency deficit (i.e. functional deficiency) for binocular stimulation in those patients with glaucoma, but no binocular summation effect was found in the normal control group.

The effect of binocular summation has also been evaluated in patients with traumatic optic neuropathy (TON) and ON (Ikejiri *et al.*, 2002). He found binocular peak amplitudes were more delayed in ON patients rather in TON study group. Mizota et al. (2003) investigated binocular summation of pattern evoked cortical potentials in patients with unilateral ON. According to the results of heir study, binocular P100 peak latencies were significantly delayed when the affected eye was stimulated, but the

amplitudes were not different in the two eyes. He also suggested that the binocular responses were more determined by the better eye.

In our previous studies (James *et al.*, 2004; Ruseckaite *et al.*, 2004) and CHAPTER I and II, we investigated visual responses of ON and multiple sclerosis (MS) patients obtained to dichoptically presented multifocal visual stimuli. The data were recorded to four different temporal multifocal modulation schemes or sparseness. We found that temporally sparser stimuli produced more reliable results than conventional contrast reversing mfVEP stimuli (for more details see CHAPTER I and II).

In the current study, mfVEP recordings are obtained to the Pattern Pulse stimulus having monocular (left and right) stimuli and binocular stimuli interleaved (James, 2003). The goal of this study is to compare the monocular and binocular responses, their latencies and amplitudes recorded to the Pattern Pulse stimulus in Normal, MS and ON study groups.

Methods

Stimuli

A detailed description of the dichoptic visual stimuli, used our experiments is presented in the previous studies (James, 2003; James *et al.*, 2004; Ruseckaite *et al.*, 2004). To produce dichoptic stimulation we used a single monitor and interleaved the image sequences for the left and right eyes on alternate video frames. This was achieved by means of a liquid crystal stereoscopic modulator (or shutter) (Tektronix, Inc., Beaverton, OR, USA). The non-interlaced frame rate of the monitor was 101.5 Hz, producing 50.75 Hz images/eye following the shutter. A complete description of the dichoptic stimulation is given by James et al. (2004).

In the current study we examine the Pattern Pulse visual stimulus (James, 2003), which is a "very sparse" stimulus (Fig. 4.1), given that the non-null stimuli appears at a mean rate of 2 presentations/s/eye. For the Pattern Pulse stimulus, two consecutive presentations in a given region were separated by an interval uniformly distributed between 400 and 600ms. Each presentation could be left-eye, right-eye, or binocular, with equal probability. Thus each of the left-eye, right-eye and binocular conditions appeared at a mean rate of 2/3 per second (James, 2003).

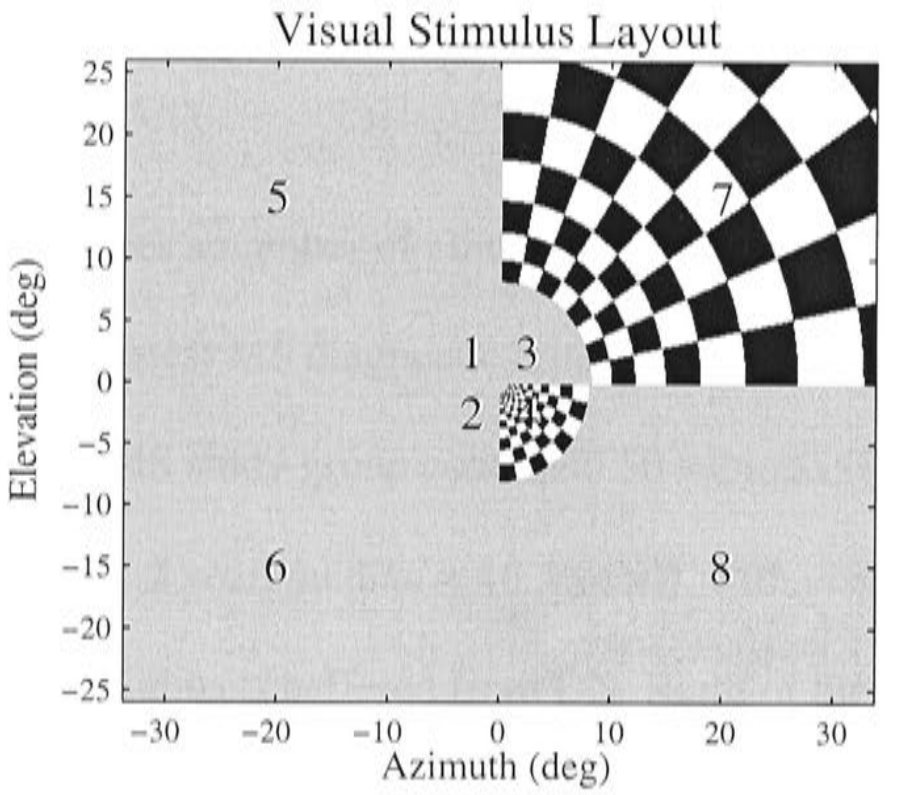

Figure 4.1 Example of the visual stimulus. Dichoptic stimulation provided 8 independent stimuli per eye. The numbers (1…8) are the indices to the eight different regions.

Recording

MfVEPs were recorded by using gold cup electrodes (diameter = 8 mm) secured on the scalp by the conductive paste EEG Ten20 (D.O.Weaver and Co, Aurora, LO). Electrodes were attached 3 cm above and 4 cm below the inion (Klistorner *et al.*, 1998). An earth electrode was attached to the right ear lobe. Each stimulus sequence lasted 40.4 s, or 4096 video frames. Four records for each subject were obtained during the experiment.

Subjects

The diagnosis of MS requires a number of clinically recognizable attacks and objective lesions. We employed the latest MS diagnostic criteria (McDonald *et al.*, 2001) to classify our subjects. The MS study group contained 50 subjects (8 men and 42 women, age range 25 to 64 (45 ± 15.2 year, median = 46.5 year)), with normal or corrected to 6/9 refraction. Twenty-six subjects suffered from ON. Eight of the twenty-six ON patients had remyelination (as evidenced by their clinical history) of the optic nerve. MS type was Relapsing Remitting (RR) for all patients. The Normal study group contained 19 subjects (12 men and 7 women, age range 22 to 44 (31.2 ± 13.1 year, median = 38 year)), with normal or corrected to normal refraction. The subjects' data are summarized in Table 4.1.

A Frequency Doubling Technology (FDT) perimeter (Humphrey, San Leandro, CA) was used to test subjects' visual fields before the first test session. Each subject was first given the C-20 screening test followed by the Full Threshold C-20 program of the FDT. The research followed the tenets of the Declaration of Helsinki, under the Australian National University's Human Experimentation Ethics Committee under

protocol M9901. Informed written consent was obtained from the subjects after the nature and possible consequences of the study were explained to them.

Table 4.1 Subject data. The two columns at the left indicate the two study groups (MS and Normal) and the number of subjects who participated in the experiments. The average age of the MS group was 45 (median = 46.5) and 31.2 (median = 38) years for Normal subjects. mfVEPs were recorded for 8 MS and 12 Normal men (see *Sex*). MS subjects had suffered from the disease on average 8.72 years (see *Duration of MS*), and during this time they had approximately 9.46 clinical attacks (see *N of attacks*). 26 subjects had optic neuritis (*ON* column) and for 16 of them a cerebrospinal (CSF) oligobanding test was positive (*CSF* column).

Study group	N	Age ± SE (yr)	Sex (M/F)	Duration of MS (yr)	N of attacks	ON	CSF	MS type
MS	50	45 ± 15.2	8/42	8.72 ± 7.2	9.46± 5.2	26	16	RR
Normals	19	31.2 ± 13.1	12/7	NA	NA	NA	NA	NA

Data Analysis

Multiple Linear Regression

Multiple linear regression (Johnson & Wichern, 1992) was used to quantify the major effects determining the monocular and binocular responses between Normal subjects and patients. The regression coefficients were examined for the Pattern Pulse visual stimulus, superior, nasal and left visual field locations. The same method was used to fit response latencies and amplitudes.

Peak Amplitudes and Relevant Latencies

Within each response we analysed two time periods. For the Normal study group the first two peaks of all the responses were contained in the temporal windows 59.4 to 99 ms and 100 to 158 ms. Since these two time windows contained the first negativity (N1) and the first positivity (P1), the peaks and their associated temporal windows are referred to as the N1 and P1 peaks and windows (James *et al.*, 2004). Before finding the maximum deflection in N1 and P1, the waveforms from the inferior regions 2, 4, 6 and 8 monocular and binocular viewing conditions were inverted to make the first peak negative within each time window. The N1 and P1 amplitudes were calculated in MS and ON study groups. A detailed description of the algorithm in described in the CHAPTER II or the paper of Ruseckaite et al. (2004).

We were also interested to examine whether any single Peak amplitude (eg. N1 or P1) was more reliable than the Peak to Peak (i.e. N1 + P1). To determine the differences between those measures we employed multiple regression analysis. In this case we fitted only the binocular amplitudes of Normal subjects.

TEMPLATE Method in Binocular Responses

Scientific studies (Halliday *et al.*, 1972; Chiappa, 1983; Andersson & Siden, 1995; Frederiksen & Petrera, 1999; McDonald *et al.*, 2001) showed that MS responses were delayed and consisted of aberrant waveforms. In our previous study (Ruseckaite *et al.*, 2004) we decomposed the monocular MS and ON responses, obtained to four different levels of temporal sparseness (James *et al.*, 2004), into a few delayed components of normal response waveforms. To do that developed the TEMPLATE algorithm, based on multiple linear regression. The TEMPLATE model allowed us to regress the individual MS waveforms onto a template consisting of delayed versions of the average response waveforms for each stimulus region of the Normal subjects. We found that mainly the waveforms of 18 ON patients consisted of more than one delayed component (for the detailed description of the TEMPLATE and the results see CHAPTER II).

In our current study we compared the waveforms obtained to the monocular and binocular stimulation in Normal, MS and ON subjects. We were interested to decompose the binocular responses into a few delayed versions of normal monocular left or right eye waveforms. Our purpose was to find out whether the binocular responses could be influenced by any single eye or by both eyes. For this task we employed the TEMPLATE method, described above and in the CHAPTER II.

Results

General Findings

Figure 4.2 presents some example Normal data waveforms. The figure shows the responses recorded to the Patter Pulse stimulus, for the left (OS), right (OD) and binocular (BIN) viewing conditions. The binocular responses have larger amplitudes than those of any single eye. They also appear to be more consistent in shape across all the stimulus regions. Considering these subjective findings, we were interested to know, whether the binocular responses had larger amplitudes and latencies than the responses from any single eye and whether their waveforms were consistent in all subjects including those with MS and ON.

Figure 4.3 illustrates the averaged N1 amplitudes and their SD recorded from Normal, ON and MS subjects to the Patten Pulse stimulus. The left column shows the monocular data obtained from the left eye, the middle column represents data from the right eye and the right column indicates data obtained from the binocular recordings. The first row represents the N1 of Normal subjects, the middle row shows ON subjects, and the last one – data from the MS (without ON) study groups. The first negativities are smaller in the ON study group, but they are larger in BIN viewing condition in all subjects.

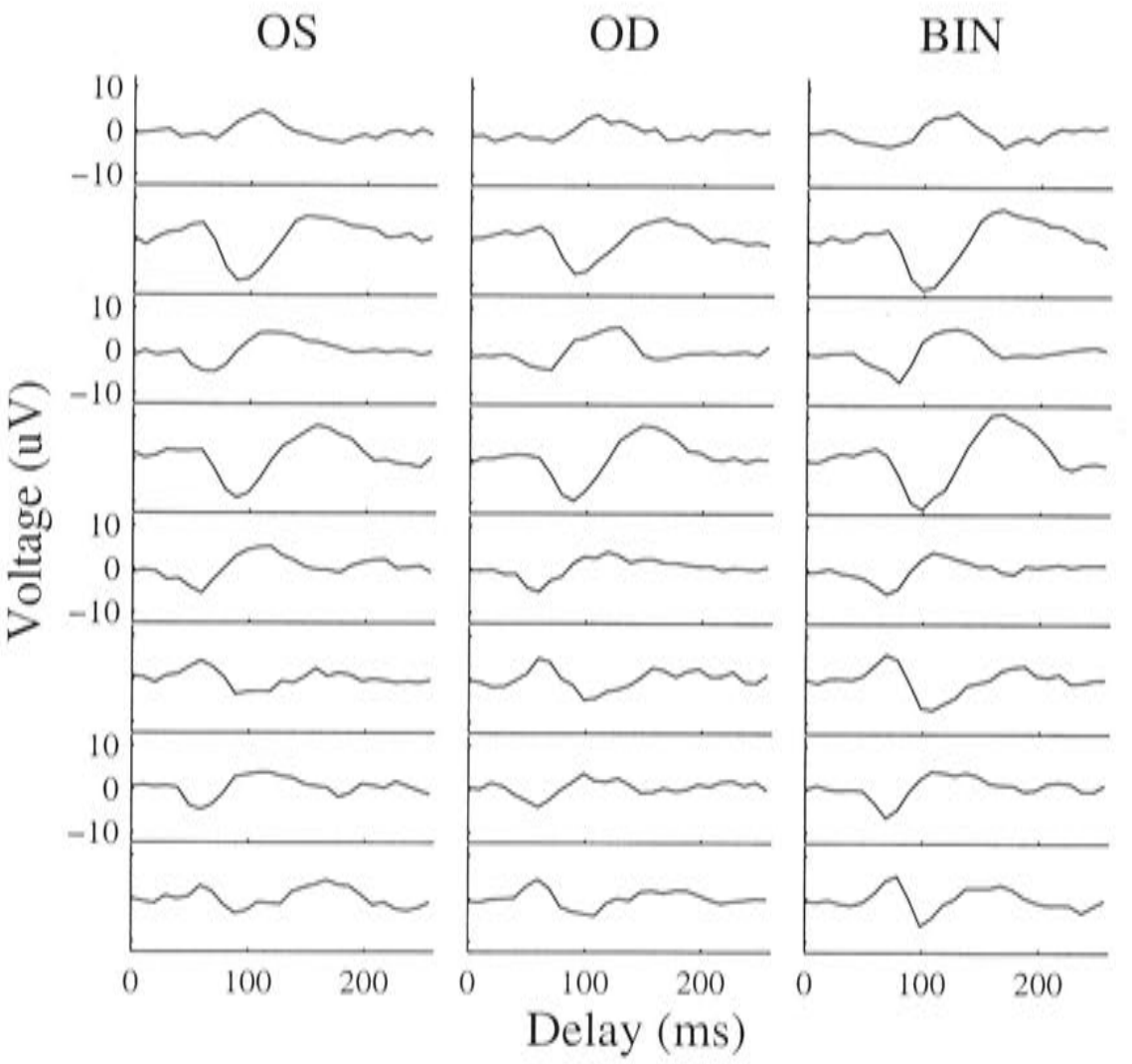

Figure 4.2 Exemplary multifocal VEPs for a Normal subject in response to the Pattern Pulse stimulus, for the left, right and binocular viewing conditions. The left panel shows multifocal responses from the left (OS) eye, the middle panel- for the right (OD) eye. The right panel (BIN) represents the binocular responses.

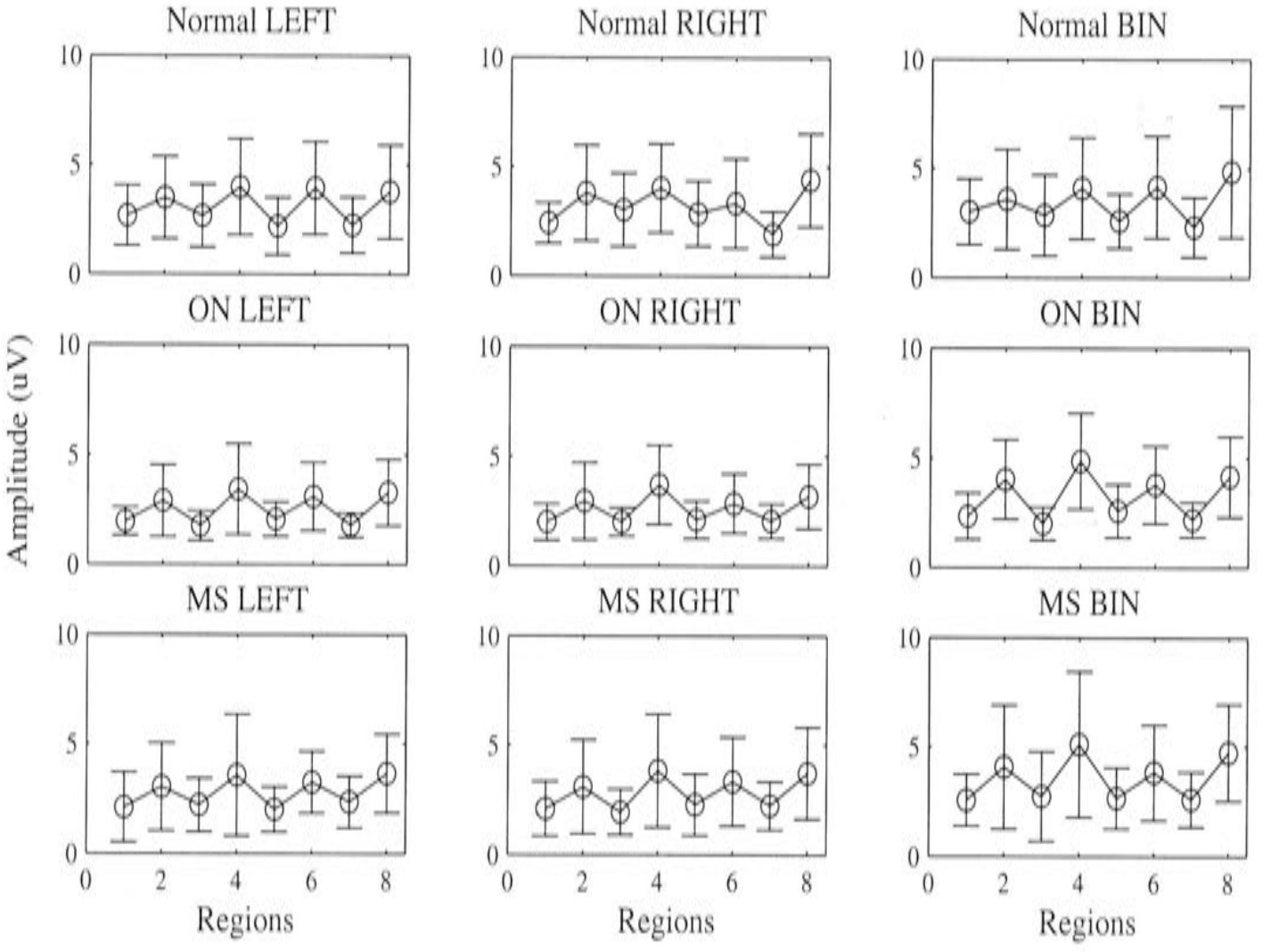

Figure 4.3 Illustration of mean N1 amplitudes in Normal, ON and MS subjects. The left –most columns indicates the N1 for the left eye, the middle column shows the data obtained from the right eye and the right column represents binocular data. N1 data are averaged across the subjects for each of 8 stimulated visual field regions (horizontal axis). See Figure 4.1 for region numbers.

Figure 4.4 illustrates the mean NT (implicit times) and their SD from Normal, ON and MS subjects. As in the Figure 4.3, the left column shows the monocular data obtained from the left eye, the middle column represents data from the right eye and the right column indicates latencies obtained from the binocular recordings. The first row represents the NT of Normal subjects, the middle row represents ON subjects, and the last one – data from the MS (without ON) study groups. Prolonged monocular and binocular responses appear in MS and ON patients.

Are the N1 Amplitudes Better than Peak to Peak Amplitudes?

In our previous and current studies (see CHAPTERS I, II and III) we examined N1 amplitudes of the Normal and MS subjects. To answer the question, why these measures were chosen in particular, we simultaneously fitted the N1, P1 and the Peak to Peak (N1 + P1) amplitudes, obtained from the binocular stimulus, in Normal subjects. Subject - wise effects were also fitted. Multiple regression results for the N1/P1 vs. N1+ P1 (in decibels) are given in the Table 4.2 The *N1 Normals* condition (8.42 dB ± 0.50 SE) corresponds to the size of N1. The *P1 Normals* condition (8.76 dB ± 0.59 SE) indicates the P1 amplitude. The coefficient for the N1 + P1 is equal to 15.09 dB ± 1.93 SE. At the same time, when comparing the *t*-statistics (b / SE) of the measures, we found that the mean *t* value for N1 + P1 was 7.81, when for N1 and P1 *t* values were equal to 16.60 and 14.84 respectively. Usually the size of *t* value determines the quality of the measure, and here we see that it is bigger in N1 than in N1 + P1, which mean that the N1 measure is more reliable than N1 + P1.

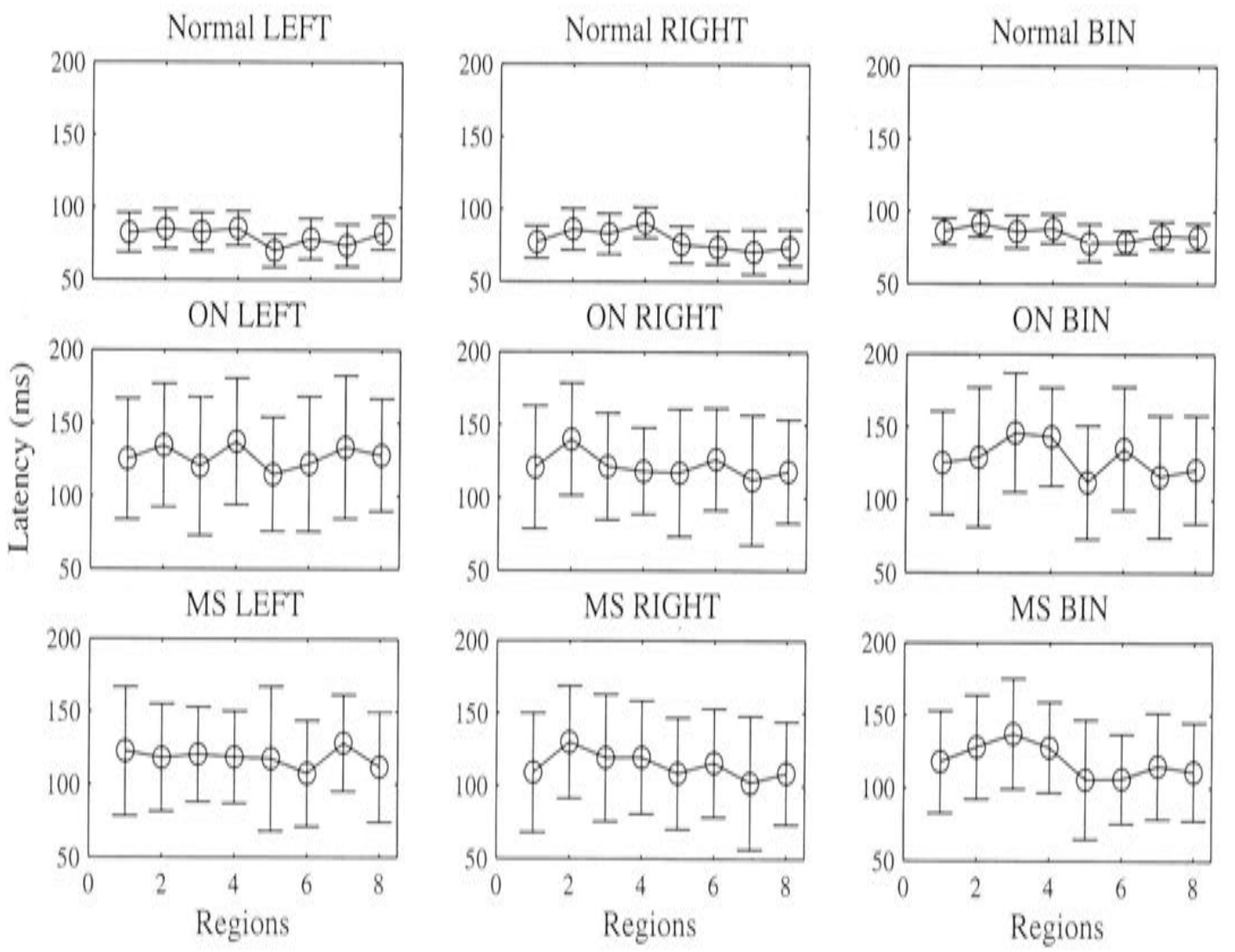

Figure 4.4 Illustration of NT in Normal, ON and MS subjects. The left – most column indicates the NT for the left eye, the middle column shows the data obtained from the right eye and the right column represents binocular data. NT data are averaged across the subjects, for each of 8 stimulated visual field regions (horizontal axis).

Table 4.2 Summarized multiple regression results for N1, P1 and N1 + P1 in Normal subjects, binocular stimulation. The *Condition* column indicates the fitted factors in dB. The *SE* indicates the standard error of the coefficient. The *t* value indicates t-statistics and the *p* value shows the probability of the coefficient. The column labelled *Multiplier* indicates the multiplicative factor corresponding to each dB gain or suppression. *-95%CL* and *+95%CL* determine the 95% confidence limits of the coefficients.

Condition	Coefficient (dB)	SE(dB)	t	p	Multiplier	-95%CL	+95%CL
N1 Normals	8.42	0.50	16.60	0.0000	2.63	2.34	2.95
P1 Normals	8.76	0.59	14.84	0.0000	2.75	2.39	3.13
N1 + P1 Normals	15.09	1.93	7.81	0.0000	5.68	3.67	8.77

Findings in the Data of Normal and MS Subjects

In our study we fitted the N1 responses of Normal subjects vs. the data of the MS patients. The results of the multiple regression analysis are presented in the Table 4.3. The variance accounted for was $r^2 = 0.74$. The reference condition (*Binocular (N)*) (8.94 dB) corresponds to the mean N1 obtained from binocular stimulation in Normal subjects. The coefficients for *LE* (-0.30dB ± 0.58 SE) and *RE* (-0.64 μV ± 0.58 SE) conditions show (non-significant) effects of the left (*LE*) and right (*RE*) eyes in Normal and MS subjects. The coefficients for the *LE * MS*, *RE*MS* and *Binocular * MS* interactions indicate a significant ($p < 0.05$) decrease of N1 in the left, right and binocular stimulation in MS patients. The -95%CL and +95%CL columns indicate the confidence intervals for the fitted coefficients. Subject-wise effects were also fitted as nuisance factor, but they are not shown here. From the Table 4.3 we find that the monocular and binocular responses are smaller in MS patients compared to the binocular amplitudes in Normal subjects. These results can also be seen in the Figure 4.3.

We also compared the data of LE, RE eyes with BIN obtained in Normal and MS study groups. The goal of this analysis was to detect how much the data of any single eye were different from the binocular stimulation. Together with the N1 peaks we fitted the effects of superior, nasal and inner visual fields. Tables 4.4A and 4.4B summarize the model fit results for both study groups respectively. The variance accounted in Normal subjects was $r^2 = 0.75$, and 0.72 in MS patients. The *Condition* column in both Table 4.4A and 4.4B indicates the fitted effects, such as *LE*, *RE*, *Sup VF* (Superior Visual Field), *Nasal VF* (Nasal Visual Field) and *Inner VF* (Inner Visual Field). The multiple regression model fit between any single eye and binocular responses is illustrated in Figures 4.5 and 4.6. Figure 4.5 shows the residuals (in '+') between the binocular N1 responses and the responses from the left (panel **a**) or right

Table 4.3 Summarized multiple regression results for Normal subjects vs. MS patients. The *Condition* column indicates the fitted factor; the *Coefficient* shows the regression coefficients in dB. The *SE* indicates the standard error of the coefficient. The *t* value shows t-statistics and *p* value shows the probability of the coefficient. The column labelled *Multiplier* indicates the multiplicative factor corresponding to each dB gain or suppression. *-95%CL* and *+95%CL* determine the 95% confidence limits of the coefficients.

Condition	Coefficient (dB)	SE (dB)	t	p	Multiplier	-95%CL	+95%CL
Ref = Binocular (N)	8.94	0.41	21.70	0.0000	2.79	2.55	3.07
LE	-0.30	0.58	-0.53	0.6135	0.96	0.84	1.10
RE	-0.64	0.58	-1.10	0.2824	0.92	0.81	1.06
LE * MS	-1.48	0.48	-3.06	0.0024	0.84	0.75	0.93
RE* MS	-1.59	0.48	-3.31	0.0134	0.83	0.74	0.92
Binocular * MS	-1.29	0.48	-2.68	0.0152	0.87	0.77	0.96

Table 4.4

A. Summarized multiple regression results for Normal subjects, N1 amplitudes.

Condition	Coefficient	SE	t	p	-95%CL	+95%CL
LE	0.44	0.08	5.27	0.0000	0.28	0.61
RE	0.49	0.08	6.08	0.0000	0.33	0.65
Sup VF	-0.22	0.55	-0.40	0.7063	-1.32	0.87
Nasal VF	3.09	1.59	1.94	0.0574	-0.02	6.21
Inner VF	3.50	1.58	2.21	0.0308	0.39	6.60

B. Summarized multiple regression results for MS patients, N1 amplitudes.

Condition	Coefficient	SE	t	p	-95%CL	+95%CL
LE	0.40	0.04	9.19	0.0000	0.31	0.49
RE	0.31	0.04	6.54	0.0000	0.21	0.40
Sup VF	-1.89	0.29	-6.44	0.0000	-2.47	-1.32
Nasal VF	6.44	1.12	5.72	0.0000	4.23	8.64
Inner VF	6.30	1.10	5.70	0.0000	4.13	8.46

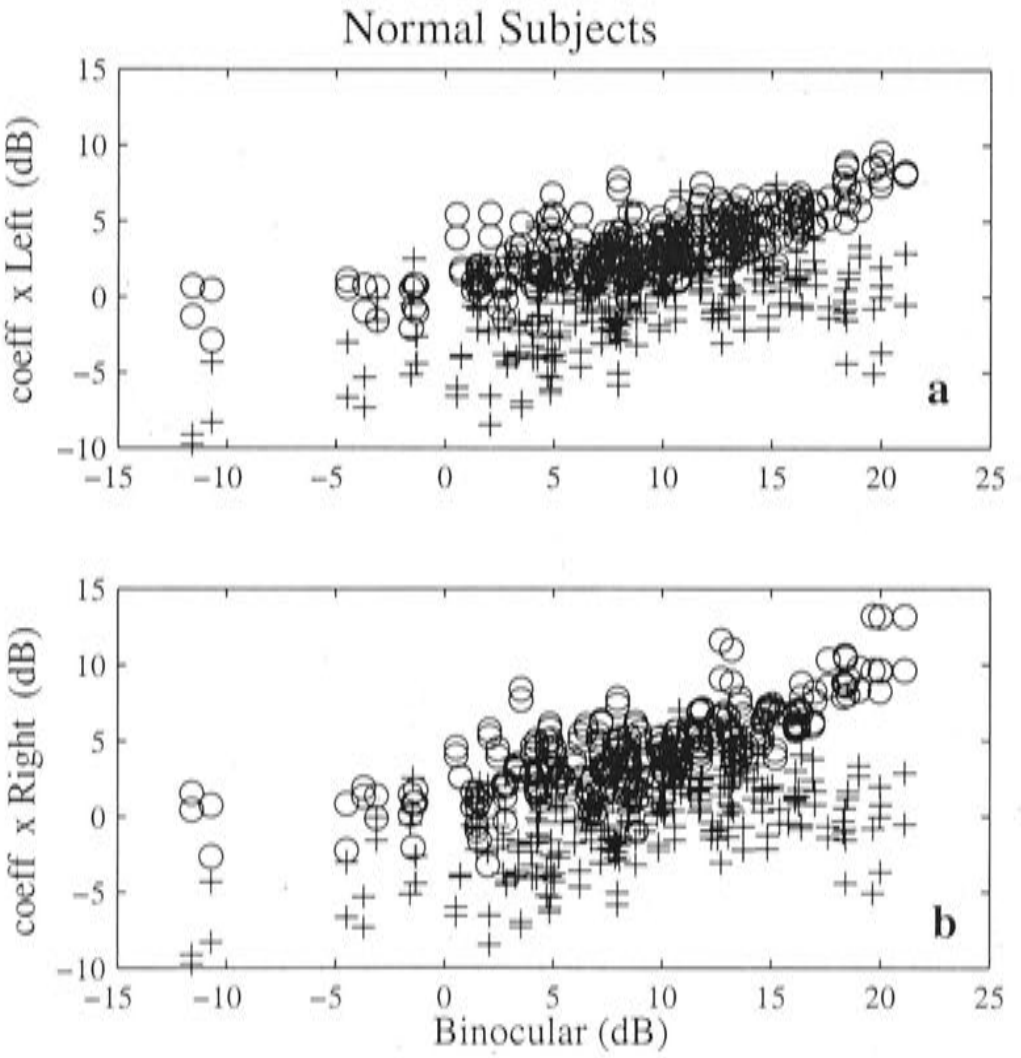

Figure 4.5 Multiple regression fit between the monocular and binocular responses in Normal subjects. The **a)** panel shows the data of the left eye, the panel **b)** represents the right eye. The horizontal axis shows N1 of binocular stimulation (in voltages). The data of a single eye, multiplied by the regression coefficient are shown in '**o**'. The '**+**' symbolizes residuals between the binocular responses and the model fit.

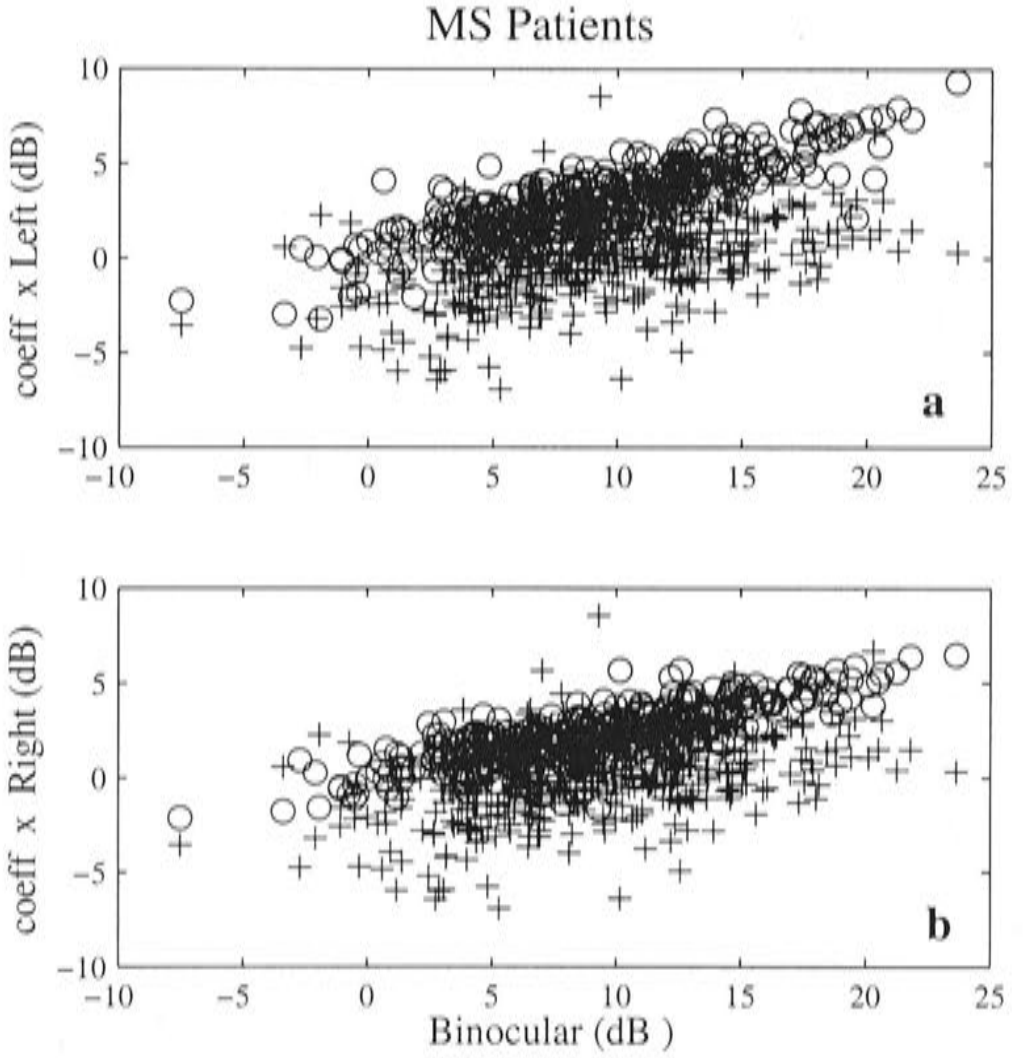

Figure 4.6 Multiple regression fit between the monocular and binocular responses in MS patients. The **a)** panel shows the data of the left eye, the panel **b)** represents the right eye. The horizontal axis shows N1 of binocular stimulation (in voltages). The data of a single eye, multiplied by the regression coefficient are shown in '**o**'. The '**+**' symbolizes residuals between the binocular responses and the model fit.

(panel **b**) obtained from Normal subjects. The fitted single eye responses are presented in '**o**'. Figure 4.6 illustrates the model fit in MS subjects.

TEMPLATE and Binocular Responses

We were interested to know whether binocular responses were influenced mainly by one of the eyes only, or they were determined by both eyes equally. For this purpose we employed the TEMPLATE method, described in the CHAPTER II. Binocular responses of Normal and MS patients were simultaneously fitted on the TEMPLATE, containing averaged delayed Normal responses, obtained from the left and right eyes. Thus, we obtained a set of multiple regression coefficients for each eye. The best coefficient was determined by its p and t values and the longest fitted delay NT_F^L and NT_F^R was chosen for the left and the right eye respectively. At the next stage we added the above mentioned delays to the averaged normal delays from the left and right eyes. The obtained values were compared to the binocular implicit times NT. We examined the differences between the binocular NT and fitted values of the left and the right eyes. We also considered the average of both eyes and calculated the differences between the binocular NT and this average (Eq.4.1).

$$NT_F^U = (NT_F^L + NT_F^R) / 2 \qquad (4.1)$$

As shown in Figure 4.7, the differences vary across the eyes, but they are smaller when the average of both eyes is considered (see the white bars in the Figure 4.7). The results show, that the values of fitted delays are close to the implicit times.

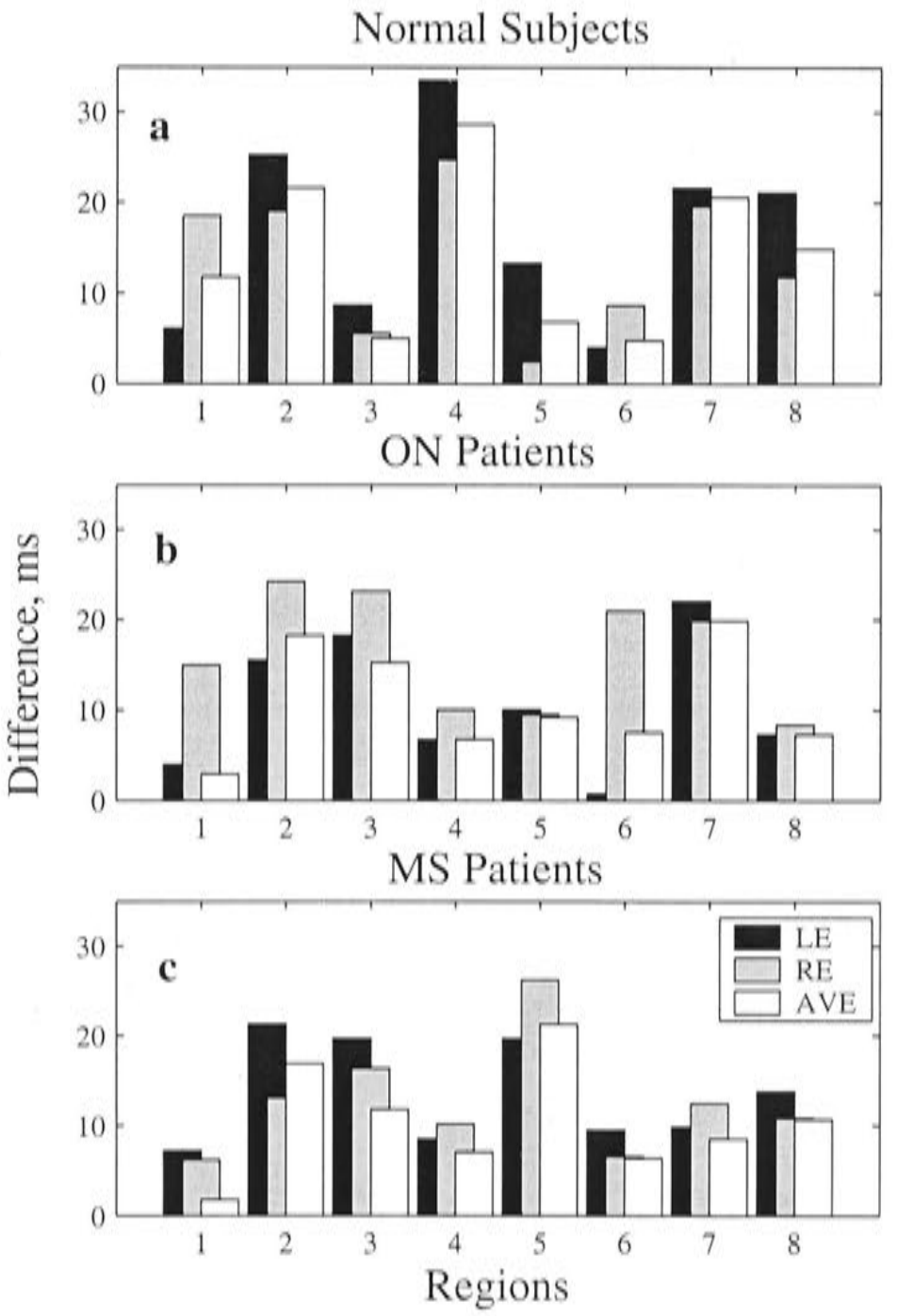

Figure 4.7 Differences between fitted left, right and the average of both eyes delays NT_F and binocular NT for Normal, ON and MS subjects. Black bars represent the left eye, grey bars show the right eye and the white bars indicate the differences between the average of the delays in both eyes and binocular NT.

To answer the question, whether the binocular implicit times are predicted by one of the eyes, we examined the data from the best and the worst eyes. We fitted multiple regression models, containing the response delays obtained from the best and the worst eye versus the data from binocular viewing condition. The subject - wise effects were considered as well. In our analysis the best eye had shorter implicit times compared to the other eye. In this case, for the model fit we selected only those data from the worst eye that were delayed by 10 ms or more compared to the best eye. The regression analysis results for the NT and NT_F are presented in the Table 4.5.

At first we fitted the implicit times (NT) of the Normal subjects (Table 4.5A) ($r^2 = 0.63$). The *Condition* column shows the regression coefficients for the *Worst* (0.95 ± 0.08 SE) and *Best* (1.11 ± 0.13 SE) eyes. The coefficients here show the multiplicative effect of the fitted conditions. Note, that these coefficients are dimensionless having units of ms/ms. The column *p* indicates the significance of these coefficients. Table 4.5B summarizes the fitted coefficients for the NT_F ($r^2 = 0.65$) in Normal subjects. Tables 4.5C ($r^2 = 0.64$) and 4.5D ($r^2 = 0.62$) summarize multiple regression results in MS patients. These results suggest that the binocular delays in all subjects are not influenced by either of the eyes particularly, but are intermediate.

Table 4.5

A. Summarized multiple regression results for Normal subjects, NT

Condition	Coefficient	SE	t	p	-95%CL	+95%CL
Worst	0.95	0.08	11.87	0.0003	0.79	1.10
Best	1.11	0.13	8.53	0.0008	0.86	1.37

B. Summarized multiple regression results for Normal subjects, NT_F

Condition	Coefficient	SE	t	p	-95%CL	+95%CL
Worst	0.92	0.11	8.36	0.0004	0.71	1.13
Best	1.19	0.14	8.50	0.0016	0. 92	1.46

C. Summarized multiple regression results for MS patients, NT

Condition	Coefficient	SE	t	p	-95%CL	+95%CL
Worst	0.85	0.09	9.44	0.0009	0.67	1.03
Best	1.26	0.12	10.50	0.0011	1.03	1.49

D. Summarized multiple regression results for MS patients, NT_F

Condition	Coefficient	SE	t	p	-95%CL	+95%CL
Worst	0.89	0.05	17.81	0.0006	0.79	0.98
Best	1.24	0.10	12.40	0.0009	1.04	1.43

Discussion

Monocular and binocular VEPs were investigated in the previous studies (Russell Harter *et al.*, 1973; Shea *et al.*, 1987; McCulloch & Skarf, 1991; Tobimatsu & Kato, 1996; Amaya *et al.*, 1998; Shimoyama *et al.*, 1998; Di Summa *et al.*, 1999; Sloper *et al.*, 2001; Ikejiri *et al.*, 2002; Sato *et al.*, 2002; Anlar *et al.*, 2003; Mizota *et al.*, 2003), but the researchers did not find any significant differences in terms of sizes or latencies of binocular responses in most of these studies; however, abnormal binocular VEPs having delayed implicit times and smaller amplitudes were noticed in ON (Mizota *et al.*, 2003) and TON patients (Ikejiri *et al.*, 2002).

In our study, we compared the monocular and binocular mfVEPs of patients, suffering from MS and ON. mfVEPs were recorded to the Pattern Pulse visual stimulus when eight visual regions were stimulated simultaneously. Our goal was to find whether the binocular responses were significantly different from monocular ones, whether they had abnormal waveforms, smaller amplitudes or delayed latencies.

General Findings

We examined N1 and their implicit times in both Normal and MS study groups. The binocular N1 were larger than monocular N1 in both study groups (Fig.4.3), but were smaller in ON patients. Their implicit times were almost the same in monocular and binocular cases; however, the responses were more delayed in MS and ON patients (Fig.4.4).

We found that N1 peaks were more reliable than N1 + P1. It was illustrated by their *t* statistics in the Table 4.2. Larger *t* values in N1 showed a better reliability of the measure.

Table 4.3 shows the multiple regression results obtained by fitting the effect of monocular and binocular vision in Normal vs. MS patients. The responses in MS patients are suppressed, as it is described in the CHAPTER II, and there is no significant effect to the binocular condition left or right eye compared.

Tables 4.4A, 4.4B, Figures 4.5 and 4.6 present the multiple regression model fits in Normal and MS subjects respectively. The figures illustrating the model fits and the residuals show no significant differences between the monocular and binocular responses in either study group.

Fitted Delays

The TEMPLATE model was applied to the binocular responses of Normal and MS subjects. We expected the binocular responses to contain one or more significant delayed waveforms of the averaged responses, recorded from the Normal subjects, for any single eye. We were also interested to find out whether the binocular NT responses were determined by the average of both eyes, or by the one eye only. Figure 4.7 illustrates the differences between the NT and NT_F in the left, right and binocular viewing conditions in Normal subjects, ON and MS patients. It is clearly shown, that these differences are smallest when the average of both eyes is considered in all study groups. For the same purpose we also fitted the implicit times obtained from the best and the worst eyes. In this case we also found that the binocular responses were not influenced by any single eye, as illustrated in the Table 4.5. This differs from the results of Mizota et al. (2003) who reported that the delay of binocular responses was determined by the better eye. His data were obtained for separate trials, rather than being determined concurrently, as in the present case.

Bibliography

AMAYA, K., ADACHI-USAMI, E., TSUYAMA, Y., KAWABATA, H. & SHIJO, Y. (1998). Binocular summation of visually evoked potentials in normal tension glaucoma (absract). In *ISCEV 1998*.

ANDERSSON, T. & SIDEN, A. (1995). An analysis of VEP components in optic neuritis. *Electromyogr Clin Neurophysiol* **35,** 77-85.

ANLAR, O., KISLI, M., TOMBUL, T. & OZBEK, H. (2003). Visual evoked potentials in multiple sclerosis before and after two years of interferon therapy. *Int J Neurosci* **113,** 483-489.

CHIAPPA, K. (1983). *Evoked potentials in clinical medicine*. Raven Press, New York.

DI SUMMA, A., FUSINA, S., BERTOLASI, L., VINCENTINI, S., PERLINI, S., BONGIOVANI, L. & POLO, A. (1999). Mechanism of binocular interaction in refraction errors: study using pattern-reversal visual evoked potentials. *Doc Ophthalmol* **98,** 139-151.

FREDERIKSEN, J. & PETRERA, J. (1999). Serial visual evoked potentials in 90 untreated patients with acute optic neuritis. *Survey Ophthalmol* **44,** 54-62.

HALLIDAY, A., MCDONALD, W. & MUSHIN, J. (1972). Delayed visual evoked response in optical neuritis. *Lancet* **1,** 982-985.

IKEJIRI, M., ADACHI-USAMI, E., TSUYAMA, Y., MIYAUCHI, O. & SUEHIRO, S. (2002). Pattern visual evoked potentials in traumatic optic neuropathy. *Opthalmologica* **216,** 415-419.

JAMES, A. (2003). The pattern pulse multifocal visual evoked potential. *Invest Opthalmol Vis Sci* **44,** 879-890.

JAMES, A., RUSECKAITE, R. & MADDESS, T. (2004). Effect of temporal sparseness and dichoptic presentation upon multifocal visual evoked potential. *Visual Neurosci* **submitted**.

JOHNSON, R. & WICHERN, D. (1992). *Applied multivariate statistical analysis*. Prentice-Hall, Inc.

KLISTORNER, A., GRAHAM, S., GRIGG, J. & BILLSON, F. (1998). Electrode position and the multi-focal visual-evoked potential: role in objective visual field assessment. *Aust N Z J Ophthalmol* **26(Suppl.),** 91-94.

LEGUIRE, L., ROGERS, G. & BREMER, D. (1991). Visual-evoked response binocular summation in normal and strabismic infants. Defining the critical period. *Invest Ophthalmol Vis Sci* **32,** 126-133.

MARSHMAN, W., DAWSON, E., NEVEU, M., MORGAN, M. & SLOPER, J. (2001). Increased binocular enhancement of contrast sensitivity and reduced stereoacuity in Duane syndrome. *Invest Ophthalmol Vis Sci* **42,** 2824-2825.

MCCULLOCH, D. & SKARF, B. (1991). Development of the human visual system: monocular and binocular pattern VEP latency. *Invest Ophthalmol Vis Sci* **32,** 2372-2381.

MCDONALD, W., COMPSTON, A., EDAN, G., GOODKIN, D., HARTUNG, H., LUBLIN, F., MAFARLAMD, H., PARTY, D., POLMAN, C., REINGOLD, S., SANDBERG-WOLLHEIM, M., SIBLEY, W., THOMPSON, A., VAN DEN NOORT, S., WEINSHENKER, B. & WOLINKSY, J. (2001). Recommended diagnostic criteria for multiple sclerosis: guidelines from the international panel on the diagnosis of multiple sclerosis. *Ann Neurol* **50,** 121-127.

MCKERRAL, M., LACHAPELLE, P., TREMBLAY, F., POLOMENO, R., ROY, M., BENEISH, R. & LEPORE, F. (1995). Monocular contribution to the peak time of the binocular pattern visual evoked potential. *Doc Ophthalmol* **91,** 181-193.

MIZOTA, A., HOSHINO, A., SATO, E., TSUYAMA, Y. & ADACHI-USAMI, E. (2003). Binocular summation of PVECPS in patients with unilateral optic neuritis. In *ISCEV 2003*, Nagoya, Japan.

RUSECKAITE, R., MADDESS, T. & JAMES, A. C. (2004). Sparse multifocal stimul for the detection of multiple sclerosis. *Visual Neurosci* **submitted**.

RUSSELL HARTER, M., SEIPLE, W. & SALMON, L. (1973). Binocular summation of visually evoked responses to pattern stimuli in humans. *Vis Res* **13,** 1433-1446.

SATO, E., TANIAI, M., MIZOTA, A. & ADACHI-USAMI, E. (2002). Binocular interaction reflected in visually evoked cortical potentials as studied with pseudorandom stimuli. *Invest Ophthalmol Vis Sci* **43,** 3355-3358.

SHEA, S., ASLIN, R. & MCCULLOCH, D. (1987). Binocular VEP summation in infants and adults with abnormal binocular histories. *Invest Ophthalmol Vis Sci* **28,** 356-365.

SHIMOYAMA, I., NAKAJIMA, Y., SHIBATA, T., ITO, T., ABLA, D., KANSAKU, K. & MIZOTA, J. (1998). Binocular interactions in visual evoked cortical potentials with two light-emitting - diodes. *Doc Ophthalmol* **97,** 1-7.

SLOPER, J., GARNHAM, C., GOUS, P., DYASON, R. & PLUNKETT, D. (2001). Reduced binocular beat visual evoked responses and stereoacuity in patients with Duane syndrome. *Invest Ophthalmol Vis Sci* **42,** 2826-2830.

TOBIMATSU, S. & KATO, M. (1996). The effect of binocular stimulation on each component of transient and steady-state VEPs. *Electroencephalogr Clin Neurophysiol* **100,** 177-183.

Summary

Summary

In my thesis that investigates of normal vision and neuro-ophthalmic disorders using nonlinear systems identification methods I introduced a new VEP recording method based on sparse multifocal stimuli. This method differs from the previous studies, where the evoked responses were obtained by using a binary contrast reversing (CR) stimulus (Halliday *et al.*, 1972; Chiappa, 1983; Jones, 1993; Andersson & Siden, 1995; Hood *et al.*, 2000). The thesis consists of four independent chapters, each of them covering different experiments and results.

In the first chapter of my thesis I compared the CR stimulus with novel temporally sparse stimuli. I showed that temporally sparse stimuli, recorded to dichoptic viewing conditions, produced larger and more reliable responses in Normal subjects. I therefore expected that sparser stimuli would also be able to produce more reliable signals in patients, suffering from neuro-ophthalmic disorders such us optic neuritis (ON). This hypothesis proved to be correct and allowed me to detect parameters that could be applied to accurately diagnosing ON and MS. In my study I also showed that the recording time to sparser stimuli could be shortened compared to CR stimuli given the increase in signal to noise ratio. This is very important when recording from patients. In summary, I showed that temporally sparse multifocal stimuli are more useful than traditional CR stimuli.

The responses to multifocal stimulation described in my thesis were recorded to the mean luminance of the monitor of 7.6 cd/m^2. This effect was achieved by means of dichoptic stimulation while using the special shutter and spectacles which reduced initial mean luminance of the monitor from 45cd/m^2. A related study on sparse multifocal stimulation, but based on higher light levels was reported by (James, 2003). Thus it would appear that light level does not produce any significant difference in the

size of quality of the responses. (Winkles, 2003) in her Honours thesis also showed that higher levels of luminance 45cd/m^2 did not change the responses in any way.

Based on the findings, described in the first chapter of my thesis, I was interested to know whether even sparser stimuli could be used in the clinical study or not. In the second part of my thesis I introduced a new, so called Pattern Pulse stimulus (James, 2003), which is a very sparse stimulus, given that the non-null stimuli appear at a mean rate of 4/3 presentations/s/eye. The responses to the above described four visual stimuli were recorded from another 27 Normal subjects and 50 MS patients, 26 of whom had a history of ON. The results showed that the mfVEPs of MS and ON patients were on average twice as small as those of Normal subjects. The responses also had strange looking waveforms and their communalities for a linear combination of 2 waveform principal components were smaller too. Based on the PCA, responses obtained to the sparser stimuli were more reliable than the responses recorded to the CR stimulus in terms of variance account from by a two PC model. I also found that responses of MS and ON patients were delayed by 24 ms on average compared to Normal subjects. Some of the patients had more than one delayed component in the responses recorded from the visual field regions 2, 4, 7 and 8. This was true for 18 ON patients and it could be possibly explained by the location of the optic nerve demyelination.

In the second chapter of the thesis I also investigated and described discriminant models for classifying MS and ON patients as being distinct from normal subjects. I showed that size, shape and implicit time of mfVEPs, recorded to the sparse Pattern Pulse stimulus, provided high sensitivities of ~90% in MS patients at low false positive rates. A surprising result was obtained when examining fitted latencies in MS and ON patients. Bootstrapped ROC models predicted excellent performance of sparser stimuli for less advanced patients. The results showed better classification performance than the

sensitivities and specificities obtained for IgG (Brasher *et al.*, 1998; McMillan *et al.*, 2000), sVCAM-1 (McMillan *et al.*, 2000) or serum antibodies to myelin (Chamczuk *et al.*, 2002). Taken together, my findings suggest that the mfVEP method could provide cost effective monitoring and treatment of MS.

The previous studies of Maddess et al. (Maddess *et al.*, 1997; Maddess *et al.*, 1999; Maddess & Severt, 1999; Maddess *et al.*, 2000b, a) showed that the spatial frequency doubling (FD) illusion was a useful tool in examining visual functions. Since ON is one of the most serious disorders of the optic nerve, I was interested to find out whether FD based technologies could be applied for assessing optic nerve and detecting ON or MS. Therefore in the third part of my studies I examined and described dichoptic multifocal FD stimulation in Normal and MS subjects. The mfVEPs were also compared with FDT perimetry thresholds. The FD mfVEPs showed significant amplitude reductions in ON patients, especially in those older than 40 years of age. By means of multivariate linear regression I described the significant differences between the responses of Normal subjects and patients. Of particular interest were the responses recorded from different visual field locations. As shown in the second chapter of my thesis, only responses in the superior visual field regions were significantly different compared to the other regions of the visual field. That is, bar a scaling difference for the superior field, no other patterns of amplitude difference were found across visual field locations. This was true both in the FDT perimetry thresholds and mfVEP responses. I this study I have also shown that FDT thresholds combined with the parameters of multifocal responses obtained to sparser chequerboard stimuli are able to provide high diagnostic sensitivity as well.

In the fourth part of my thesis I examined the effect of binocularity of multifocal Pattern Pulse VEPs in Normal and MS patients. Previous studies by Ikejiri et al. (2002) and Mizota et al. (2003) evaluated the binocular responses recorded to conventional

stimulus in traumatic optic neuropathy and ON patients. I was curious to use multifocal stimulation in order to find out whether there was a significant influence of the binocular stimulation in the above mentioned patients. Unlike the previous studies I could concurrently determine binocular and monocular responses providing a better basis for comparison. As expected the results showed that binocular responses were bigger than the monocular VEPs in both study groups. The binocular responses in MS and ON patients were delayed as well but, contrary to the previous authors' findings, this delay was not significantly different from the latencies in any single eye.

Each chapter of my thesis shows that multifocal stimulation is a useful tool in assessing ON and MS. The positive results of multifocal Pattern Pulse stimulation and discriminant models based upon the latencies lead us to a future where MS could be detected at its early stage and the proper treatment and rehabilitation could be applied at lower cost.

Bibliography

ANDERSSON, T. & SIDEN, A. (1995). An analysis of VEP components in optic neuritis. *Electromyogr Clin Neurophysiol* **35,** 77-85.

BRASHER, G., FOLLENDER, A. & SPIEKERMAN, A. (1998). The clinical value of commonly used spinal fluid diagnostic studies in the evaluation of patients with suspected multiple sclerosis. *Am J Manag Care* **4,** 1119-1121.

CHAMCZUK, A., URSELL, M., O'CONNOR, P., JACKOWSKI, G. & MOSCARELLO, M. (2002). A rapid ELISA-based serum assay for myelin basic protein in multiple sclerosis. *J Immun Methods* **262,** 21-27.

CHIAPPA, K. (1983). *Evoked potentials in clinical medicine*. Raven Press, New York.

HALLIDAY, A., MCDONALD, W. & MUSHIN, J. (1972). Delayed visual evoked response in optical neuritis. *Lancet* **1,** 982-985.

HOOD, D., ODEL, J. & ZHANG, X. (2000). Tracking the recovery of local optic nerve function after optic neuritis: a multifocal VEP study. *Invest Ophthalmol Vis Sci* **41,** 4032-4038.

IKEJIRI, M., ADACHI-USAMI, E., MIZOTA, A., TSUYAMA, Y., MIYAUCHI, O. & SUEHIRO, S. (2002). Pattern visual evoked potentials in traumatic optic neuropathy. *Ophthalmol* **216,** 415-419.

JAMES, A. (2003). The pattern pulse multifocal visual evoked potential. *Invest Opthalmol Vis Sci* **44,** 879-890.

JONES, S. (1993). Visual evoked potentials after optic neuritis. Effect of time interval, age and disease dissemination. *J Neurol* **240,** 489-494.

KELLY, D. (1966). Frequency doubling in visual responses. *J Opt Soc Am* **56,** 1628-1633.

KELLY, D. (1981). Nonlinear visual responses to flickering sinusoidal gratings. *J Opt Soc Am* **71,** 1051-1055.

MADDESS, T., BEDFORD, S., JAMES, A. & ROSE, K. (1997). A multiple - frequency, multiple-region pattern electroretinogram investigation of non-linear retinal signals. *Aust Nz J Ophthalmol* **25,** 94-97.

MADDESS, T., GOLDBERG, I., WINE, S., DOBINSON, J., WELSH, A. H. & JAMES, A. C. (1999). Testing for glaucoma with the spatial frequency doubling illusion. *Vision Res* **39,** 4258-4273.

MADDESS, T., JAMES, A., GOLDBERG, I., WINE, S. & DOBINSON, J. (2000a). Comparing a parallel PERG, automated perimetry, and frequency-doubling thresholds. *Invest Ophthalmol Vis Sci* **41,** 3827-3832.

MADDESS, T., JAMES, A., GOLDBERG, I., WINE, S. & DOBINSON, J. (2000b). A spatial frequency - doubling illusion -based pattern electroretinogram for glaucoma. *Invest Ophthalmol Vis Sci* **41,** 3818-3826.

MADDESS, T. & SEVERT, W. (1999). Testing for glaucoma with the frequency-doubling illusion in the whole, macular and eccentric visual fields. *Aust N Z J Ophthalmol* **27,** 194-196.

MCMILLAN, S., MCDONNELL, G., DOUGLAS, J. & HAWKINS, S. (2000). Evaluation of the clinical utility of cerebrospinal fluid (CSF) indices of inflammatory markers in multiple sclerosis. *Acta Neurol Scand* **101,** 239-243.

MIZOTA, A., HOSHINO, A., SATO, E., TSUYAMA, Y. & ADACHI-USAMI, E. (2003). Binocular summation of PVECPS in patients with unilateral optic neuritis. In *ISCEV 2003*, Nagoya, Japan.

WINKLES, N. (2003). An investigation of the effects of pulse rate, pulse length, eccentricity and spatial density on multifocal visual evoked potentials (honour thesis). In *Visual Sciences, RSBS*. ANU, Canberra.

General Conclusions

Conclusions and Future Directions

Many previous studies (Halliday *et al.*, 1972; Dawson *et al.*, 1982; Chiappa, 1983; Matthews & Small, 1983; Andersson & Siden, 1995; Hood *et al.*, 2000a; Hood & Zhang, 2000; Hood *et al.*, 2000b) have shown that VEP is a very useful tool in assessing neurological diseases, such as glaucoma, ON or MS. MS is one of the "secret" diseases, having a high prevalence in Australia and world wide (Waxman, 1983; Swank & Dugan, 1987; Van der Mei *et al.*, 2001). So far nobody knows what causes this CNS disease; it is very difficult to diagnose and many patients suffering from it do not know that they suffer from MS, particularly those with Progressive MS. ON is one of the first and most common symptoms of MS (Ebers, 1985; Kurtzke, 1985; Celesia *et al.*, 1990).

Previous studies (Halliday *et al.*, 1972; Chiappa, 1983; Jones, 1993; Andersson & Siden, 1995; Hood *et al.*, 2000a) have shown that VEPs of patients suffering from ON are prolonged, they have smaller amplitudes and strange looking waveforms. Most of those studies were done using a traditional contrast reversing (CR) stimulus, whereby the responses were recorded stimulating the whole visual field. ON can affect any part of the optic nerve, therefore it is important to detect the location of optic nerve demyelination as precisely as possible. A potential solution to this problem are multifocal VEPs, allowing multiple areas of the visual field and optic nerve to be examined concurrently. Fortune et al. (Fortune *et al.*, 2002; Fortune & Hood, 2003) compared conventional and multifocal VEPs. They showed that mfVEPs are more reliable than conventional ones; offering a substantial improvement for objective detection of glaucomatous dysfunction for the superior visual field and are not directly related to conventional VEPs.

Based on these assumptions I was interested to examine the mfVEPs recorded from MS and ON patients. In my research I introduced a set of novel sparse multifocal

stimuli when the previous evoked response studies were done using a binary contrasts reversing (CR) stimulus.

In the first chapter of my thesis I showed that temporally sparser stimuli, recorded to dichoptic viewing conditions, produced larger and more reliable responses in Normal subjects. I expected that sparser stimuli would also be able to produce more reliable signals in MS patients, allowing me to detect the diagnostic parameters. I have also found that the recording time to sparser stimuli could be shortened compared to CR stimuli. This is very important when recording from patients.

In the second part of my thesis I investigated and described discriminant models for classifying MS and ON patients. Compared to the traditional MS diagnostic techniques, such as MRI, or conventional VEPs which are able to produce the sensitivities of only 83% (Sand *et al.*, 1990; Frederiksen *et al.*, 1991; Roder, 1991; Duska & Denislic, 2000; Rovaris *et al.*, 2003; Sicotte *et al.*, 2003), my results illustrate much higher diagnostic value for mfVEPs.

I my study I have also examined the FD illusion in MS patients and shown that FDT thresholds combined with the parameters of multifocal responses obtained to sparser chequeboard stimuli are able to provide high diagnostic sensitivity as well.

In conclusion, I have shown that mfVEPs recorded to the Pattern Pulse stimulus are a useful tools for diagnosing MS and ON.

This research has many potential perspectives and will be continued in future. For example it would be interesting to apply these techniques to patients recovering from ON. Brusa et al. (2001) in her study suggested that VEPs do not change after remyelination of the optic nerve. Nevertheless, the question, as to whether the responses after the remyelination change, or not, is not answered yet. To answer this question it would be interesting to record mfVEPs to sparser stimuli and compare them with the responses before and after the restoration of the optic nerve.

Alternatively a large scale clinical trial of first presenting patients could be initiated to compare the ability of the new mfVEPs and gadolinium enhanced MRI to predict conversion to clinically definite MS. This should be done in conjunction with assessments of the test-retest variability of the mfVEP method.

The method described in my thesis could be combined with already existing MS diagnostic technologies, such as MRI or CSF markers. Those combined techniques would raise the diagnostic sensitivities and help to detect the disease as soon as possible. If detected in time, MS symptoms could be blocked or alleviated by prescribing the correct medications at the correct dosage, both of which could potentially be monitored with the mfVEP method.

The other advantage of this method is that it could be applied in evaluating many other visual field neuro-ophthalmic disorders, such as diabetic retinopathy, retinitis pigmentosa, glaucoma, and many others.

Bibliography

ANDERSSON, T. & SIDEN, A. (1995). An analysis of VEP components in optic neuritis. *Electromyogr Clin Neurophysiol* **35,** 77-85.

BRUSA, A., JONES, S. & PLANT, G. (2001). Long-term remyelination after optic neuritis. A 2-year visual evoked potential and psychophysical serial study. *Brain* **124,** 468-489.

CELESIA, G., KAUFMAN, D., BRIGELL, M., TOLEIKIS, S., KOKINAKIS, D., LORANCE, R. & LIZANO, B. (1990). Optic neuritis: a prospective study. *Neurology* **40,** 919-923.

CHIAPPA, K. (1983). *Evoked potentials in clinical medicine*. Raven Press, New York.

DAWSON, W., MAIDA, T. & RUBIN, M. (1982). Human pattern-evoked retinal responses are altered by optic atrophy. *Invest Ophthalmol Vis Sci* **22,** 796-803.

DUSKA, M. & DENISLIC, M. (2000). Diagnostic sensitivity of neurophysiological tests in multiple sclerosis. In *6th Internet World Congress for Biomedical Sciences*.

EBERS, G. (1985). Optic neuritis and multiple sclerosis. *Arch Neurol* **42,** 702-704.

FORTUNE, B. & HOOD, D. (2003). Conventional pattern-reversal VEPs are not equivalent to summed multifocal VEPs. *Invest Ophthalmol Vis Sci* **44,** 1364-1375.

FORTUNE, B., HOOD, D. & JOHNSON, C. (2002). Comparison of conventional and multifocal VEPs. In *ARVO*, pp. 2126, Ft. Lauderdale.

FREDERIKSEN, J., LARSSON, H., OLESEN, J. & STIGSBY, B. (1991). MRI, VEP, SEP and biothesiometry suggest monosymptomatic acute optic neuritis to be a first manifestation of multiple sclerosis. *Acta Neurol Scand* **83,** 343-350.

HALLIDAY, A., MCDONALD, W. & MUSHIN, J. (1972). Delayed visual evoked response in optical neuritis. *Lancet* **1,** 982-985.

HOOD, D., ODEL, J. & ZHANG, X. (2000a). Tracking the recovery of local optic nerve function after optic neuritis: a multifocal VEP study. *Invest Ophthalmol Vis Sci* **41,** 4032-4038.

HOOD, D. & ZHANG, X. (2000). Multifocal ERG and VEP responses and visual fields: comparing disease - related changes. *Doc Ophthalmol* **100,** 115-137.

HOOD, D., ZHANG, X., GREENSTEIN, V., KANGOVI, S., ODEL, J., LIEBMANN, M. & RITCH, R. (2000b). An interocular comparison of the multifocal VEP: a possible technique for detecting local damage to the optic nerve. *Invest Ophthalmol Vis Sci* **41,** 1580-1587.

JONES, S. (1993). Visual evoked potentials after optic neuritis. Effect of time interval, age and disease dissemination. *J Neurol* **240,** 489-494.

KURTZKE, J. (1985). Optic neuritis and multiple sclerosis. *Arch Neurolog* **42,** 704-710.

MATTHEWS, W. & SMALL, M. (1983). Prolonged follow-up of abnormal visual evoked potentials in multiple sclerosis: evidence for delayed recovery. *J Neurol Neurosurg Psych* **46,** 639-642.

RODER, H. (1991). [VEP in the determination of multiple lesions in the visual system in patients with multiple sclerosis]. *EEG EMG Z Elektroenzephalogr Elektromyogr Verwandte Geb* **22,** 234-238.

ROVARIS, M., AGOSTA, F., SORMANI, M., INGLESE, M., MARTINELLI, V., COMI, G. & FILIPPI, M. (2003). Conventional and magnetization transfer MRI predictors of clinical evolution: a medium-term follow-up study. *Brain* **126,** 2323-2332.

SAND, T., SJAASTAD, O., ROMSLO, I. & SULG, I. (1990). Brain-stem auditory evoked potentials in multiple sclerosis: the relation to VEP, SEP and CSF immunoglobulins. *J Neurol* **237,** 376-378.

SICOTTE, N., VOSKUHL, R., BOUVIER, S., KLUTCH, R., COHEN, M. & MAZZIOTTA, J. (2003). Comparison of multiple sclerosis lesions at 1.5 and 3.0 Tesla. *Invest Radiol* **38,** 423-427.

SWANK, R. & DUGAN, B. (1987). *The multiple sclerosis diet book. A low-fat diet for the treatment of MS*. Doubleday, New York.

VAN DER MEI, I., PONSONBY, A., BLIZZARD, L. & DWYER, T. (2001). Regional variation in multiple sclerosis. Prevalence in Australia and its association with ambient ultraviolet radiation. *Neuroepidemiology* **20,** 168-174.

WAXMAN, S. (1983). The demyelinating diseases. *Clinical Neurosci* **1,** 609-643.